

Progressive collapse of damaged ship structures

Arriya Leelachai

Submitted for the degree of Doctor of Philosophy

March 2020

School of Engineering

Faculty of Science, Agriculture and Engineering

Newcastle University

Newcastle upon Tyne, UK

@2018 Arriya Leelachai

School of Engineering

Armstrong Building

Newcastle University

NE1 7RU

United Kingdom

Abstract

This research investigates the progressive collapse of stiffened panels in a ship's structure under several damaged conditions. The main focus is on the behaviour of stiffened panels under three conditions: intact condition; damage represented by a circular, clear-cut-out hole; and damage represented by penetration simulations. The same damage conditions have also been applied to double bottom box girders. The results of these analyses are used to better understand the behaviour of damaged ship structures and develop a novel modification to a simplified method for predicting a ship's ultimate strength.

The non-linear, finite element method is used in order to simulate the damaged condition and to estimate ultimate strength behaviour in both undamaged and damaged stiffened panels. The damaged conditions are divided into two categories: damage represented by a circular, clear-cut hole and damage represented by penetration with an indenter. The damaged scenario assumes the damage to be located in the middle of the stiffened panel. The diameter of the damaged area and diameter of indenter are controlled by a ratio between the diameter of damaged area (D) or diameter of indenter (D_{in}) and the width of the stiffened panels (W) respectively. Pre-existing characteristics of the structure are considered as an average level in terms of both residual stress and geometric imperfection. An in-plane compression load is applied to the stiffened panel in order to generate the ultimate strength, which is affected by the damaged condition.

The results are used to extend an existing hull girder progressive collapse method, using a novel approach to adapt the load shortening curves. A knockdown factor is generated by using regression formulae from the finite element models and is applied to modify a load shortening curve for damaged ship structures. The modification curves are combined with moment curvature to find the ultimate strength of the damaged hull girder.

The method is verified with case study analyses of double bottom box girders. The same damaged conditions applied for the stiffened panels are used with the hull girder. The damaged area is located in the middle of the bottom part of the structure. The hogging condition is applied for the verification model. The validation results show excellent agreement between the finite element method and modified hull girder progressive collapse method, which can be used to predict the ultimate strength of a damaged ship structure.

Acknowledgements

The five years of my PhD could not have been completed without an amazing group of people who always supported and had faith in me.

First, I would like to express my very great appreciation to my first supervisor, Prof Robert Dow, who gave me an opportunity to continue my study journey as a PhD student, who always listened to me and helped me in both my studies and my life. Thank you for your kind support, understanding and lovely smile. Moreover, I would like to offer my special thanks to Myra Dow, who gives very warm hugs and understanding. Thank you both of you for a very warm welcome to an international student like me.

I also wish to thank my second supervisor, Dr Simon Benson, who was always there to help me throughout my study. Thank you for listening, and for supporting me. Thank you for spending your own time to help and explain things to me when I was stuck with my study.

Thank you to both of my supervisors for making me feel at home in the marine school. You are not just my supervisors; you are friends and family to me. Thank you so much!

I would like to send a big thank you to ONR for the opportunity provided by sponsoring me through my research.

Special thanks to John Garside, who came to school with a warm heart to help and support me through the five years of my study.

To my family, who supported me though this journey, especially my husband who was always beside me to help, listen and take care of me. Thank you, Op, for believing in me. Thanks to Mom, Dad and other member of my family for their support and having faith in me.

To my office mate in 2.66 Armstrong building and the Marine Special Collection people, Dr Brian Newman, Mr Richard Carter and Prof Ian Buxton, (a special group of friends) who make me feel like I have a little family here.

Thank to my lovely neighbours, Smokey and Gill Robinson, who make amazing chocolate cake for me every time I stress out, and who always look after me while I am studying.

To the amazing groups of aunts and uncles in Brunswick church, who are volunTrs in the coffee shop, thank you for giving me very warm hugs every time we met, and thank you for having

faith in me.

Last but not least, to my special person, my granddad, thank you for teaching me to be the way I am today. Wherever you are, I would like to say 'Finally, I can make it Grand!'

Contents

| | |
|---|------|
| Abstract | V |
| Acknowledgements | VII |
| Contents | IX |
| List of Figures | XIII |
| List of Tables | XIX |
| Nomenclature | XXI |
| Chapter 1 Introduction | 1 |
| 1.1 Introduction..... | 1 |
| 1.2 Impact on ship structure..... | 1 |
| 1.2.1 MV Prestige | 2 |
| 1.2.2 USS Cole..... | 3 |
| 1.3 Aims and objectives..... | 4 |
| Chapter 2 Background | 5 |
| 2.1 Introduction..... | 5 |
| 2.2 Ship structural design..... | 5 |
| 2.3 Design methods..... | 6 |
| 2.3.1 The limit state design method | 7 |
| 2.3.2 The progressive collapse method | 7 |
| 2.3.3 Idealised structural unit method (ISUM) | 8 |
| 2.3.4 The finite element analysis method | 9 |
| 2.4 Strength of ship structure | 10 |
| 2.4.1 Strength of steel plates | 11 |
| 2.4.2 Strength of stiffened panels..... | 12 |
| 2.4.3 Ultimate strength of hull girder..... | 15 |
| 2.4.4 Initial imperfections | 16 |
| 2.4.5 Rationale | 18 |
| 2.5 Strength of accidentally damaged ship structure | 21 |
| 2.5.1 Representation of Damage | 22 |
| 2.5.2 Realistic damage mechanism | 25 |

| | |
|--|----|
| 2.6 Factors in finite element analysis..... | 31 |
| 2.6.1 Mesh..... | 31 |
| 2.7 Software development. | 32 |
| 2.8 Summary | 36 |
| Chapter 3 Material and Structural Properties..... | 37 |
| 3.1 Introduction..... | 37 |
| 3.2 Material Properties..... | 37 |
| 3.2.1 Material Characteristics | 38 |
| 3.3 Panel Geometries | 43 |
| 3.4 Damaged Stiffened Panels | 47 |
| 3.4.1 Damage represented by circular clear-cut out..... | 49 |
| 3.4.2 Damage represented by penetration with indenter | 51 |
| 3.5 Boundary conditions | 52 |
| 3.6 Initial conditions | 54 |
| 3.6.1 Residual stress..... | 55 |
| 3.6.2 Distortions..... | 55 |
| 3.7 Finite element program | 57 |
| 3.8 Element type | 58 |
| 3.9 Mesh..... | 59 |
| 3.10 Steps..... | 60 |
| 3.10.1 Relaxation step..... | 60 |
| 3.10.2 Compression load..... | 61 |
| 3.10.3 Damaged step..... | 61 |
| 3.11 Analysis procedure..... | 64 |
| 3.11.1 Intact analysis procedure..... | 64 |
| 3.11.2 Damaged area represented by circular clear-cut hole. | 65 |
| 3.11.3 Damaged area represented by penetration with indenter | 66 |
| 3.12 Summary | 67 |
| Chapter 4 Strength of intact and damaged stiffened panels..... | 69 |
| 4.1 Introduction..... | 69 |
| 4.2 Intact stiffened panels | 69 |
| 4.3 Damaged stiffened panels | 75 |
| 4.3.1 Damage represented by circular clear-cut hole..... | 75 |

| | |
|--|-----|
| 4.3.2 Damage represented by penetration with indenter | 91 |
| 4.4 Summary | 101 |
| Chapter 5 The extended progressive collapse method..... | 103 |
| 5.1 Introduction..... | 103 |
| 5.2 Overview of the simplified method | 103 |
| 5.3 Modified process..... | 105 |
| 5.3.1 Comparison of intact stiffened panel results | 105 |
| 5.3.2 Knockdown factor from damaged stiffened panels | 105 |
| 5.3.3 Re-creating damage results under the simplified method in ProColl..... | 109 |
| 5.4 Comparison of damaged stiffened panels between ABAQUS and ProColl. | 111 |
| 5.5 Validation – double bottom box girder | 112 |
| 5.5.1 Model description | 112 |
| 5.5.2 Scope of analysis..... | 114 |
| 5.5.3 Damage on double bottom box girder..... | 116 |
| 5.5.4 Results of double bottom box girder..... | 119 |
| 5.6 ProColl results for other cases with box girder..... | 131 |
| 5.6.1 Model description | 131 |
| 5.6.2 Ultimate strength results from ProColl | 133 |
| 5.7 Summary | 134 |
| Chapter 6 Conclusions and Recommendations..... | 135 |
| 6.1 Conclusions..... | 135 |
| 6.1.1 Intact stiffened panels | 135 |
| 6.1.2 Damaged stiffened panels | 136 |
| 6.1.3 Extended progressive collapse method | 138 |
| 6.2 Recommendations for future work | 139 |
| References | 141 |
| Appendix A: Intact panels' details..... | 145 |
| Plate slenderness ratio (β) = 1.0..... | 146 |
| Plate slenderness ratio (β) = 2.0..... | 149 |
| Plate slenderness ratio (β) = 3.0..... | 152 |
| Plate slenderness ratio (β) = 4.0..... | 155 |
| Appendix B: Strength of intact stiffened panels | 159 |

| | |
|--|-----|
| Beta 1.0: Average imperfection | 159 |
| Beta 1.0: Stress and Strain curve | 161 |
| Beta 2.0: Average imperfection | 165 |
| Beta 2.0: Stress and Strain curve | 167 |
| Beta 3.0: Average imperfection | 171 |
| Beta 3.0: Stress and Strain curve | 173 |
| Beta 4.0: Average imperfection | 177 |
| Beta 4.0: Stress and Strain curve | 179 |
| Appendix C: Strength of damaged clear-cut hole stiffened panels..... | 183 |
| Beta 1.0 | 183 |
| Beta 2.0 | 187 |
| Beta 3.0 | 191 |
| Beta 4.0 | 195 |
| Appendix D: Strength of penetration damage with indenter. | 199 |
| Beta 1.0 | 199 |
| Beta 2.0 | 202 |
| Beta 3.0 | 204 |
| Beta 4.0 | 207 |
| Appendix E: Strength of double bottom box girder..... | 211 |
| Comparison of double bottom box girder with damaged clear-cut hole between ABAQUS and ProColl. | 211 |
| Comparison of double bottom box girder with penetration damage with indenter between ABAQUS and ProColl. | 217 |

List of Figures

| | |
|--|----|
| Figure 1.1 The sinking of the MV Prestige (gCaptain, 2016) | 3 |
| Figure 1.2 The <i>USS Cole</i> (left) is towed away from the port city of Aden in Yemen, Damage to <i>USS Cole</i> destroyer (DDG 67) (right) anchored at port of Aden, Yemen (Sgt. Don L. Maes, 2000) | 3 |
| Figure 2.1 Combination of hull girder (Hughes, 1988). | 6 |
| Figure 2.2 ISUM flow diagram..... | 9 |
| Figure 2.3 Stress-strain curve of plates under longitudinal compression (Dow, 1997)..... | 11 |
| Figure 2.4 Inter-frame buckling..... | 13 |
| Figure 2.5 Overall buckling. | 13 |
| Figure 2.6 Load-shortening curves for stiffened panels with T-bar stiffeners (Stiffened area ratio $ASA = 0.2$ with average imperfections) (Dow, 1997). | 14 |
| Figure 2.7 Heat effect zone from welding (Benson, 2011)..... | 15 |
| Figure 2.8 Stress distribution from welding in plates (Benson, 2011). | 17 |
| Figure 2.9 Stress distribution from welding in stiffened panels (Dow, 1997)..... | 17 |
| Figure 2.10 Typical Load Shortening curve (Chalmers, 1993). | 18 |
| Figure 2.11 Column strength curve – average imperfections with stiffener area ratio $ASA = 0.1$ (Smith and Anderson, 1991). | 20 |
| Figure 2.12 Column strength curve – average imperfections with stiffener area ratio $ASA = 0.2$ (Smith and Anderson, 1991). | 20 |
| Figure 2.13 Column strength curve – average imperfections with stiffener area ratio $ASA = 0.4$ (Smith and Anderson, 1991). | 21 |
| Figure 2.14 Examples of damage case studies Left: damaged singular stiffened, Right: damage in line with the central stiffener of the panel (Underwood et al., 2012). | 23 |
| Figure 2.15 Rectangular opening in unstiffened plate (Yu and Lee, 2012)..... | 24 |
| Figure 2.16 Opening cases in stiffened panels (Yu et al., 2015). | 25 |

| | |
|---|----|
| Figure 2.17 Resistance of stiffened panels to penetration damage (AbuBakar and Dow, 2013). | 26 |
| Figure 2.18 Vertical grounding displacement on the main floor of models (AbuBakar and Dow, 2013). | 27 |
| Figure 2.19 Box girder cross section (Benson et al., 2013b). | 28 |
| Figure 2.20 Penetration damage with indenter (Benson et al., 2013b). | 29 |
| Figure 2.21 Simplified progressive collapse method with damage model. (a) top damage. (b) side damage and (c) bottom damage (Benson et al., 2013a). | 30 |
| Figure 2.22 Raking damage of <i>HMS Nottingham</i> on ship hull (Bole, 2007). | 32 |
| Figure 2.23 The Seagoing Paramarine program (Bole, 2007). | 33 |
| Figure 2.24 Irregular panel calculation flow diagram (Benson et al., 2015). | 35 |
| Figure 3.1 Engineering Stress – Strain curve. | 39 |
| Figure 3.2 Idealised stress-strain curves (Chen and Han, 1988). | 40 |
| Figure 3.3 Typical material response showing progressive damage (ABAQUS 6.13, Systèmes (2013)). | 41 |
| Figure 3.4 Resistance simulation on stiffened panel under penetration damage (AbuBakar and Dow, 2013). | 42 |
| Figure 3.5 Overall collapse in a stiffened panel. | 44 |
| Figure 3.6 Stiffened panel geometries. | 45 |
| Figure 3.7 Stiffener geometries. | 46 |
| Figure 3.8 Damage clear-cut hole diagram. | 49 |
| Figure 3.9 Change of transverse frame height. | 51 |
| Figure 3.10 Indenter geometry. | 51 |
| Figure 3.11 Boundary conditions of stiffened panel. | 53 |
| Figure 3.12 Imperfection in a stiffened panel. | 55 |
| Figure 3.13 Dimension of a plate in a stiffened panel. | 56 |

| | |
|---|----|
| Figure 3.14 Distortions of the length of steel plate ‘a’. | 57 |
| Figure 3.15 Distortions of the width of steel plate ‘b’. | 57 |
| Figure 3.16 Shell element type S4R. | 58 |
| Figure 3.17 Comparison between element type S4 and S4R. | 59 |
| Figure 3.18 Mesh size for stiffened panel. | 60 |
| Figure 3.19 Quad-domination type. | 60 |
| Figure 3.20 Compression load | 61 |
| Figure 3.21 Penetration damage. | 62 |
| Figure 3.22 Analysis procedure. | 65 |
| Figure 4.1 Stress-strain curve of stiffened panels with Beta of 2.0, stiffened area ratio (ASA) of 0.2 and 5’ long-stalk T bar. | 72 |
| Figure 4.2 Average imperfection of plate slenderness ratio (β) 2.0, stiffener area ratio ASA 0.1. | 74 |
| Figure 4.3 Average imperfection of plate slenderness ratio (β) 2.0, stiffener area ratio ASA 0.2. | 74 |
| Figure 4.4 Average imperfection of plate slenderness ratio (β) 2.0, stiffener area ratio ASA 0.4. | 75 |
| Figure 4.5 Comparison between intact stiffened panel and damaged clear-cut hole panel. | 77 |
| Figure 4.6 Stress-strain curve of damaged clear-cut hole with plate slenderness ratio (β) = 2.0, column slenderness ratio (λ) = 0.3, stiffener area ratio ASA = 0.2 and ALS3. | 77 |
| Figure 4.7 Ultimate strength of damaged clear-cut hole panels with plate slenderness ratio (β) = 1.0, column slenderness ratio (λ) = 0.2, stiffener area ratio ASA = 0.2 and ALS3. | 85 |
| Figure 4.8 Ultimate strength of damaged clear-cut hole panels with plate slenderness ratio (β) = 2.0, column slenderness ratio (λ) = 0.2, stiffener area ratio ASA = 0.2 and ALS3. | 86 |
| Figure 4.9 Ultimate strength of damaged clear-cut hole panels with plate slenderness ratio (β) = 3.0, column slenderness ratio (λ) = 0.2, stiffener area ratio ASA = 0.2 and ALS3. | 86 |
| Figure 4.10 Ultimate strength of damaged clear-cut hole panels with plate slenderness ratio (β) = 4.0, column slenderness ratio (λ) = 0.2, stiffener area ratio ASA = 0.2 and ALS3. | 87 |

| | |
|--|-----|
| Figure 4.11 Ultimate strength of damaged represented by circular clear-cut hole panels..... | 88 |
| Figure 4.12 Stress-strain curve of penetration damage with indenter on the stiffened panel with plate slenderness ratio (β) = 2.0, column slenderness ratio (λ) = 0.2, stiffener area ratio ASA = 0.2 and ALS3. | 91 |
| Figure 4.13 the measurement of damaged diameter in penetration with indenter..... | 97 |
| Figure 4.14 Ultimate strength of penetration damage with indenter on the stiffened panels with plate slenderness ratio (β) = 1.0, column slenderness ratio (λ) = 0.2, stiffener area ratio ASA = 0.2 and ALS3. | 98 |
| Figure 4.15 Ultimate strength of penetration damage with indenter on the stiffened panels with plate slenderness ratio (β) = 2.0, column slenderness ratio (λ) = 0.2, stiffener area ratio ASA = 0.2 and ALS3. | 98 |
| Figure 4.16 Ultimate strength of penetration damage with indenter on the stiffened panels with plate slenderness ratio (β) = 3.0, column slenderness ratio (λ) = 0.2, stiffener area ratio ASA = 0.2 and ALS3. | 99 |
| Figure 4.17 Ultimate strength of penetration damage with indenter on the stiffened panels with plate slenderness ratio (β) = 4.0, column slenderness ratio (λ) = 0.2, stiffener area ratio ASA = 0.2 and ALS3. | 99 |
| Figure 4.18 Ultimate strength of damage represented by penetration with indenter..... | 100 |
| Figure 5.1 Overview of modified simplified method (ProColl). | 104 |
| Figure 5.2 Idealise of small panel (Benson, 2011) | 105 |
| Figure 5.3 Knockdown factors for damage represented by circular clear-cut hole..... | 107 |
| Figure 5.4 Knockdown factors for damage represented by penetration with an indenter. | 109 |
| Figure 5.5 Load shortening curve for damage with a clear-cut hole. (ProColl with β = 2.0)..... | 110 |
| Figure 5.6 Comparison of load shortening curve between ABAQUS and ProColl for damage with a clear-cut hole panel with β = 2.0 and DW = 0.50. | 111 |
| Figure 5.7 Layout of double bottom box girder..... | 113 |

| | |
|---|-----|
| Figure 5.8 Front view of double bottom box girder..... | 113 |
| Figure 5.9 Boundary conditions of the double bottom box girder..... | 115 |
| Figure 5.10 Double bottom box girder with damaged clear-cut hole area. | 118 |
| Figure 5.11 Double bottom box girder with penetration damage with indenter..... | 119 |
| Figure 5.12 Behaviour of intact structure for double bottom box girder..... | 120 |
| Figure 5.13 Comparison between ABAQUS and ProColl with damage represented by circular clear-cut hole at 57 per cent damage..... | 122 |
| Figure 5.14 Comparison of ultimate strength for double bottom box girder between two different damage types in ABAQUS. | 127 |
| Figure 5.15 Comparison of ultimate strength for double bottom box girders between two different damage types in ProColl. | 128 |
| Figure 5.16 Penetration damage of double bottom box girder with damaged area ratio $DW =$ 0.65..... | 129 |
| Figure 5.17 Comparison of ultimate strength for double bottom box girder with damage from a clear-cut hole between ABAQUS and ProColl..... | 130 |
| Figure 5.18 Comparison of ultimate strength for double bottom box girder with penetration damage with indenter between ABAQUS and ProColl..... | 130 |
| Figure 5.19 Front view of single bottom box girder (Case1). | 131 |
| Figure 5.20 Front view of single bottom box girder (Case2). | 132 |
| Figure 5.21 Layout of single bottom box girder (Case2)..... | 133 |
| Figure 5.22 Ultimate strength of three cases of box girder with ProColl. | 134 |
| Figure 6.1 Comparison of ultimate strength in damaged stiffened panels with Beta 2.0. | 138 |
| Figure A.0.1 Dimension of stiffened panel..... | 145 |

List of Tables

| | |
|--|----|
| Table 2.1 Assumed imperfection levels..... | 16 |
| Table 2.2 Box girder properties (Benson et al., 2013b)..... | 28 |
| Table 2.3 Comparison between different mesh sizes and time consumed in the analysis (Benson et al., 2013a)..... | 31 |
| Table 3.1 Advantages and disadvantages of steel (Chalmers, 1993)..... | 38 |
| Table 3.2 Scope of analysis in intact stiffened panels. | 43 |
| Table 3.3 The UK Admiralty Research Establishment..... | 46 |
| Table 3.4 Scope of analysis for damaged stiffened panel..... | 47 |
| Table 3.5 Size of damaged clear-cut hole..... | 50 |
| Table 3.6 Size of indentation damaged hole, DINW | 52 |
| Table 3.7 Boundary condition of stiffened panels | 53 |
| Table 3.8 Imperfection properties for stiffened panels. | 54 |
| Table 3.9 Definition of initial deformation in this research (Dow and Smith, 1984)..... | 56 |
| Table 3.10 Penetration with different speeds..... | 63 |
| Table 4.1 Intact panels' behaviour for set of stiffened panels with plate slenderness ratio (β) of 2.0, stiffened area ratio ASA of 0.2 and 5' long-stalk T bar..... | 70 |
| Table 4.2 The behaviour of damaged clear-cut hole panels with plate slenderness ratio (β) of 2.0, column slenderness ratio (λ) = 0.3, stiffener area ratio ASA = 0.2 and ALS3..... | 79 |
| Table 4.3 Coefficient of Variation between regression lines and ABAQUS data in Figure 4.11. 88 | |
| Table 4.4 Comparison of different transverse frame height in stiffened panels. | 89 |
| Table 4.5 The effect of penetration damage with an indenter on the stiffened panels with plate slenderness ratio (β) of 2.0, column slenderness ratio (λ) = 0.2, stiffener area ratio ASA = 0.2 and ALS3. | 93 |
| Table 4.6 Coefficient of Variation between regression lines and ABAQUS data in Figure 4.18. | |

| | |
|---|-----|
| | 101 |
| Table 5.1 Turning point of knockdown formulae in penetration damage. | 108 |
| Table 5.2 Double bottom box girder parameters. | 114 |
| Table 5.3 Boundary condition of double bottom box girder. | 116 |
| Table 5.4 Diameter of damaged area in both damage cases. | 117 |
| Table 5.5 Diameter of clear-cut hole in double bottom box girder. | 120 |
| Table 5.6 Post collapse of double bottom box girder with damage from a clear-cut hole. | 123 |
| Table 5.7 Diameter of penetration damage with indenter in double bottom box girder. | 126 |

Nomenclature

| Symbol | Definition |
|------------------|---|
| A | Total cross section area of the whole structure |
| A _s | The cross section area of the stiffeners |
| a | Longitudinal dimension of plate panel between stiffeners |
| b | Transverse dimension of plate panel between stiffeners |
| b _f | Stiffener flange width |
| b _p | Plate width/ spacing between adjacent longitudinal stiffeners |
| b _t | Tensile residual stress width |
| D | Diameter of damage area |
| D _{IN} | Diameter of indenter |
| E | Young's modulus |
| E _t | Tangent modulus |
| h _w | Stiffener web height |
| h _{wy} | Transverse frame height |
| I _x | Second moment of area of the plate-stiffener cross section |
| RP | Reference point |
| r | Radius of gyration of plate and stiffener combination = $\sqrt{\frac{I_x}{A}}$ |
| t _p | Plating thickness |
| t _f | Stiffener flange thickness |
| t _w | Stiffener web thickness |
| t _{wy} | Transverse frame thickness |
| U1 | Force in X-axis direction |
| U2 | Force in Y-axis direction |
| U3 | Force in Z-axis direction |
| UR1 | Moment about X-axis |
| UR2 | Moment about Y-axis |
| UR3 | Moment about Z-axis |
| W | Width of stiffened panel |
| W ₀ | Initial plate displacement |
| W _{0pl} | Plate imperfection |
| W _{0s} | Stiffener imperfection |
| β | Plate slenderness ratio = $\left(\frac{b}{t}\right) \sqrt{\left(\frac{\sigma_y}{E}\right)}$ |
| ε | Material strain |
| ε ₀ | Material yield strain (steel) |
| δ ₀₁ | Plate distortion |
| δ ₀₂ | Plate distortion |
| λ | Stiffened panel slenderness/column slenderness ratio = $\left(\frac{a}{\pi r}\right) \sqrt{\frac{\sigma_y}{E}}$ |
| σ | Stress |

| | |
|----------------|---|
| σ_0 | Material yield stress (steel) |
| σ_{rc} | Residual stress magnitude |
| σ_{rcx} | Compressive residual stress magnitude in longitudinal direction |
| σ_{rcy} | Compressive residual stress magnitude in transverse direction |
| σ_{rtx} | Tensile residual stress magnitude in longitudinal direction |
| σ_{rty} | Tensile residual stress magnitude in transverse direction |
| σ_y | Yield stress of material |
| ν | Poisson's ratio |

Abbreviations

| | |
|---------|---|
| ALS | Admiralty Long Stalk T-bar stiffener |
| FLD | Forming Limit Diagram |
| HAZ | Heat Affected Zone |
| ProColl | Compartment level Progressive Collapse Program |
| S4 | Shell element with four nodes element |
| S4R | Shell element with four nodes element with reduce integration and hourglass control |

Chapter 1 Introduction

1.1 Introduction

The consequences of accidental damage in ship structures have been extensively studied over the past decades. Once a ship suffers major structural damage, there is risk of severe consequences such as economic and environmental costs, loss of the ship or loss of life.

To reduce these consequences, ship structures should be able to withstand some degree of damage. It is important to evaluate and understand the residual damaged strength of a typical vessel in order to help to develop damage tolerant designs and improve decision making for the recoverability of the ship.

This chapter presents some case studies of ships that sustained damage and which provide an inspiration to this study. The aims and objectives of the study are then described.

1.2 Impact on ship structure

A major concern is the ability of a ship to withstand some degree of damage when the structure suffers a situation such as an unpredictable extreme environment or an accident. The damage to ship could caused by collision, grounding, explosion and excessing environmental loads.

To improve durability and prevent unfavourable outcomes, engineer should be able to understand the behaviour of ships' structures while an accidental event; moreover, with greater understanding, the ship industry can develop suitable equipment to repair and maintenance of the damage ship's structure. To explore this, several case studies have been considered below.

1.2.1 MV Prestige

The *MV Prestige* (Wikipedia, 2002-2017) was an oil tanker which broke in half and sank in November 2002. The moment the ship sank is illustrated in Figure 1.1. More than 63,000 tonnes of oil spilled along the coastlines of northern France, Spain and Portugal. The oil spill especially affected the ecology and economy of Spain, as offshore fishing had to be suspended for six months because of the heavy coastal pollution.

Investigation of failure in MV Prestige was carried out by ABS (Ship Structures Committee, 2018). The cause of initial failure of the ship can be separated into four possible scenarios:

1. Due to the bursting of a tank in heavy seas, flooding of the ship created a single failure in the hull girder by increasing the maximum stresses in the deck and double bottom.
2. The structure itself could have been weakened by the residual stresses from welded plates.
3. The dynamic load from successive lightening operations in port and then successive wave loads during transit could have created a permanent deformation into the structure. The bending stress then surpassed the buckling level, which created a failure of the ship structure.
4. There were also failures of the maintenance schedule. ABS suggested that any damage, which can cause the serious threat to the ship, should have been repaired before the next operation.

The scenarios show the importance of the strength of the structure. A better understanding of the strength in the structure can improve the maintenance and reduce the risk of catastrophic hull girder failure.



Figure 1.1 The sinking of the MV Prestige (gCaptain, 2016)

1.2.2 USS Cole

The *USS Cole* (Wikipedia, 2000 - 2017) is shown in Figure 1.2. She was the target of two suicide bombers in Aden harbour in Yemen. The explosion occurred at the side of the ship and 17 were killed immediately. After the attack, the ship was carried back to shore for repairs. She was returned to the sea three years later, in 29 November 2003.



Figure 1.2 The *USS Cole* (left) is towed away from the port city of Aden in Yemen, Damage to *USS Cole* destroyer (DDG 67) (right) anchored at port of Aden, Yemen (Sgt. Don L. Maes, 2000)

A reduction in strength due to impact can reduce the serviceability limit state of the structure. The structure should be designed to withstand this damage and keep its stability until a return to port for repairs.

The investigation of the ultimate strength of a damaged ship such as the *USS Cole* could be difficult with such a large-scale rupture. Limited time could be one of the key factors

constraining the investigation. To improve the situation, this research will provide a supporting tool with an efficient methodology to develop the investigation, using the basis of the progressive collapse method.

This research provides a foundation that includes the data set of different damage effects from small to large scale ruptures in the ship's structure. The extension of the simplified progressive method, developed from the dataset of the research, aims to improve the accuracy of ultimate strength results, in order to design, maintain or aid ships in extreme situations such as collision, grounding or terrorist incidents, as with the *USS Cole*. The research methodology might thus save lives, improve economics in the ship industry and reduce environmental impacts.

1.3 Aims and objectives

The aim of this research is to investigate the effect of realistic damage mechanisms which occur on a ship's structure and to provide a better understanding of the residual ultimate strength behaviour of the damaged structure. The main outcome and novel contribution of this study is the development of an extension to the simplified progressive collapse method, to include damage effects.

The objectives of this research are as follows:

- Define a comprehensive dataset of intact, stiffened panels used as the main structural components for providing the longitudinal strength of the ship. The dataset includes a range of plate and column slenderness covering all normal ship type structures.
- Develop two representative damage scenarios: idealised damage represented by a circular, clear-cut hole and realistic damage represented by the penetration of an indenter.
- Complete non-linear finite element analysis to simulate in-plane compression load on the dataset of stiffened panels in intact and damaged conditions.
- Propose a simplified method to adjust the load shortening curve and ultimate strength of the damaged stiffened panels, to represent the effects of damage area in the structure.
- Extend and validate an implementation of the progressive collapse method for calculating the ultimate strength of ship structure, including damage effects.

Chapter 2 Background

2.1 Introduction

This chapter presents research relevant to the development of the analysis method presented in this thesis, case studies of damage on ship structures and the original development of simplified software to complete these calculations. An overview of ship structural design is included in the beginning of this chapter, in order to give a general view of the ship design industry.

The research builds on previous literature, in order to improve understanding of damage effects on ship structure. The focus is on the behaviour of local structure because the damage effect is applied to stiffened panels, based on previous literature.

2.2 Ship structural design

A principal purpose of a ship's structure is to withstand the global bending moment which appears on the longitudinally continuous structure which comprises the main hull girder. The global bending strength of ship structure is a combination of an individual strength in each of the local structure members, such as plates or stiffeners, under external loads such as dead load or wave loading. These external loads generate bending moments in the main hull structure and exert an internal load to the sub-member of the ship structure. Figure 2.1 shows the internal loads which occur in the hull girder.

Internal loads are the main focus in this research in order to understand stiffened panels' behaviour. Even so, external and internal loads are not only the factors affecting the ship's structures. The strength of the ship can be influenced by other factors, which influence the initial strength of the structure. For example, these might include an initial imperfection, an accident or the age of the ship.

Initial imperfections in the structural geometry are a major factor with an effect on the overall strength behaviour of the ship's structure. These initial imperfections, which are a combination of distortion during fabrication and residual stress from welding, can create a strength reduction in the structure. Dow and Smith (1984) demonstrate an effect of localised imperfection in long, rectangular plates. Fourteen case studies were set up under three conditions, which are local

imperfection, periodic (ripple) distortion and dents, which occurred in a few different locations in the steel plate. The residual stress effect was eliminated in the study. The study shows that the local deformation, affected by the imperfection, can cause a reduction of compressive strength in the plate. Further information regarding initial imperfections is used in this simulation, and is discussed in Chapter 3.

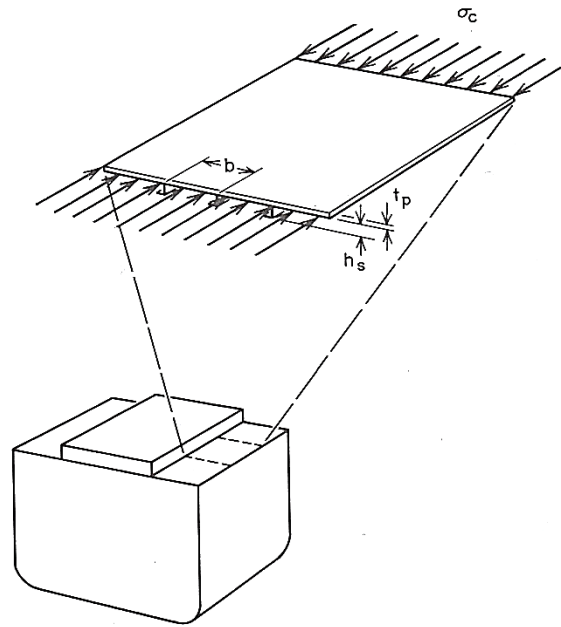


Figure 2.1 Combination of hull girder (Hughes, 1988).

2.3 Design methods

The behaviour of ship structures should be considered in order to improve the capability of ship hulls and maintain the reliability of the structure. Nowadays, naval architecture uses design standards such as Lloyd's Register (register, 2014) or their own design rules to reduce time and simplify the process; however, fundamental design methods are needed to understand failure mechanisms during the design process.

At the simplest level, classical beam theory could be used to assess hull girder strength. This assumes the hull girder functions as a beam under distribution loads; however, buckling effects are not taken in to account. To consider the compression effect on the ship structure, there are more accurate methods which have been adopted and are relevant to this research.

2.3.1 The limit state design method

The limit state method is a design philosophy that needs to identify a strength limit in a structure. The method is separated into four categories;

- Ultimate limit state or collapse limit state (ULS);
- Serviceability limit state (SLS);
- Fatigue limit states (FLS);
- Accidental limit state (ALS);

This study is mainly focussed on the ultimate limit state, which requires the direct assessment of the ultimate strength of ship structures. The ultimate strength of a hull girder is affected by both welding and accidental damage, which create initial residual stress. Reduction of the ultimate strength limit occurs, which means that the ship cannot support the same load capacity. To prevent this situation, the ultimate strength of damaged, stiffened panels is investigated in order to develop an understanding of damaged behaviour in stiffened panels.

2.3.2 The progressive collapse method

The progressive collapse method, often known as the Smith method, was first pioneered by Caldwell (1965) and then developed by Faulkner to investigate the ultimate strength of hull girders under longitudinal bending moment in both sagging and hogging. Furthermore, the development of the method by Smith (1977, 1988) included post-buckling behaviour, which came from initial imperfections, and applied in large defects in elasto-plastic analysis.

The full method can be found in several papers such as those by Yao and Nikolov (1991), Smith (1977), Dow (1997).

The Smith method employs a simple procedure, as follows:

- 1) The hull girder cross section is selected. It is usually in the mid part of the ship, because that is where the maximum bending moment occurs.
- 2) The cross section is divided into small elements in the form of plates and stiffeners, which act independently.

- 3) Each element is analysed and a load shortening curve is generated under incremental increases of compression and tension.
- 4) The neutral axis of the hull girder cross section is calculated.
- 5) Vertical curvature of the hull girder is assumed to gradually increase under certain circumstances;
 - a. The plane section remains plane.
 - b. The bending occurs about the instantaneous elastic (tangent) neutral axis of the cross section.
 - c. An adjustment of the neutral axis occurs when the cross section loses stiffness over a compressive strain area in the hull girder.
- 6) Increments of element stresses are derived from the slope of the load shortening curve.
- 7) Stresses are integrated over the cross section to obtain the bending moment increments.
- 8) Incremental curvatures and bending moments are summed to provide cumulative values.

2.3.3 Idealised structural unit method (ISUM)

Another method for estimating ultimate strength is called the ‘Idealised structural unit method’ (ISUM) and is a numerical method. Ueda and Rashed (1974) presented one version this method to use with a large structure such as ships but also with offshore platform. ISUM represents a structure’s response in the form of a stress-strain curve by using non-linear analysis. The method reduces the number of freedom to decrease the unknown in the finite matrix. Figure 2.2 shows a flow diagram for this method.

The stress-strain curves in each element are created by increasing displacement or load in the structure. The ultimate strength of the structure is calculated in the final process.

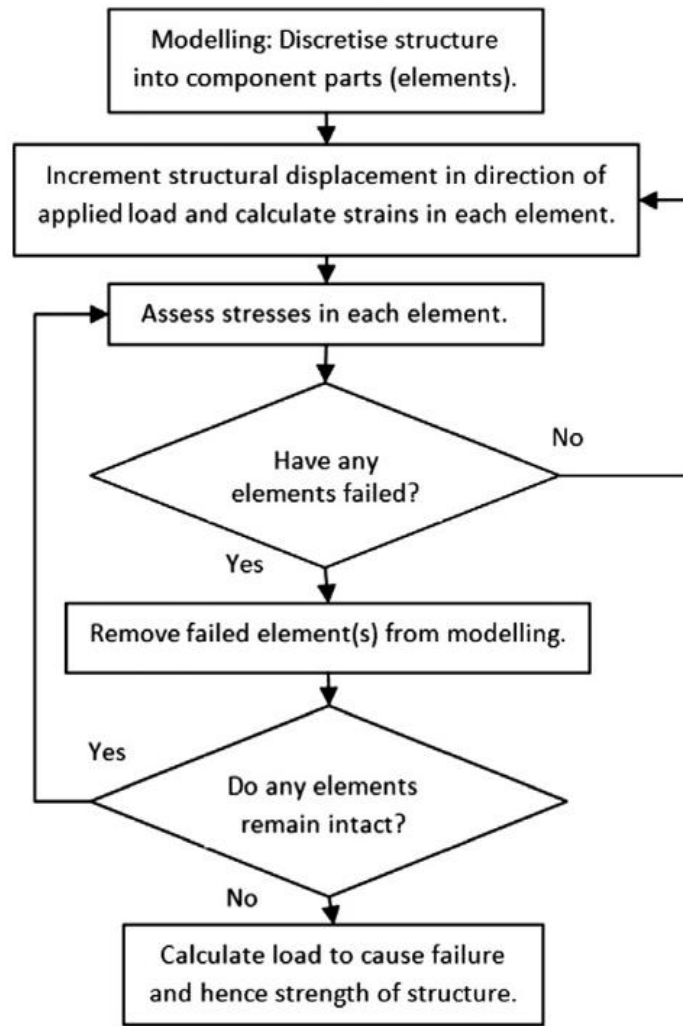


Figure 2.2 ISUM flow diagram.

ISUM is one well-known method, and is adopted in several research studies such as by Underwood et al. (2012), but the method is not considered in this research.

2.3.4 The finite element analysis method

The finite element analysis method (FEA) is a powerful tool for use in ship design, especially with specific areas or an individual section of a structure. In this research, non-linear finite element analysis is used to simulate residual stress in damaged stiffened panels. The investigation has been carried out with both static and dynamic analyses; moreover, dynamic

analysis is used to simulate a quasi-static analysis.

- ***Static non-linear analysis***

The static non-linear analysis method uses a combination of Riks arc length and a modified Newton-Raphson value (D. Cook et al., 2002) to provide a basic, incremental procedure to produce iterative values for equilibrium in the structure; moreover, plasticity of a stiffened model is represented by the von Mises yield criterion and a true stress-strain relationship.

- ***Dynamic non-linear analysis***

Dynamic non-linear analysis can be separated into two types: implicit analysis and explicit analysis. In the ultimate strength calculations quasi-static analysis is replaced by explicit dynamic analysis to overcome convergence problems in the quasi-static methodology.

However, the problem of explicit analysis is one of controlling the kinetic energy and damping in the structure, while with the explicit is possible to produce an overestimate of ultimate strength.

In this research, the explicit analysis is adopted and assumed to give a quasi-static solution by using a small incremental procedure to control the level of kinetic energy and damping. The accuracy of this method depends on small time steps being used since no equilibrium check is carried out.

The disadvantage of this method is the time consuming process; moreover, the method requires a large computing capability to support a large amount of data in the procedure. More details of the analysis process will be presented in Chapter 3.

2.4 Strength of ship structure

Based on the design method in section 2.3, the strength of a ship's structure originates from a combination of steel plates and stiffeners in the hull girder. The improvement of understanding of the behaviour of plates and stiffened panels is thus beneficial for the assessment of the ultimate strength limit in the ship's hull. Since 1965, the development of theory related to this has been continuous until the present day.

2.4.1 Strength of steel plates

In 1977, Smith and Dow published work on complex elasto-plastic behaviour in stiffened and unstiffened panels under in-plane compression loads. The initial imperfections are included in the experiments, because initial imperfections gradually decrease the compressive strength of the structure and change the failure mode. The investigation started with the strength of steel plates under in-plan compression loads, as presented in Figure 2.3. The tangent stiffness of plating was assessed from the slope of the stress-strain curve and demonstrated numerically in the computer program.

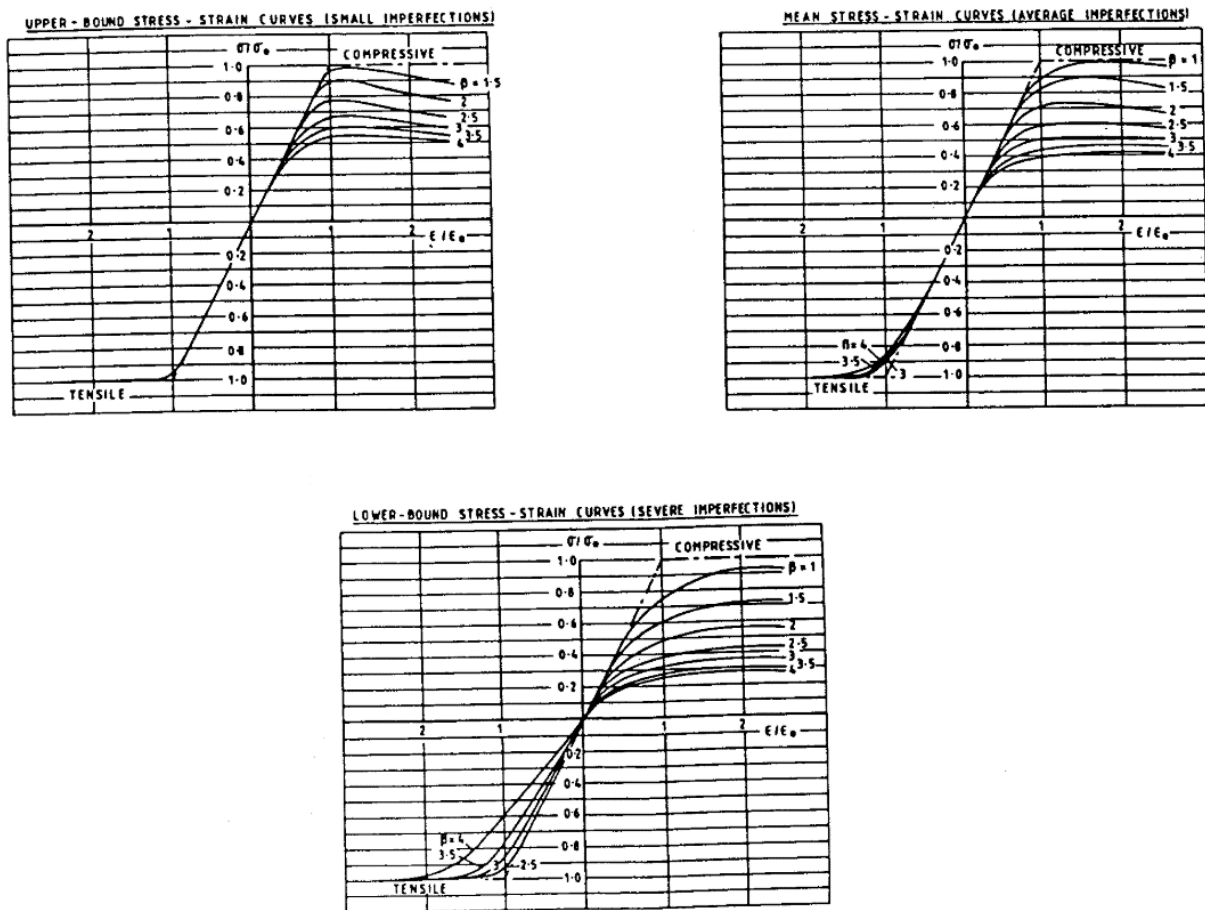


Figure 2.3 Stress-strain curve of plates under longitudinal compression (Dow, 1997).

The possibility of damage effects in plating which cause a strength reduction can be described below (Dow, 1997):

1. Static or dynamic impact loads, which occur during fabrication or in service, can cause an isolated dent. Compressive strength in the rectangular plate is decreased due to the isolated dent and can be equal to an effect from periodic or ripple distortion of the same level of amplitude.
2. Hungry horse deformation is created from hydrodynamic impact (slamming) or underwater explosion.

To reduce these effects in plating, Dow (1997) suggests that the plate aspect ratio $\left(\frac{a}{b}\right)$ should be bigger than 2, with a combination of low or intermediate slenderness (β) less than 2.5.

2.4.2 Strength of stiffened panels

Smith (1977) studied the possibility of compressive failures in stiffened panels. The collapse modes of interest to this research are inter-frame failure mode and overall collapse mode, as presented in Figures 2.4 and 2.5 respectively.

- **Inter-frame failure mode**

The loss of stiffness due to buckling and yielding of the plating can cause the inter-frame failure mode, as illustrated in Figure 2.4. Both distortions and residual stresses from welding can affect collapse strength in the panels. Smith (1977) explained that the sensitivity of imperfections is greatest in stiffened panels with high column slenderness (λ); moreover, the panel can be sensitive to the direction of buckling.

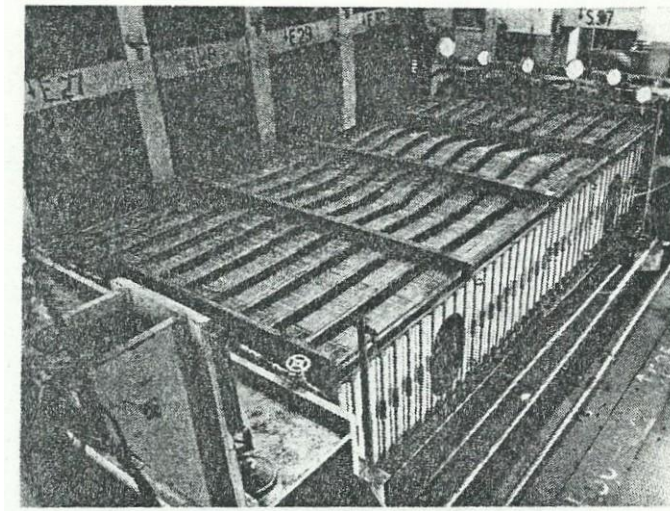


Figure 2.4 Inter-frame buckling.

- Overall buckling mode

This mode of failure occurs because of the bending in both transverse and longitudinal stiffeners, as shown in Figure 2.5.

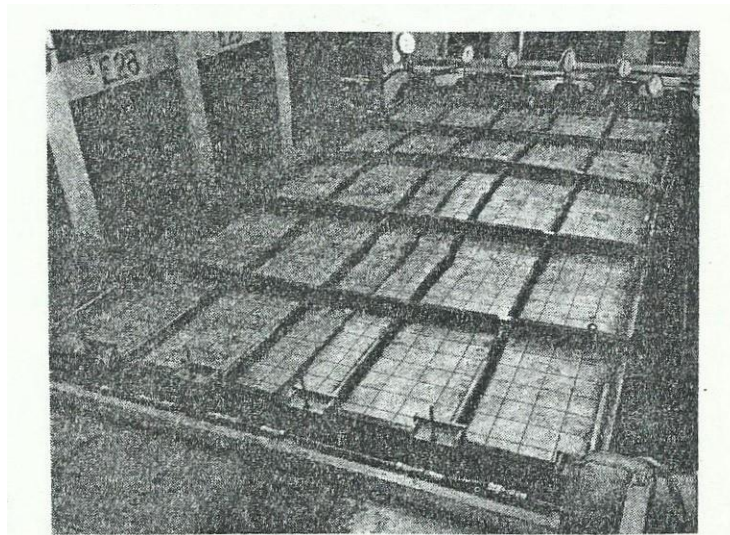


Figure 2.5 Overall buckling.

The local compressive failure mode is generally inter-frame collapse mode; however, the failure mode can be overall buckling mode in the case of a structure which has lightly stiffened panels.

Dow (1997) set up the experiments with different stiffened panels with T-bar stiffeners under in-plane compression loads. The plates were divided into three levels of imperfection: slight, average and severe, under in-plane compression and tension. The levels of imperfections used in the experiment are showed in Table 2.1. This is relevant as the ultimate strength of a longitudinally framed hull is dependent on the size of the stringer.

Figure 2.6 shows the average level of imperfection applied to the experiments. The load shortening curve is first developed to use in the standard design. The load shortening curves are controlled with several plate slenderness (β) and column slenderness ratios (λ) under a stiffened area ratio ($\frac{A_s}{A}$) at 0.2.

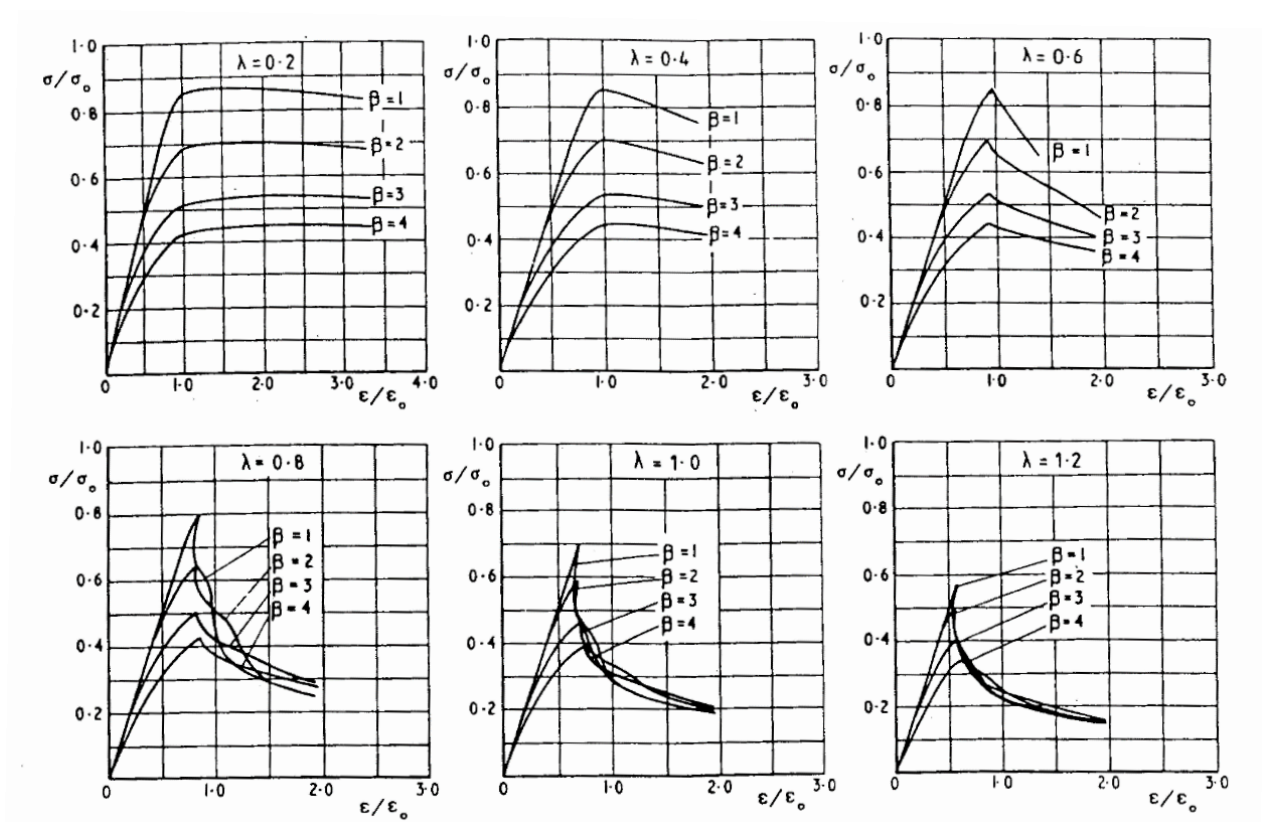


Figure 2.6 Load-shortening curves for stiffened panels with T-bar stiffeners (Stiffened area ratio

$$\frac{A_s}{A} = 0.2 \text{ with average imperfections) (Dow, 1997).}$$

2.4.3 Ultimate strength of hull girder

Studies on the ultimate strength of hull girders have been carried out by researchers such as Dow (1997). This research develops the ultimate limit state design method as a design standard for naval architecture, moreover, the pre-collapse loss from initial imperfection is considered and taken into account in the experiments. This is because the load carry behaviour of the ship's structure is affected by the ultimate strength reduction.

The experiments show an ultimate strength reduction which comes from the initial distortions and residual stresses from welding areas. The pre-collapse strength is formed by the heat effect zone, which presents in Figure 2.7, and introduces imperfections into the structure. The imperfection level is presented in Table 2.1 in section 2.4.4.

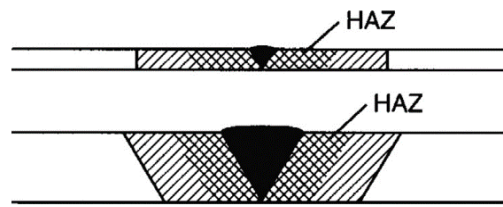


Figure 2.7 Heat effect zone from welding (Benson, 2011).

Dow (1997) recommended that the column slenderness (λ) for stiffened panels in both primary deck and bottom shell structure should be less than 0.45 and never exceed 0.55. Furthermore, plate slenderness (β) should be less than 2.0 and never exceed 2.5. On the other hand, the redundancy and damage tolerance can be improved by using double bottom box girders instead of single box girders.

Recently, ISSC committee III demonstrated eight factors which have an effect on the ultimate strength of the structure (Yoshikawa et al., 2015);

1. Component scantlings (plate thickness, scantling of stiffener, supported span and space of plate and stiffeners, etc.)
2. Material properties (elastic modulus, yield strength, stress-strain curve after yielding, etc.)

3. Initial imperfections (initial distortion and residual stress)
4. Load type (static or dynamic (ratio between duration and natural period of structure), etc.)
5. Additional loads (thermal load, lateral load in hull girder strength, etc.)
6. Age-related deteriorations (corrosion, fatigue cracks)
7. Accidental issues (collision, grounding, and fire)
8. Human factors

This list shows imperfections as one of the effective parameters which influences the ultimate strength. In case of a stiffened panel with an in-plane compression load, the combination of distortions and residual stresses can create a reduction in the ultimate strength of the structure; moreover, strength reduction can be caused by an accidental load such as a collision or grounding.

2.4.4 Initial imperfections

Dow and Smith (1984) divided imperfections into three levels: slight, average and severe, as shown in Table 2.1. These imperfections are a result of fabrication processes together with the consequences of damage such as collisions, grounding, hydrodynamic impacts or weapon effects. The important factors in structural imperfections include initial deformation and residual stresses caused by welding and cold forming. This can affect the pre-collapse loss of stiffness and post collapse load carrying capacity of the structure.

Table 2.1 Assumed imperfection levels

| Level | Initial Deformation $\frac{W_{omax}}{t}$ | Residual stress $\frac{\sigma_{RC}}{\sigma_o}$ |
|---------|--|--|
| Slight | $0.025\beta^2$ | 0.05 |
| Average | $0.1\beta^2$ | 0.15 |
| Severe | $0.3\beta^2$ | 0.3 |

The welding created residual stress areas in both plates and stiffeners due to heat and cooling

effects from the welding process. The residual stress area is estimated based on the stress distribution in Figures 2.8 and 2.9, which present the stress distribution on plates and stiffened panels respectively.

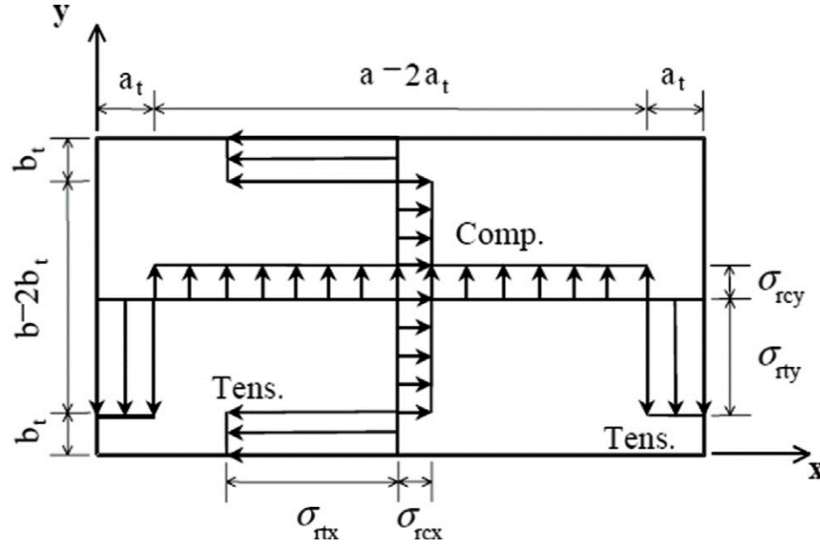


Figure 2.8 Stress distribution from welding in plates (Benson, 2011).

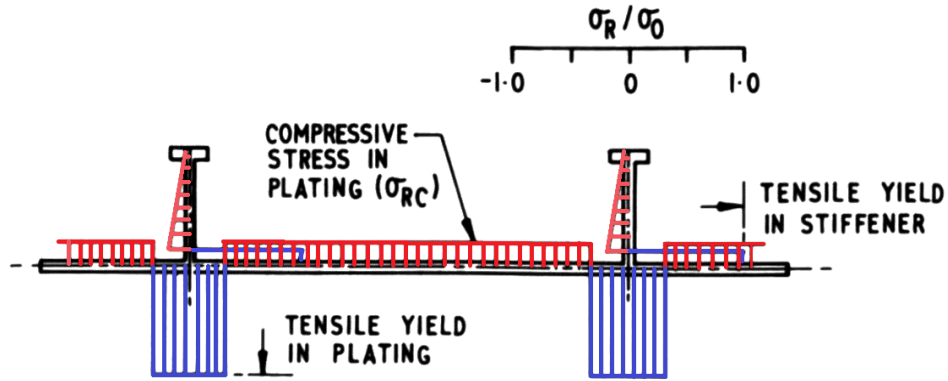


Figure 2.9 Stress distribution from welding in stiffened panels (Dow, 1997).

The welding process also created residual deformation (distortions) in stiffened panels. The distortion is based on the Fourier formula, which is a component of initial half-wavelength:

$$W_0 = \overline{W}_0 \sin \frac{m\pi x}{a} \sin \frac{\pi y}{b}$$

In this research, the Fourier formula is adopted with the combination of five half-wavelengths

and a single half-wavelength, in transverse and longitudinal respectively. The formula of single half-wavelengths is formed as:

$$W_0 = \overline{W}_0 \sin \frac{\pi x}{a} \sin \frac{\pi y}{b}$$

five half-wavelengths is formed as:

$$W_0 = \overline{W}_0 \sin \frac{5\pi x}{a} \sin \frac{\pi y}{b}$$

2.4.5 Rationale

Smith (1988) studied the plate element behaviour with initial imperfections. The distortion and residual stress from welding are applied into the plate. The research was carried out with numerical analysis which was a non-linear finite element method over a range of plate configurations. This valuable research created data for load-shortening behaviour, which can be used for estimating the hull girder strength of the plate. An example of the load shortening curves is presented in Figure 2.10.

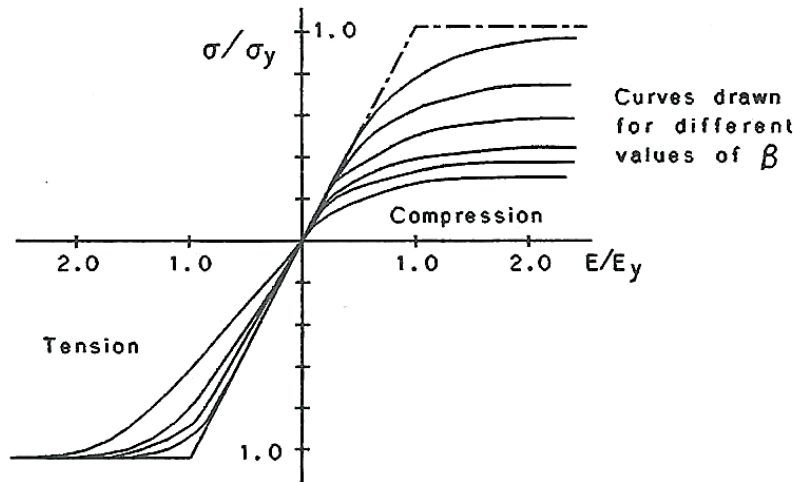


Figure 2.10 Typical Load Shortening curve (Chalmers, 1993).

The design curves are in the form of stress and strain curves in term of elastic-plastic tension and compression. Moreover, The parametric control of geometric and material properties is based on the systematic data set from the UK Admiralty Research Establishment, which is presented in

several sources (Chalmers, 1993). These show a standard load-shortening curve to use in the design process.

The design curve shows the limit state design of the structural elements, divided into three levels as small, average and large imperfection, and represented in Table 2.1 for initial plate displacement (W_0) and compressive residual stress (σ_{RC}), respectively. The column strength curves have been created only with the slenderness area ratio ($\frac{A_s}{A}$) at 0.2.

Smith and Anderson (1991) extended the designing with slenderness area ratio ($\frac{A_s}{A}$) from 0.1 to 0.4 with T-bar and flat-bar stiffeners under in-plane compressive load. The structures were defined with a range of different plate slenderness ratios (β) and column slenderness ratios (λ). The results of this study show that imperfections become more influential for a slender structure that has λ over 0.8.

The average imperfection has been chosen for this research with the level of slenderness area ratio ($\frac{A_s}{A}$) as 0.1, 0.2 and 0.4, as presented in Figures 2.11, 2.12 and 2.13. The full series of the column strength curves is provided in Appendix A.

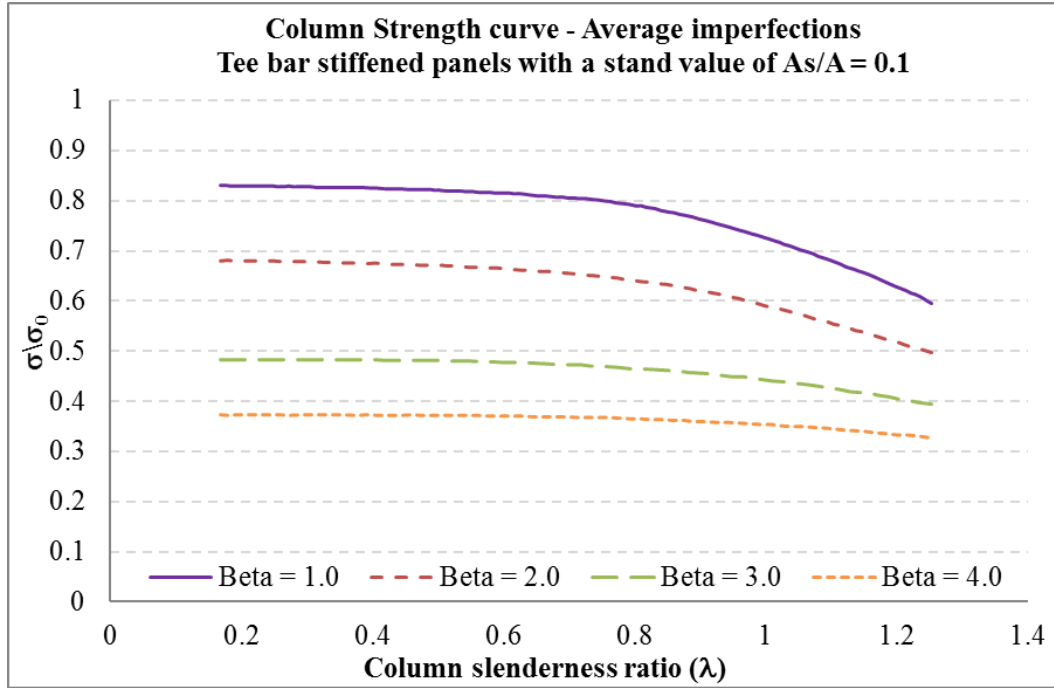


Figure 2.11 Column strength curve – average imperfections with stiffener area ratio $\left(\frac{A_s}{A}\right) = 0.1$ (Smith and Anderson, 1991).

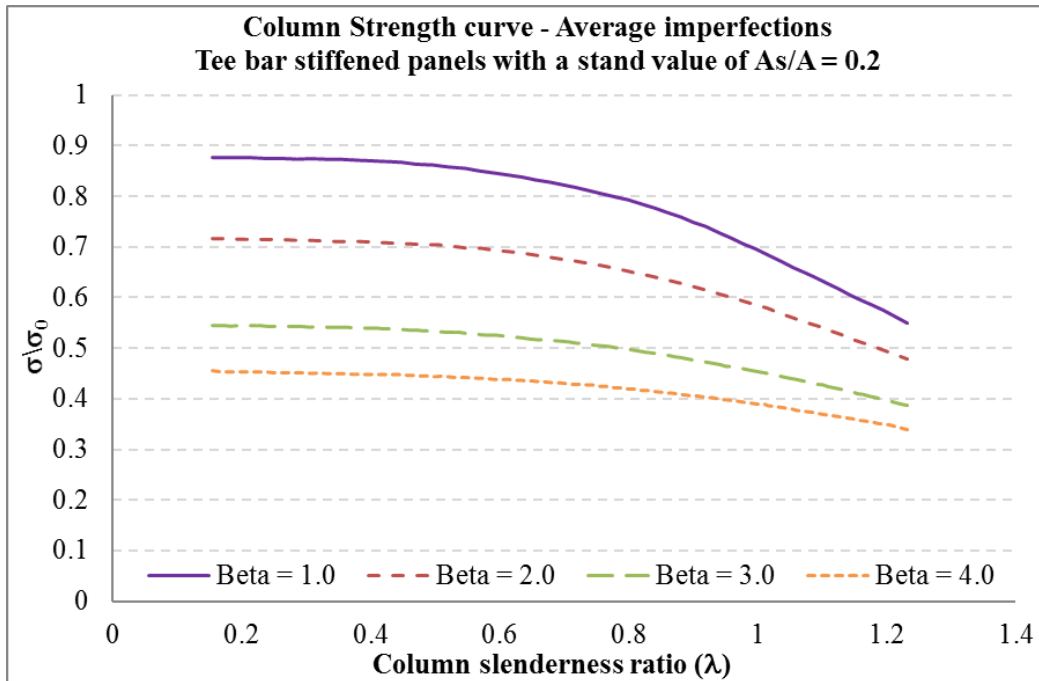


Figure 2.12 Column strength curve – average imperfections with stiffener area ratio $\left(\frac{A_s}{A}\right) = 0.2$

(Smith and Anderson, 1991).

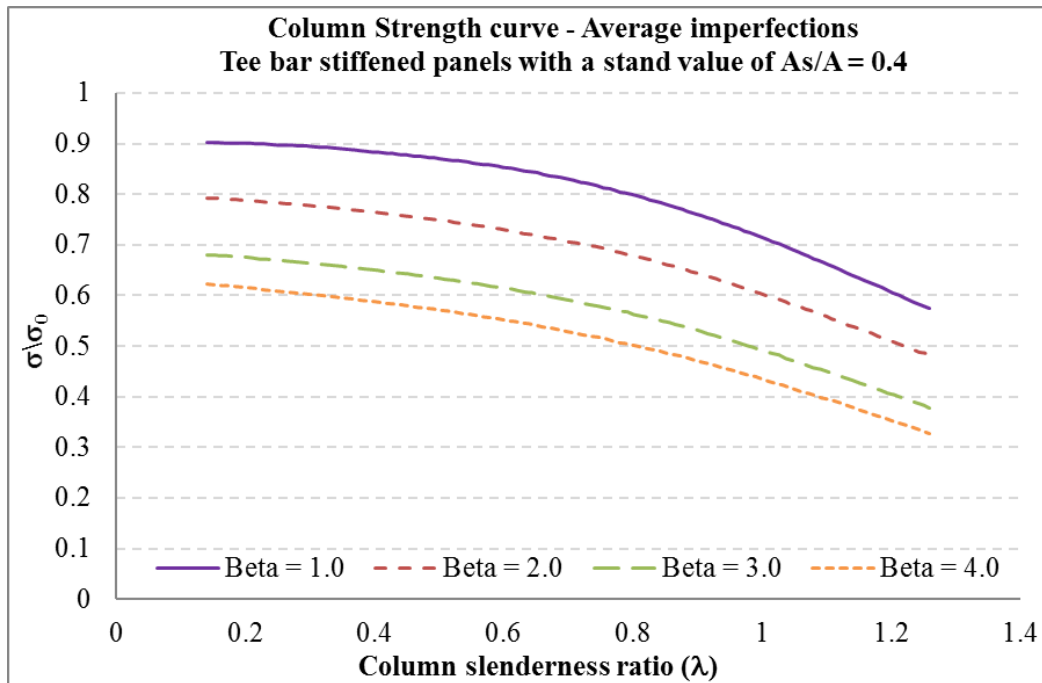


Figure 2.13 Column strength curve – average imperfections with stiffener area ratio $\left(\frac{A_s}{A}\right) = 0.4$ (Smith and Anderson, 1991).

2.5 Strength of accidentally damaged ship structure

The accidental loads in ship design can be describe as (Chalmers, 1993):

- Ship collision and impact
- Ship grounding
- Fire/explosion
- Freak waves

The assessment of residual ultimate strength which comes from damage conditions in ship structures has become more important to the ship industry. The capability of damaged ships can be estimated and predicted by understanding the ship's response to certain types of damage. If damage can be predicted it can be used to design a more damage tolerant structure.

2.5.1 Representation of Damage

Even in an intact state, holes are present in ship structures. Cut outs can be placed in the structure under some considerations, (Chalmers, 1993) which are represented as follows:

- The hole can be located in the low stress area; however, in highly stressed areas, holes should be kept to minimum. The hole can decrease the ability of structure to carry loads and increase the local stress.
- Size and shape of the hole should be considered. Sharp corners should be avoided because of fatigue cracking and the high stress produced.
- The longest dimension of the hole should be in the direction of maximum stress.
- Necessary reinforcement is provided to prevent further damage.

However, an unpredictable accident can occur on ships and create a large opening area which decreases the ultimate strength of the hull girder, and at the worst this can cause the loss of the ship. To prevent major damage in the shipping industry, an assessment of residual stress which occurs after an accident is a key parameter for improvements in design and repairs for ships. For four decades, the ultimate strength of hull girders under damaged conditions has been the subject of major studies.

The realistic damage mechanism is a complex process to represent in the analysis; however, the simple cut out area is another option to use in order to re-create a damaged area. Several researchers have been representing the shape of this cut out differently. The recommendation in design of ships' structure (Chalmers, 1993) suggests that it should be a circular or elliptical hole, which should be as close to the natural axis as possible, due to the ideal stress flow and easier analysis.

Underwood (2012) assumed the shape of the damaged area, which is located in the centre of the panel, to take rectangular, elliptical or triangular form. The cut out took place in both unstiffened and stiffened panels to investigate the ultimate strength and develop the Idealised Structural Unit Method (ISUM) which is similar to the progressive collapse method (Smith method).

These investigations explored the influence of a damage-hole on the ultimate collapse strength of steel grillage arrangements by using finite element analysis, controlling the size and dimensions

of damage, which are represented by the hole in the structure. The investigation was carried on with commercial finite element software ANSYS. The model was created with four-noded quadrilateral isoparametric linear shell elements (SHELL181) with simply supported boundary conditions along the loaded and reactive edges. The results of Underwood's work show that damage aperture may influence the type of collapse depending on the slenderness of the plate. The need to assess both inter-frame and overall collapse modes is pointed out to ensure a good prediction of the ultimate strength of a damaged structure.

Case studies for this research have been divided into three cases: intact stiffened panels, damaged stiffened panels where damage was located only in the plate itself with the position of centre halfway between two stiffeners (as shown in Figure 2.14 Left), and damaged stiffened panels with the damage location resulting in the loss of a single stiffener through its position at the centre of the damage (as shown in Figure 2.14 Right).

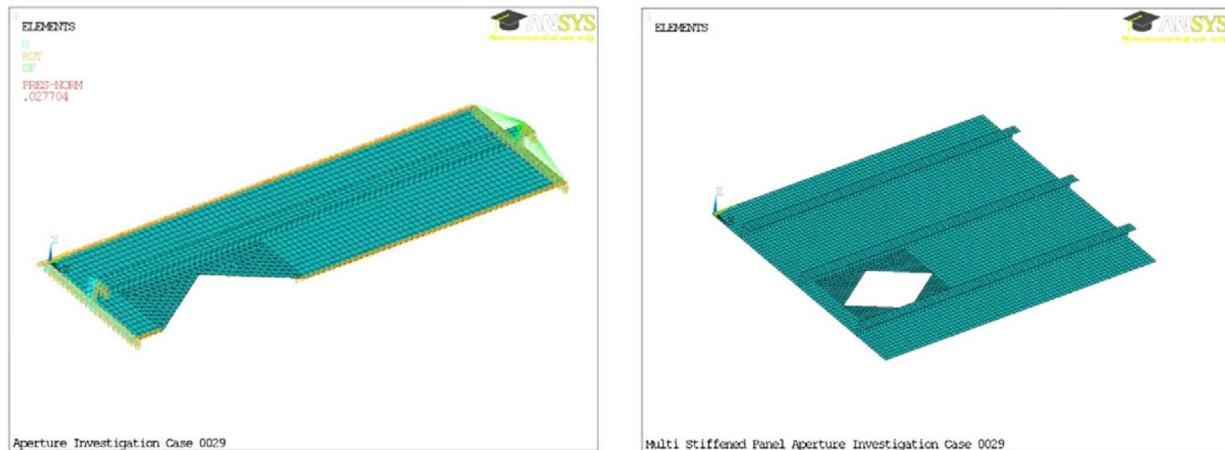


Figure 2.14 Examples of damage case studies Left: damaged singular stiffened, Right: damage in line with the central stiffener of the panel (Underwood et al., 2012).

The results show that the ratio of the damaged area to the overall plate increases as the failure load of the panel reduces; moreover, the shape of the damage has minimal effect on the ultimate strength of the stiffened panel.

Other studies have been carried out by Yu and Lee (2012), Lee (2012), Yu et al. (2015). This research focusses on the opening area in rectangular openings in different dimension of unstiffened panel by using non-linear finite element analysis approaches.

Yu and Lee (2012), Lee (2012) studies focus on a rectangular opening area in the unstiffened plates, because opening areas in ship and offshore are generally located in the plate for piping, ducts and maintenance. Numerical models were set up in two cases with the aim to investigate an effect of the opening area, as shown in Figure 2.15.

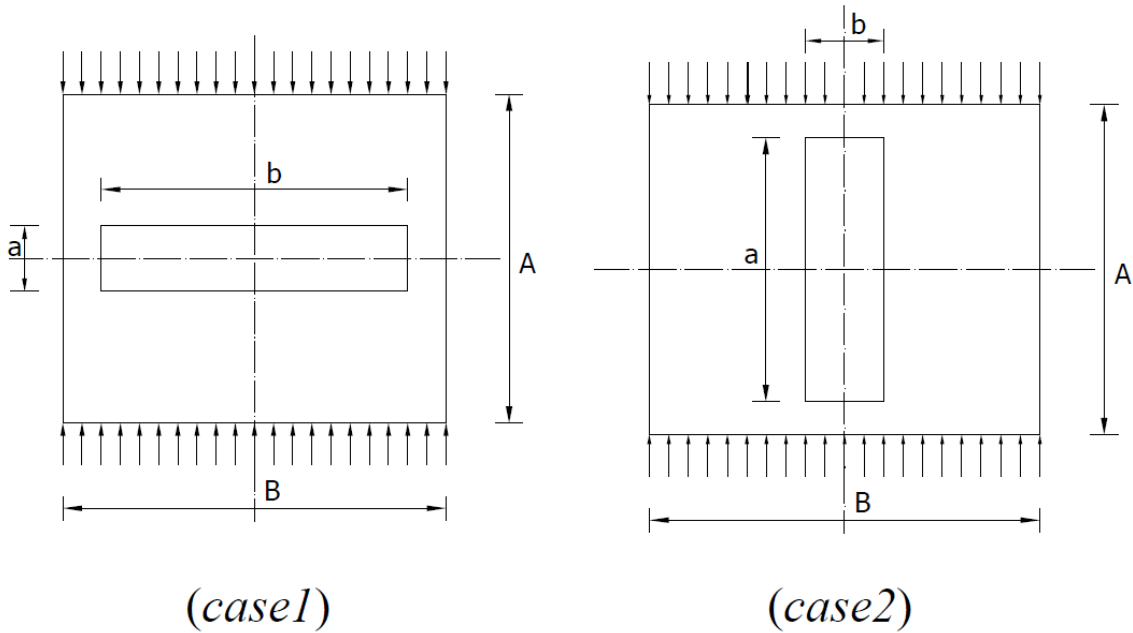


Figure 2.15 Rectangular opening in unstiffened plate (Yu and Lee, 2012).

The investigation was carried out with an elastic-plastic material using the ABAQUS static-Riks solver. The results show that the ultimate strength of the model is influenced by plate slenderness (β) and the loss of cross section area, which is considered in the same direction with longitudinal axial compression.

The investigation has been carried out with stiffened panel type 1 and type 2 in Figure 2.16 (Yu et al., 2015). The rectangular opening is controlled by variables of the width or the length of opening area which are applied on panel type 1 and type 2 respectively. The ultimate strength of the stiffened panels is set up with combined loads, which are axial compression and constant lateral load; moreover, initial imperfections are applied at the beginning of the analysis.

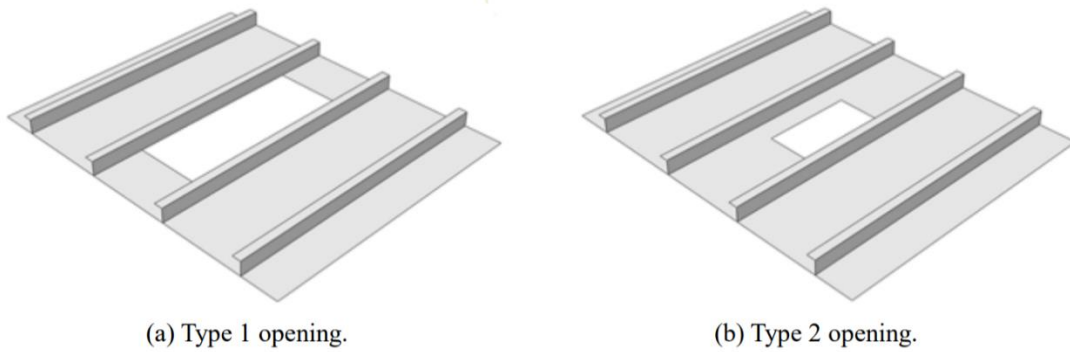


Figure 2.16 Opening cases in stiffened panels (Yu et al., 2015).

The results show that the ultimate strength of stiffened panels can be affected by the width of the opening area more than the length of it.

Those three studies demonstrate agreement that the opening areas in unstiffened panels show the behaviour of ultimate strength reduction when a cross sectional area of panel has been reduced by the cut-out area; moreover, the ultimate strength is influenced by plate slenderness (β).

The literature on the opening areas in unstiffened and stiffened panels shows the relationship between the ultimate strength of the structure and the opening area, under the control of the plate slenderness (β). This conclusion shows a good agreement with research presented in this thesis on damage represented by clear-cut holes in the stiffened panel under in-plane compression loads (Benson et al., 2013e, Leelachai A et al., 2015).

2.5.2 Realistic damage mechanism

Several researchers have used realistic damage mechanism in order to improve understanding of the behaviour of damaged ship structures. Collision and grounding are two major accidental topics at the moment. The studies have carried out both experiments and numerical analyses.

In 2013, AbuBakar and Dow compared experimental data of a stiffened panel rupture with numerical simulation using finite element analysis with ABAQUS. The comparison aimed to demonstrate the capabilities of the finite element method. The simulations were set up with an explicit analysis. The forming limit diagram (FLD) was used as a material failure mode. The

comparison was divided into two groups: penetration with indenter on stiffened panels and grounding damage of double bottom structures.

Figure 2.17 shows the first group of comparison with three different sets of stiffened panels. The indenter was penetrated on a flat panel, on the stiffener of a single stiffened panel, or between stiffeners of a stiffened panel in (a), (b) and (c) respectively. Several sizes of meshes were adopted in the simulation in order to investigate an appropriate mesh size which can be used for optimisation of accuracy, computer resources and computational time.

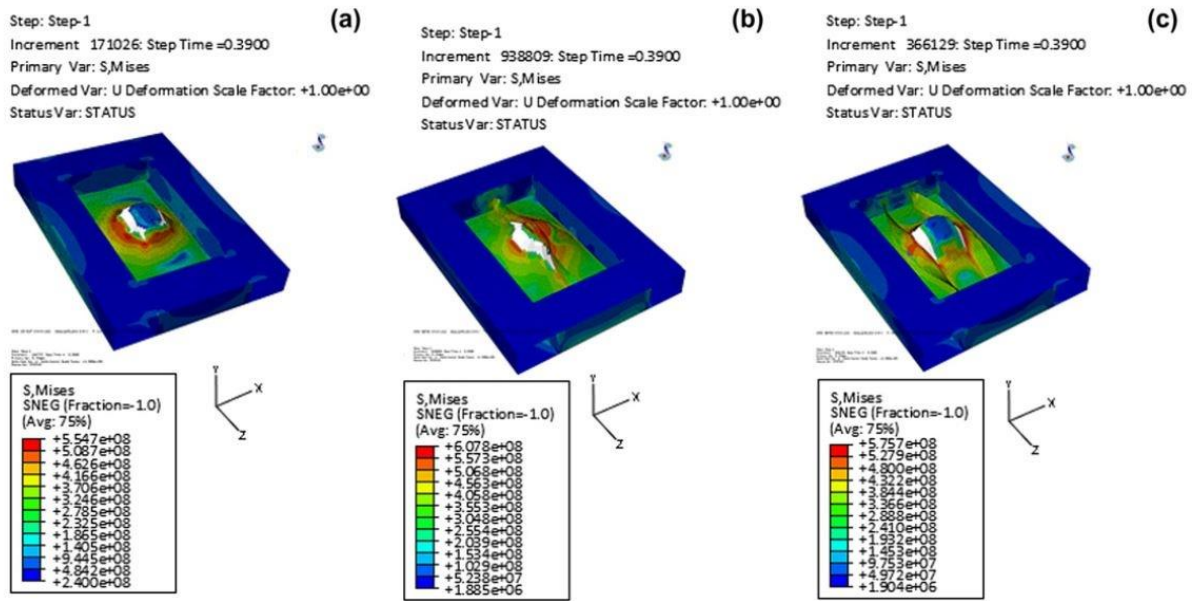


Figure 2.17 Resistance of stiffened panels to penetration damage (AbuBakar and Dow, 2013).

The results show that fine meshes, of 15 mm, gave the best comparison results for the forming limit diagram (FLD), moreover, fine meshes generated more realistic and more accurate results than the larger mesh size. This is because fine meshes represent a better stress concentration and a better prediction of strain in the element.

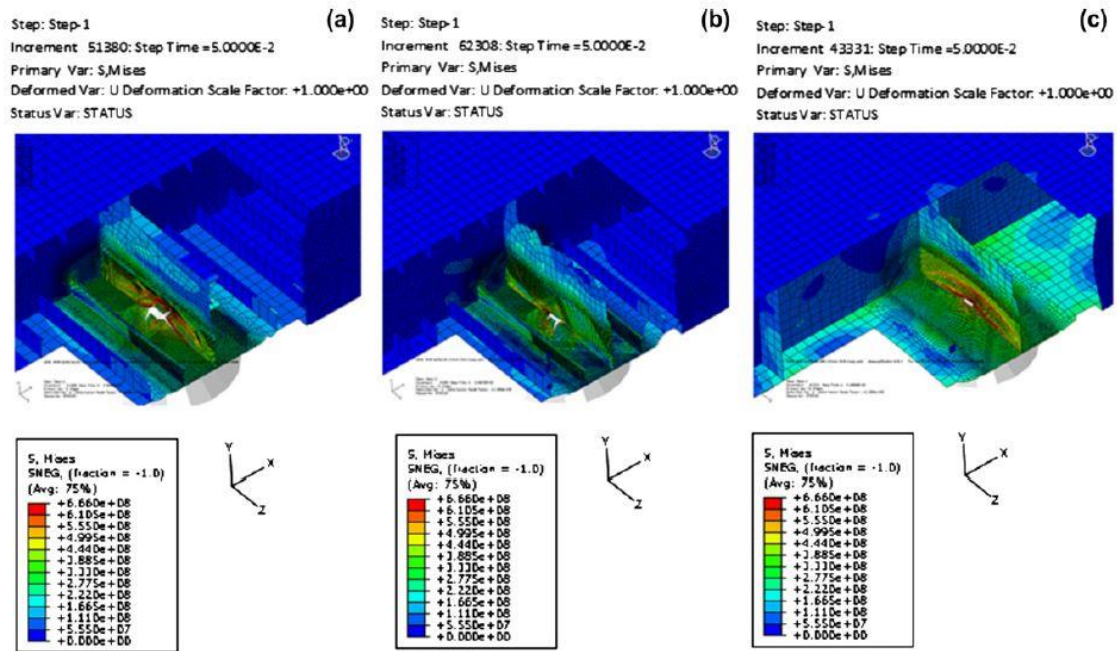


Figure 2.18 Vertical grounding displacement on the main floor of models (AbuBakar and Dow, 2013).

The second group in the comparison was the grounding effect on double bottom structure. The simulations were set up with three different sets of the models, which were double bottom with all longitudinal stiffeners (Model A), all longitudinal stiffeners except stiffeners on longitudinal floors (Model B) and no longitudinal stiffeners (Model C). The grounding effect was located at the main transverse frames and in between the main transverse frames. Figure 2.18 shows the first effect, located at the main transverse frame. Further information is in AbuBakar and Dow (2013).

The second group of results demonstrated the ability of a double bottom hull girder to withstand rupture from grounding. Flexibility of hull girders can increase the resistance of a ship's hull to rupture effects. From both groups of studies, finite element analysis is an appropriate approach to use to investigate the behaviour of ship structures during an accident; moreover, the material rupture effect is excellently predicted using finite element software.

Benson et al. (2013b) studied the girder with ruptured penetrations simulated using a large indenter to represent damage, which represented the significance of the residual stress sustained

in the damage simulation. The study used the finite element method in both static and dynamic analysis with ABAQUS. The static implicit analysis adopted the Riks arc length method or modified Newton-Raphson method. In the other hand, dynamic explicit analysis was used for analysis of impact damage and rupture with slow time steps.

Table 2.2 Box girder properties (Benson et al., 2013b).

| Specimen Length (mm) | Frame Spacing (mm) | Plate Thickness (mm) | Stiffener Height (mm) | Stiffener Thickness (mm) |
|-------------------------|-----------------------|-------------------------|--------------------------|-----------------------------|
| 1000 | 200 | 4 | 20 | 4 |

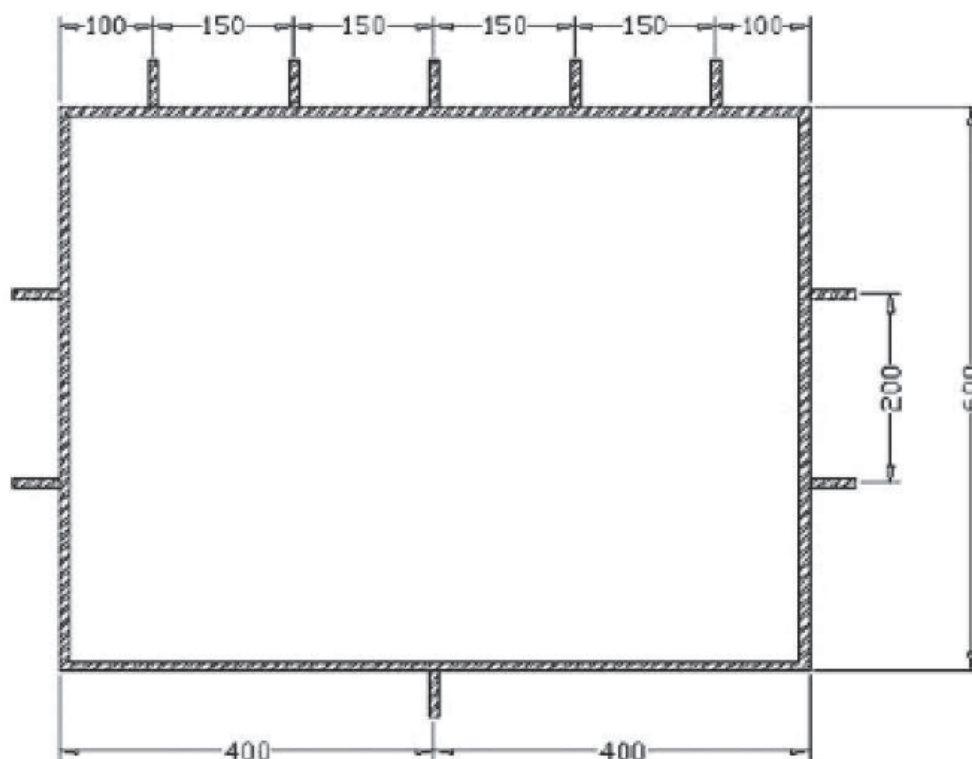


Figure 2.19 Box girder cross section (Benson et al., 2013b).

Table 2.2 and Figure 2.19 show the box girder details and cross section area. High tensile steel grade (S690) was adopted with yield strength at 690 MPa and Young's modulus at 200 GPa. The

material failure was based on the forming limit diagram method (FLD).

The damage mechanism was represented by using an indenter, which is a rigid body cylinder with half of sphere tip, as shown in Figure 2.20. The analysis was set up with three case studies: implicit analysis without residual stress from a damaged area, then explicit analysis with and without residual stress from damage.

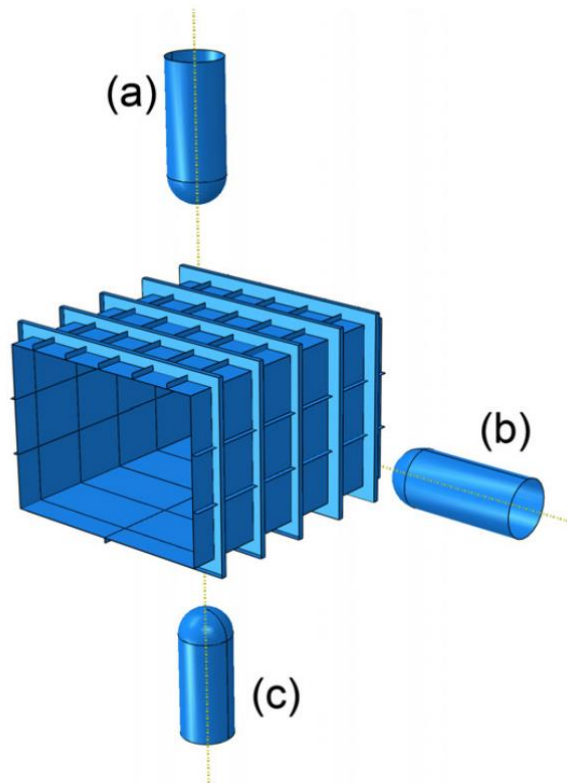


Figure 2.20 Penetration damage with indenter (Benson et al., 2013b).

The results show a major impact of the residual stress from damage area on the ultimate strength of box girders. The residual stress can affect the tensile zone, which is close to the rupture region, by increasing strength up to 10%.

The extent of the study was expanded on by Benson et al. (2013a). A similar set of box girders were used and compared using different methods. The experiments were first set up to compare the ultimate strength of the box girder with and without residual stresses by using dynamic

explicit, implicit and static analysis. The numerical experiments show that the static finite element analysis has the same rupture geometry as both forms of dynamic analysis; however, the residual stress from penetration cannot be taken into account due to the complexity of the analysis procedure. On the other hand, the static method brings a benefit to the analysis since it can reduce the simulation time, while neglecting damping effects and kinetic energy in the model.

The results of the box girder tests were compared with the simplified progressive collapse method presented in section 2.7 (Benson, 2011). Figure 2.21 shows the cross section of a damaged box girder which was used in the simplified progressive collapse analysis. The comparison shows a good correlation of results, and indicates that the simplified progressive collapse method can be used instead of the computationally expensive finite element program.

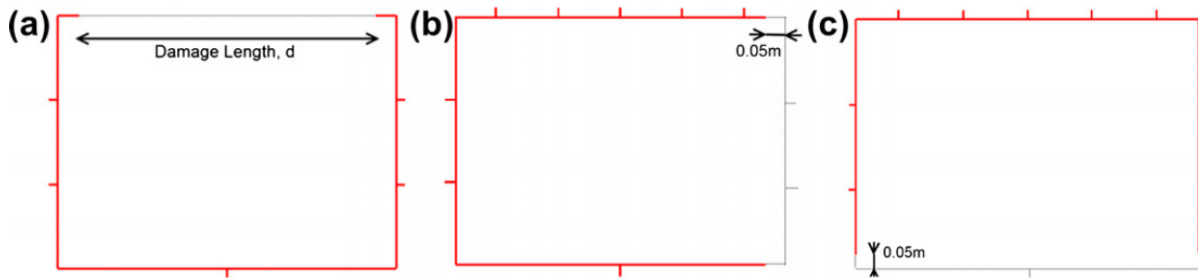


Figure 2.21 Simplified progressive collapse method with damage model. (a) top damage. (b) side damage and (c) bottom damage (Benson et al., 2013a).

Based on the literature review, the damage mechanisms used in this research are divided into two categories, which are damage represented by a circular clear-cut out and damage represented by penetration with an indenter. Both groups of damage take place in the middle of the stiffened panel. The damage scenarios are considered appropriate to represent realistic damage mechanisms. The nonlinear finite element method is used to find the ultimate strength of the damaged stiffened panels. This is applied with appropriate boundary conditions and in-plane compression load. The simplified progressive collapse method (Benson, 2011) is then modified in order to include the damaged effect in the calculation.

2.6 Factors in finite element analysis

2.6.1 Mesh

The fundamentals of finite element method is using a matrix frame analysis, in which each structural element can be represented as an interconnection with a number of nodes used for calculating equilibrium in the structure. These nodes, moreover, can represent the stress concentration and other elements. The accuracy of the finite element analysis will depend on the number of elements used in the simulation and the type of element. This number can be shown as an element size or mesh size, which is one of the important factors for the analysis in this research. Increasing the number of elements will increase the computation time, therefore increasing the cost of the process. The appropriate size of mesh can give the appropriate results within an acceptable time. Benson et al. (2013a) compared different sizes of mesh, as presented in Table 2.3.

Table 2.3 Comparison between different mesh sizes and time consumed in the analysis (Benson et al., 2013a).

| Mesh size (mm.) | Number of elements | CPU time^a (s) | Time penalty (compared to 20 mm mesh model) |
|----------------------------|---------------------------|---------------------------------|--|
| 50 | 2929 | 160 | 0.2 x |
| 20 | 10,547 | 710 | - |
| 10 | 42,017 | 3,774 | 5.3 x |
| 5 | 166,130 | 28,800 | 40.5 x |

^a Using a single processor on an Intel Core i7-2600@ 3.40 GHz with 16 GB Ram.

Different sizes of mesh are used in the investigation. The experiment shows that an accurate result is generated by fine meshes such as a mesh size of 5 mm. However, the comparison shows

the close results between mesh sizes at 20 mm and 5 mm. To reduce the simulation time, the 20mm mesh size can be used instead of the finer mesh size.

2.7 Software development.

Numerical software which is used in the structure design has been developed over four decades. For examples, Dow and Smith (1986) developed FABSTRAN, which is used in the area of elasto- plastic behaviour in frames and beam-columns under static and dynamic loading, to calculate the load shortening curve, as shown in Smith (1977, 1988).

Bole (2007) considered damage in the ship's structure. Bole's case study was *HMS Nottingham*, shown in Figure 2.22. An accident occurred in a way which shows potential problems of communication between crews and the support team, affecting the amount of time for crews and support teams to make a decision and come to help before the loss of the ship. The possibility of ship failure was considered necessary for the improvement of the software.



Figure 2.22 Raking damage of *HMS Nottingham* on ship hull (Bole, 2007).

Bole (2007) introduced a tool called 'The Seagoing Paramarine' to help crews in decision-making in an emergency situation. The software has the ability to check the stability of the ship, including damage stability such as grounding and fatigue failure. The software is installed on board and aims to be of benefit to both crews and to a support team onshore who have the experience and regularly train for emergency situations.

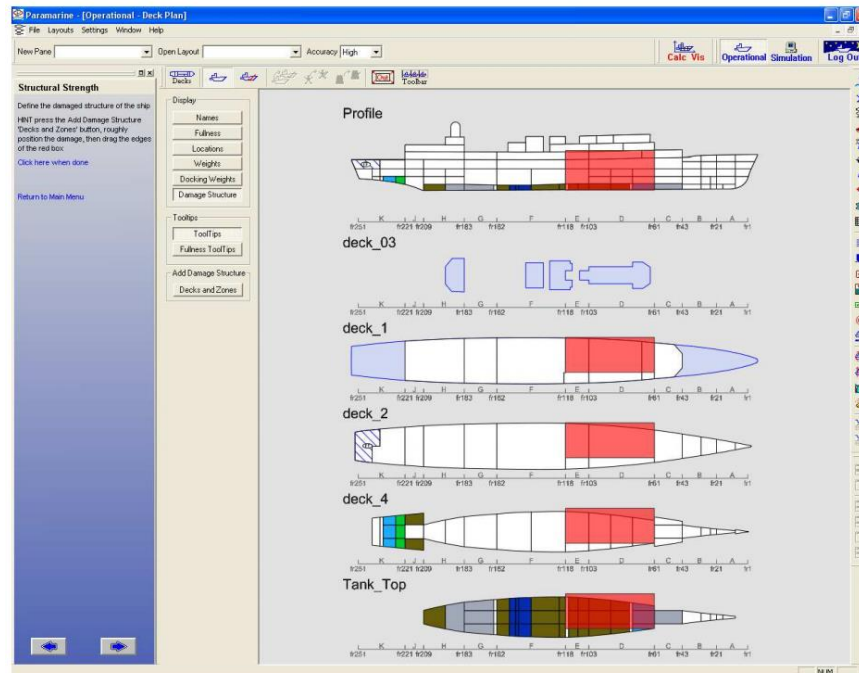


Figure 2.23 The Seagoing Paramarine program (Bole, 2007).

Figure 2.23 demonstrates an overview of the Seagoing Paramarine which can respond to the emergency situation. The red area in the figure shows the response of the damaged area in the program.

Lee et al. (2013) suggest that time is one of the most important factors which needs to be considered. Captains and crew members must understand their situation based on the basic information at hand. This information will help them to understand the situation in a clearer way, letting them communicate more straightforwardly with the assisting team onshore. Moreover, having ultimate limit strength information for a ship's structure will help crews and support teams to make the right decision in a short period of time. Ultimate limit strength helps engineers to predict the behaviour of a damaged ship structure and allows crews on board to make a quick decision regarding whether to attempt maintenance or move the damage ship structure to a closed port for repair.

Even with the software was installed into a ship's structure, some accidental damage will still happen. For that reason, several major research projects have investigated different damage

mechanisms in ship structures. The understanding of damage behaviour has resulted in incredible tools for preventing and controlling the effects of damage to a ship's structure.

Some researchers explore the effect from the different angle of ship collisions which can create different damage mechanisms in the ship's structure (AbuBakar et al., 2010). In some cases full-scale simulations of marine accidents have been used to investigate the cause of the actual accident by using highly advanced modelling and simulation (M&S) (Lee et al., 2013, Lee et al., 2017).

This research will set up the groups of damage scenarios with a range of stiffened panels, to generate accurate data with the finite element method under static and dynamic analysis, with the ABAQUS program used to generate the stress and strain curve. The behaviour of the damaged stiffened panels will be more understandable. Advanced analytical techniques to determine longitudinal ultimate strength, such as the progressive collapse method (Smith, 1977) are adopted to recalculate the ultimate strength of a damaged hull girder (Dow, 1997).

Since 2011, an extension of the simplified method has been developed (Benson, 2011, Benson et al., 2013c, Benson et al., 2015). The method is explained with a load shortening curve which represents the behaviour of a grillage panel and can show both inter-frame and overall collapse in the structure; after this the ultimate strength of hull girder is calculated with the progressive collapse method.

The extension method is adapted to a large deflection orthotropic plate method, with the capability to predict gross buckling of stiffened panels over multiple frame spaces (Benson et al., 2013b). The method is used in predicting compartment level collapse modes of lightweight hull girders.

The simplified progressive collapse method is represented in the ProColl program, which has the ability to predict hull girders' ultimate strength, including both inter-frame and overall grillage collapse. Figure 2.24 explains the process of analysis in ProColl. In the beginning, the hull girder is divided into small elements such as plates and stiffeners. The load shortening curves are calculated for each element before the load shortening curves are summarised for each panel. At this moment, each element of the orthotropic plate is calculated to generate another set of load

shortening curves. Finally, all the load shortening curves are added up to the final load shortening curve, which shows the strength of the ship's hull.

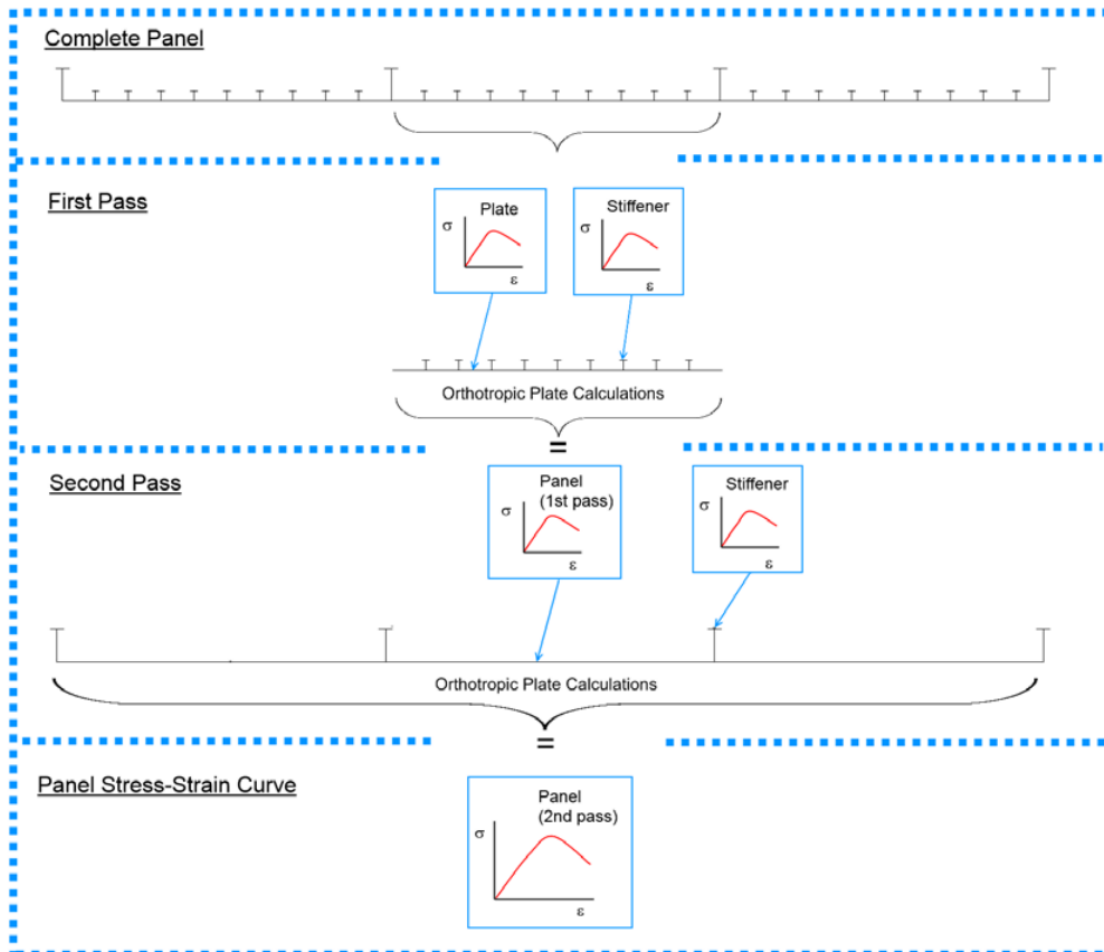


Figure 2.24 Irregular panel calculation flow diagram (Benson et al., 2015).

ProColl gives accurate results compared to finite element analysis (Benson et al., 2013a). The finite element analysis is a time-consuming process, especially in dynamic analysis. ProColl is thus one of the better options to use in order to reduce time in analysis with accurate results.

This research aims to use an understanding of the damaged structures to modify the simplified progressive collapse method to include damage effects in the calculation. The new, modified version of ProColl will help to reduce the amount of time in the analysis process and generate an accurate result which includes the damage effect area.

2.8 Summary

The literature review shows relevant research which has been taken into account in this study. Based on the literature, the research will proceed in a way where the ultimate limit state is represented by the strength of the structure in both stiffened panels and box girder with the use of the finite element method.

To generate the damage effect in the stiffened panel, the literatures shows a few different type of damage areas such as damage represented by clear-cut out area or realistic damage mechanism, which is close to collision and grounding effects. In this study, the different behaviours of damage effects are considered by comparing the clear-cut out damage to penetration with an indenter. In addition, the damage scenario is aimed to investigate the effect of stiffeners which is remove by the damaged area to the panel strength.

The ultimate strength of the damage stiffened panel is used in order to extend the simplified progressive method to include damage effects at the end of the research.

Chapter 3 Material and Structural Properties.

3.1 Introduction

The strength of a ship's structure comes from a combination of members with complex states of stress. An understanding of the material properties involved is important to provide a representative structural behaviour and stress limit, which are used in the designing process. Material properties in this study are chosen to be typical of a large merchant or naval ship. The panels are flat and regularly stiffened.

A representative set of stiffened panels are used to complete the computational analyses in this research. The panel model extends over ten longitudinal stiffeners and four transverse frame spaces. The longitudinal stiffeners are composed of T-bar. The transverse frames of the panel are flat bar and divide the stiffened panel into five bays; this transverse frame is vital to control buckling behaviour to make it either an inter-frame or overall collapse mode in this study. The boundary conditions are chosen to reasonably represent the influence of adjacent structures. The geometric dimensions are adjusted parametrically to give a range of panels with controlled values of:

- Plate slenderness ratio (β)
- Column slenderness ratio (λ)
- Stiffened area ratio ($\frac{A_s}{A}$)

The simulation has been carried out with non-linear finite analysis using the program ABAQUS. The design process is demonstrated for both intact and damaged stiffened panel models.

3.2 Material Properties

Steel is the dominant material used for ship structures. Choices of steel grade depend on the reliability of the structure, as well as optimisation for the designer and ship owner in terms of cost, time and maintenance. In this research, mild steel is chosen, because of its main characteristics as a ductile material and as it has a resistance to cracks. Advantages and disadvantages of steel are summarised in Table 3.1.

Table 3.1 Advantages and disadvantages of steel (Chalmers, 1993).

| Advantage | Disadvantages |
|---|-----------------------------|
| Normally Ductile | Corrodes readily |
| Virtually isotropic | Has no lower fatigue limit |
| Easily formed and fabricated | Heavy |
| Plentiful | Brittle at low temperatures |
| Easily alloyed or heat treated for special properties | (Magnetic) |
| Easily repaired | |

3.2.1 Material Characteristics

In 1678, Robert Hooke discovered the relationship between load and extension in materials, which is presented in Figure 3.1. This stress-strain curve represents the capacity of a material to withstanding tensile loads before collapsing. The proportional limit takes place in the beginning of the curve, which can be explained by Hooke's law that materials have an ability to return to their original shape when unloaded until exposed to yield stress. The plasticity zone occurs beyond the yield point with no change of shape back to the original shape. Material strain-hardening occurs in the plastic zone. The stress of material then becomes larger and eventually reaches ultimate stress which represents the beginning of the necking zone and fracture or collapse (Carl T. F. Ross et al., 1999).

This methodology is universally used to characterise the properties of ductile materials, such as steel and aluminium.

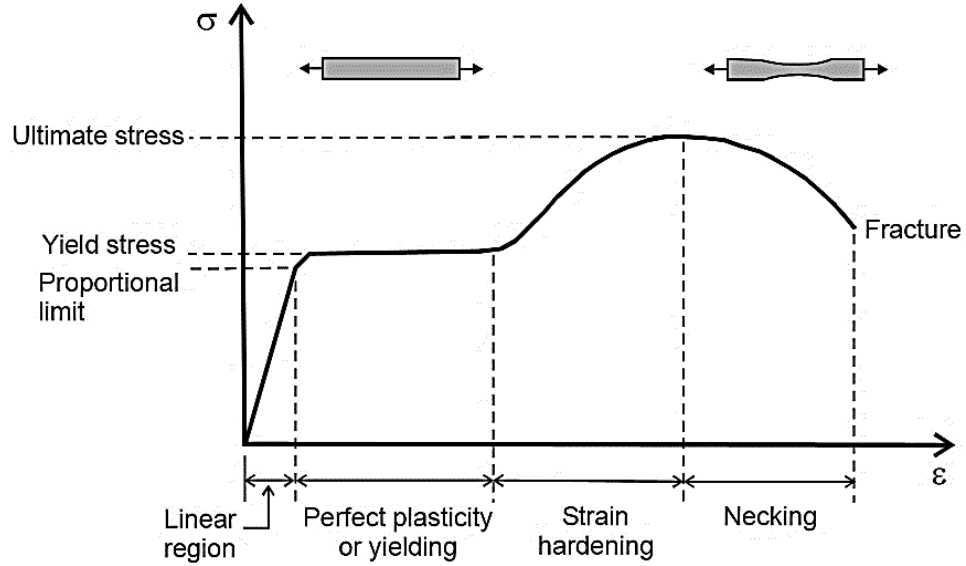


Figure 3.1 Engineering Stress – Strain curve.

In this research, the plasticity is considered, because plastic theory can represent more realistic load-carrying behaviour in materials. Moreover, stiffened panels with damage effects are applied with appropriate elastic-plastic material to make sure that the structures have a realistic response. Figure 3.2 is a group of four different, idealised stress-strain curves which are applied to the analysis. The elastic–perfectly plastic model eliminates the work of hardening and assumes perfectly plastic performance after the yield point (Figure 3.2 (a)). To include the work of hardening into the curve, Figure 3.2 (b) shows the strain hardening with the slope of the tangent modulus (E_t) after the yield point. The relationship of the stress-strain curve in Figure 3.2 (b) can be represented as

$$\varepsilon = \frac{\sigma}{E}$$

$$\varepsilon = \frac{\sigma_0}{E} + \frac{1}{E_t} (\sigma - \sigma_0)$$

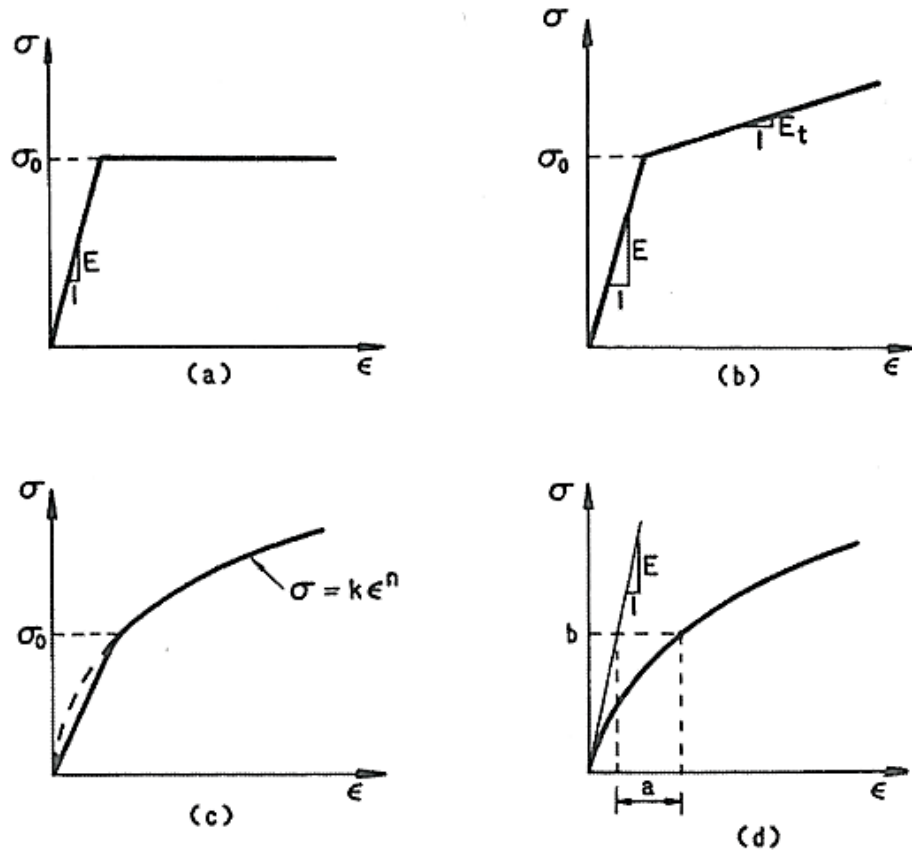


Figure 3.2 Idealised stress-strain curves (Chen and Han, 1988).

Figures 3.2 (c) and (d) which are more suitable for true stress-strain curves, are the demonstrated elastic-exponential hardening model and Ramberg-Osgood model respectively. The true stress-strain curve is used to represent the plastic performance of a material which includes damage responses after the necking point.

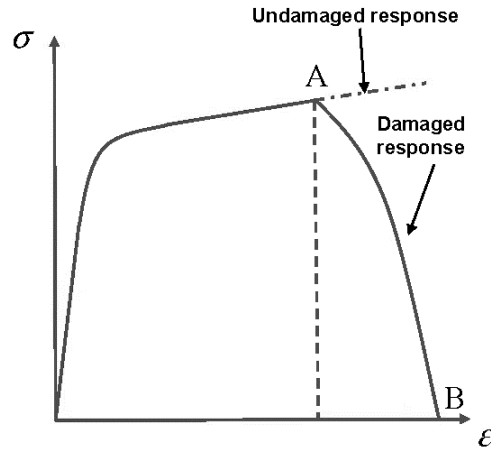


Figure 3.3 Typical material response showing progressive damage (ABAQUS 6.13, Systèmes (2013)).

Typical damaged responses of material can be demonstrated in terms of the true stress-strain curve in Figure 3.3. Point A represents the maximum load capacity a material can resist, and is called ultimate stress. From point A, the softening of material occurs and shows the beginning of the necking region, before rupture at point B.

A simple understanding of damage response (Figure 3.3) can apply to other structures such as plates, stiffened panels or other types of structure, and shows the ability of the structure to withstand load before rupture. AbuBakar and Dow (2013) studied resistance in stiffened panels under collision and grounding by using the same damage response curve (Figure 3.3). A comparison of difference methods, which have ability to predict damage in the ship structure, such as the forming limit diagram (FLD), the Rice-Tracey and Cockcroft-Latham (RTCL) and the Bressan, Williams and Hill (BWH), was set up to investigate their capabilities in the finite element program.

In this study the material was assumed to be elastic-plastic with isotropic hardening, made from mild steel. The forming limit diagram was used in the numerical simulations to investigate the resistance of stiffened panels after penetration. Several conditions of stiffened panels have been set up and demonstrated in Figures 3.4 (a), (b) and (c). These represent penetration on flat plate, on the stiffener or in between stiffeners respectively.

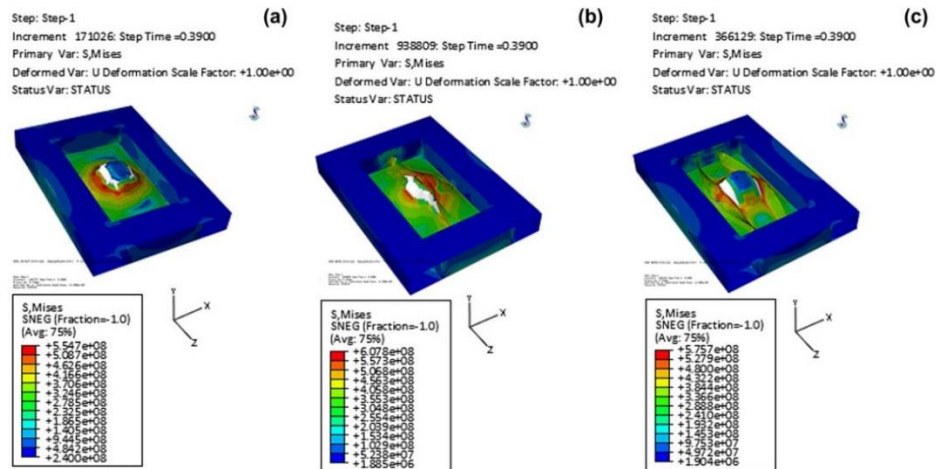


Figure 3.4 Resistance simulation on stiffened panel under penetration damage (AbuBakar and Dow, 2013).

The comparison between other methods and numerical simulations shows good agreement, although the results depend on the type of element and size of mesh, which should be an appropriate size to represent acceptable stress concentration and predict onset failure in the structure.

The simulation has been carried out with a double bottom structure to find the resistance for grounding effects under two conditions, for example, the ability of a rigid and flexible structure to withstand damage, and the abilities of fully plastic materials to do this with and without material failure. The flexible structure shows a higher ability of the structure to withstand force and displacement than rigid structures. In addition, the material failure in the fully plastic structure is an important factor to consider, because the difference in resistance to damage between with and without failure mode tests can be around 15 to 50 per cent. The structure without failure mode can continue to absorb more force than the failed structure.

This demonstrates important factors, which play a significant role in the serviceability of the ship, such as, element type, appropriate size of mesh, the plasticity of material and material failure.

This research focusses on the ultimate strength of the structure, which represents the ability of the structure to survive loads, and a principal consideration for ship structures. Stiffened panels are assumed to be mild steel material which have an elastic-plastic and isotropic behaviour. The failure mode is included and can be simulated from the forming limit diagram (FLD) in finite element analysis. The von Mises plastic deformation is used to represent local failure in the panels. The load shortening curve is provided from the numerical analysis, while the average level of design curve from section 2.4.5 is used in comparison with both damaged and undamaged stiffened panels

3.3 Panel Geometries

In this study, a stiffened panel is assumed to be made from mild steel which has ten T-bar longitudinal stiffeners with five bays. This significant size of the models has been selected to support a large scale of damage. Moreover, the odd number of the spacing in the stiffened panel is used to control the damage which takes place in the middle of the panel. The bays are separated with four flat-bar transverse frames. The intact panels are controlled by several parameters such as the plate's slenderness ratio (β), the column slenderness ratio (λ) and the stiffener area ratio ($\frac{A_s}{A}$). The models are set-up with plate slenderness ratio (β) values from 1.0 to 4.0, column slenderness ratio (λ) values in between 0.2 and 1.0 and stiffener area ratio ($\frac{A_s}{A}$) values from 0.1 to 0.4, as presented in Table 3.2.

Table 3.2 Scope of analysis in intact stiffened panels.

| Parameter | Intact |
|--|-----------------------------|
| <u><i>Material Properties</i></u> | |
| Yield stress (σ_y) | 245 MPa. |
| Young's modulus (E) | 207 GPa. |
| Poisson's ratio (ν) | 0.3 |
| <u><i>Structure Parameters</i></u> | |
| Plate slenderness ratio (β) | $1 \leq \beta \leq 4$ |
| Column slenderness ratio (λ) | $0.2 \leq \lambda \leq 1.0$ |

| | |
|--|-----------------------------------|
| Stiffener area ratio ($\frac{A_s}{A}$) | $0.1 \leq \frac{A_s}{A} \leq 0.4$ |
| Stiffener shape | Admiralty long-stalk T bar |
| Transverse frame shape | Flat bar |
| Transverse frame thickness (t_{wy}) | 10 mm. |
| Transverse frame height (h_{wy}) | 450 mm. |

The longitudinal T-bar stiffeners, which have values from 3' long-stalk T to 10' long-stalk T, have been used in this study. The inter-frame collapse mode has been picked and used for controlling the main behaviour of the stiffened panel because the inter-frame frame collapse mode creates less effect on the surrounding structure than the overall collapse mode.

To prevent the overall collapse mode, as represented in Figure 3.5, the stiffened panel model was applied with an appropriate boundary condition, which is presented in section 3.5, and appropriate size of transverse frame. The transverse frames adopted in this study are flat-bar frames 10 millimetres thick and 450 millimetres high.

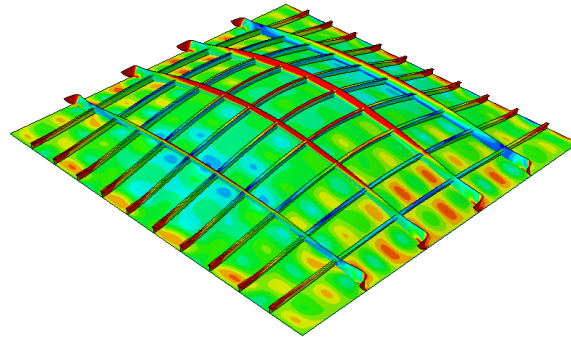


Figure 3.5 Overall collapse in a stiffened panel.

Several parameters are used to control the characterises of the stiffened panel, including:

- Plate slenderness ratio (β);

$$\beta = \frac{b}{t_p} \sqrt{\frac{\sigma_y}{E}}$$

- Stiffened panel slenderness (λ);

$$\lambda = \left(\frac{a}{\pi r} \right) \sqrt{\frac{\sigma_y}{E}}$$

Where the radius of gyration is;

$$r = \sqrt{\frac{I_x}{A}}$$

I_x is the second moment of area of the plate stiffener cross section:

$$I_x = b_p t_p^3 \left[z_0 - \frac{t_p}{2} \right]^2 + t_w h_w^3 + t_w h_w \left[z_0 - t_p - \frac{h_w}{2} \right]^2 + b_f t_f^3 + b_f t_f \left[z_0 - t_p - h_w - \frac{t_f}{2} \right]^3$$

- Stiffened area ratio

$$\frac{A_s}{A} = \frac{h_w * t_w + b_f * t_f}{h_w * t_w + b_f * t_f + b * t}$$

The geometric features of the stiffened panel are shown in Figure 3.6, below.

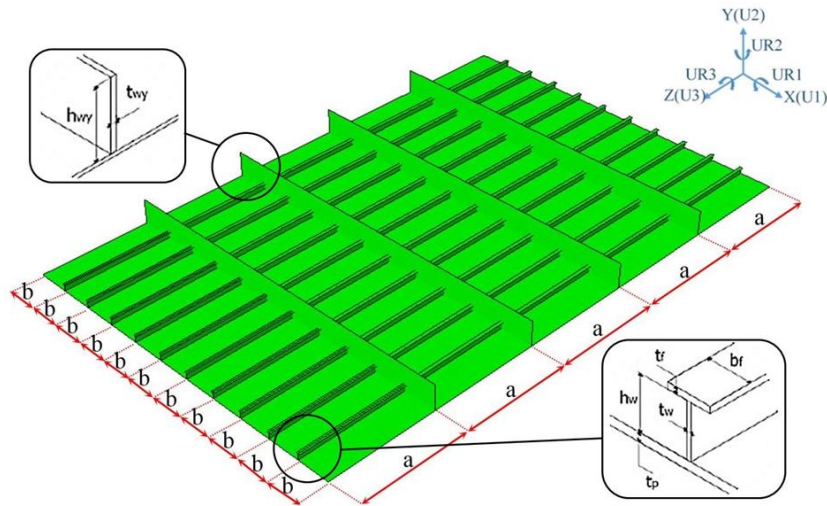


Figure 3.6 Stiffened panel geometries.

The dimensions of T-bar longitudinal stiffeners first developed by the UK Admiralty Research Establishment are used and are shown in Table 3.3 and Figure 3.7. Seven types of T-bar stiffener are used in the simulation of an intact stiffened panel to investigate the effect of the stiffener size on the strength of the stiffened panel.

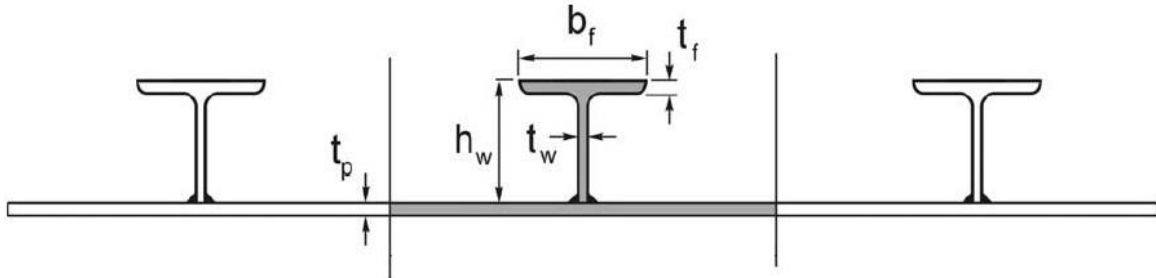


Figure 3.7 Stiffener geometries.

Table 3.3 The UK Admiralty Research Establishment.

| Stiffener type | h_{wx} (mm) | t_{wx} (mm) | b_{ft} (mm) | t_{ft} (mm) | A_{sx} (mm ²) | I_x (mm ⁴) |
|----------------|------------------|------------------|------------------|------------------|--------------------------------|-----------------------------|
| ALS1 | 69.8 | 4.4 | 25.4 | 6.4 | 469.7 | 279548 |
| ALS2 | 104.8 | 5.1 | 44.5 | 9.5 | 957.2 | 1263323 |
| ALS3 | 113.6 | 6.65 | 63.5 | 13.4 | 1606.3 | 2438715 |
| ALS4 | 138.2 | 7.15 | 76.2 | 14.2 | 2070.2 | 4589788 |
| ALS5 | 162.6 | 7.65 | 88.9 | 15.2 | 2595.2 | 7885356 |
| ALS6 | 186.9 | 8.15 | 101.6 | 16.3 | 3179.3 | 12661097 |
| ALS7 | 235.7 | 9.15 | 127 | 18.3 | 4480.8 | 28091475 |

3.4 Damaged Stiffened Panels

Generally, opening areas in a ship's structure can be used for rivets, pipe lines or humans. The opening area can also be applied in the course of a maintenance process. However, the opening area can become dangerous to the structure because of its size and placement, which can introduce initial residual strength to the ship's structure.

To increase understanding of damaged ship structures, an investigation was set up with two types of damage scenarios: clear-cut hole damage and damage from penetration by an indenter. The mild steel material is assumed to be elastic perfectly plastic and isotropic. A failure criterion in the material used the forming limit diagram (FLD) to represent realistic rupture behaviour in the material.

Table 3.4 represents the scope of the analysis in both damage effects. The simulation has been narrowed down to focus on only one stiffener, which is a 5' long stalk T (ALS3). The damage area is controlled by the ratio between the diameter of the damage area (D) and the width of the stiffened panel (W) in damage represented by a clear-cut hole and the ratio between diameter of indenter (D_{IN}) and the width of panel (W) in penetration damage. The damage area ratios increase from 5 per cent to 80 per cent. The transverse frame height of 450 mm is chosen to be large enough to ensure that the buckling occurs interframe.

Table 3.4 Scope of analysis for damaged stiffened panel.

| Parameter | Damaged clear-cut | Penetration damaged |
|--------------------------------------|-------------------|---------------------|
| <i><u>Material Properties</u></i> | | |
| Yield stress (σ_y) | 245 MPa. | |
| Young’s modulus (E) | 207 GPa. | |
| Poisson’s ratio (λ_p) | 0.3 | |
| <i><u>Interaction properties</u></i> | | |
| Surface interaction | General contact | |

| | | |
|--|-----------------------------------|--|
| Friction coefficient | 0.3 | |
| <u>Structure Parameters</u> | | |
| Plate slenderness ratio (β) | $1 \leq \beta \leq 4$ | |
| Column slenderness ratio (λ) | $0.2 \leq \lambda \leq 1.0$ | $0.2 \leq \lambda \leq 0.6$ |
| Stiffener area ratio ($\frac{A_s}{A}$) | $\frac{A_s}{A} = 0.2$ | |
| Stiffener shape | 5' long stalk T (ALS3) | |
| Transverse frame shape | Flat bar | |
| Transverse frame thickness (t_{wy}) | 10 mm. | |
| Transverse frame height (H_{wy}) | 450 mm. | 180 mm. |
| Damage area ratio | $0.05 \leq \frac{D}{W} \leq 0.80$ | $0.05 \leq \frac{D_{in}}{W} \leq 0.80$ |

3.4.1 Damage represented by circular clear-cut out

The first damage scenario of this research is that represented by a clear cut hole. The hole is represented as a circular cut out which is placed in the middle of the stiffened panel. The size of the damaged area depends on the ratio between the diameter of the hole (D) and the width of the panel (W), as shown in Figure 3.8.

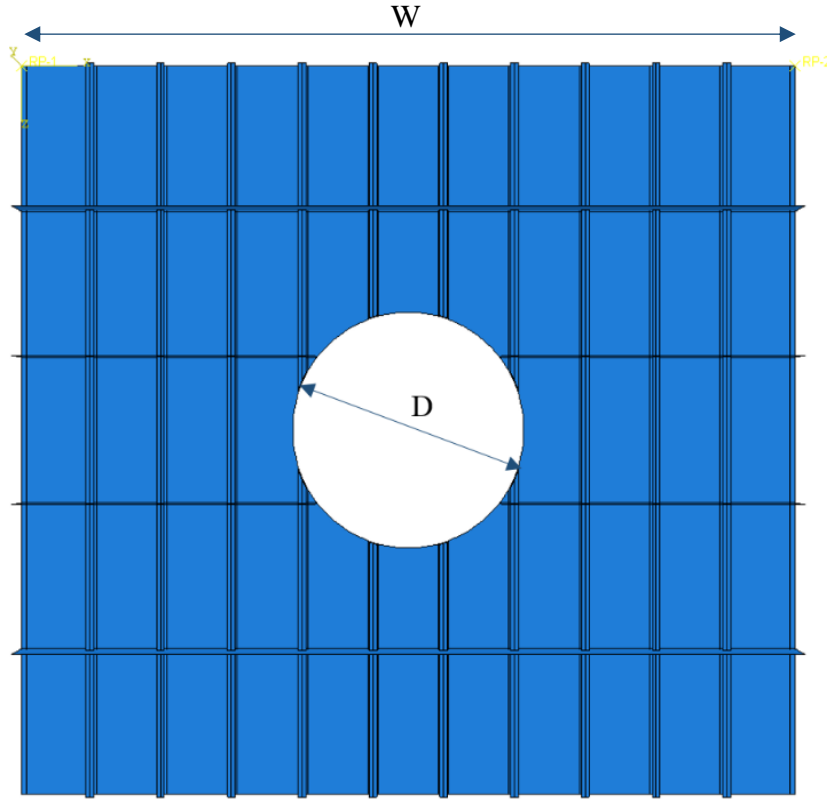


Figure 3.8 Damage clear-cut hole diagram.

The characteristics of the damaged panel shown in Table 3.5 follow the intact panel condition; however, some of the parameters such as stiffened area ratio and stiffener size are narrowed down to 0.2 and 5' long stalk T .

The size of the damage area used for representing a cut-out area is shown in Table 3.5, below.

The damage area ratio $\left(\frac{D}{W}\right)$ represents the percentage of the damage area to the width of the panel, increasing from 5 per cent to 80 per cent and depending on the slenderness area ratio (β).

Table 3.5 Size of damaged clear-cut hole

| Damaged hole diameter (mm.) | | | | |
|-----------------------------|---------------------------------|-------------|-------------|-------------|
| $\frac{D}{W}$ | $\lambda = 0.2 \text{ to } 1.0$ | | | |
| | $\beta = 1$ | $\beta = 2$ | $\beta = 3$ | $\beta = 4$ |
| 0.05 | 227 | 320 | 393 | 453 |
| 0.10 | 453 | 641 | 785 | 907 |
| 0.15 | 680 | 961 | 1178 | 1360 |
| 0.20 | 907 | 1282 | 1570 | 1813 |
| 0.25 | 1133 | 1602 | 1963 | 2266 |
| 0.30 | 1246 | 1763 | 2159 | 2493 |
| 0.35 | 1360 | 1923 | 2355 | 2720 |
| 0.40 | 1586 | 2243 | 2748 | 3173 |
| 0.45 | 1813 | 2564 | 3140 | 3626 |
| 0.50 | 2040 | 2884 | 3533 | 4079 |
| 0.55 | 2266 | 3205 | 3925 | 4533 |
| 0.60 | 2493 | 3525 | 4318 | 4986 |
| 0.65 | 2720 | 3846 | 4710 | 5439 |
| 0.70 | 2946 | 4166 | 5103 | 5892 |
| 0.75 | 3173 | 4487 | 5495 | 6346 |
| 0.80 | 3399 | 4807 | 5888 | 6799 |

Transverse frame size is also considered in this study due to the size of the transverse frame being a parameter to create and control the behaviour of the stiffened panel, which is represented as an inter-frame collapse mode. To represent more realistic transverse frame size, several sizes of transverse frame have been simulated with the simplified method to find the smallest frame, which is 180 mm high, which can prevent the overall collapse behaviour in the panels. Figure 3.9 shows the behaviour of two different transverse sizes in the research.

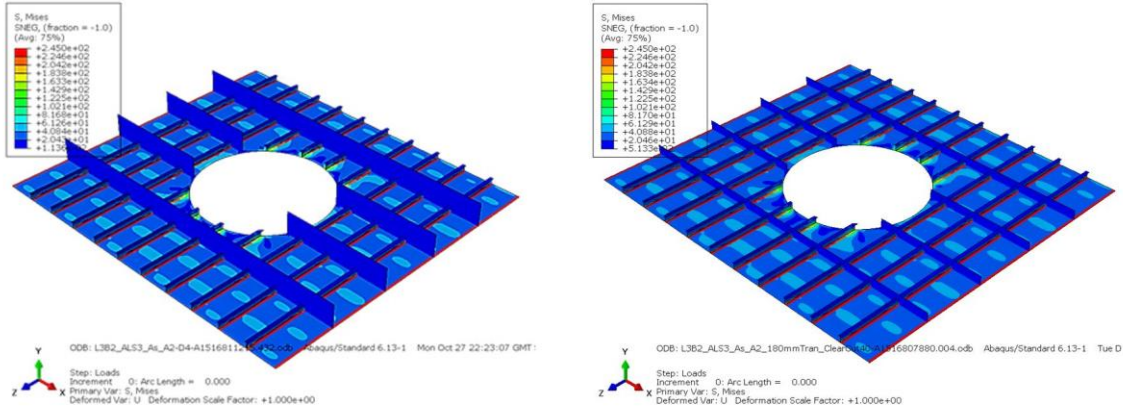


Figure 3.9 Change of transverse frame height.

3.4.2 Damage represented by penetration with indenter

The second damage scenario is represented by penetration damage. A rigid body indenter is shown in Figure 3.10, being a half sphere shape with a diameter controlled by the damage area ratio $\left(\frac{D_{IN}}{W}\right)$ as shown in Table 3.6, and 500 millimetres long. The stiffened panel is penetrated by the indenter with slow amplitude to create a realistic damage area. D_{IN} is the diameter for the indenter, however, the size of the hole depends on the speed of the penetration. Diameter of the hole is measured after penetration.

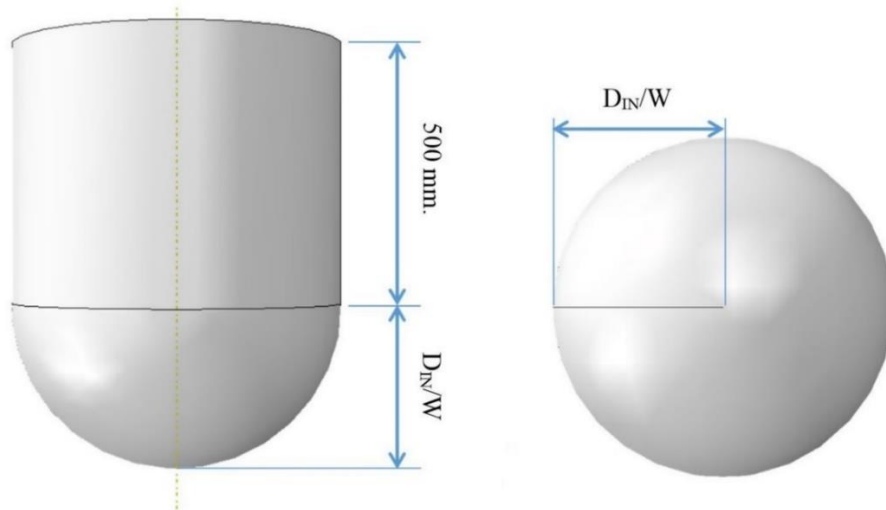


Figure 3.10 Indenter geometry.

Table 3.6 Size of indentation damaged hole, $\frac{D_{IN}}{W}$

| Damaged hole diameter (mm.) | | | | |
|-----------------------------|---------------------------------|-------------|-------------|-------------|
| $\frac{D_{IN}}{W}$ | $\lambda = 0.2 \text{ to } 0.6$ | | | |
| | $\beta = 1$ | $\beta = 2$ | $\beta = 3$ | $\beta = 4$ |
| 0.05 | 227 | 320 | 393 | 453 |
| 0.10 | 453 | 641 | 785 | 907 |
| 0.15 | 680 | 961 | 1178 | 1360 |
| 0.20 | 907 | 1282 | 1570 | 1813 |
| 0.25 | 1133 | 1602 | 1963 | 2266 |
| 0.30 | 1246 | 1763 | 2159 | 2493 |
| 0.35 | 1360 | 1923 | 2355 | 2720 |
| 0.40 | 1586 | 2243 | 2748 | 3173 |
| 0.45 | 1813 | 2564 | 3140 | 3626 |
| 0.50 | 2040 | 2884 | 3533 | 4079 |
| 0.55 | 2266 | 3205 | 3925 | 4533 |
| 0.60 | 2493 | 3525 | 4318 | 4986 |
| 0.65 | 2720 | 3846 | 4710 | 5439 |
| 0.70 | 2946 | 4166 | 5103 | 5892 |
| 0.75 | 3173 | 4487 | 5495 | 6346 |
| 0.80 | 3399 | 4807 | 5888 | 6799 |

In addition, the size of the damaged area depends on the speed of the indenter. Thus, three different speeds of penetration have been tested to investigate the appropriate speed and time for the simulation process, which will be presented in section 3.10.

3.5 Boundary conditions

The boundary conditions of the stiffened panel are set to ensure that buckling will occur in a central bay, which is the inter-frame collapse behaviour, by not allowing both ends of the transverse frame to move up, in the Y-axis. A simple support condition is assumed on the longitudinal edges.

Transversely, the model has been fixed at one end, which does not allow movement or rotation in any direction, except in the X-axis, to allow the long edges of the panel to pull in. On the other hand, the loaded end applies a uniform compressive load to the structure in the Z-axis, whilst

other constraints are fixed as for the opposite edge. The applied load is used as a controlled displacement. Longitudinally, both edges of the stiffened panel are constrained in the Y-axis direction but are free to remain straight but displace in the Z-axis direction to enable uniform compressive displacement throughout the panel's length. One edge is constrained in X-axis direction whilst the other is free to pull in, but is constrained to remain straight. Table 3.7 and Figure 3.11 show the boundary conditions of the stiffened panel.

Table 3.7 Boundary condition of stiffened panels

| Location of nodes | boundary conditions |
|-----------------------|---------------------------------|
| Along Z-axis, $X = 0$ | $U1 = U2 = 0$ |
| Along X-axis, $Z = 0$ | $U2 = UR1 = UR2 = UR3 = 0$ |
| Along Z-axis, $X = B$ | $UR2 = 0$ |
| Along X-axis, $Z = A$ | $U2 = U3 = UR1 = UR2 = UR3 = 0$ |
| At the origin | $U3 = 1$ |

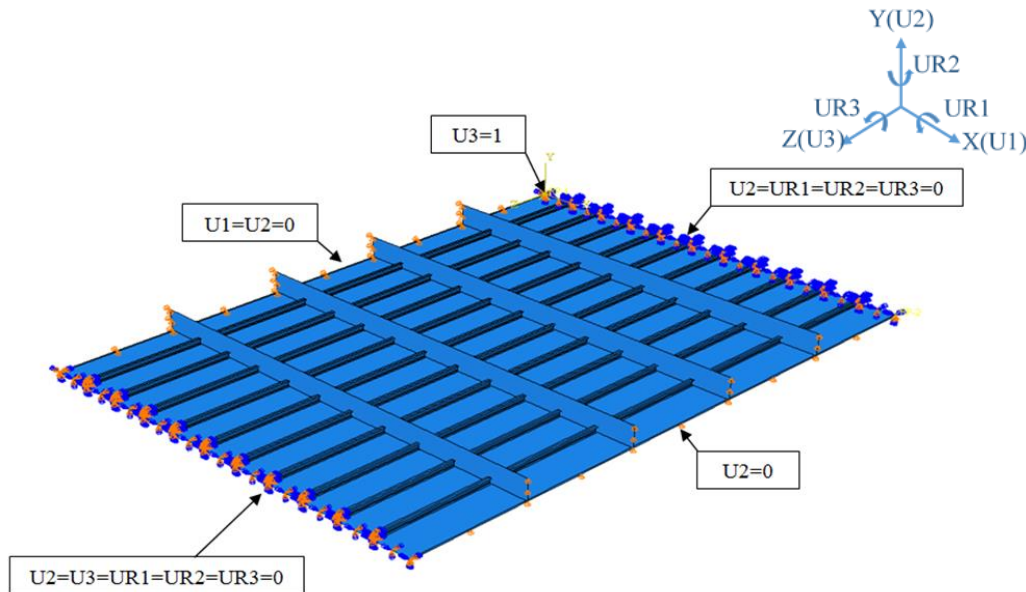


Figure 3.11 Boundary conditions of stiffened panel.

Constraints are applied to three places in this analysis. Firstly, a constraint is used at the end of the stiffened panel (Along X-axis, Z=0) to ensure that equal displacement is applied to the structure. Secondly, each side of the transverse frame is constrained to remain straight to avoid an overall buckling behaviour and reduce vibration in the dynamic analysis. Finally, constraint is used with the indenter to ensure that force is applied to the centre of the indenter.

3.6 Initial conditions

The initial conditions for the research follow the studies of Dow and Smith (1984) and Benson et al. (2013d). The imperfection is divided into two parts, which are distortion and residual stress. The average level of imperfection has been used for the whole simulation and is represented in Table 3.8.

Table 3.8 Imperfection properties for stiffened panels.

| Parameter | | Value |
|---|-----------------------------|----------------|
| Average residual stress magnitude (σ_{rc}) | | $0.15\sigma_y$ |
| Average plate imperfection (W_{0pl}) | | $0.1\beta^2t$ |
| Average stiffener imperfection (W_{0s}) | | |
| Ratio of $\frac{\delta_{01}}{a}$ | $\lambda = 0.2$ | 0.0008 |
| | $\lambda = 0.4$ | 0.0012 |
| | $\lambda \geq 0.6$ | 0.0015 |
| Ratio of $\frac{\delta_{02}}{\delta_{01}}$ | $0.2 \geq \lambda \geq 0.6$ | 0.25 |

3.6.1 Residual stress

The residual stress is applied to the stiffened panel by following the values from Table 3.8. The red line in Figure 3.12 represents the pre-set, residual stress in the model in both plates and stiffeners.

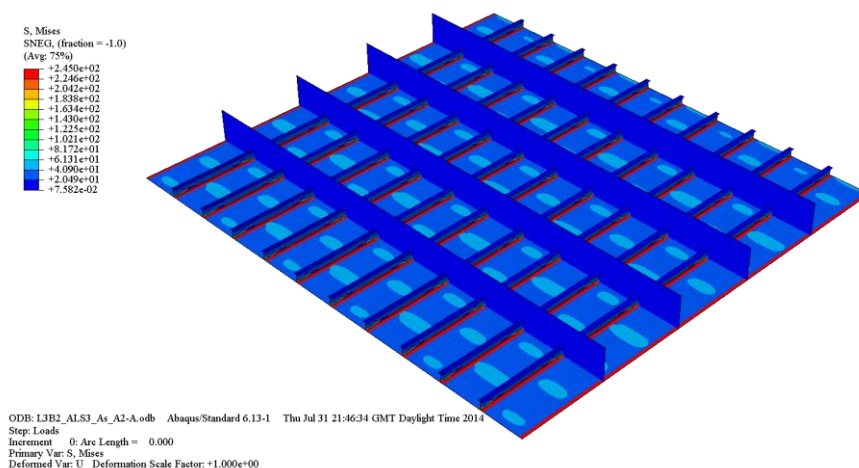


Figure 3.12 Imperfection in a stiffened panel.

3.6.2 Distortions

Distortions are applied to both directions of the steel plate. The dimensions of the plate can be showed in Figure 3.13 which shows the length and the width of the plate as ‘a’ and ‘b’ respectively.

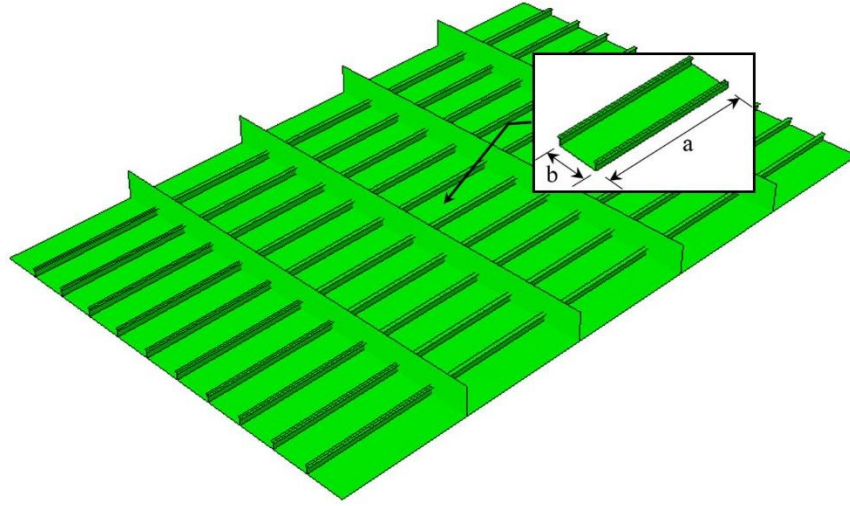


Figure 3.13 Dimension of a plate in a stiffened panel.

Table 3.9 Definition of initial deformation in this research (Dow and Smith, 1984).

| Case no. | Definition of initial deformation | |
|----------|---|--|
| 1 | $W_0 = \overline{W}_0 \sin \frac{\pi x}{a} \sin \frac{\pi y}{b},$ $\overline{W}_0 = 0.008b$ | |
| 2 | $W_0 = \overline{W}_0 \sin \frac{5\pi x}{a} \sin \frac{\pi y}{b},$ $\overline{W}_0 = 0.008b \left(\frac{x}{a} < 0.1, \frac{x}{a} > 0.9 \right)$ $W_0 = 0.008b \left(0.1 \leq \frac{x}{a} \leq 0.9 \right)$ | |
| 3 | $W_0 = \overline{W}_0 \sin \frac{5\pi x}{a} \sin \frac{\pi y}{b},$ <p>(a) $\overline{W}_0 = 0.008b$</p> <p>(b) $\overline{W}_0 = 0.016b$</p> <p>(c) $\overline{W}_0 = 0.02b$</p> | |

Table 3.9 shows a group of initial deformations used in analysis. A combination of initial deformation case 1 and 3 are applied to the length of plate ‘a’ which are a combination of an 80 per cent single half wave (case 1) and 20 percent of five half wave (case 3). Furthermore, the width ‘b’ of the plate is subjected to a single half wave (case 1).

To explain how distortions are applied into the stiffened panel, Figures 3.14 and 3.15 display details of distortions with a deformation scale factor of 1000, and represent a complete combination of distortions in the length of plate ‘a’ and single half wave of distortion in the width of plate ‘b’ respectively.

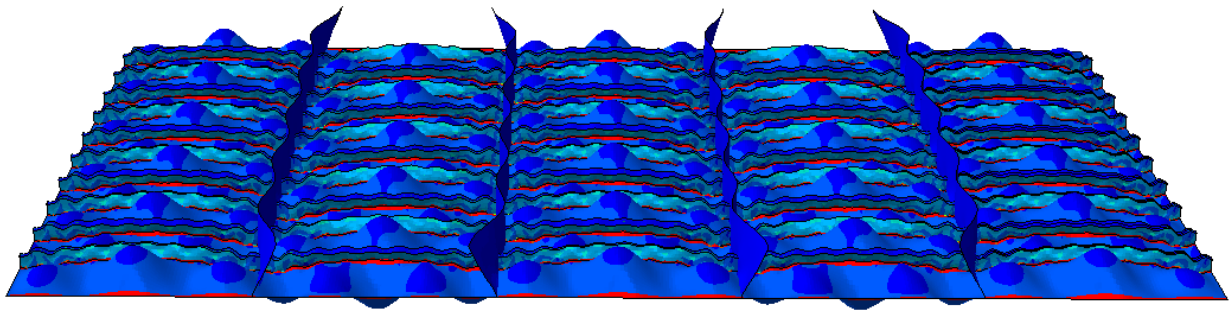


Figure 3.14 Distortions of the length of steel plate ‘a’.

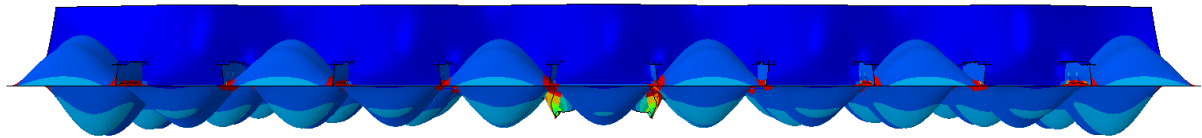


Figure 3.15 Distortions of the width of steel plate ‘b’.

3.7 Finite element program

The non-linear finite element analysis was applied by using the program ABAQUS. ABAQUS (2013) version 6.13 has been used for all simulations in this study. Static and dynamic non-linear finite element analysis methods were applied to the program, with the dynamic analysis controlled to give a quasi-static solution.

3.8 Element type

A shell element with four nodes was chosen for the simulation. However, finite element analysis is a time-consuming process. In order to reduce the total time of the analysis, the shell element type S4R, which is a shell element with four nodes, doubly curved thin or thick shell, reduced integration, hourglass control and finite membrane strains (see Figure 3.16), was used to create the stiffened panels in this research.

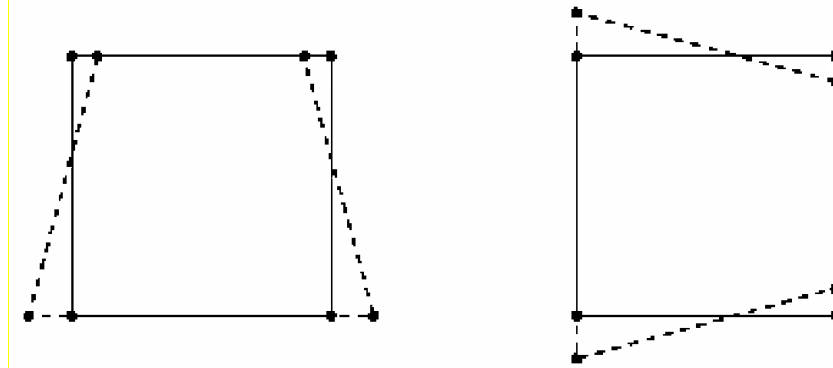


Figure 3.16 Shell element type S4R.

In order to control for accurate results, analysis has been carried out to compare both element type S4 and S4R, presented in Figure 3.17. The comparison used the same model as in the analysis, which is plate slenderness ratio (β) equal to 1, column slenderness ratio (λ) equal to 0.3, stiffener ratio ($\frac{A_s}{A}$) equal to 0.2 with stiffener type ALS3.

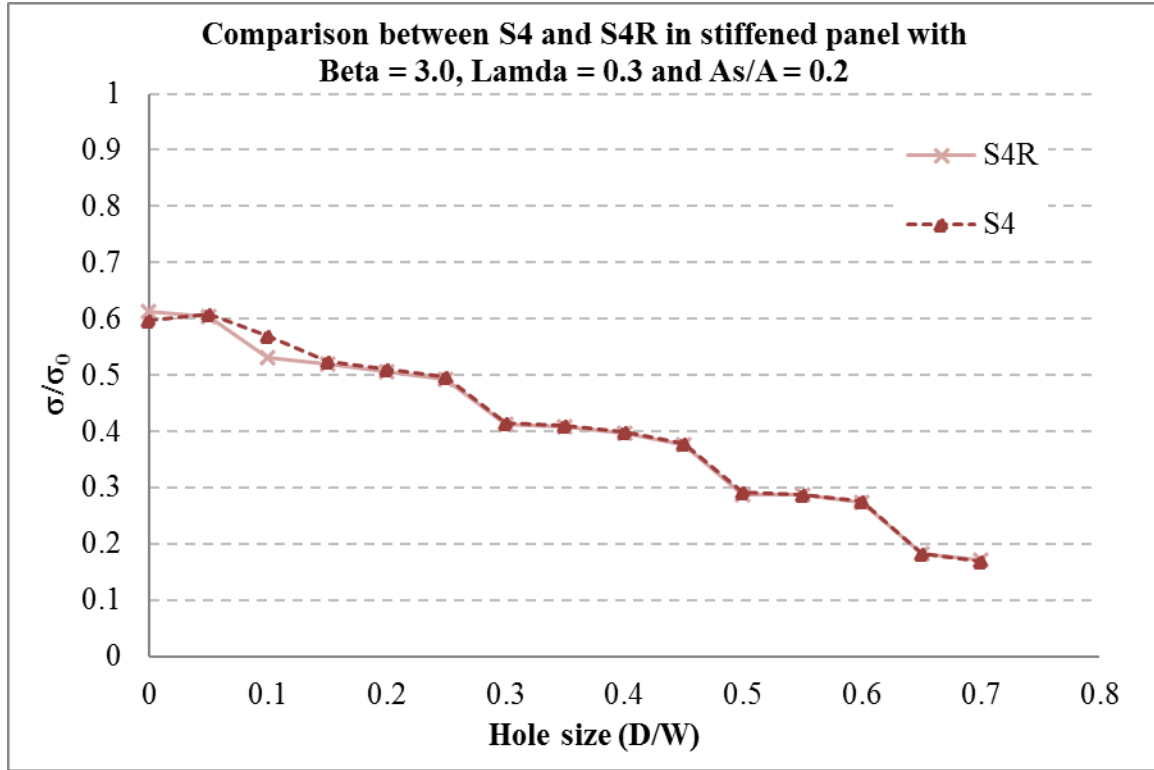


Figure 3.17 Comparison between element type S4 and S4R.

Figure 3.17 shows that results of the comparison between element type S4 and S4R are close and that they can be used as substitutes for each other in the simulation. Thus, element type S4R is a better choice for this research, because this element type can reduce run times in the analysis and give a very accurate result at the end of the simulation.

3.9 Mesh

Size of mesh is one of the elements which can be related to the time consumed in the analysis process. Benson et al. (2013a) compared the analysis time with different size of mesh, as shown in Chapter 2. Figure 3.18 shows a 25 millimetre mesh which has been used for this research, because it gives an appropriate analysis time and accurate results in the analysis.

Quad-dominated is used as an element shape to automatically generate the mesh; this allows triangles to occur in the transition region, as shown in Figure 3.19. Furthermore, this type of element shape gives better and more accurate results.

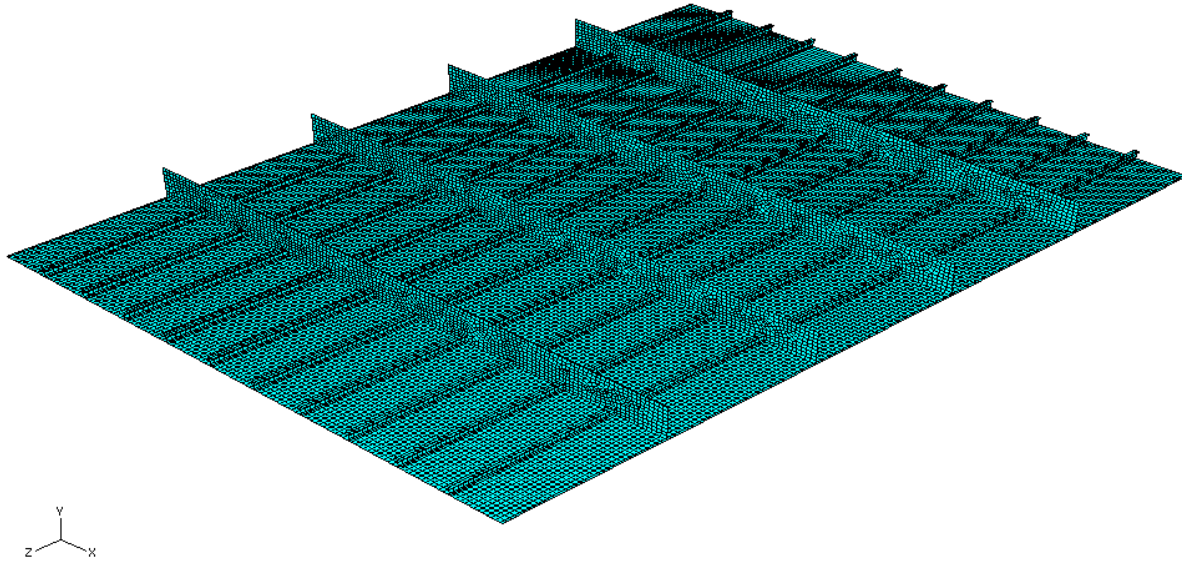


Figure 3.18 Mesh size for stiffened panel.

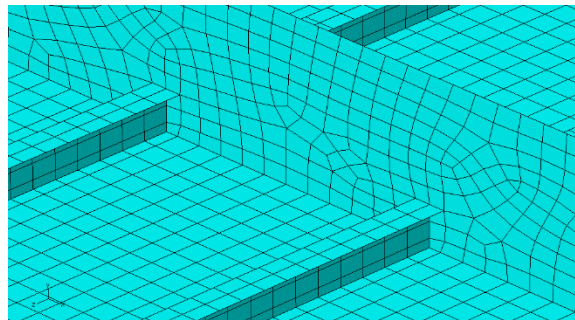


Figure 3.19 Quad-domination type.

3.10 Steps

Three important steps in analysis are used for different reasons and help to generate more realistic behaviour in ship structures.

3.10.1 Relaxation step

The relaxation step aims to find the equilibrium of the structure with zero load applied, before moving on to the next step. In intact panel analysis, the relaxation step takes place after the stiffened panel has been subjected to the initial conditions, which are initial distortions and residual stress.

For the damaged structure cases, the relaxation step takes place after initial condition is applied and after the penetration process for damage represented by the clear-cut area and damage represented by penetration respectively.

3.10.2 Compression load

Uniform end displacement is used and assumed as a compression load in this research. In-plane displacement is applied to one side of the stiffened panel. Figure 3.20 shows the reaction of the other end of the stiffened panel, which has a boundary as a fixed end. The reaction of the fixed end area can give the same amount of reaction force based on Newton's laws.

The in-plane displacement is applied to the stiffened panel which has been divided into 100 steps, where each step has movement of 1 millimetre. The Newton Raphson method is used to find the equilibrium of each step before moving on to the next step.

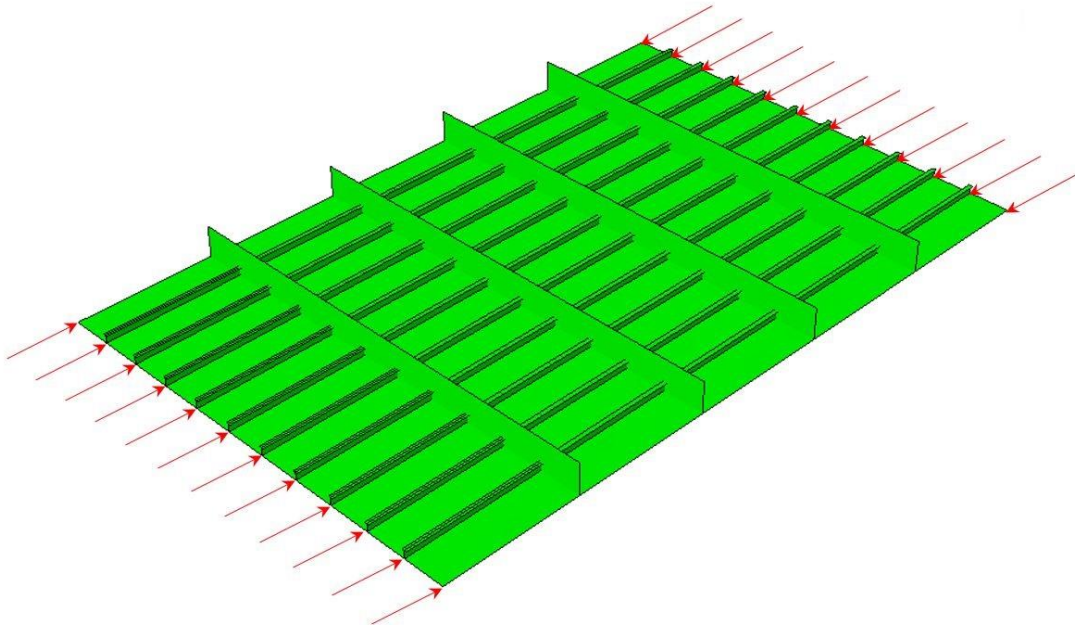


Figure 3.20 Compression load

3.10.3 Damaged step

The damage step can be divided into two separate steps, for the following type of damage scenarios:

a) Damage represented by a circular clear-cut hole.

This type of damage is applied directly to the stiffened panel by removing the elements in the circular shape. After this step, the simulation is as same as intact panel analysis.

b) Damage represented by penetration with indenter.

The indenter is set up as a rigid body and moved upward to the stiffened panel in order to create the damage area, as shown in Figure 3.21. The speed of the indenter is maintained constant and becomes an important factor to control because different speeds can create different effects on the damage area. In order to choose the appropriate speed for this research, three different speeds of indenter have been tested. The speed of indenter is set up with the amplitude in ABAQUS.

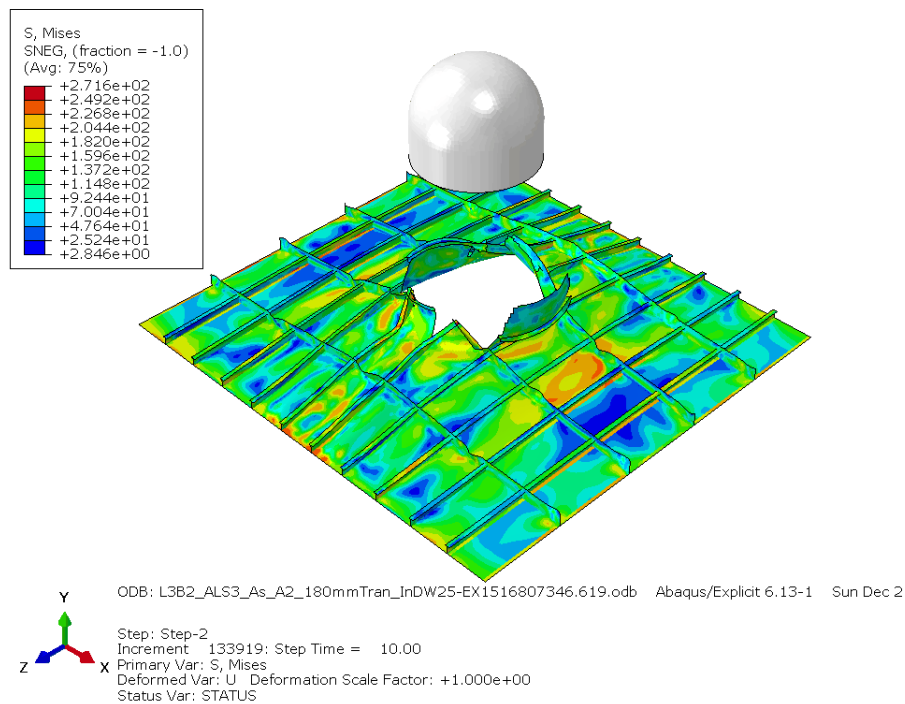
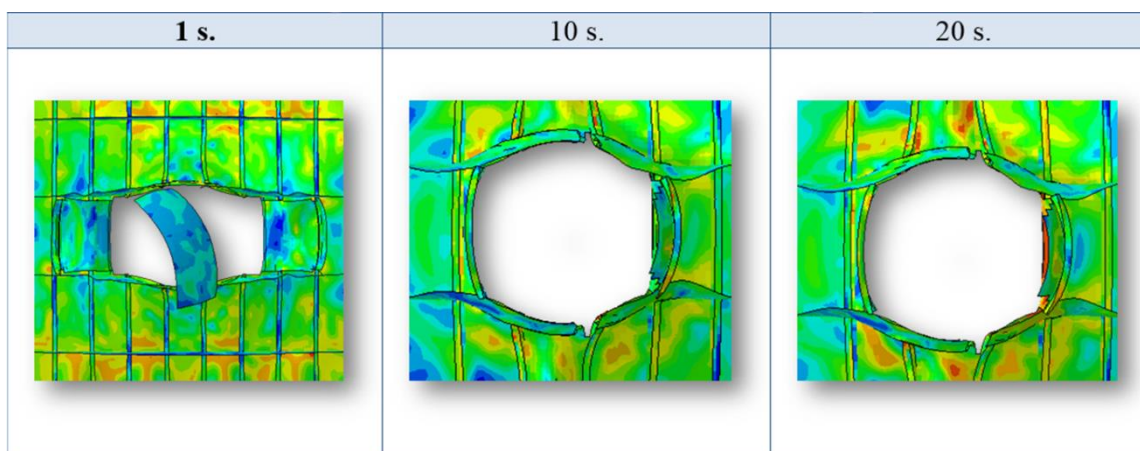


Figure 3.21 Penetration damage.

Table 3.10 shows the effect of penetration with different speeds. The indenter was placed close to the stiffened panel and set to move upward with 4000 millimetres with different amplitudes, which control the movement of the indenter from point A to point B under the amplitude of time, as 1 second, 10 seconds and 20 seconds, which is equivalent to indenter velocities of 4m/s, 0.4m/s and 0.2m/s respectively.

Table 3.10 Penetration with different speeds.



The differences in the damaged area in Table 3.10 show that the speed of the indenter can create a huge difference in the damage effect because of the transfer of the kinetic energy. A faster indenter speed is expected to transfer a greater kinetic energy to the panel than a slower speed indenter. If the indenter is too fast it can cause several unwanted effects for the purposes of this study, where a realistic and controllable damage representation is required. As shown in the example of Table 3.10, the damage mechanism is completely different. The high speed indenter causes a larger damage area where the plates adjacent to the indenter are also fractured due to the high kinetic energy imparted into the structure. With a slower indenter speed these plates remain attached to the panel and the resultant damage hole is smaller and provides a more realistic and controllable shape for parametric studies. The key parameter to control this is the magnitude of the kinetic energy throughout the simulation timestep. It was found that by keeping the total kinetic energy to below 1% of total energy was sufficient to produce parametrically equivalent damage with different indenter sizes. It was therefore found that an indenter with velocity of 0.4m/s meets the 1% kinetic energy limit.

The relaxation step is adopted after the penetration process to decrease the kinetic energy in the structure. The kinetic energy level is controlled to be close to zero before applying an in-plane compression load to the stiffened panel.

3.11 Analysis procedure

The procedure is divided into three groups and separated by both type of design and type of damage. At the beginning stage, the stiffened model is given material properties and boundary conditions as presented in the previous chapter. From this point, the procedure is explained by following Figure 3.22.

3.11.1 Intact analysis procedure

- a) Initial condition is applied to the stiffened panel.
- b) The relaxation step is applied to the model to find the equilibrium.
- c) In-plane displacement or in-plane compression loads are applied to the stiffened panel.
- d) To run the analysis, the mesh and input file are created. The input file is submitted to ABAQUS for the analysis.
- e) The results are collected at this point to create a stress and strain curve and load shortening curve.

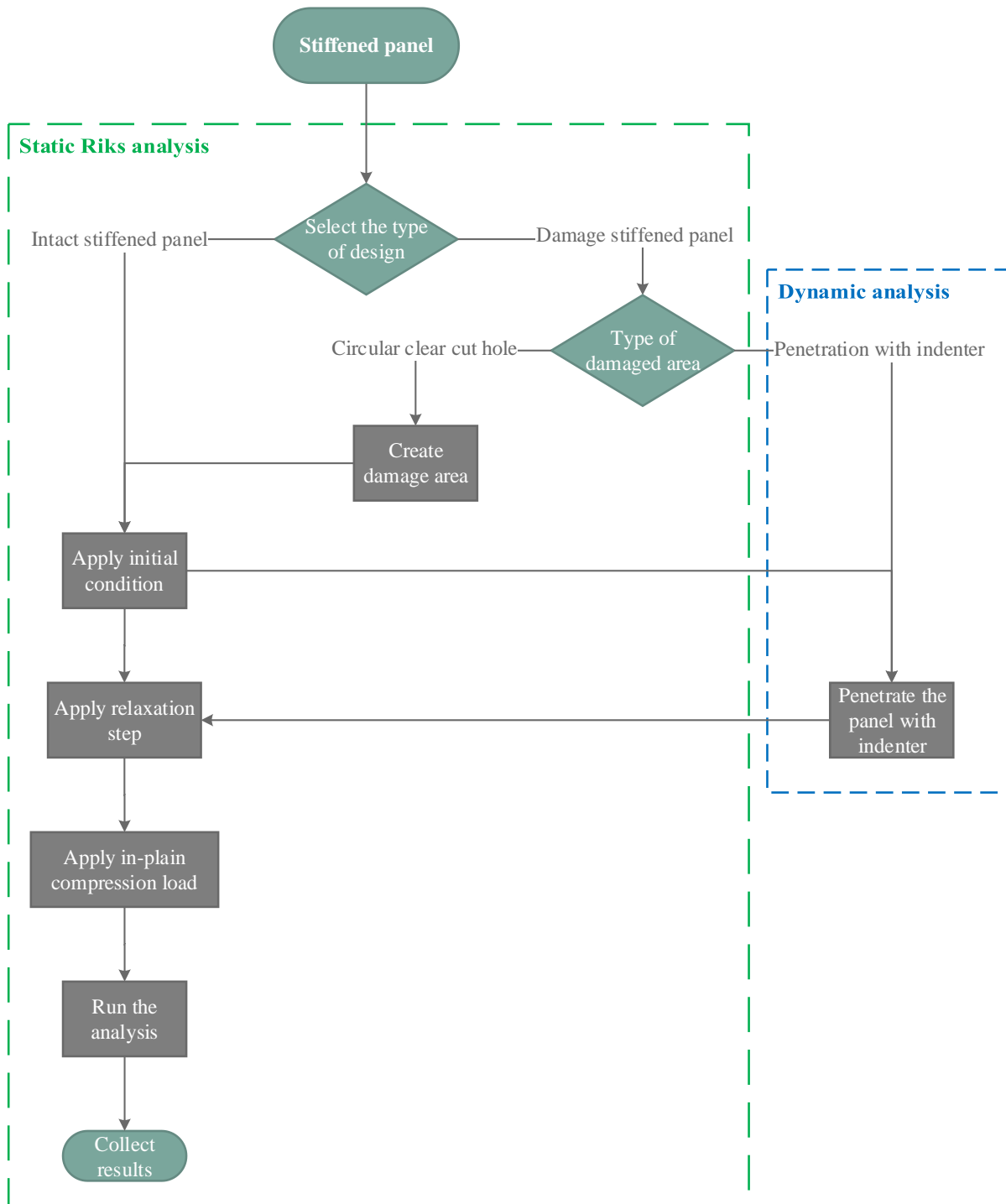


Figure 3.22 Analysis procedure.

3.11.2 Damaged area represented by circular clear-cut hole.

- The element of stiffened panel model is removed in a circular shape from the middle of

the panel. The diameter of the hole is explained in the beginning of this chapter.

- b) Initial conditions are applied to the stiffened panel.
- c) The relaxation step is applied to the model to find the equilibrium.
- d) In-plane displacement or in-plane compression load is applied to the stiffened panel.
- e) To run the analysis, mesh and input file are created. The input file is submitted to ABAQUS for analysis.
- f) The results are collected at this point to create a stress and strain curve and load shortening curve.

3.11.3 Damaged area represented by penetration with indenter

- a) Initial conditions are applied to the stiffened panel.
- b) The penetration step is used to create the damaged area by using dynamic analysis as a quasi-static analysis. The indenter moves upward in y direction with amplitude 10 seconds, with distance set at 4000 millimetres.
- c) The relaxation step is applied to the model to find the equilibrium.
- d) In-plane displacement or in-plane compression load is applied to the stiffened panel.
- e) To run the analysis, a mesh and input file are created. The input file is submitted to ABAQUS for analysis.
- f) The results are collected at this point to create a stress and strain curve and load shortening curve.

N.B.

Only the penetration damage step uses dynamic non-linear analysis. Other steps use static Riks analysis, which can produce more stable results and can reduce the kinetic energy in the penetration damage cases.

3.12 Summary

Material and geometric proprieties are very important factors for the simulation in order to introduce realistic behaviour into the structure. The serviceability of the ship is represented by appropriate factors such as type of material, element type and inclusion of non-linear material behaviour, which is one major factor in studying the damage behaviour of the structure in this research.

This chapter presented details of the geometry of the stiffened panels analysed by dividing the study into two main groups: intact and damaged structure. The damaged area is considered to be more realistic and can be used to represent the actual behaviour of the damage structure; this can be represented by both the clear-cut hole and damage represented by penetration with indenter.

The appropriate boundary and initial condition are applied to stiffened panels base on the realistic behaviour of ship structure.

The simulation uses the appropriate type of shell element and a suitable size of mesh in the analysis of the stiffened panels. The analysis involves three different type of analysis: intact panel analysis, damage represented by the circular clear-cut out and damage represented by penetration with indenter. Both static and dynamic analyses have been used in the analysis procedure to give accurate results.

Chapter 4 Strength of intact and damaged stiffened panels

4.1 Introduction

The results of the stiffened panel analysis are demonstrated in this chapter. Intact structure results are shown as baseline results and used for comparison with the damaged stiffened panels, while a comparison between standard design curves and intact structures is provided.

The damaged stiffened panels' results are presented in the form of stress-strain curves and load shortening curves in order to represent the behaviour of the stiffened panels with different sizes of damage. Finally, a mean value of ultimate strength is provided to modify the simplified method in ProColl.

4.2 Intact stiffened panels

The boundary conditions from Chapter 3 were applied to the panel with the intention of avoiding overall buckling. Table 4.1 shows the von Mises stress at the yield point and post collapse point on a set of intact stiffened panels with plate slenderness ratio (β) of 2.0, stiffened area ratio ($\frac{A_s}{A}$) of 0.2 and 5' long-stalk T bar with different column slenderness ratio (λ) value. These plots demonstrate that all the panels collapse with a inter-frame mode. A difficulty with multi-frame panel analyses is controlling the bay in which the buckling nucleates. Ideally, for the purposes of parametric analysis, nucleation should occur in the central bay. This is encouraged by seeding a favourable imperfection pattern to cause the central bay to buckle first. In the example shown in Table 4.1 this is the case for all panels with the exception of the most stocky with $\lambda = 0.2$. For this panel the buckling nucleates in the outer bay adjacent to the boundary, and is caused by a realignment of the imperfections during the simulation due to snap-through. However, this still results in an interframe collapse mode consistent with the other panels, and therefore was not a cause for concern in the parametric study. Overall, the plots show that the boundary conditions and frame sizing selected for the study are suitable for consistent analysis.

Table 4.1 Intact panels' behaviour for set of stiffened panels with plate slenderness ratio (β) of 2.0, stiffened area ratio ($\frac{A_s}{A}$) of 0.2 and 5' long-stalk T bar.

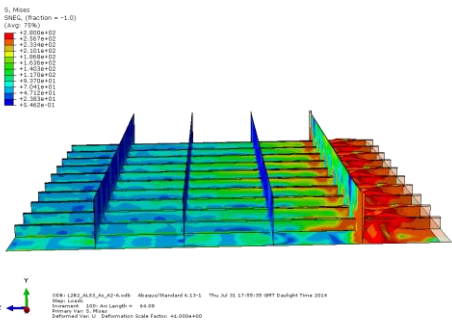
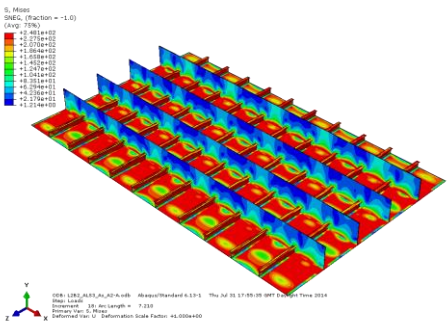
Stiffened panels with plate slenderness ratio (β) of 2.0, stiffened area ratio ($\frac{A_s}{A}$) of 0.2 and 5' long-stalk T bar.

Lamda

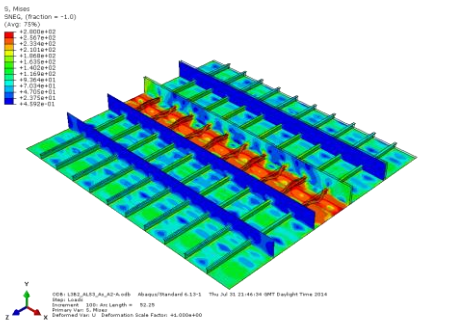
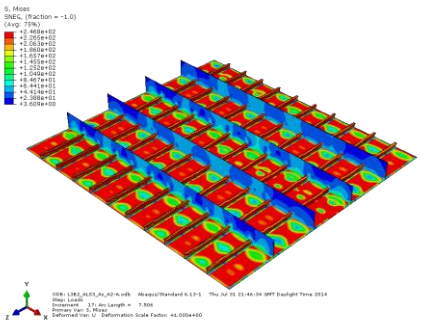
Yield point

Buckling

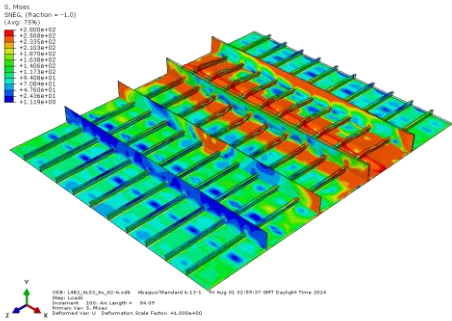
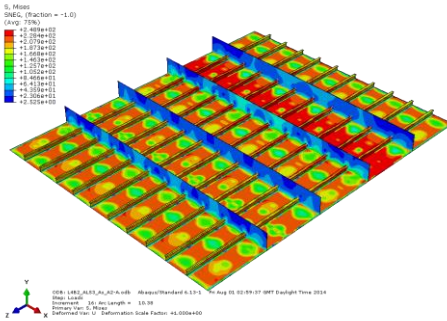
0.2



0.3



0.4



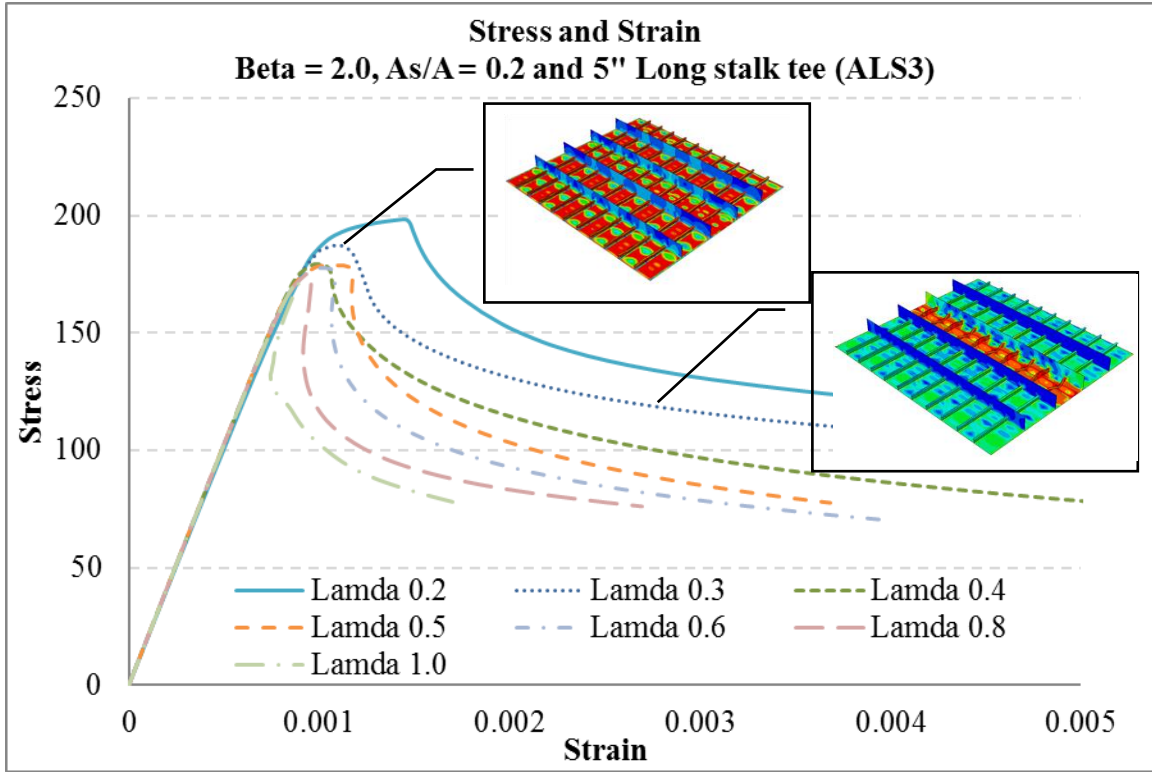


Figure 4.1 Stress-strain curve of stiffened panels with Beta of 2.0, stiffened area ratio ($\frac{A_s}{A}$) of 0.2 and 5' long-stalk T bar.

Figure 4.1 presents a comparison of the stress-strain curves between different column slenderness ratio (λ) values, in order to show the strength of the stiffened panel. The results show that the strength of stiffened panels consistently decreases when column slenderness ratio (λ) value becomes larger or the panel becomes more slender.

Furthermore, the ultimate strength of the stiffened panels is generated and compared with standard design curves which have an average value of imperfection taken from the UK Admiralty Research Establishment (Chalmers, 1993). Figures 4.2 to 4.4 show the comparison of ultimate strength in stiffened panels with a column slenderness ratio (λ) between 0.2 and 1.0 and different types of stiffeners. This group of results is controlled under a plate slenderness ratio (β) of 0.2 and stiffener area ratio ($\frac{A_s}{A}$) at 0.1, 0.2 and 0.4.

The graphs show a group of results which have a similar strength value and are very close together in the group of stiffener area ratio $\left(\frac{A_s}{A}\right)$ equal to 0.2 and 0.4, compared to a set of results with fairly spread results for the low stiffener area ratio of 0.1. This suggests that when the stiffener area ratio is very low, plate-stiffener buckling dominates the solution whereas with higher stiffener area ratio plate buckling dominates. For these higher stiffener area ratio panels this confirms the validity of the design curves such as those put forward by Chalmers, because panels with very different stiffener sizes but with the same overall slenderness demonstrate very similar levels of overall strength. This means that, for larger stiffener area ratios, a parametric study can be confined to a single stiffener size to produce results which are valid over a wide range of different scantling arrangements. However, if the stiffener area ratio is small, the validity of results for other scantling sizes is more questionable. For this study a stiffener area ratio of 0.2 was therefore selected, which is also more representative of realistic ship scantlings. In summary, these graphs demonstrated the validity to narrow the analysis down to a smaller group for the damaged panel cases which have the stiffened area ratio value $\left(\frac{A_s}{A}\right)$ at 0.2 with 5' long stalk T stiffeners (ALS3).

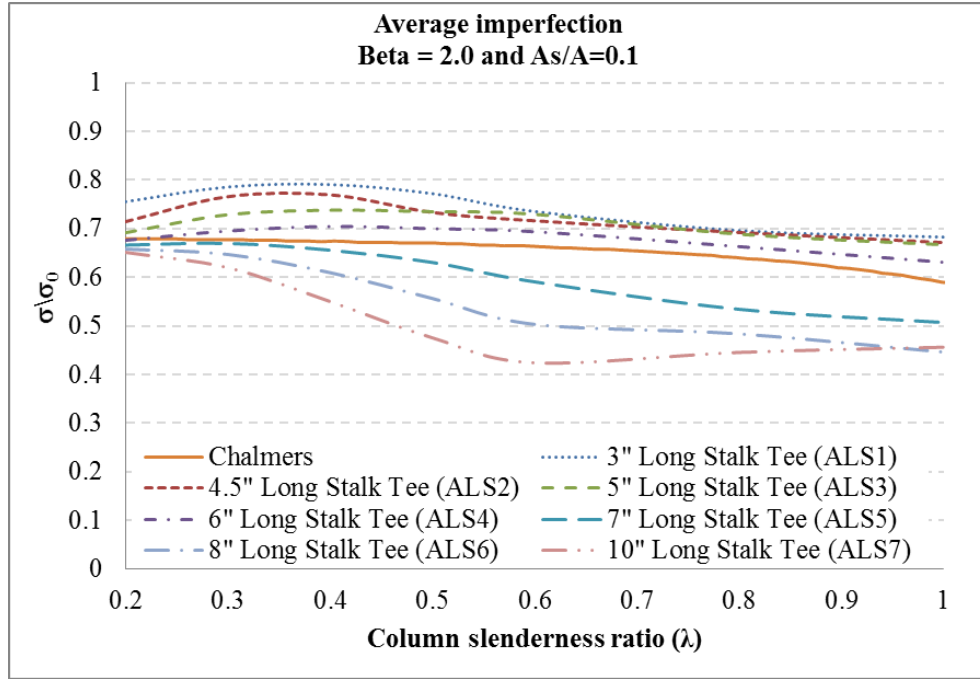


Figure 4.2 Average imperfection of plate slenderness ratio (β) 2.0, stiffener area ratio ($\frac{A_s}{A}$) 0.1.

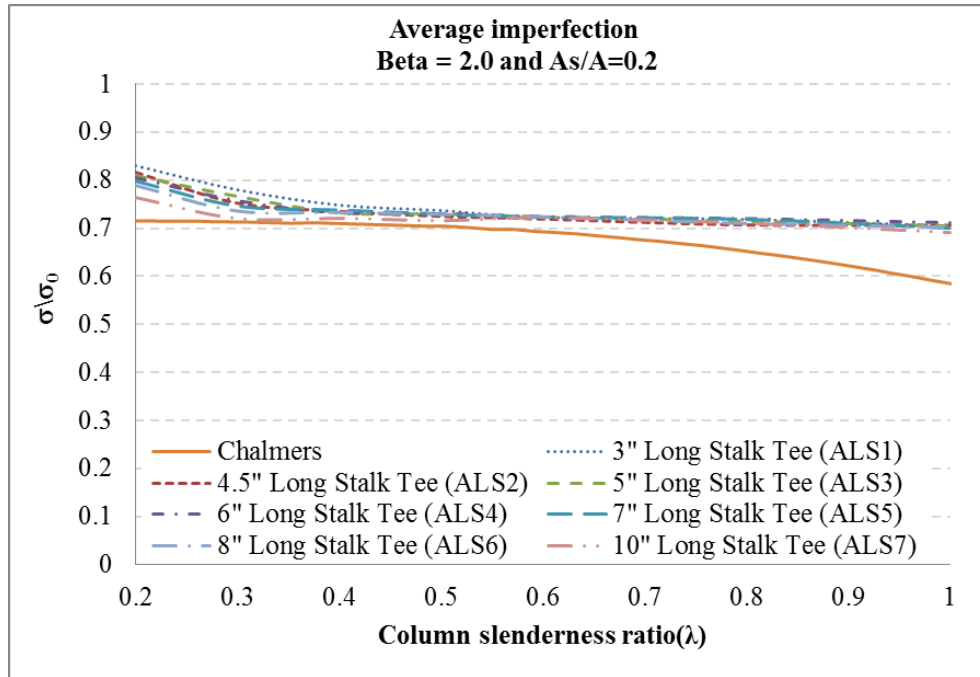


Figure 4.3 Average imperfection of plate slenderness ratio (β) 2.0, stiffener area ratio ($\frac{A_s}{A}$) 0.2.

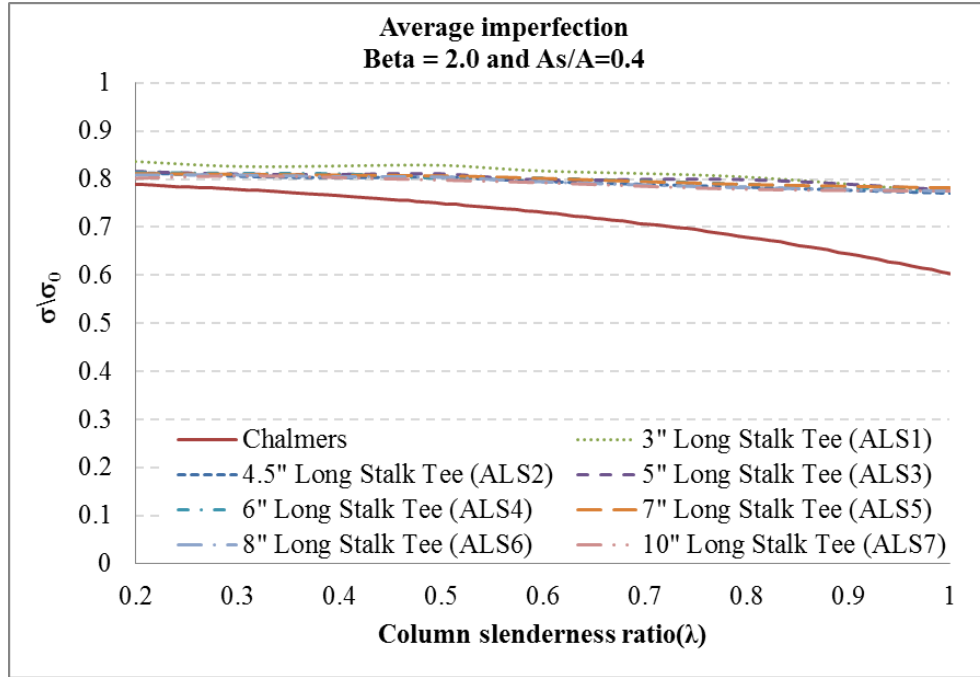


Figure 4.4 Average imperfection of plate slenderness ratio (β) 2.0, stiffener area ratio ($\frac{A_s}{A}$) 0.4.

4.3 Damaged stiffened panels

4.3.1 Damage represented by circular clear-cut hole

The damage analysis has been carried out by focusing on the stiffened area ratio value ($\frac{A_s}{A}$) at 0.2 with stiffener type ALS3. The behaviour of damaged stiffened panels with a clear-cut hole area is compared with the intact stiffened panel in Figure 4.5. Both models use the same parameters of stiffened panel which have a plate slenderness ratio (β) = 2.0, and column slenderness ratio (λ) = 0.3. The results demonstrate that the inter-frame collapse mode still occurs in the middle of the stiffened panel.

Comparison between intact stiffened panel and damaged clear-cut hole panel

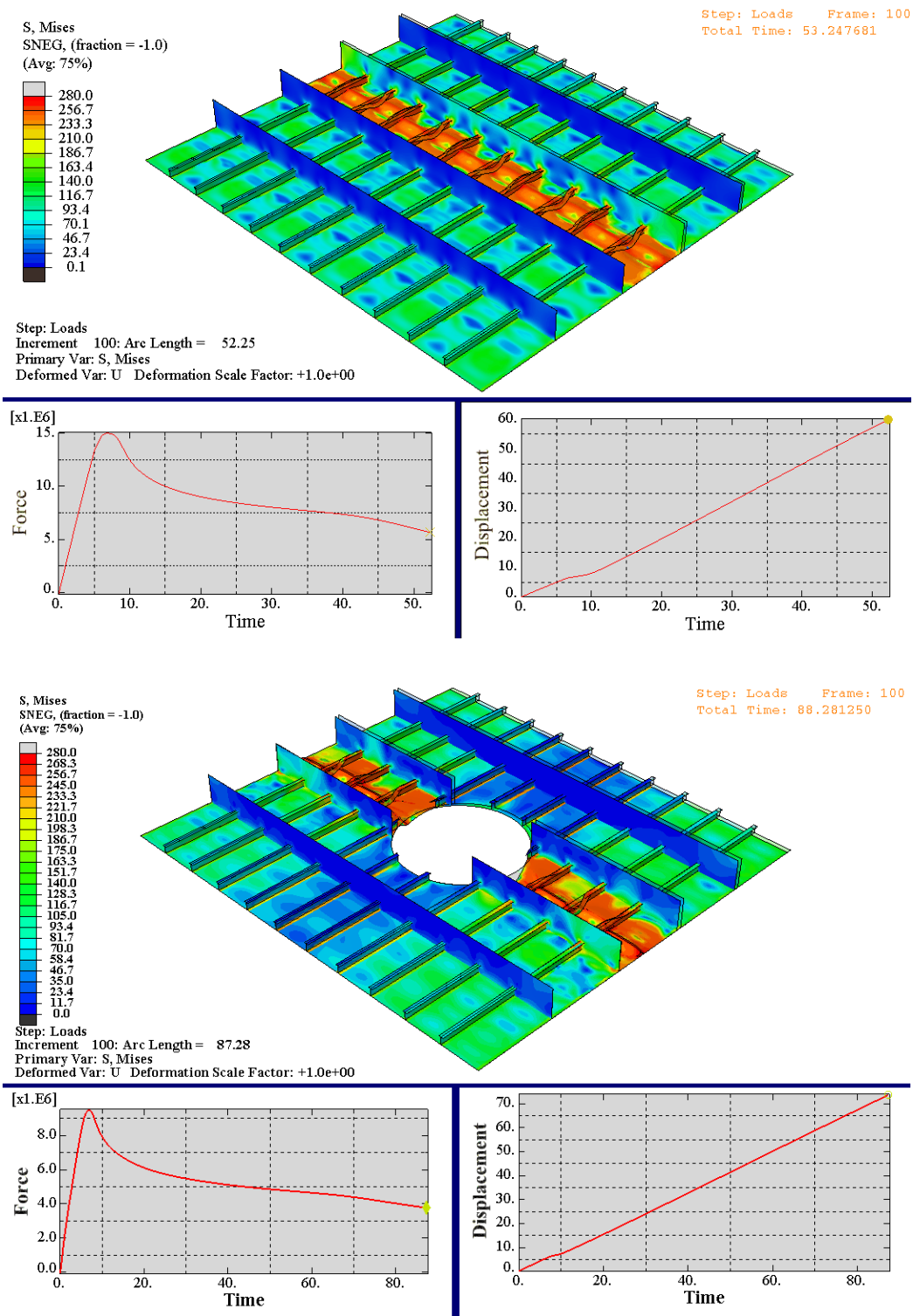


Figure 4.5 Comparison between intact stiffened panel and damaged clear-cut hole panel.

In addition, the cut-out area modifies the residual stress pattern of the stiffened panel at the beginning of the analysis. The cross sectional area of the panel is decreased by the circular cut-out. Consequently, a similar pattern with a reducing collapse strength occurs, as in Figure 4.6. The bigger the cut-out area, the larger the reduction of strength in the stiffened panel. The strain value at ultimate strength is almost constant throughout the range. This means that the pre-collapse stiffness of the load-shortening curve correspondingly reduces.

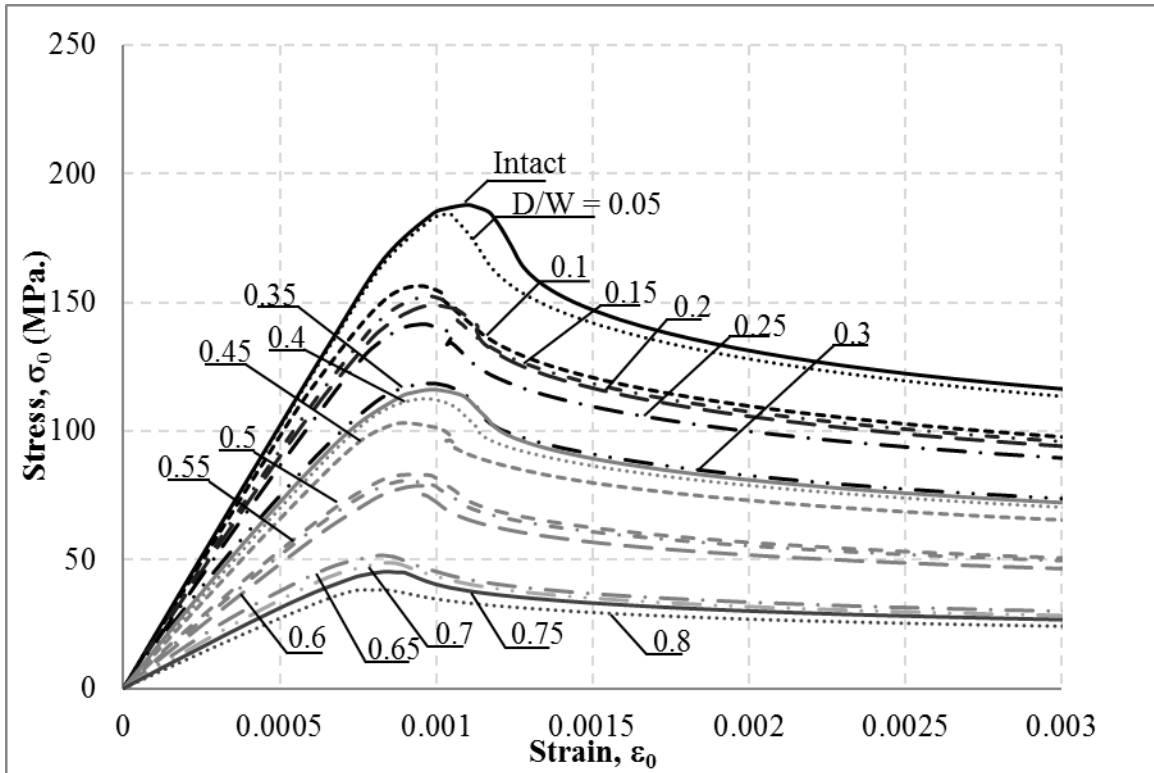


Figure 4.6 Stress-strain curve of damaged clear-cut hole with plate slenderness ratio (β) = 2.0, column slenderness ratio (λ) = 0.3, stiffener area ratio ($\frac{A_s}{A}$) = 0.2 and ALS3.

The effect of increasing the diameter of the circular cut-out area on the stiffened panels is demonstrated in finite element plots in Table 4.2. From these plots a number of observations can be made:

- The comparison shows the difference of stress distribution from the damaged area. When the damaged area ratio ($\frac{D}{W}$) increases from 0.05 to 0.8, the larger stress distribution is

introduced into the stiffened panel.

- The higher stress areas of the panel are concentrated in the zones outside of the damaged hole, where stress paths remain intact. The hole creates a “shadow” area across the longitudinal extent of the panel where the stress is relieved. This is more obvious at the yield point where stress is distributed across the entire length of the panel, whereas in the post-buckling region the stress concentrates in the nucleated region.
- When the damaged area ratio reaches 0.2, the frames adjacent to the central bay are also “cut” by the idealised hole. However, this does not have a significant effect on the buckling mode of the panel, which remains interframe. This is an important result because it demonstrates that, at least with larger frame sizes, the damage length is not a significant factor.

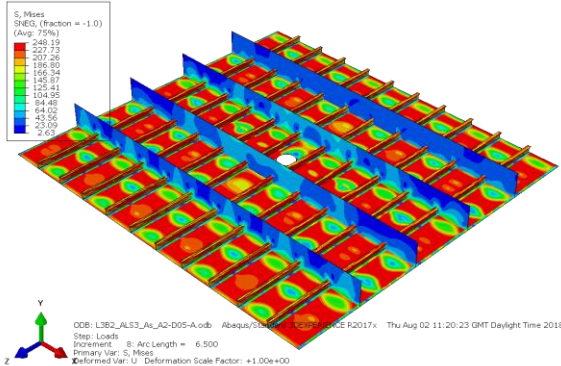
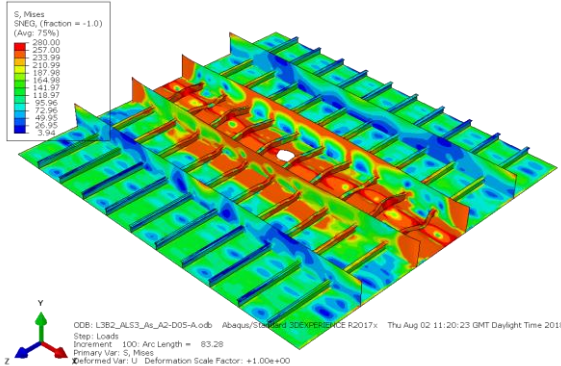
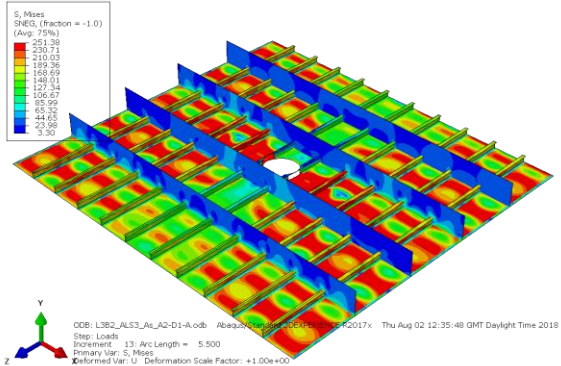
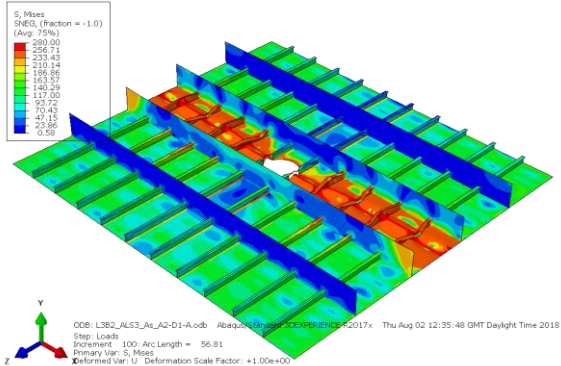
These results suggest that the ultimate strength and failure mechanism in the damaged panel is dominated by the behaviour of the structure outside the damaged zone in the transverse direction, and is not affected by the behaviour of the structure in the longitudinal “shadow” region.

However, this is only valid when the transverse frames are large enough to continue supporting the panel and therefore the resulting buckling behaviour is interframe. For the example shown in Table 4.2 this is even the case for extreme levels of damage where almost the entire panel cross-section is removed.

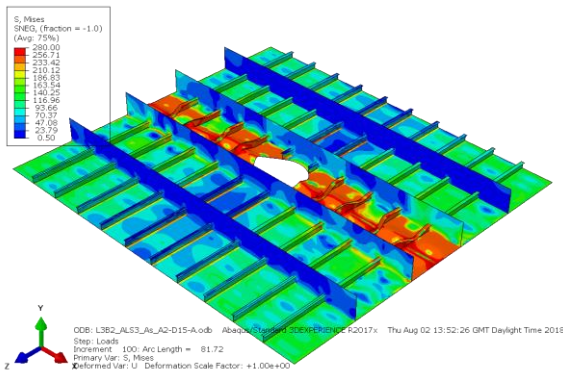
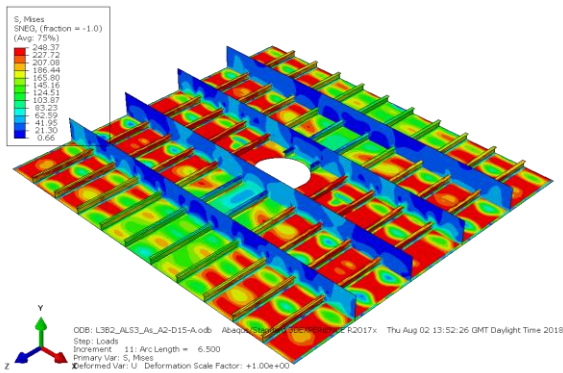
The complete set of results for this analysis is provided in Appendix C.

Table 4.2 The behaviour of damaged clear-cut hole panels with plate slenderness ratio (β) of 2.0, column slenderness ratio (λ) = 0.3, stiffener area ratio ($\frac{A_s}{A}$) = 0.2 and ALS3.

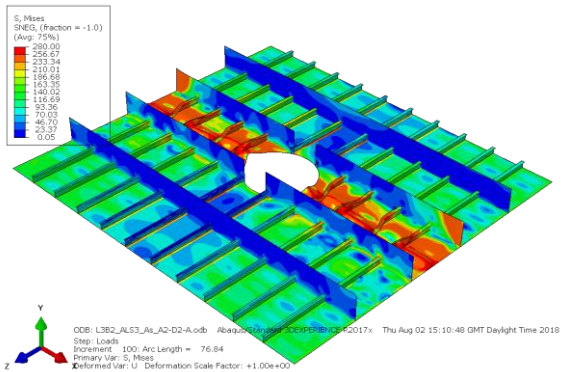
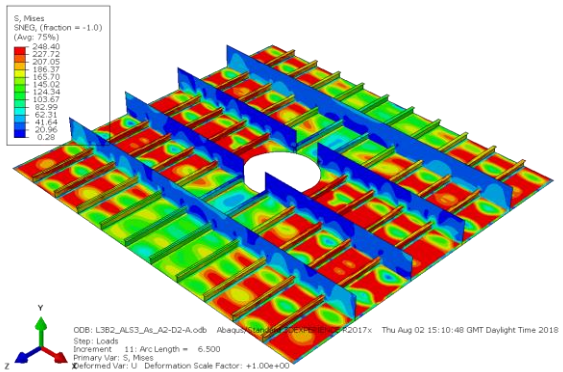
Damaged clear-cut hole panels with Beta = 2.0, Lamda = 0.3
with damaged area ratio ($\frac{D}{W}$) from 0.05 to 0.8

| $\frac{D}{W}$ | Yield point | Buckling |
|---------------|---|--|
| 0.05 |  |  |
| 0.10 |  |  |

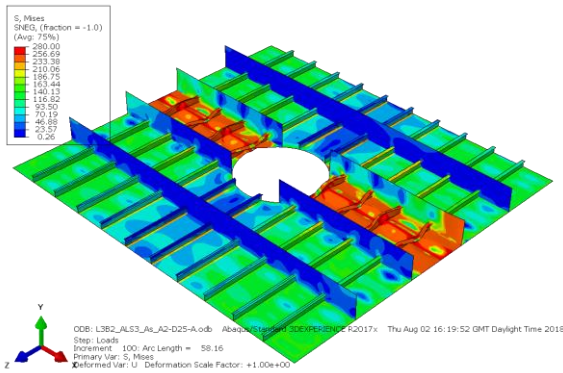
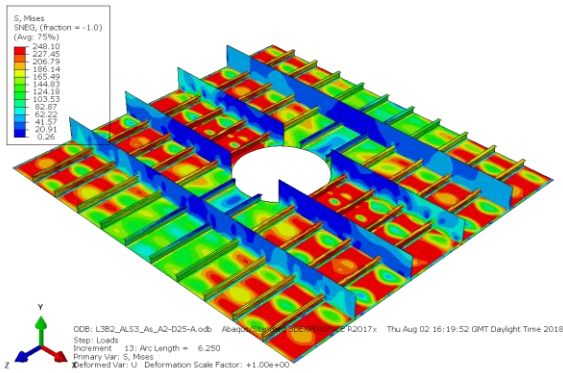
0.15



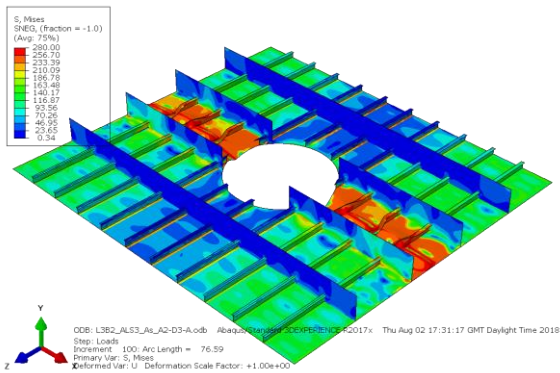
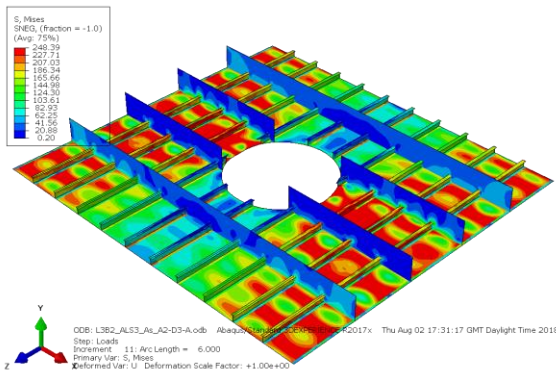
0.20



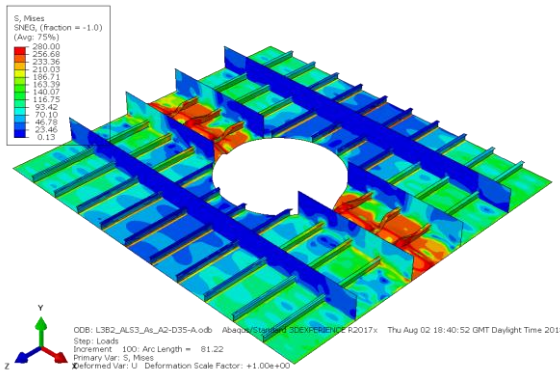
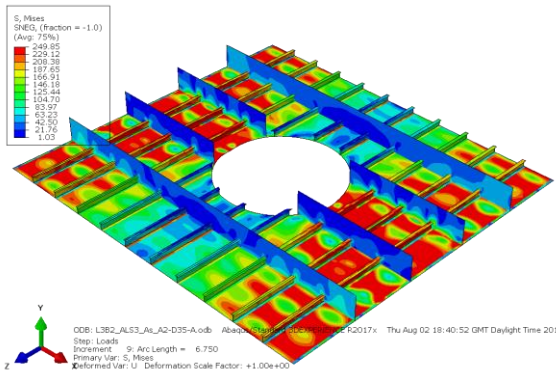
0.25



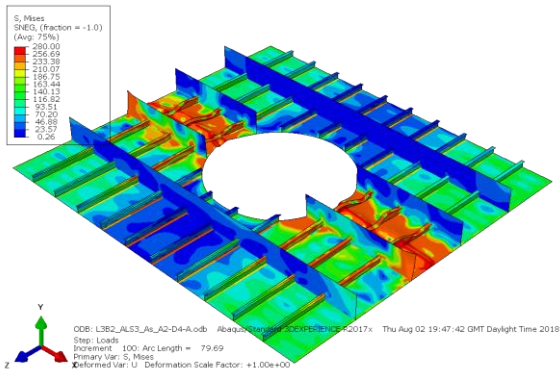
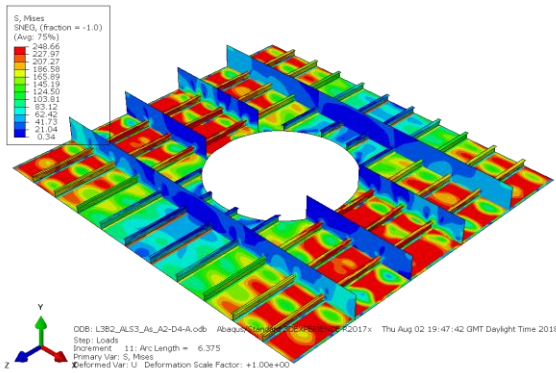
0.30



0.35

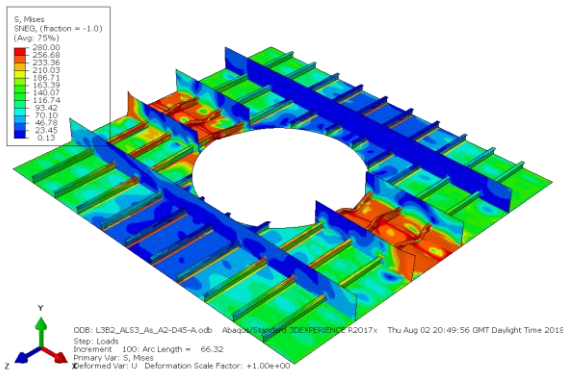
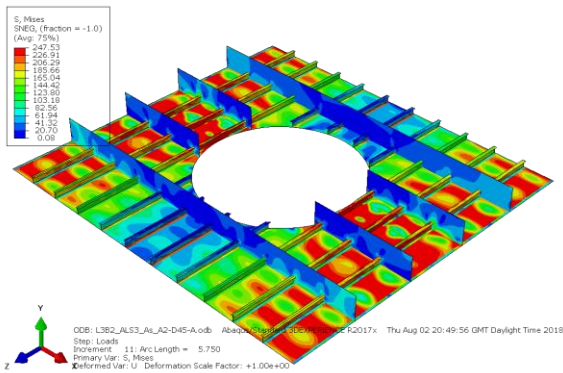


0.40

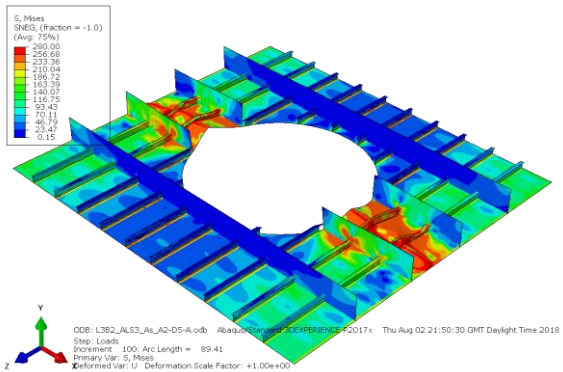
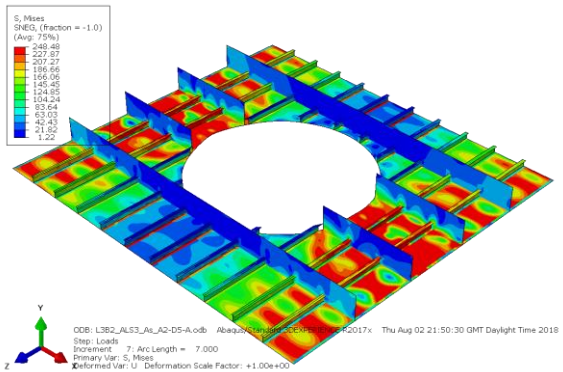


Progressive collapse of damaged ship structure

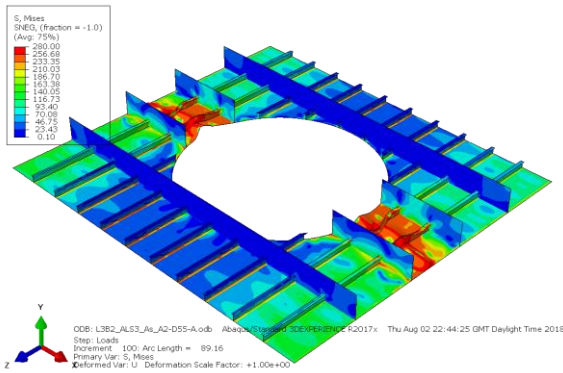
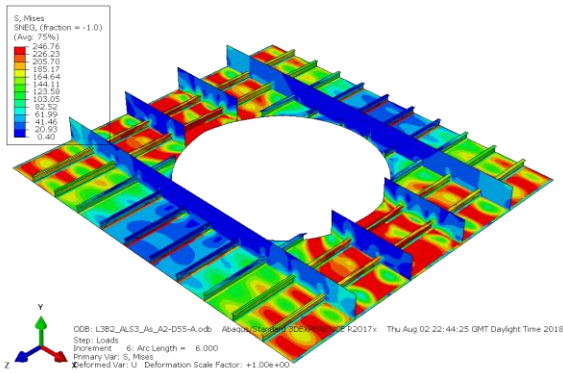
0.45



0.50

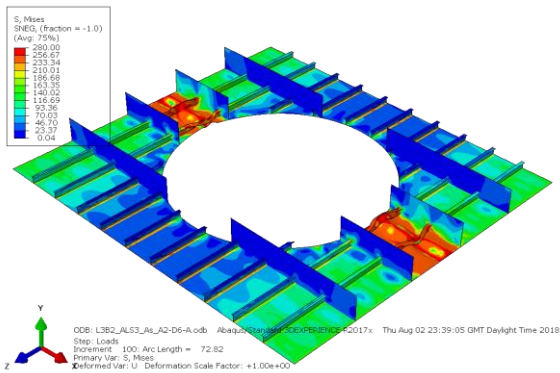
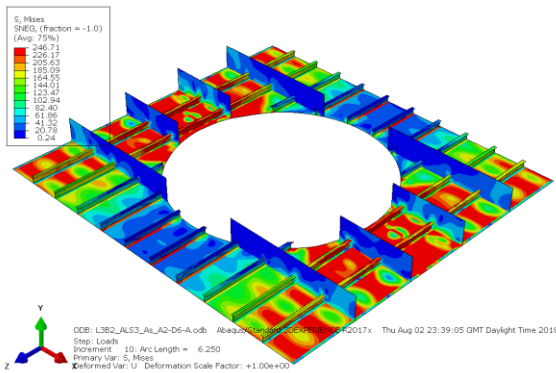


0.55

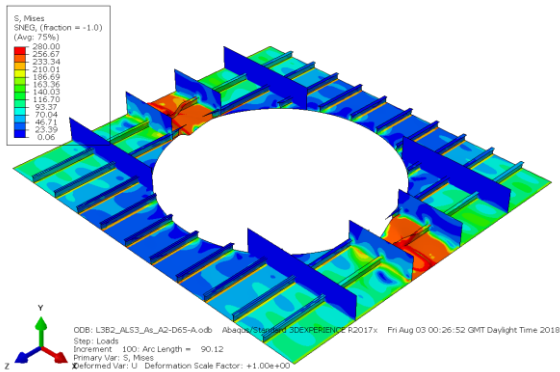
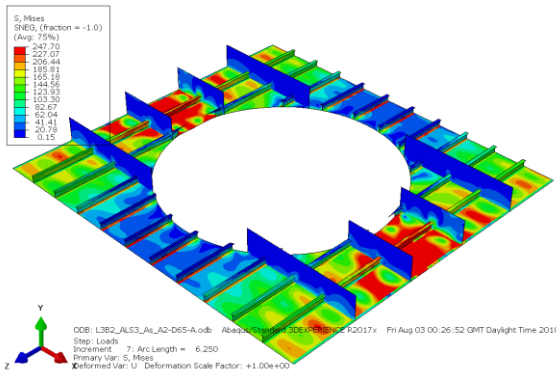


Progressive collapse of damaged ship structure

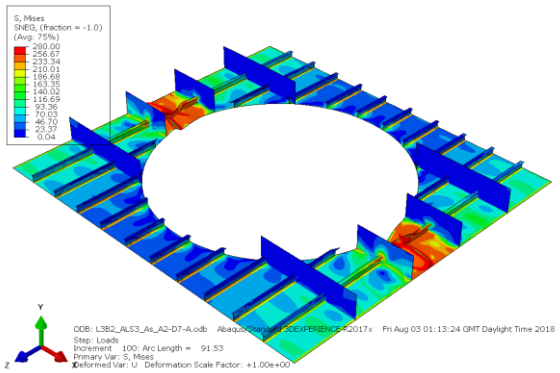
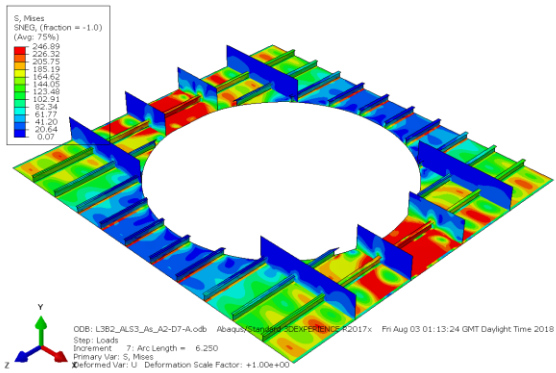
0.60



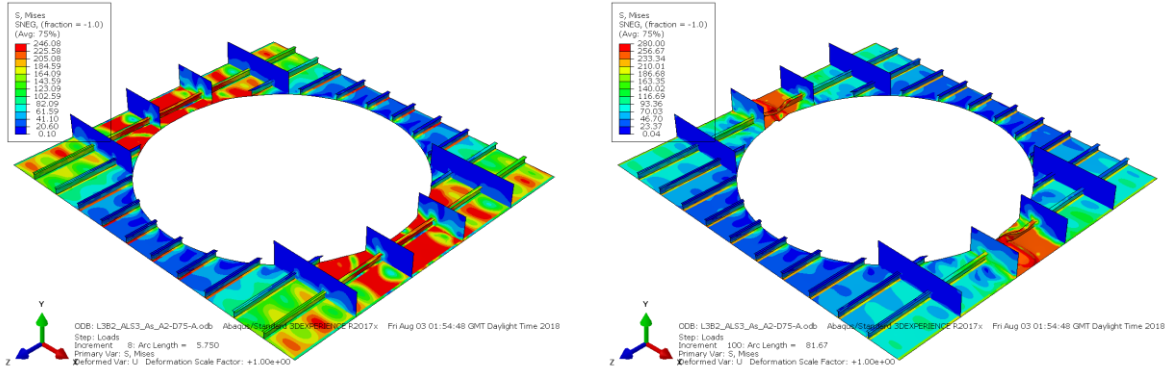
0.65



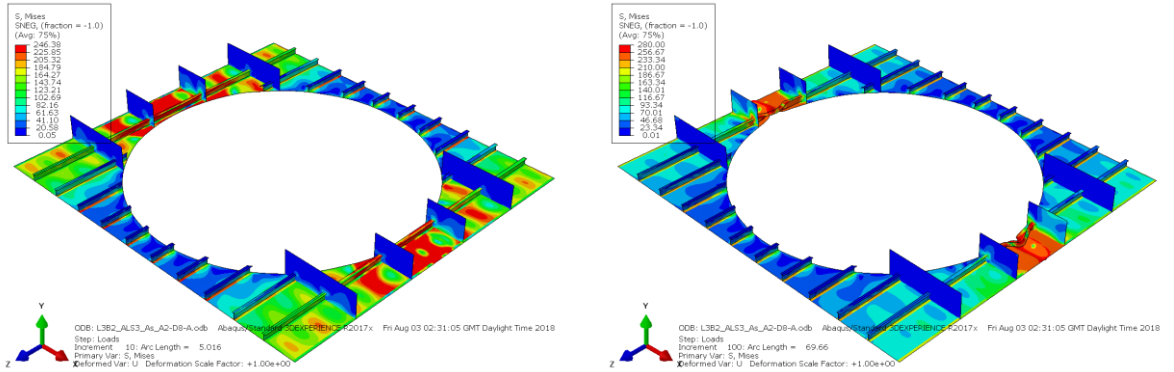
0.70



0.75



0.80



The ultimate strength of damage represented by clear-cut hole is provided for each plate slenderness ratio (β). The strength of the stiffened panels is compared with the diameter of the circular cut out area ratio ($\frac{D}{W}$) from 0.00 to 0.80. Figures 4.7 to 4.10 present the ultimate strength results, for a plate slenderness ratio (β) equal to 1.0, 2.0, 3.0 and 4.0.

The results demonstrate the ultimate strength reduction pattern which can be divided into three elements. Firstly, a growth in the damage diameter has only a slight effect on the ultimate strength of the panel when the cut-out area is limited to plating between frames. This group of results is represented as flat regions in the curve. A second group of results shows a sharp drop in the ultimate strength, because the cut-out area has been cut through longitudinal stiffeners. In this case, the hole cut through two stiffeners at the same time because the damaged area was located in the middle of the stiffened panel.

Finally, the overall behaviour of ultimate strength is affected by a slight drop in strength due to any loss of cross section area.

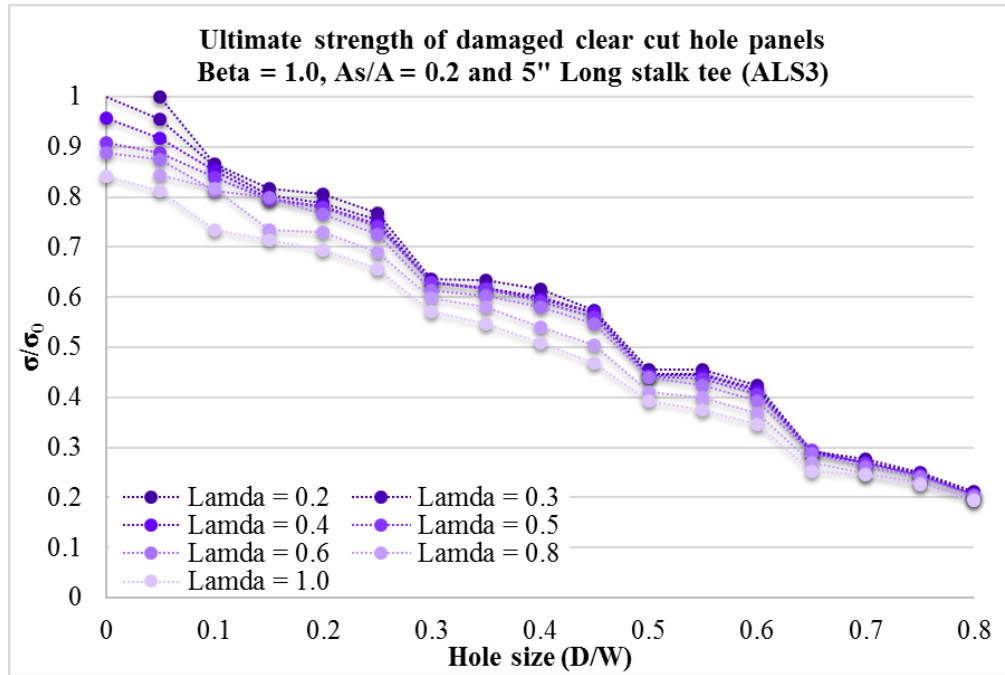


Figure 4.7 Ultimate strength of damaged clear-cut hole panels with plate slenderness ratio (β) = 1.0, column slenderness ratio (λ) = 0.2, stiffener area ratio ($\frac{A_s}{A}$) = 0.2 and ALS3.

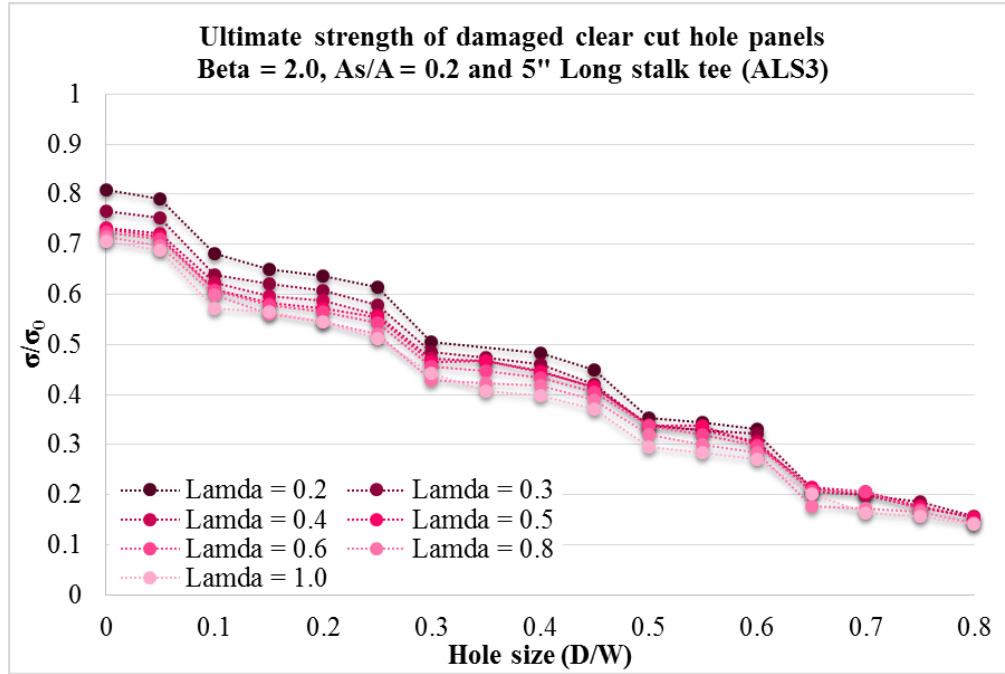


Figure 4.8 Ultimate strength of damaged clear-cut hole panels with plate slenderness ratio (β) = 2.0, column slenderness ratio (λ) = 0.2, stiffener area ratio ($\frac{A_s}{A}$) = 0.2 and ALS3.

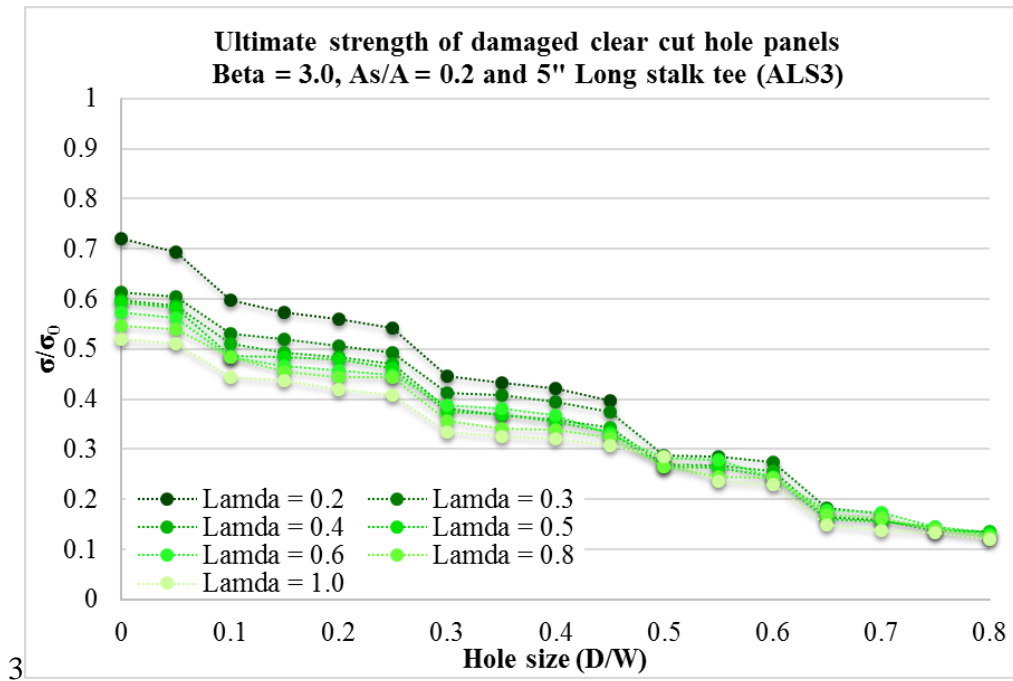


Figure 4.9 Ultimate strength of damaged clear-cut hole panels with plate slenderness ratio (β) = 3.0, column slenderness ratio (λ) = 0.2, stiffener area ratio ($\frac{A_s}{A}$) = 0.2 and ALS3.

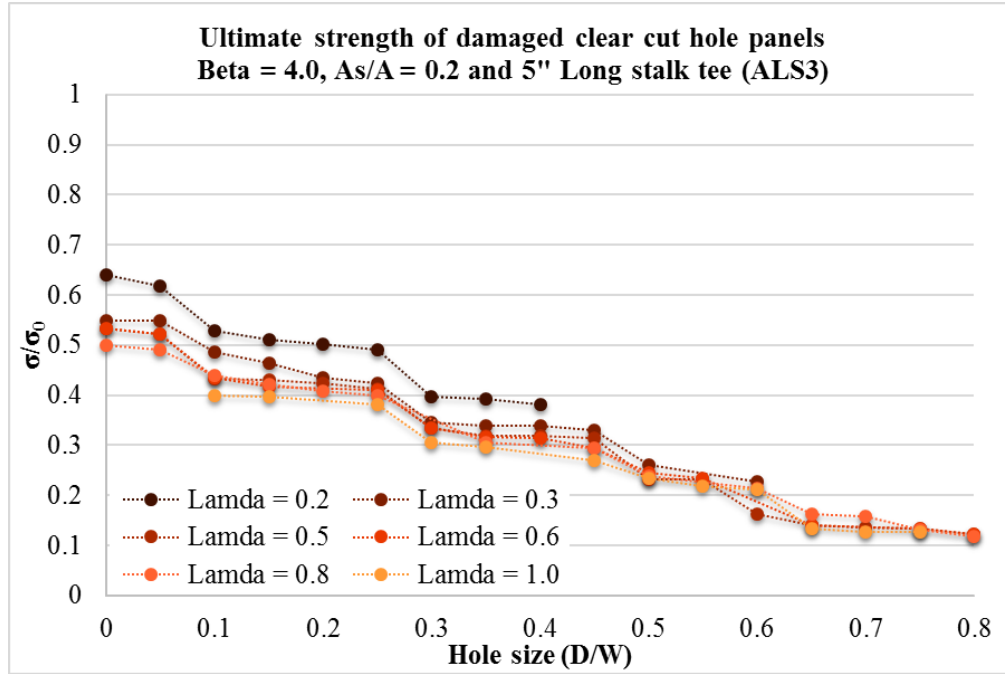


Figure 4.10 Ultimate strength of damaged clear-cut hole panels with plate slenderness ratio (β) = 4.0, column slenderness ratio (λ) = 0.2, stiffener area ratio ($\frac{A_s}{A}$) = 0.2 and ALS3.

Figure 4.11 shows all the ultimate strength results for damage represented by a circular clear-cut hole. The graphs show that plate slenderness area ratio (β) has the main effect on ultimate strength in stiffened panels, more so than the column slenderness ratio (λ) or other parameters. A mean regression line has been plotted through these results for the purpose of modifying the progressive collapse method in ProColl, as will be discussed in Chapter 5.

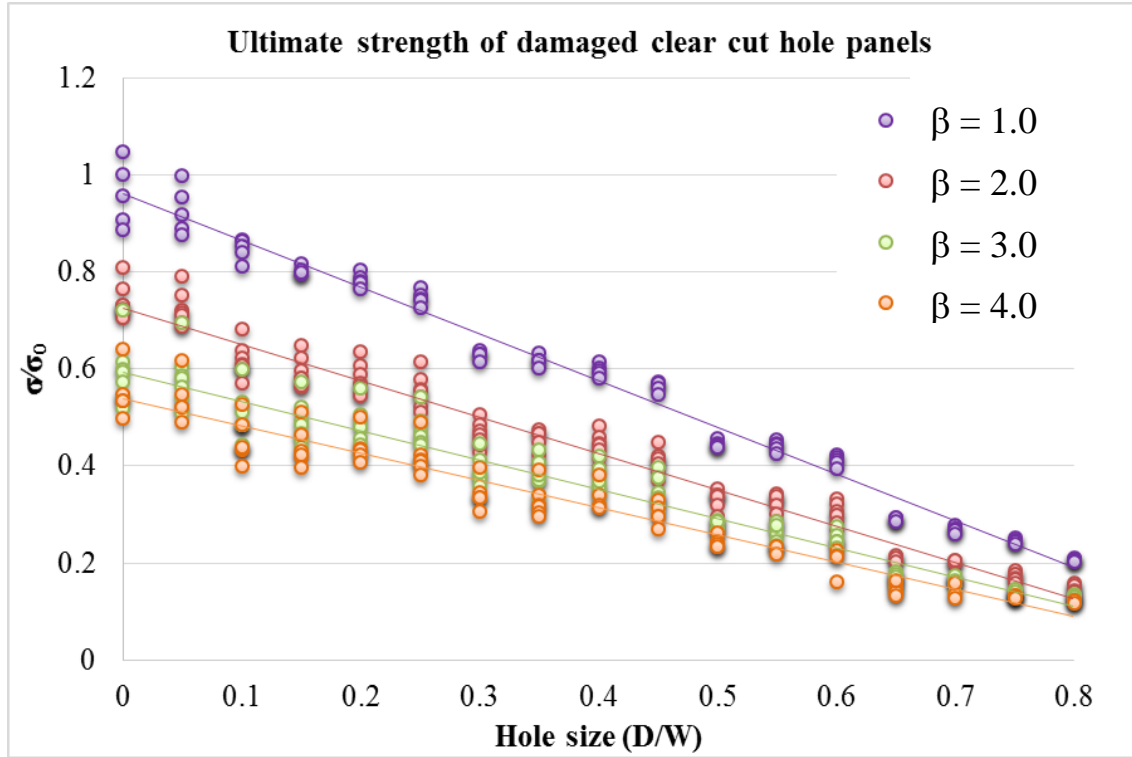


Figure 4.11 Ultimate strength of damaged represented by circular clear-cut hole panels.

To assess the upper and lower bounds of the ABAQUS data compared to the regression line, the coefficient of variation between these results is calculated and shown in Table 4.3. The coefficient of variation (COV) is calculated as the ratio of the standard deviation to the mean of the ratio of ABAQUS to formula ultimate strength. The COV values show that the regression line has good correlation to the simulation results.

Table 4.3 Coefficient of Variation between regression lines and ABAQUS data in Figure 4.11.

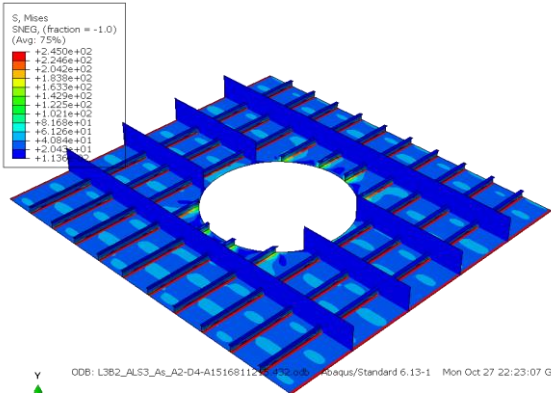
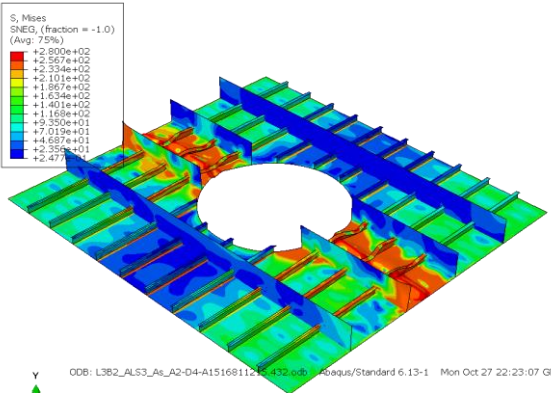
| Plate Slenderness | C.O.V. |
|-------------------|--------|
| 1 | 0.08 |
| 2 | 0.09 |
| 3 | 0.10 |
| 4 | 0.12 |

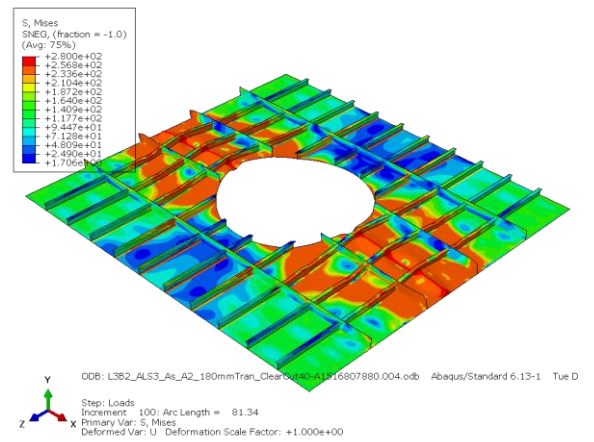
In an effort to match real world applications, this research reduced the transverse frame height from 450 mm to 180 mm to represent a commercial ship’s structure. The new transverse frame height applied similar boundary conditions in order to create an inter-frame collapse behaviour in the damaged stiffened panels, demonstrated in Table 4.3.

In the next section, this new transverse frame height is explored with damage represented by penetration with indenter.

Table 4.4 Comparison of different transverse frame height in stiffened panels.

Damaged clear-cut hole panels with $\beta = 2.0$, $\lambda = 0.3$ and $\frac{D}{W} = 0.40$

| Transverse frame height (mm) | Initial | Buckling |
|---------------------------------------|---|--|
| 450 |  |  |



4.3.2 Damage represented by penetration with indenter

Figure 4.12 shows a set of the results with plate slenderness ratio (β) = 2.0, column slenderness ratio (λ) = 0.3, stiffener area ratio ($\frac{A_s}{A}$) = 0.2 and ALS3. The results show a similar pattern of behaviour to the damage represented by circular clear-cut hole, because the stiffened panels lose their cross section area. The graph presents differences between stresses when transverse frame height decreases to 180 mm; moreover, increasing indenter diameter reduces the strength capacity level in the stiffened panels.

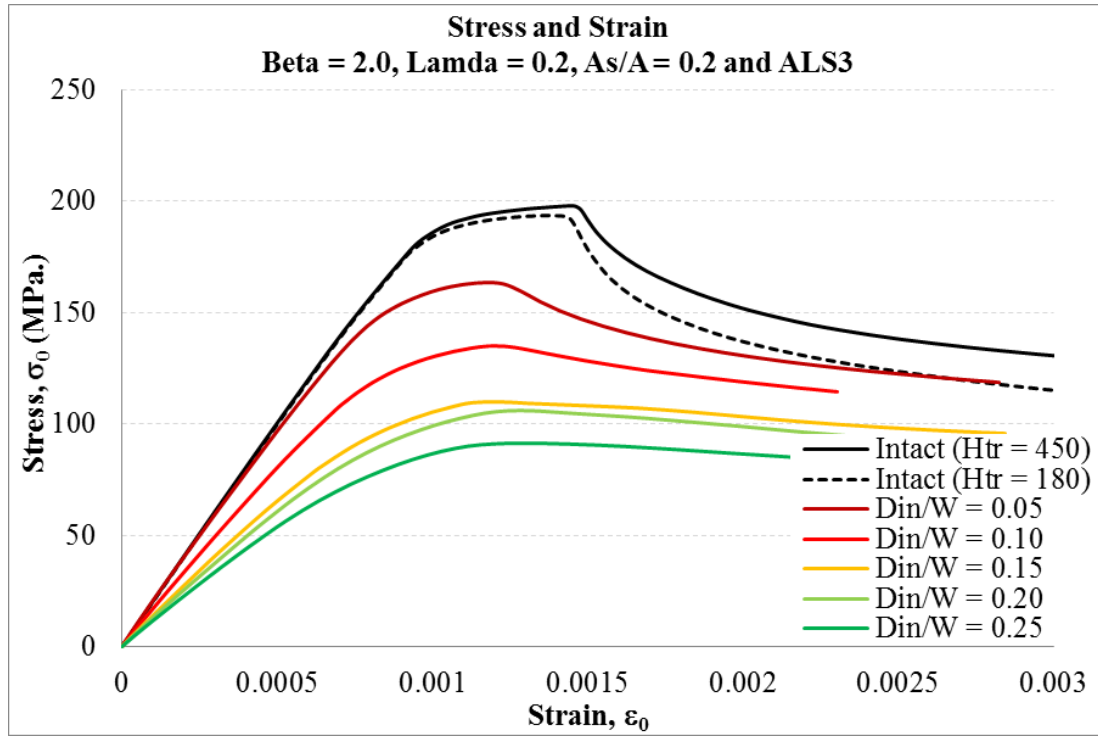


Figure 4.12 Stress-strain curve of penetration damage with indenter on the stiffened panel with plate slenderness ratio (β) = 2.0, column slenderness ratio (λ) = 0.2, stiffener area ratio ($\frac{A_s}{A}$) = 0.2 and ALS3.

The effect of penetration damage with an indenter is shown in Table 4.4. The stiffened panels with plate slenderness ratio (β) = 2.0, column slenderness ratio (λ) = 0.2, stiffener area ratio ($\frac{A_s}{A}$) = 0.2 and ALS3 are demonstrated. The first two rows in the table compares the inter-frame collapse behaviour between two different sizes of transverse frame in intact stiffened panels. The remaining rows in the table compares the collapse behavior of the panel with different damaged

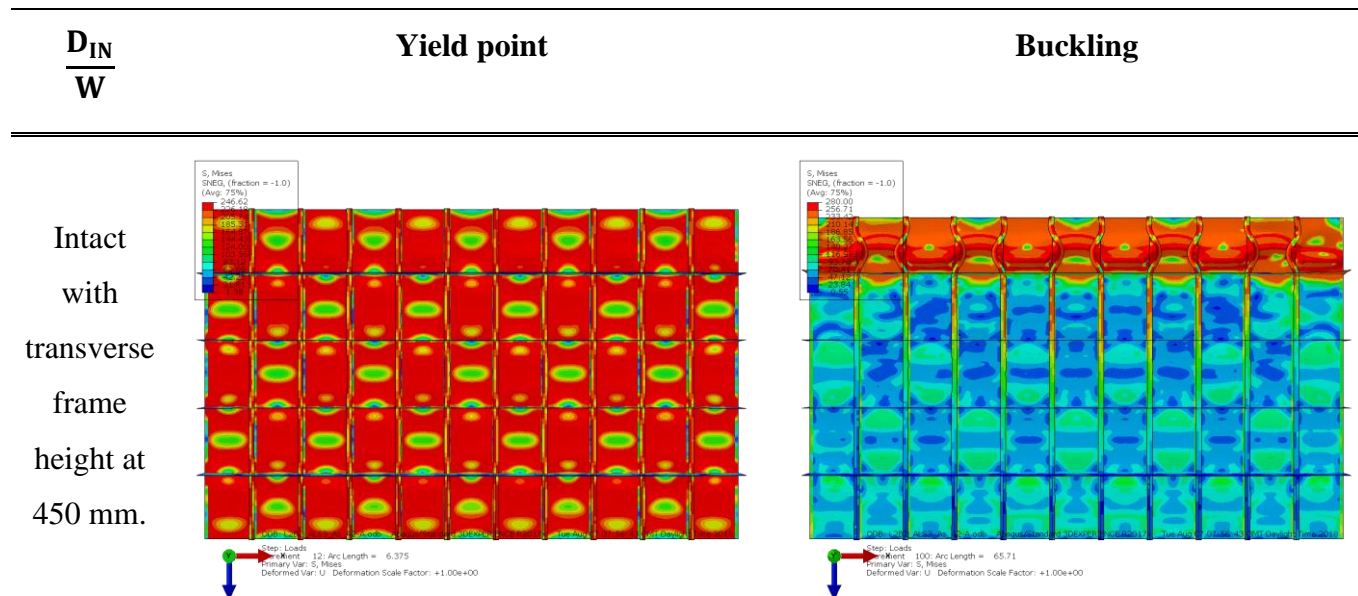
areas generated by penetration with an indenter by control damaged area ratio $\left(\frac{D_{IN}}{W}\right)$, which is represented by the ratio between the diameter of the indenter and the width of the stiffened panel, between 0.05 and 0.25. Unlike the clear cut hole cases, the indenter damage causes a large deformation of the panel surrounding the ruptured hole before any in-plane loading is applied. This also dominates the stress plots, which means it is more difficult to see the subsequent nucleation of buckling when in-plane load is applied. It is apparent that the collapse shape spreads over the entire panel even with a relatively small indenter size. The associated strength reduction plots in Figures 4.14 to 4.17 show a markedly different relationship to the clear cut hole but still demonstrate that the ultimate strength is a function of the ruptured hole size.

This finding means that, in these cases, the penetration has created a bigger damaged area than the diameter of the indenter and if this area can be estimated a relationship with the damaged ultimate strength can be made. Thus, the measurement of the damaged area is considered in this section. The circular area is placed to cover all of the damaged area by controlling the centre of the circle's area to match the centre of the stiffened panel, as shown in Figure 4.13. The diameter of the actual damaged area is used to provide the ultimate strength of the stiffened panels.

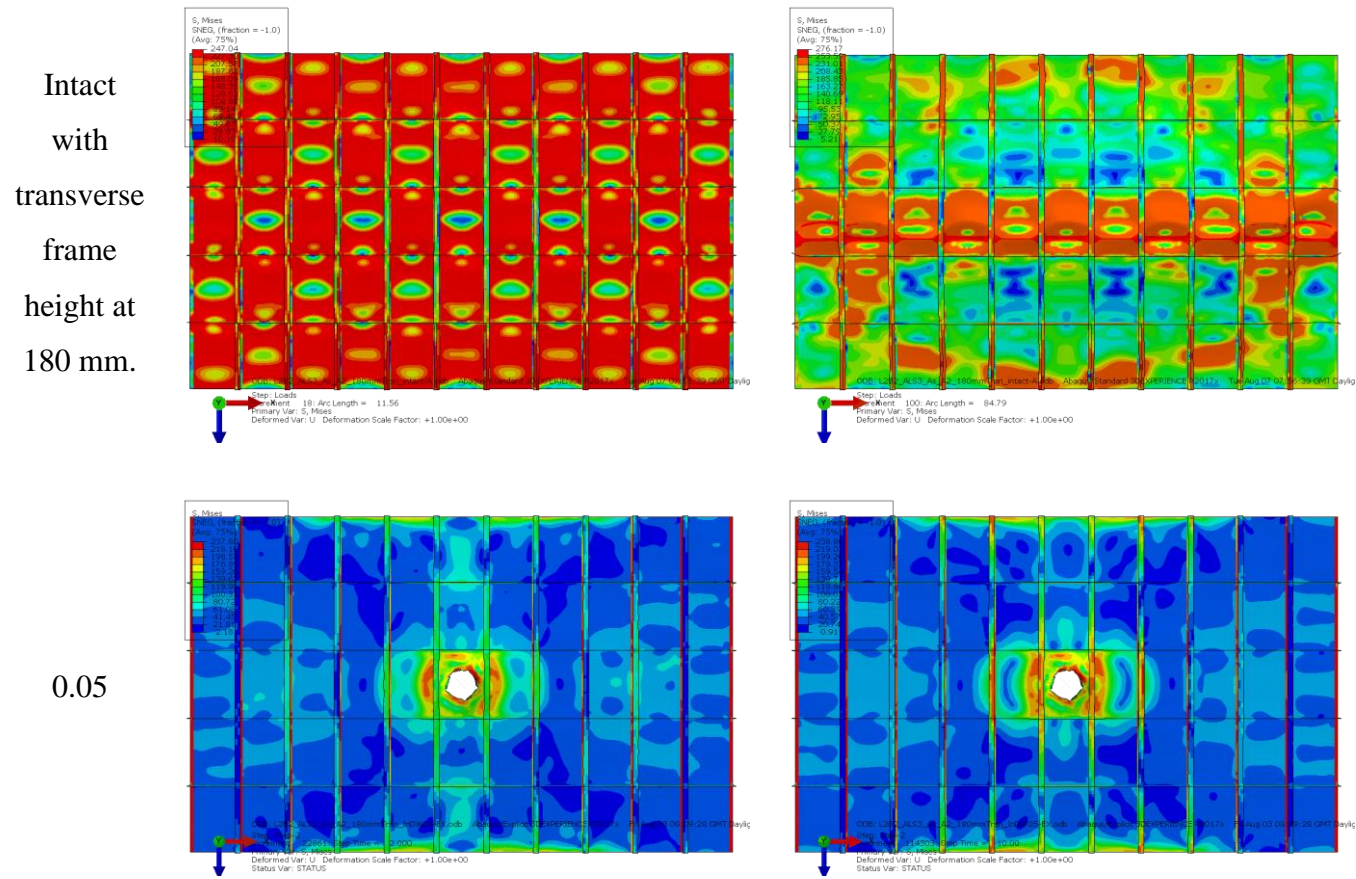
Table 4.5 The effect of penetration damage with an indenter on the stiffened panels with plate slenderness ratio (β) of 2.0, column slenderness ratio (λ) = 0.2, stiffener area ratio $\left(\frac{A_s}{A}\right) = 0.2$ and ALS3.

Damaged clear-cut hole panels with Beta = 2.0, Lamda = 0.2

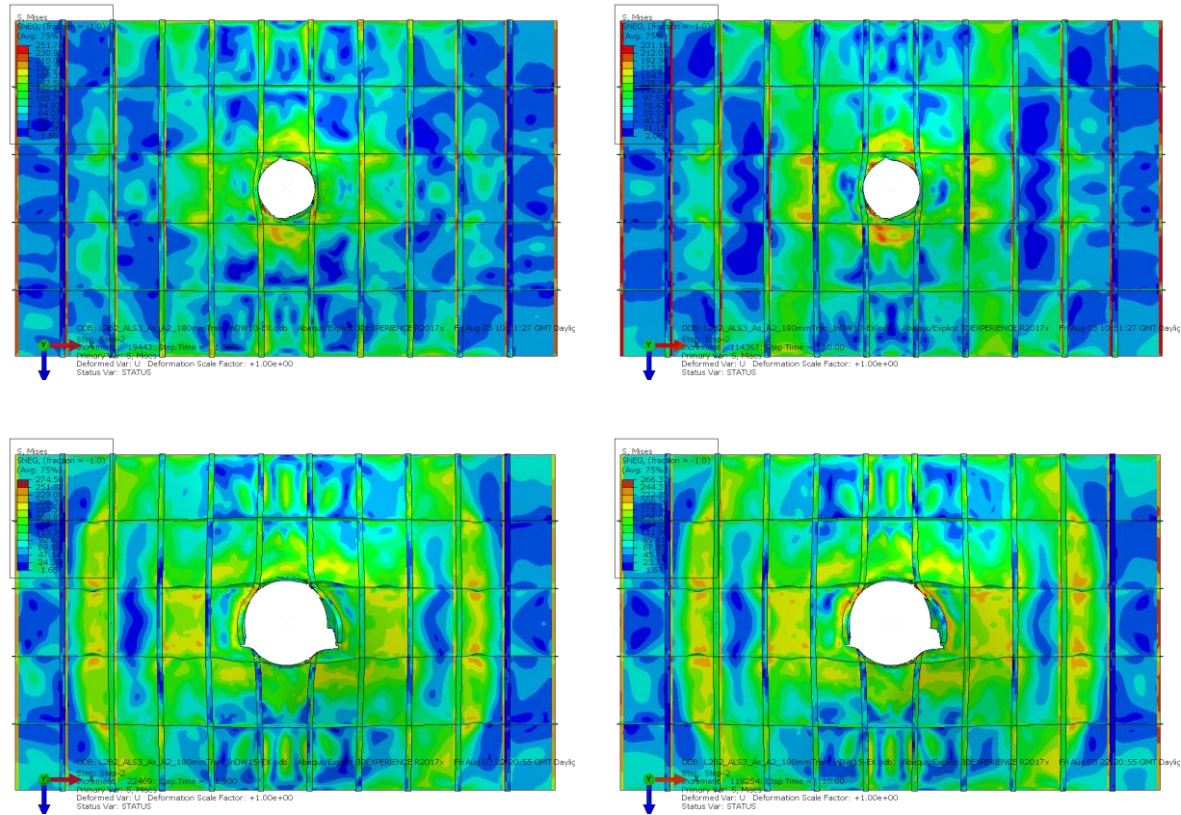
with intact panel and damaged area ratio $\left(\frac{D}{W}\right)$ from 0.05 and 0.25



Progressive collapse of damaged ship structure



0.15



0.25

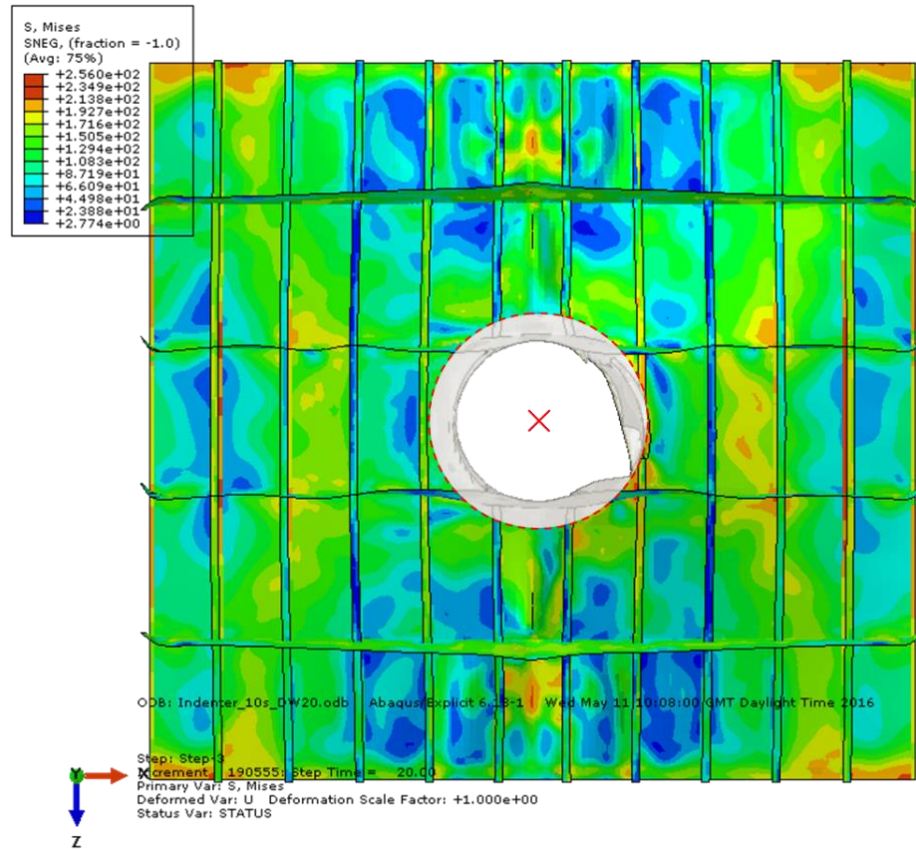


Figure 4.13 the measurement of damaged diameter in penetration with indenter.

The ultimate strength from penetration damage with indenter is provided for each plate slenderness ratio (β). Figures 4.14 to 4.17 present the ultimate strength results for plate slenderness ratios (β) equal to 1.0, 2.0, 3.0 and 4.0.

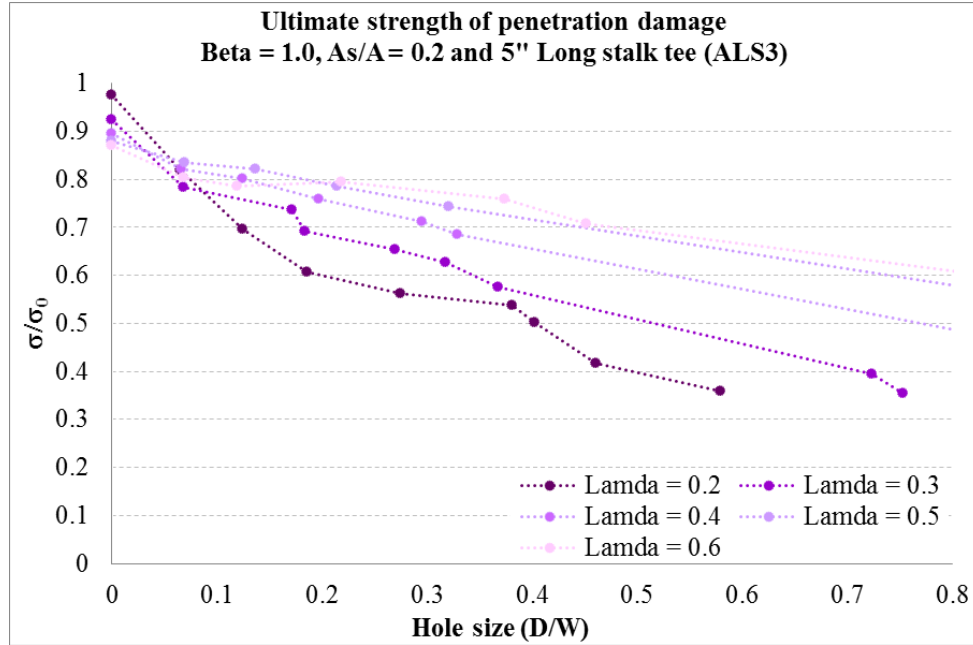


Figure 4.14 Ultimate strength of penetration damage with indenter on the stiffened panels with plate slenderness ratio (β) = 1.0, column slenderness ratio (λ) = 0.2, stiffener area ratio ($\frac{A_s}{A}$) = 0.2 and ALS3.

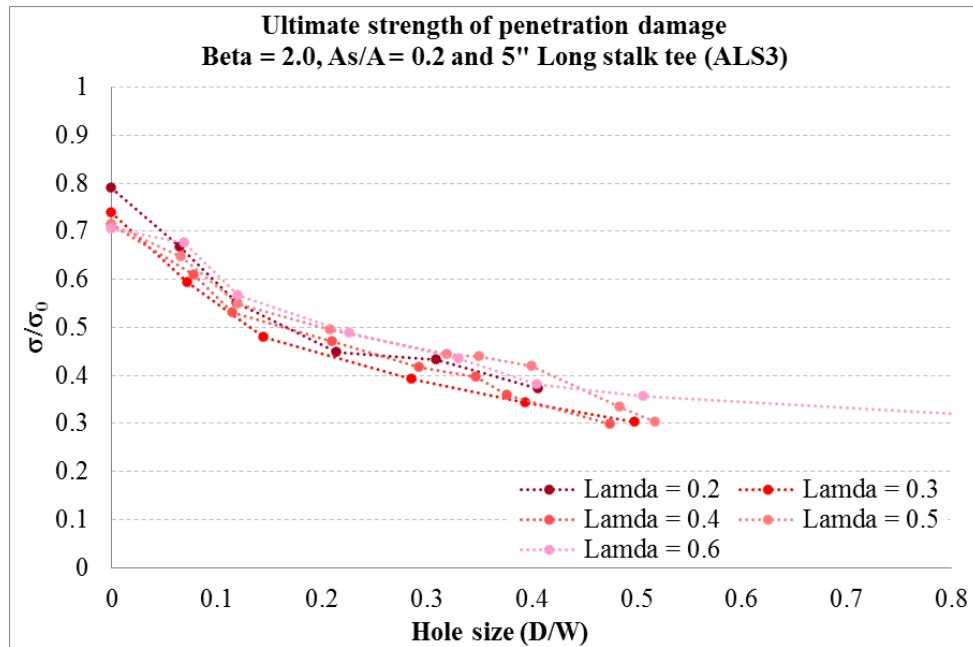


Figure 4.15 Ultimate strength of penetration damage with indenter on the stiffened panels with plate slenderness ratio (β) = 2.0, column slenderness ratio (λ) = 0.2, stiffener area ratio ($\frac{A_s}{A}$) = 0.2 and ALS3.

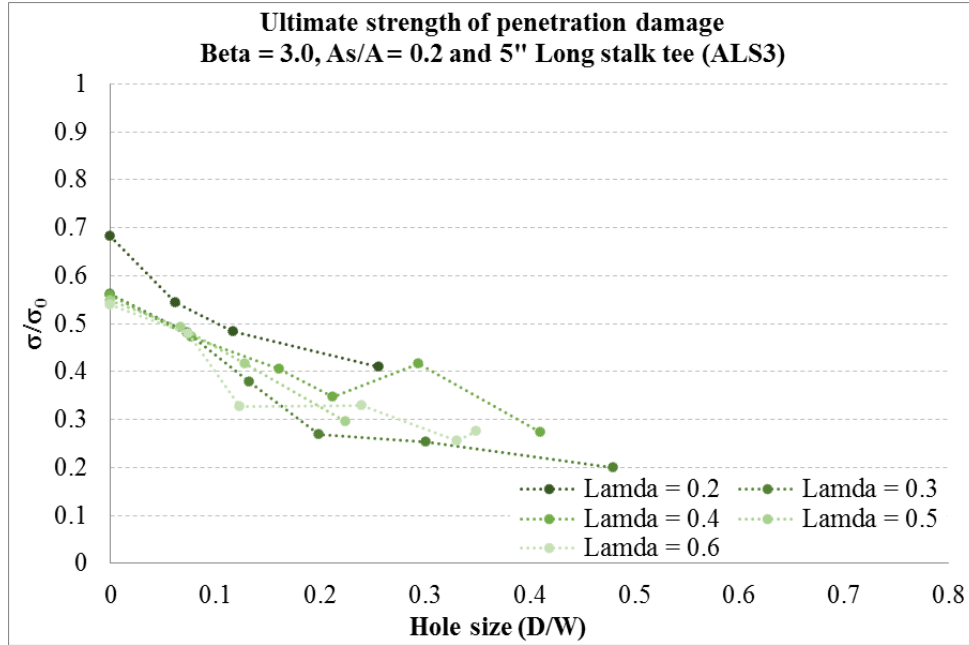


Figure 4.16 Ultimate strength of penetration damage with indenter on the stiffened panels with plate slenderness ratio (β) = 3.0, column slenderness ratio (λ) = 0.2, stiffener area ratio ($\frac{A_s}{A}$) = 0.2 and ALS3.

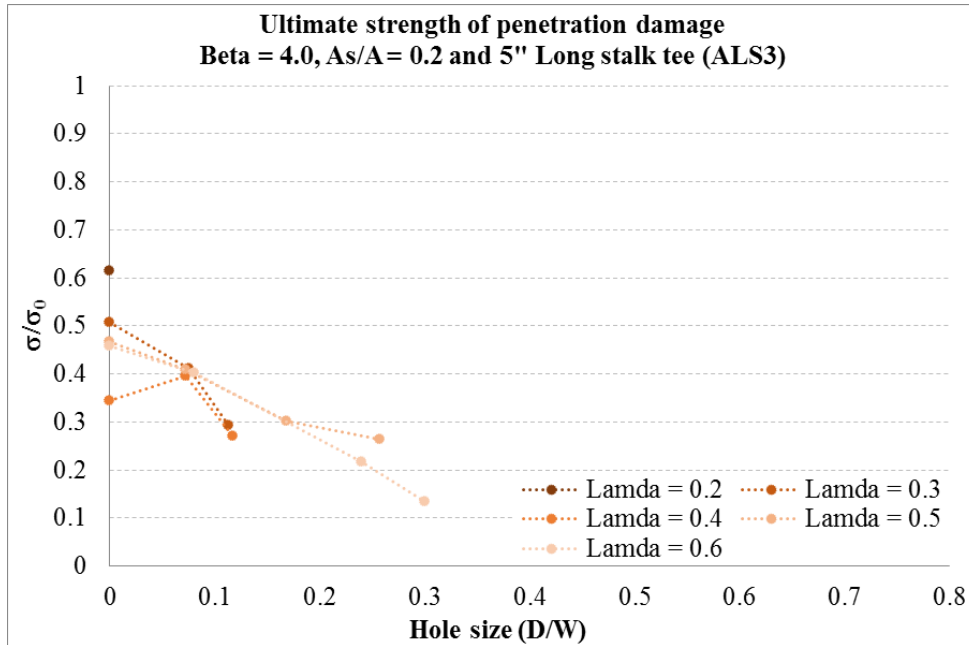


Figure 4.17 Ultimate strength of penetration damage with indenter on the stiffened panels with plate slenderness ratio (β) = 4.0, column slenderness ratio (λ) = 0.2, stiffener area ratio ($\frac{A_s}{A}$) = 0.2 and ALS3.

For this set of results, some solutions were not completed in the simulation because of the capabilities of ABAQUS. All stress and strain curves for penetration damage are provided in Appendix C.

Even so, Figures 4.14 to 4.17 showed similar trends between both damaged groups. The plate slenderness ratio (β) is still a main parameter which has more effect on ultimate strength than the column slenderness ratio (λ). Moreover, ultimate strength reduction occurred because of the cross-section area in stiffened panel which was decreased by penetration.

Mean values for the penetration damage results were generated as a bi-linear line at this stage in order to modify the simplified method in ProColl. Figure 4.18 shows the mean value of four different plate slenderness ratios (β).

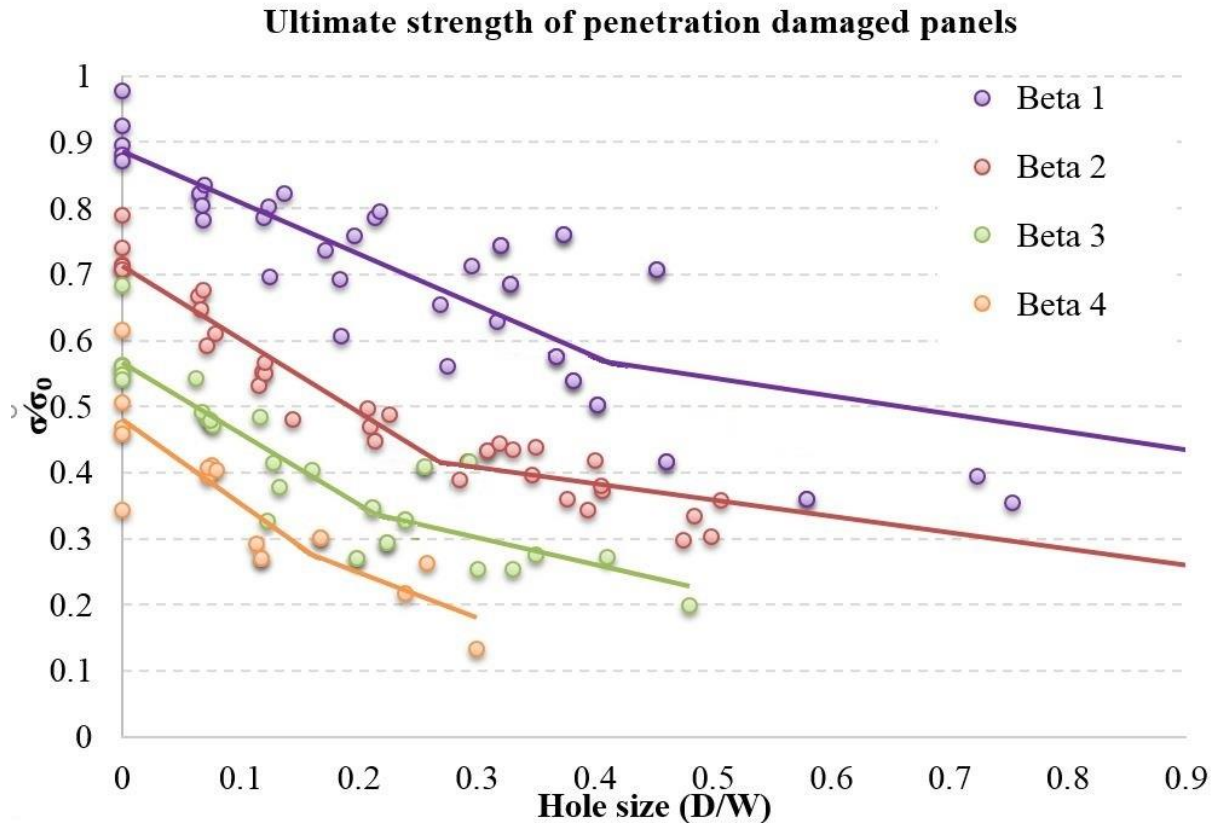


Figure 4.18 Ultimate strength of damage represented by penetration with indenter.

Using the same method as for the clear cut hole, the upper and lower bounds of the ABAQUS

data is compared to the regression line using the coefficient of variation as shown in Table ???. As expected, the larger values of COV show somewhat greater scatter in the data when compared to the clear cut hole.

Table 4.6 Coefficient of Variation between regression lines and ABAQUS data in Figure 4.18.

| Plate Slenderness | C.O.V. |
|-------------------|--------|
| 1 | 0.16 |
| 2 | 0.08 |
| 3 | 0.14 |
| 4 | 0.17 |

4.4 Summary

This chapter presents results from three case studies on stiffened panels in this research. The results are controlled under several parameters, notably plate slenderness ratio (β), stiffened panel slenderness (λ) and stiffened area ratio $\left(\frac{A_s}{A}\right)$.

Intact stiffened panels' results show a close match in behaviour between finite analysis and a standard design curve. On the other hand, the damage case studies show signs of significant effects on the strength of stiffened panels based on one parameter: plate slenderness ratio (β). The strength reduction is caused by the damaged area, which reduces the cross-sectional area of the stiffened panels.

The mean value of ultimate strength has been prepared for further modification of the progressive collapse method in ProColl.

Chapter 5 The extended progressive collapse method

5.1 Introduction

This chapter shows an extension to the simplified progressive method (ProColl) which includes damaged areas in the calculation process. The results of previous studies are used to generate the knockdown factor and put it into the simply method. The chapter shows the development of the program and a validation with a box girder is included in the damage effect.

5.2 Overview of the simplified method

In general, the simplified method (ProColl) has been developed from the progressive collapse method by Benson et al. (2013d), Benson et al. (2015). It aims to reduce the time spent on analysis and give accurate results to the designer. The modified simplified method which includes damage effects should be a more beneficial program for commercial ship design.

Figure 5.1 demonstrates an overview of the modified ProColl with damage effect.

1. ProColl uses the simplified progressive collapse method to generate a load shortening curve for an individual element in the hull girder cross section area.
2. In the damaged structure cases, the damage type is chosen, either being damage represented by circular clear-cut out or damage represented by penetration with an indenter.
3. The diameter of the damaged area in stiffened panels is added in the form of a damaged area ratio.
4. ProColl re-calculates the load shortening curve for the damage panel by using the knockdown factor that is presented in section 5.2.
5. The new load shortening curve for damage panel is sent back to be analysed with other elements in the hull girder and generate incremental curvatures and moments to obtain total cumulative values for the hull girder.

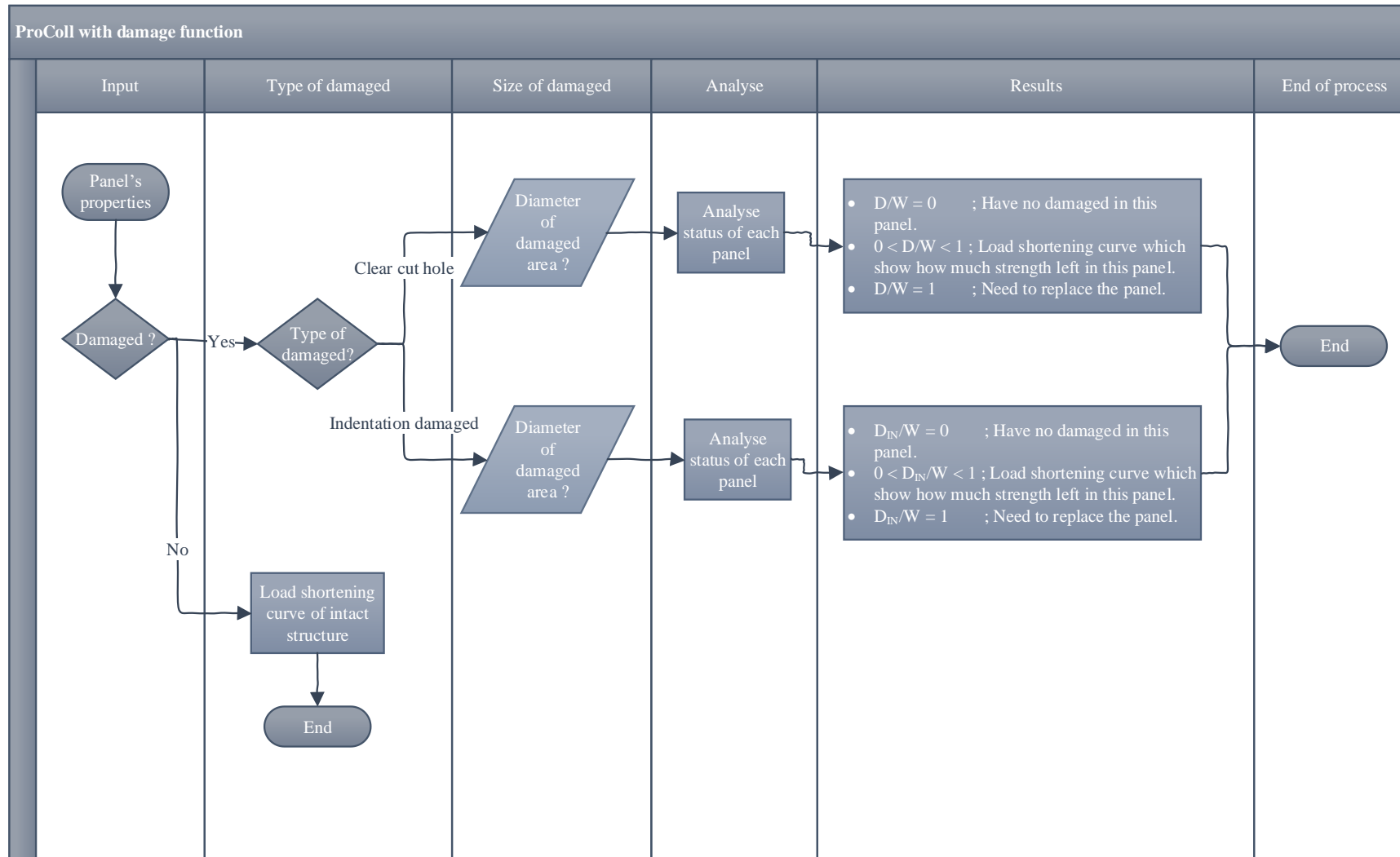


Figure 5.1 Overview of modified simplified method (ProColl).

5.3 Modified process

The modifications to the simplified progressive collapse method are presented in several steps, as shown in the sub-sections below.

5.3.1 *Comparison of intact stiffened panel results*

The comparison between ABAQUS and ProColl is presented in this section in order to verify the results by using key assumptions of the progressive collapse method. The progressive collapse method considers the strength of independent members in the structure (Benson, 2011). A combination of a single plate and stiffener can be used to represent the behaviour of an entire stiffened panel. Figure 5.3 shows an ideal small panel which is used in a comparison between ABAQUS and ProColl in this section.

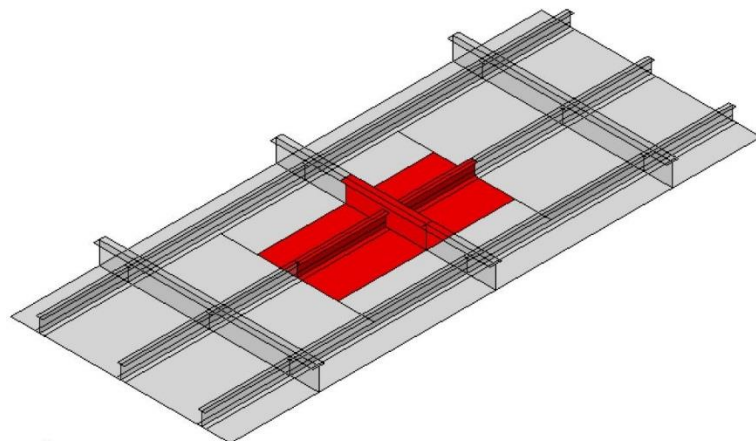


Figure 5.2 Idealise of small panel (Benson, 2011)

5.3.2 *Knockdown factor from damaged stiffened panels*

The modification of the simplified method begins with the knockdown factor, which is a key formula to generate a load shortening curve with a damage effect. The use of a knockdown factor was chosen for the following reasons:

- Knockdown factors are a convenient and fast method to re-evaluate the load shortening curve within the iterative analytical progressive collapse method, enabling fast re-

evaluation of the global ultimate strength

- It was found that the load shortening curve keeps the same overall shape and stiffness characteristics after damage has been applied to it.
- The principal change to the load shortening curve is the reduction in the ultimate strength. The applied strain at which ultimate strength is attained remains at the same value as for the intact case. This implies that the damage load shortening curve can be redefined by adjusting the applied stress only.
- Use of a knockdown factor follows a similar philosophy and terminology to the use of factors in classification rules and guidance such as the IACS common structural rules, where the simplified progressive collapse method is stipulated. This means that the application of a knockdown factor here enables the use of this method in an industrial context, for example the potential for the method to be incorporated into classification rules.

The ultimate strength of a damaged stiffened panel is presented in Chapter 4, and used to create the knockdown formula by finding the mean value of each set of results in damaged clear-cut hole panels and penetration damage with indenter, as shown in Figures 4.11 and 4.18 respectively.

Both linear and bi-linear line fit have been used to fit this set of non-dimension curves, which are separate as a group of plate slenderness ratios (β) from 1 to 4. Figure 5.3 shows the set of non-dimensions of damaged clear-cut hole panels with the linear line. Each line is represented with the knockdown formula in the box on the left-hand side. Intermediate values of slenderness are evaluated using linear interpolation.

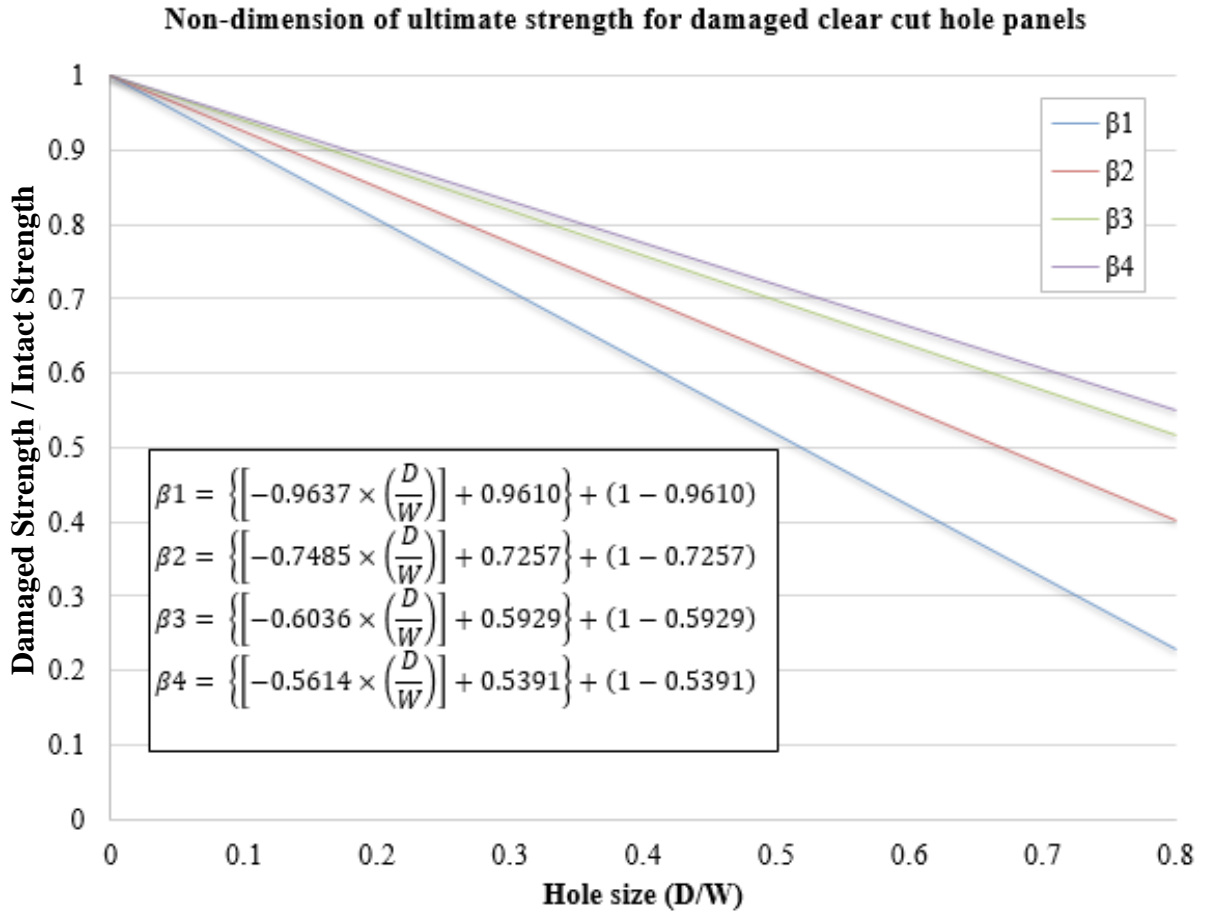


Figure 5.3 Knockdown factors for damage represented by circular clear-cut hole.

On the other hand, the knockdown formula for penetration damage is developed from a bi-linear line which includes a turning point to switch between knockdown formulas, as presented in Table 5.1.

Table 5.1 Turning point of knockdown formulae in penetration damage.

Turning point of knockdown formula in penetration damage

| <i>Plate slenderness ratio (β)</i> | <i>Damage area ratio</i> |
|---|--------------------------|
| β_1 | 0.45 |
| β_2 | 0.30 |
| β_3 | 0.25 |
| β_4 | 0.20 |

The turning point is used for change first group of knockdown formula to second group of formula in Figure 5.4 which presents a non-dimension of penetration damage.

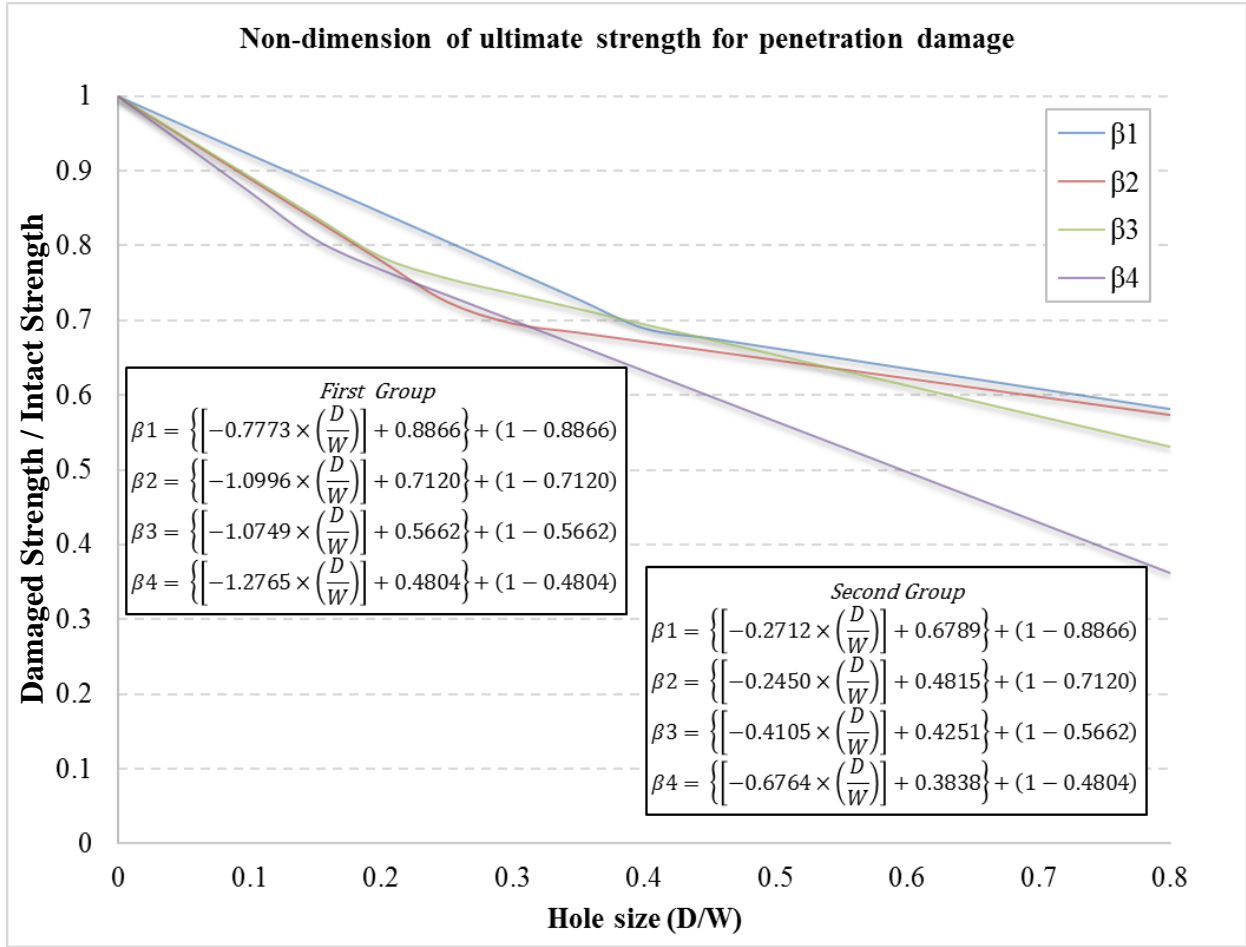


Figure 5.4 Knockdown factors for damage represented by penetration with an indenter.

5.3.3 Re-creating damage results under the simplified method in ProColl.

In general, ProColl is used for generating a load shortening curve for each stiffened panel in a box girder base using the simplified method (Benson et al., 2015); however, knockdown formulae are used for the damaged cases. The knockdown formula is used to generate a knockdown factor which is specific for each type and diameter of damaged area to decrease the strength value of the undamaged stiffened panel in original ProColl.

For example, the box girder has a damaged area in one of the stiffened panel, which has damage as a clear-cut hole with a damaged area ratio $\left(\frac{D}{W} \right)$ at 0.50 with plate slenderness ratio (β) at 2.0. The knockdown formula at $\beta = 2.0$ is used in this case. The formula is presented below:

$$\beta_2 = \left\{ \left[-0.7485 \times \left(\frac{D}{W} \right) \right] + 0.7257 \right\} + (1 - 0.7257)$$

The formula to calculate the knockdown factor for a damaged area ratio at 50 per cent of the width of the panel. In this case the knockdown factor is equal to 0.49528574, which is multiplied with the original stress value from ProColl to give a load shortening curve for the intact panel.

Figure 5.5 shows the load shortening curve for the damaged panel. The blue curve in Figure 5.5 represents intact panel strength. The red curve shows the strength reduction of a damaged stiffened panel with 50 per cent damaged clear-cut hole area.

This new load shortening curve with a damaged clear-cut hole, in red, is sent back to re-calculate the moment curvature of the box girder in ProColl.

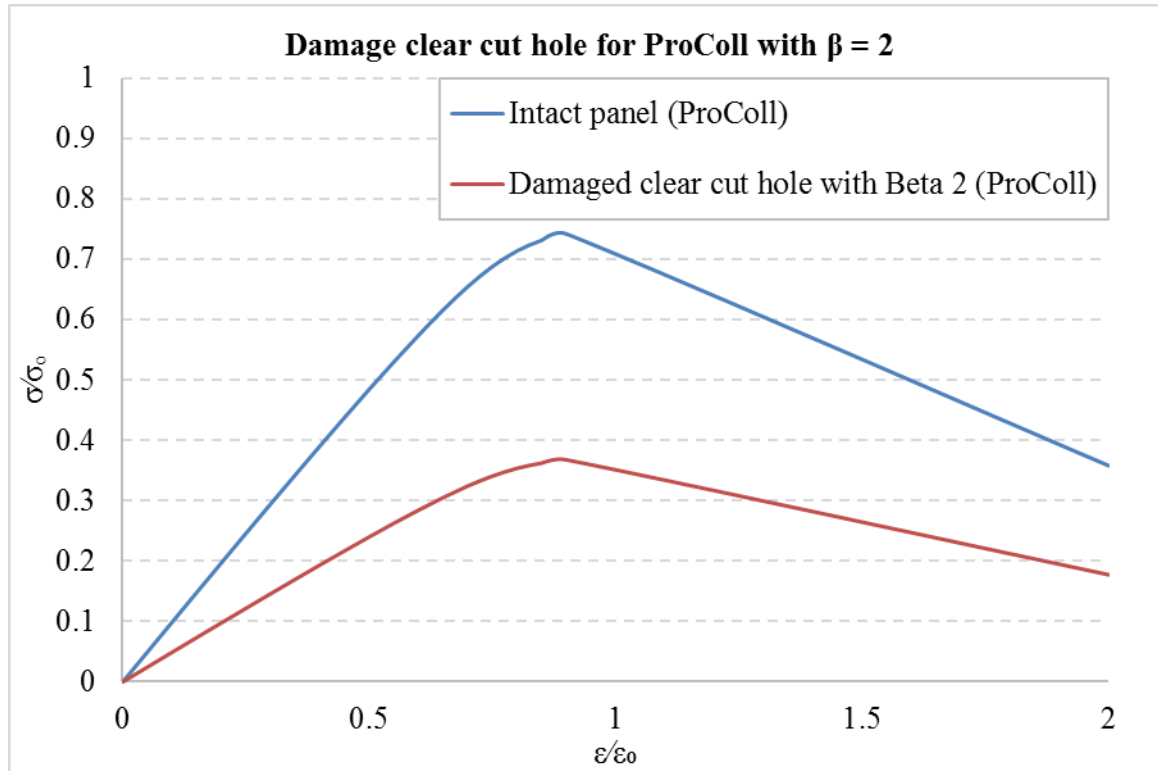


Figure 5.5 Load shortening curve for damage with a clear-cut hole. (ProColl with $\beta = 2.0$).

The load shortening curve for penetration damage is calculated in the same way. However, more attention is necessary in this calculation because of the turning point of the knockdown equation.

5.4 Comparison of damaged stiffened panels between ABAQUS and ProColl.

To be more accurate in the calculation, the results between ABAQUS and ProColl are compared as shown in Figure 5.6. The graph shows a comparison between ABAQUS and ProColl's results in both intact and damaged clear-cut hole panels. The results show comparable results between ABAQUS and ProColl in both groups of results.

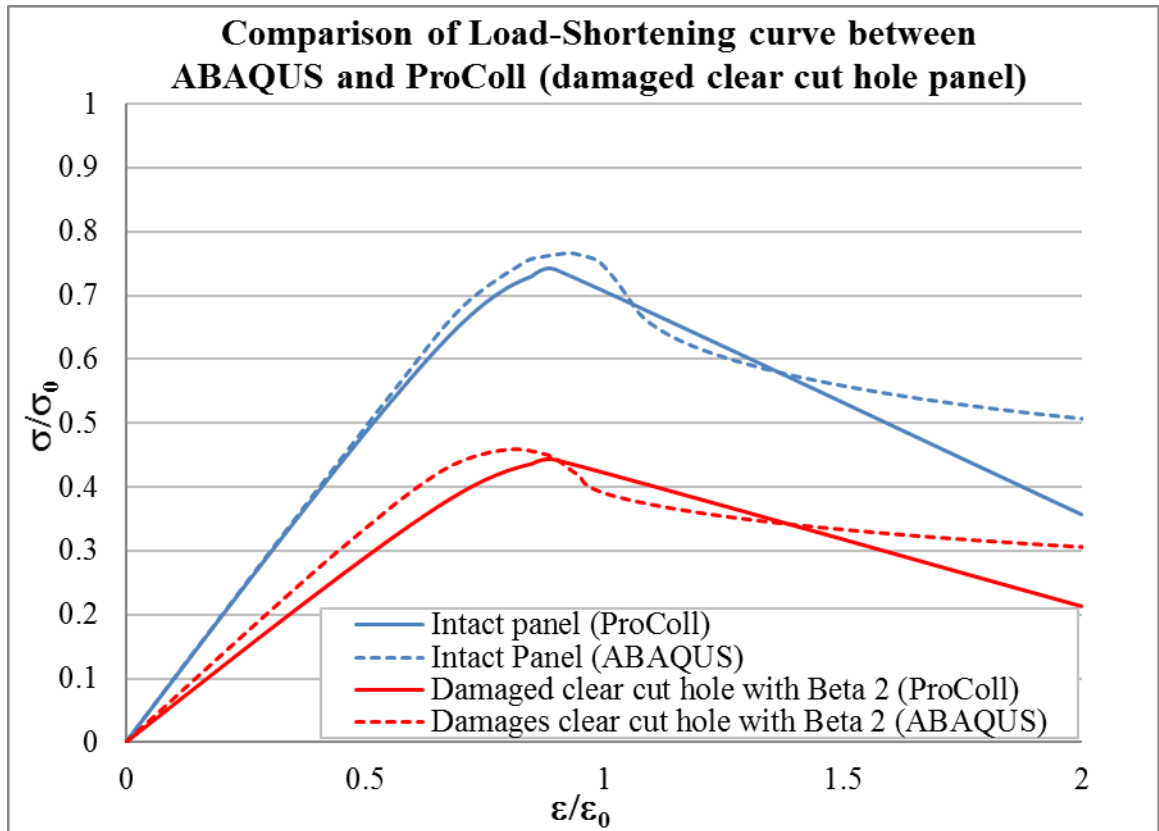


Figure 5.6 Comparison of load shortening curve between ABAQUS and ProColl for damage with a clear-cut hole panel with $\beta = 2.0$ and $\frac{D}{W} = 0.50$.

5.5 Validation – double bottom box girder

5.5.1 Model description

Originally, ProColl was used to investigate the strength of the box girder by generating a load shortening curve for each panel and then producing the moment curvature relationship. In addition, the validation of the program took place by using double bottom box girder as a case study. The section was designed to represent a conventional ship-type structural arrangement but with simplifying features to enable reasonable computation times, especially for damage simulations. Furthermore, the scantlings of the box girder are equivalent to the flat-panels analysed in Chapter 4. This is suitable for validation because the box girder exhibits an ultimate strength failure equivalent to larger cross sections typical of real ship structures.

Figures 5.7 and 5.8 show a steel double bottom box girder 12600 millimetres wide, 8400 millimetres high and 12600 millimetres long. A T-bar stiffener which is ALS3 was used with 600 millimetre spacing, along with a flat bar transverse frame at 180 millimetres high. The compartment length was separated into seven bays.

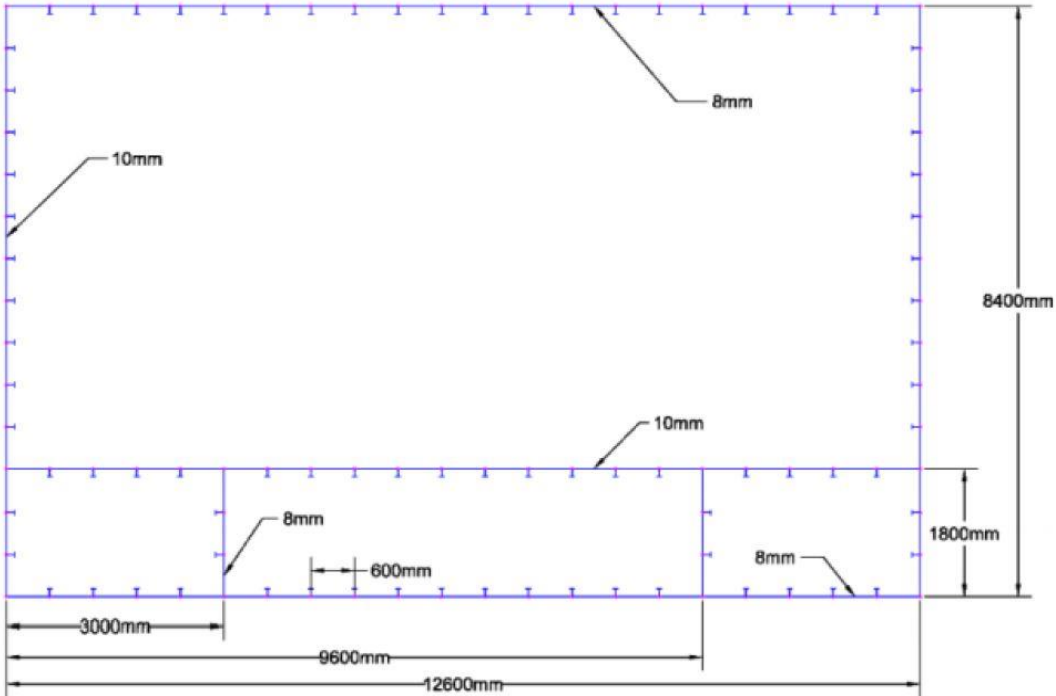


Figure 5.7 Layout of double bottom box girder.

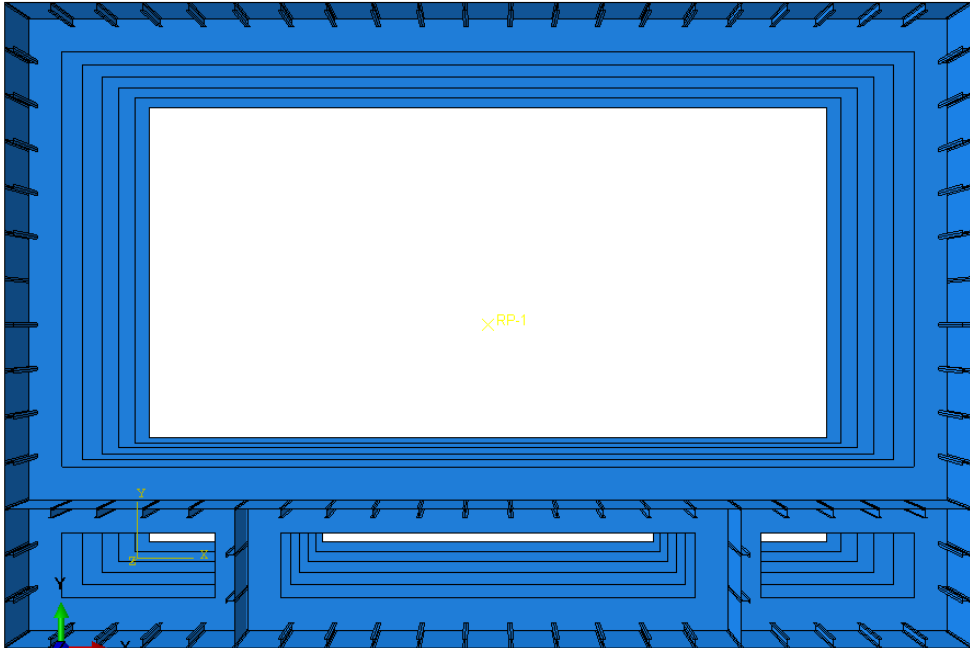


Figure 5.8 Front view of double bottom box girder.

The plate slenderness ratio (β) and column slenderness ratio (λ) controlled using the thickness of the steel plate. Table 5.2 shows the parameters of the double bottom box girder with two different thickness values.

Table 5.2 Double bottom box girder parameters.

| Plate thickness, t_p | Yield stress (σ_y), MPa | Young's modulus (E), GPa. | β | λ | a (mm.) | b (mm.) | $\frac{A_s}{A}$ | Stiffened Type |
|------------------------------|--|---------------------------------|---------|-----------|------------|------------|-----------------|---------------------------|
| 8 | 245 | 207 | 2.58 | 0.43 | 1800 | 600 | 0.30 | 5' long stalk T (ALS3) |
| 10 | 245 | 207 | 2.06 | 0.46 | 1800 | 600 | 0.25 | 5' long stalk T (ALS3) |

5.5.2 Scope of analysis

A double bottom box girder was set up in ABAQUS using non-linear finite element analysis (Quasi –static analysis). The condition of box girder was set up in the same way as the stiffened panel studies in the previous chapter except for the boundary condition and force applied to the structure.

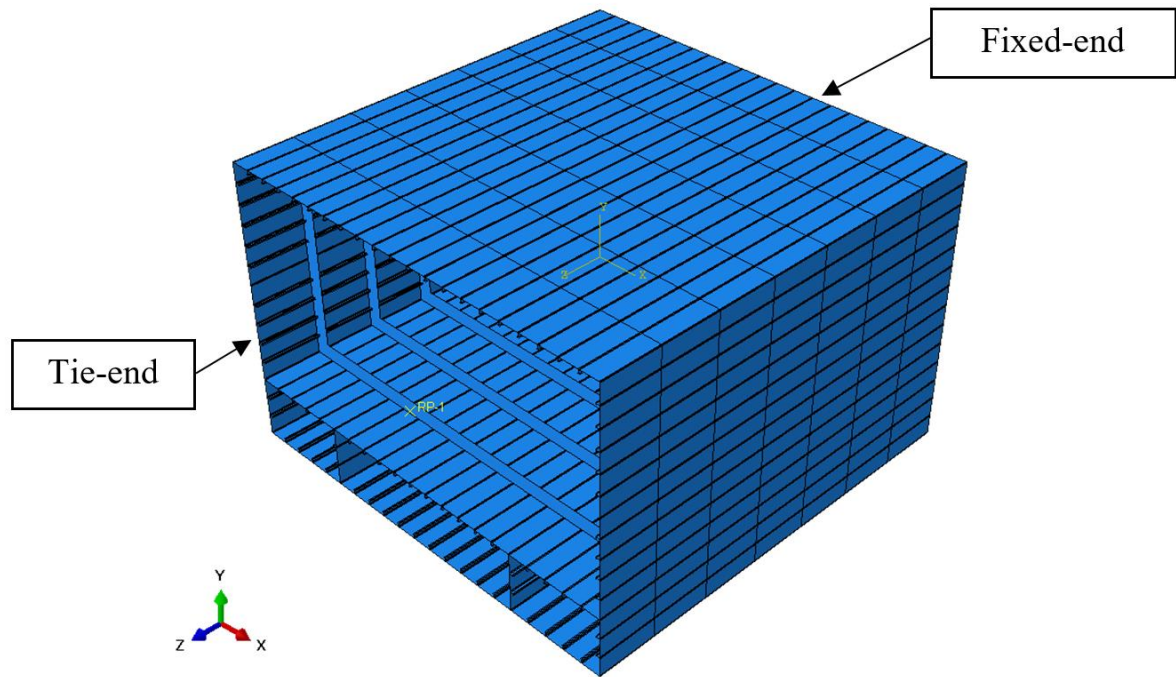


Figure 5.9 Boundary conditions of the double bottom box girder.

Figure 5.9 shows that the box girder was set up with two types of boundary condition, as presented in Table 5.3. The fixed-end condition did not allow any displacement to occur. At the same time constraint was applied at the tie-end side to tie all elements in that side together with the tip-point (reference point) which is RP1. The curvature was applied to the reference point (RP1) at 0.5. An amplitude with smooth steps was used to control the curvature with a rate of 0.0125 radius per second.

Table 5.3 Boundary condition of double bottom box girder.

| Location of Nodes | Boundary conditions |
|----------------------------------|------------------------------------|
| Along X-axial, Z = 0 (Fixed-end) | $U1=U2 = U3 = UR1 = UR2 = UR3 = 0$ |
| Along X-axial, Z = A (Tie-end) | $UR1 = 0.5$ |

An imperfection at an average level was applied to the structure before applying any damaged areas to the structure. Tensile residual stress area was assumed as being 25 millimetres wide to represent the welding area in the box girder.

5.5.3 Damage on double bottom box girder.

The outer bottom of the box girder was subjected to two types of damage, which are damage represented by a circular clear-cut hole and penetration damage with an indenter. The damage was in the middle of the bottom part of the box girder. The damaged area ratio in this particular study was calculated by using the width of the middle panel at the bottom part of the box girder, which had a value of 6600 millimetres.

The penetration damage used an indenter to create a damage area by moving the indenter up in the y-direction for 1800 millimetres with a speed of 400 millimetres per second. After the damaged area was created, the indenter was moved away from the box girder to a distance of 2000 millimetres with a speed of 400 millimetres per second. This part of the analysis was carried out as an explicit dynamic analysis in ABAQUS.

Table 5.4 presents the diameter of the damaged area in both cases; however, the damaged area through penetration damage was stopped at $\frac{D_{IN}}{W} = 0.35$ because the damaged area depended on the distance of indenter in order to create a damaged area in the box girder.

Table 5.4 Diameter of damaged area in both damage cases.

| Damage represented by a circular clear-cut hole | | Damage represented by penetration with an indenter | | |
|---|--------------------------------|--|---------------|--------------------------------|
| $\frac{D}{W}$ | Diameter of damaged area (mm.) | $\frac{D_{IN}}{W}$ | $\frac{D}{W}$ | Diameter of damaged area (mm.) |
| 0.10 | 630 | 0.05 | 0.148 | 973.77 |
| 0.19 | 1260 | 0.10 | 0.277 | 1827.27 |
| 0.29 | 1890 | 0.15 | 0.372 | 2454.55 |
| 0.38 | 2520 | 0.20 | 0.543 | 3584.25 |
| 0.48 | 3150 | 0.25 | 0.653 | 4311.26 |
| 0.57 | 3780 | 0.30 | 0.776 | 5124.00 |
| 0.67 | 4410 | 0.35 | 0.792 | 5226.46 |
| 0.76 | 5040 | | | |
| 0.86 | 5670 | | | |
| 0.95 | 6300 | | | |

Figures 5.10 and 5.11 show a cross section of the damaged area at the bottom part of the box girder before applying the moment. In addition, penetration introduced more initial residual stress into the box girder because of the effect of the indenter going through the stiffened panel.

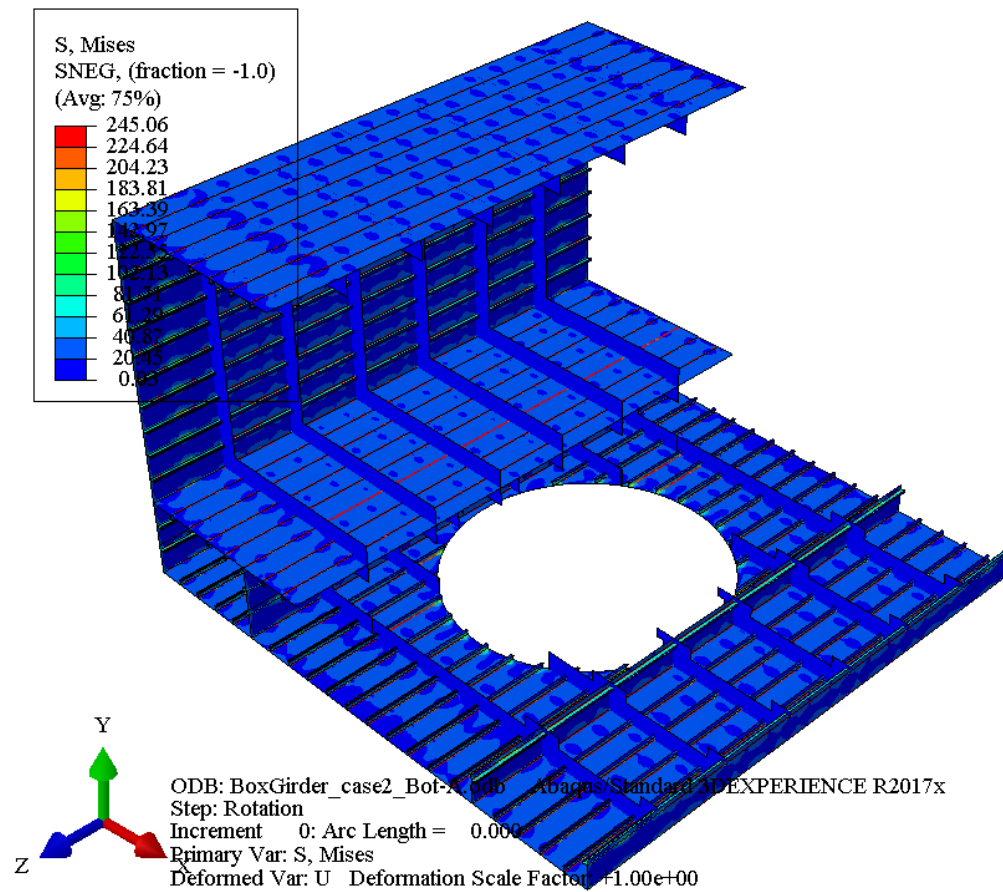


Figure 5.10 Double bottom box girder with damaged clear-cut hole area.

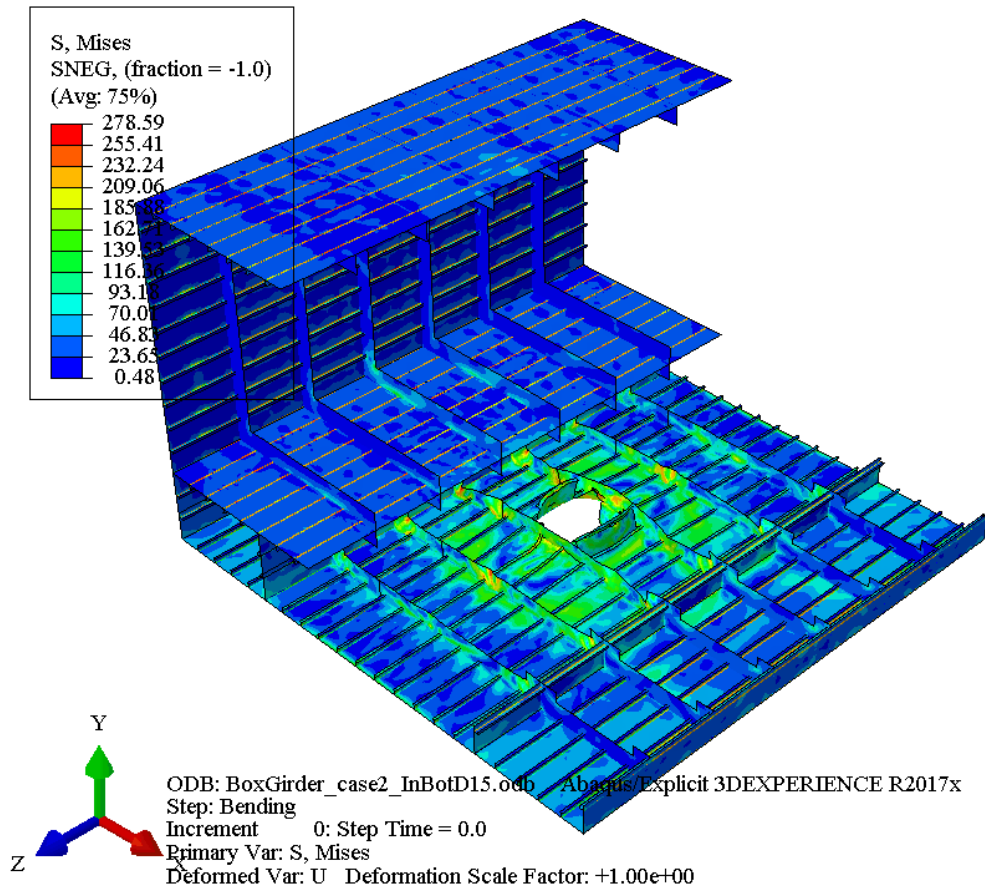


Figure 5.11 Double bottom box girder with penetration damage with indenter.

After this step, the curvature was applied to the box girder and assumed to be a hogging bending moment.

5.5.4 Results of double bottom box girder.

Figure 5.12 shows the results for an intact box girder which had curvature applied as a hogging bending moment. The strength of the intact double bottom box girder represents an inter-frame buckling at the bottom part of the structure. The investigation can be compared to the box girder with a damaged area.

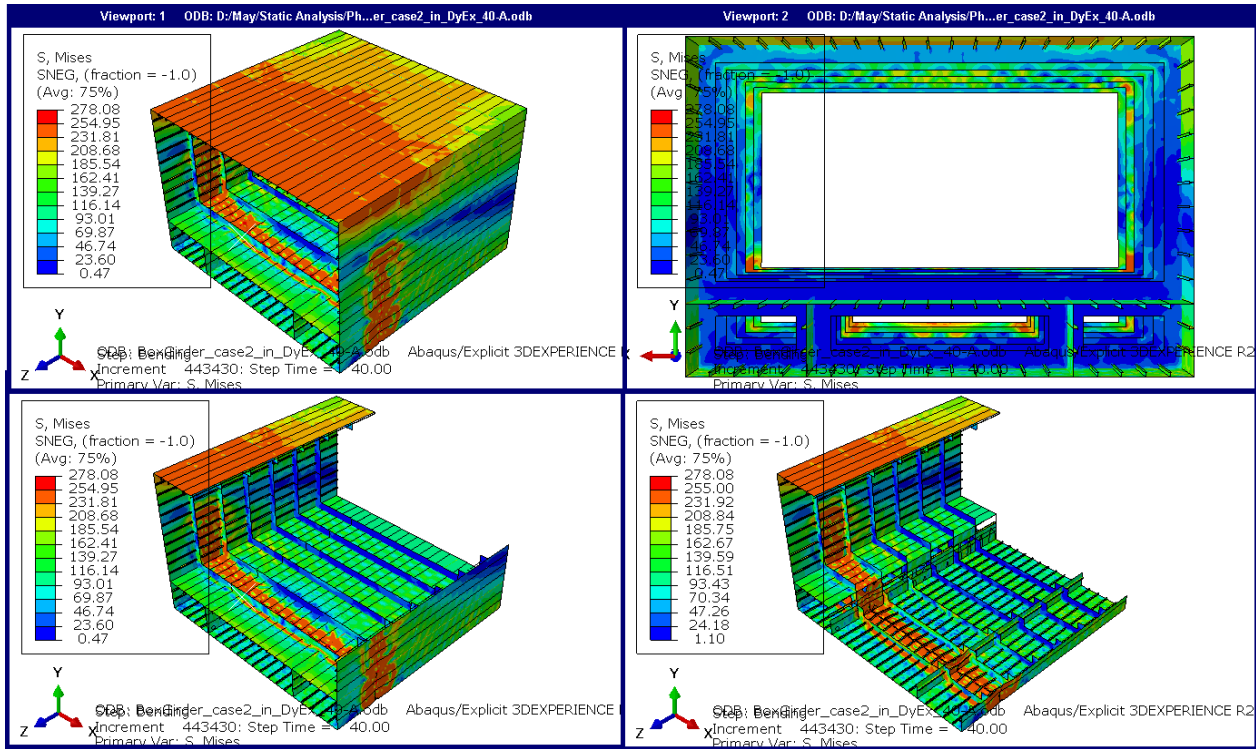


Figure 5.12 Behaviour of intact structure for double bottom box girder.

Table 5.5 presents the diameter of damage represented by a circular clear-cut hole in the bottom part of the double bottom box girder. The damaged area ratio in this case study is considered the ratio between diameter of the damaged area and the width of the middle stiffened panel in the bottom part of the box girder.

Table 5.5 Diameter of clear-cut hole in double bottom box girder.

| Name | Damaged area ratio $\left(\frac{D}{W}\right)$ | Diameter of damage clear-cut hole (mm.) |
|----------------------|---|--|
| Clear-cut damage_D10 | 0.10 | 630 |
| Clear-cut damage_D19 | 0.19 | 1260 |
| Clear-cut damage_D29 | 0.29 | 1890 |
| Clear-cut damage_D38 | 0.38 | 2520 |

| | | |
|----------------------|------|------|
| Clear-cut damage_D48 | 0.48 | 3150 |
| Clear-cut damage_D57 | 0.57 | 3780 |
| Clear-cut damage_D67 | 0.67 | 4410 |
| Clear-cut damage_D86 | 0.86 | 5670 |
| Clear-cut damage_D95 | 0.95 | 6300 |

The comparison between ABAQUS and ProColl for the double bottom box girders both intact and damaged by circular clear-cut out area is shown in Figure 5.13. The comparison represents a good fit between both programs.

The results show a good agreement not only regarding the strength of the damaged box girder but also for the initial stiffness of the box girder, shown by the initial slope of the stress-strain curve. More stress and strain curves for double bottom box girder with damaged clear-cut hole are provided in Appendix E.

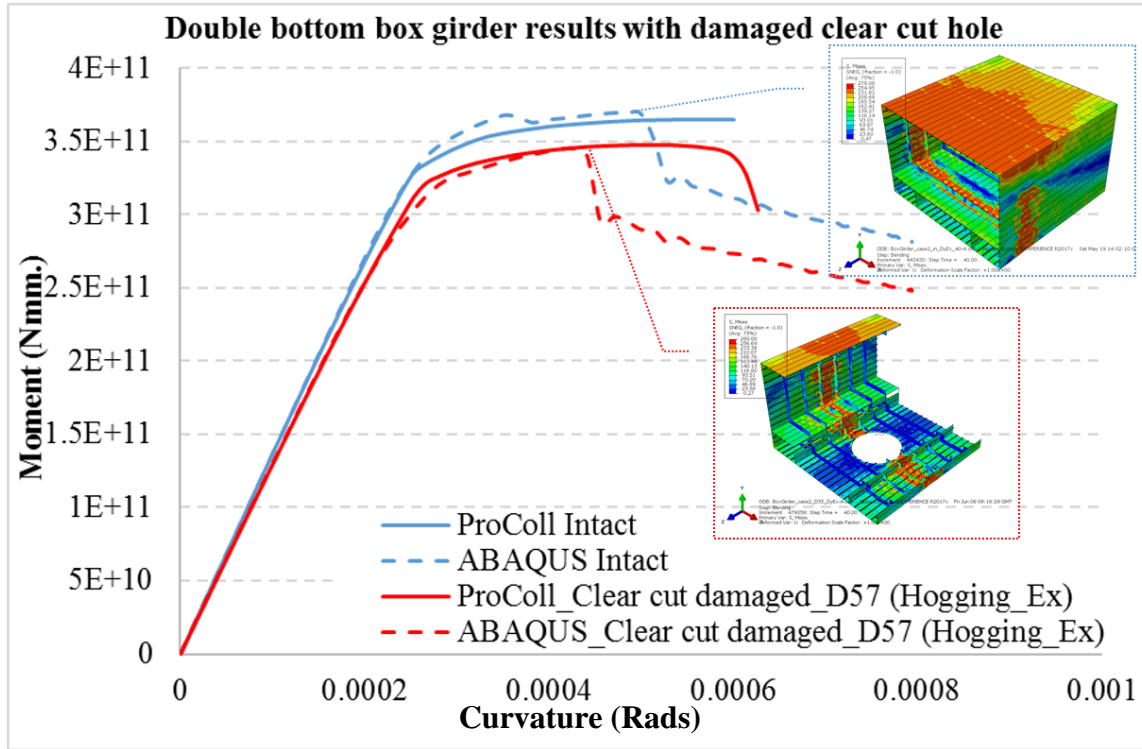


Figure 5.13 Comparison between ABAQUS and ProColl with damage represented by circular clear-cut hole at 57 per cent damage.

The set of behaviour in double bottom box girders with damage from a clear-cut hole is demonstrated in Table 5.6. The intact structure shows buckling nucleation into a different frame space compared to the damage scenarios where the damage is placed in the central frame of the compartment. However, the intact result is still valid for direct comparison to the damage results because the nucleation still occurs away from the boundaries. The damage scenarios exhibit the main characteristics as observed in the flat panel studies in Chapter 4. The buckling continues to nucleate into the central frame space even when the damage extent is large and spreads over several frame spaces. The hole creates a “shadow” area across the longitudinal extent of the panel where the stress is relieved. The failure mechanism in other regions of the structure such as the side shell are unaffected by the presence of the damage. This indicates that the methodology proposed in this study, where only the load shortening curves in way of damage are adjusted through knockdown factors, is reasonable.

Table 5.6 Post collapse of double bottom box girder with damage from a clear-cut hole.

Damaged area

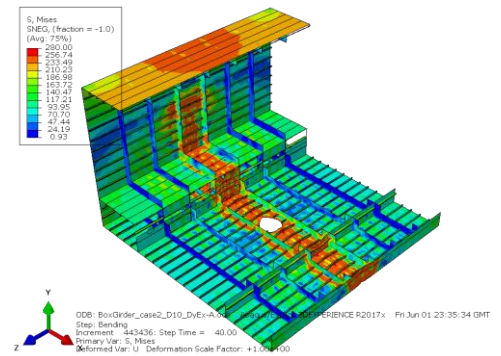
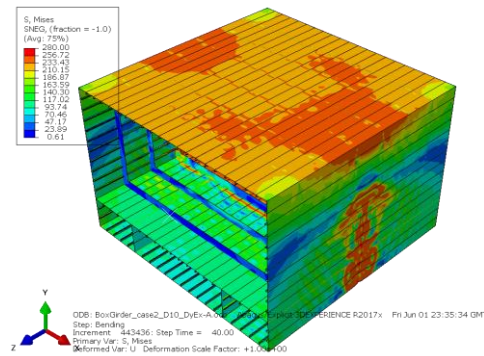
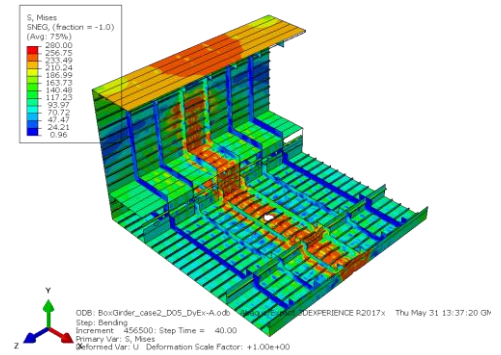
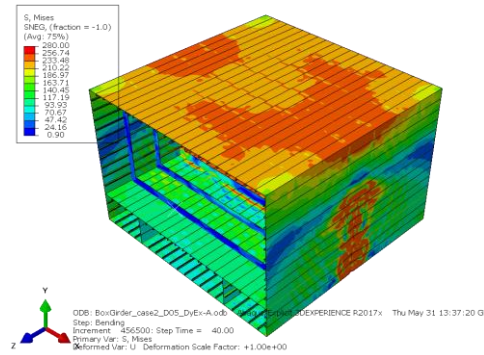
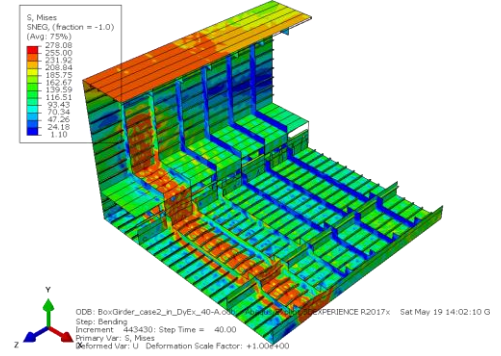
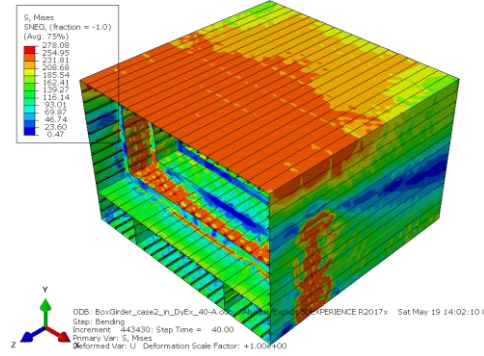
$$\text{ratio} \left(\frac{D}{W} \right)$$

Post collapse

Intact structure

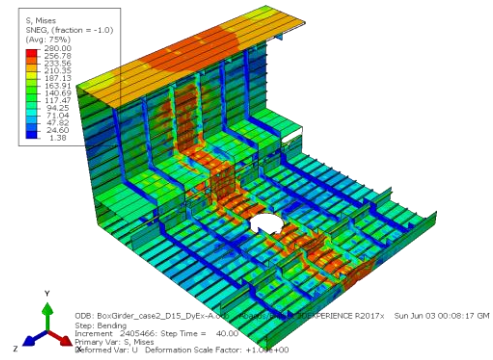
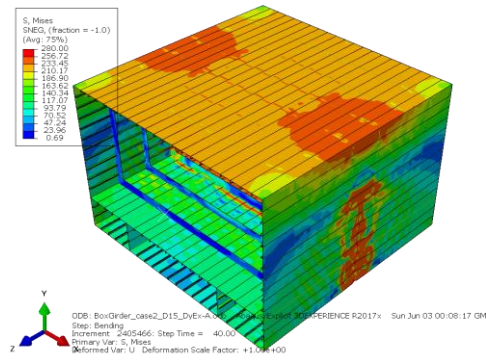
0.10

0.19

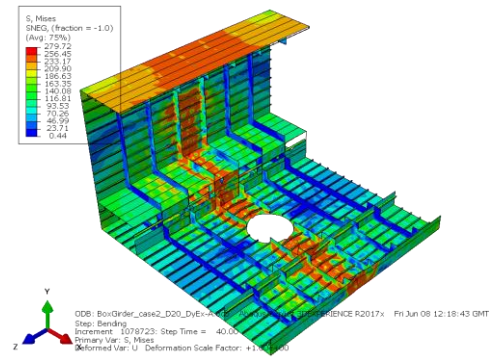
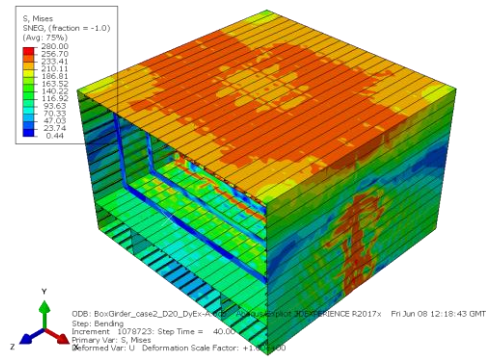


Progressive collapse of damaged ship structure

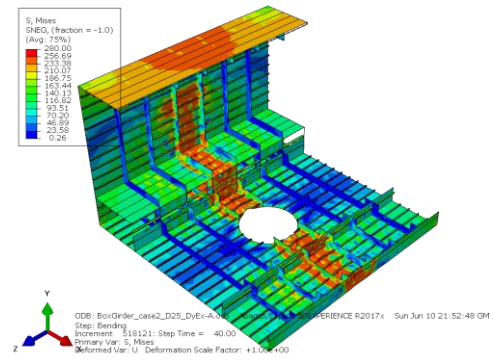
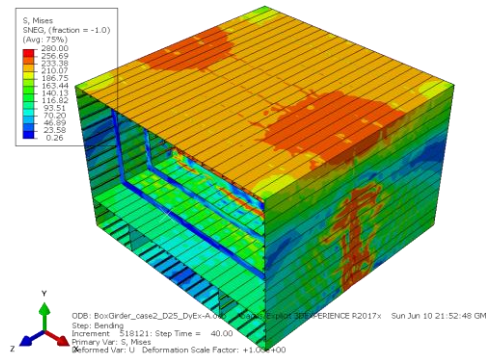
0.29



0.38

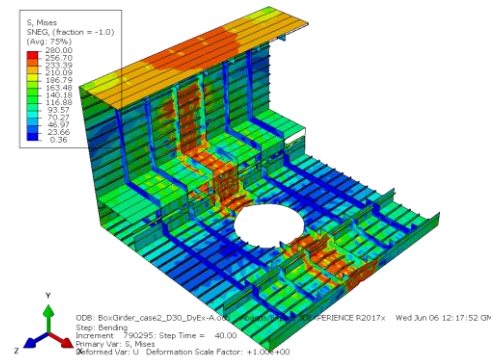
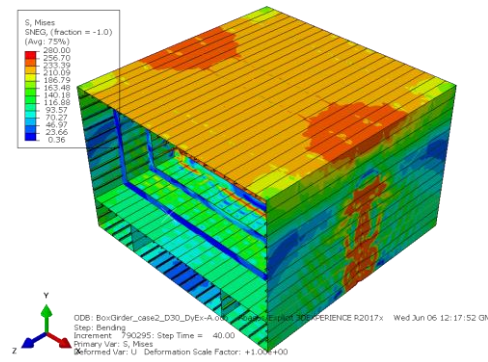


0.48

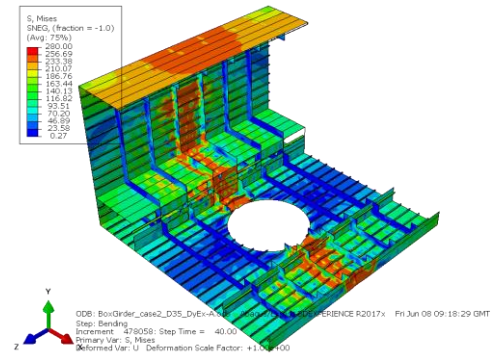
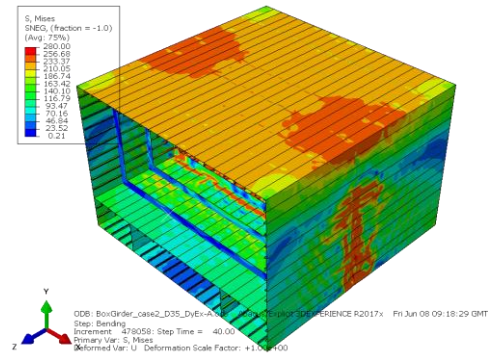


Progressive collapse of damaged ship structure

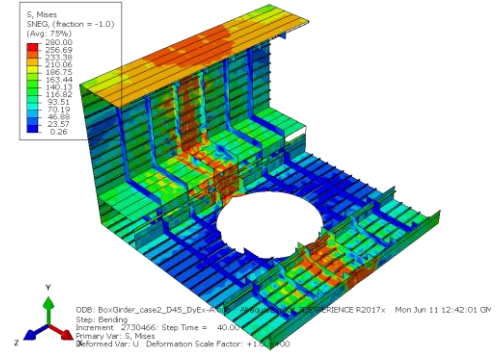
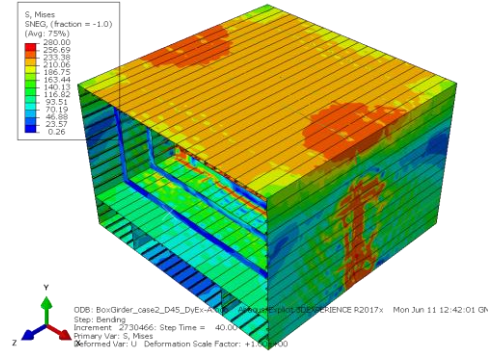
0.57

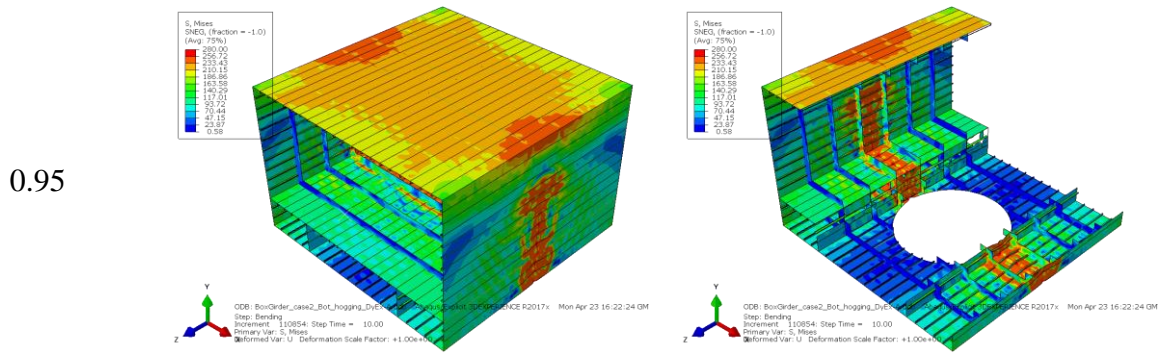


0.67



0.86





Research was carried out with the penetration damaged scenario using the damage area ratios in Table 5.7.

Table 5.7 Diameter of penetration damage with indenter in double bottom box girder.

| Name | Damaged area ratio $\left(\frac{D}{W}\right)$ | Diameter of actual hole damage (mm.) |
|-------------------------|--|---|
| Penetration damage_D15 | 0.15 | 973.77 |
| Penetration damage _D28 | 0.28 | 1827.27 |
| Penetration damage _D37 | 0.37 | 2454.55 |
| Penetration damage _D54 | 0.54 | 3584.25 |
| Penetration damage _D65 | 0.65 | 4311.26 |
| Penetration damage _D78 | 0.78 | 5226.46 |

Figures 5.14 and 5.15 present an ultimate set of results for the double bottom box girder by comparing two types of damage scenario. The results show that both damage scenarios have a good agreement regarding the ultimate strength reduction which occurs after the cross-section

area of the box girder decreases.

A view of the ABAQUS simulation with large-scale damage is shown in Figure 5.16. Figures 5.17 and 5.18 show the comparison between ABAQUS and ProColl with damage represented by a circular clear-cut hole and damage represented by penetration respectively. The results show the following:

- There is close agreement between ABAQUS and ProColl in terms of the reduction gradient of strength as the damage extent increases. This demonstrates the validity of ProColl with the use of knockdown factors to represent damage.
- The representation of damage with a clear cut hole shows a shallower gradient of strength reduction as the damage extent increases. This is expected because the knockdown factors are also less.

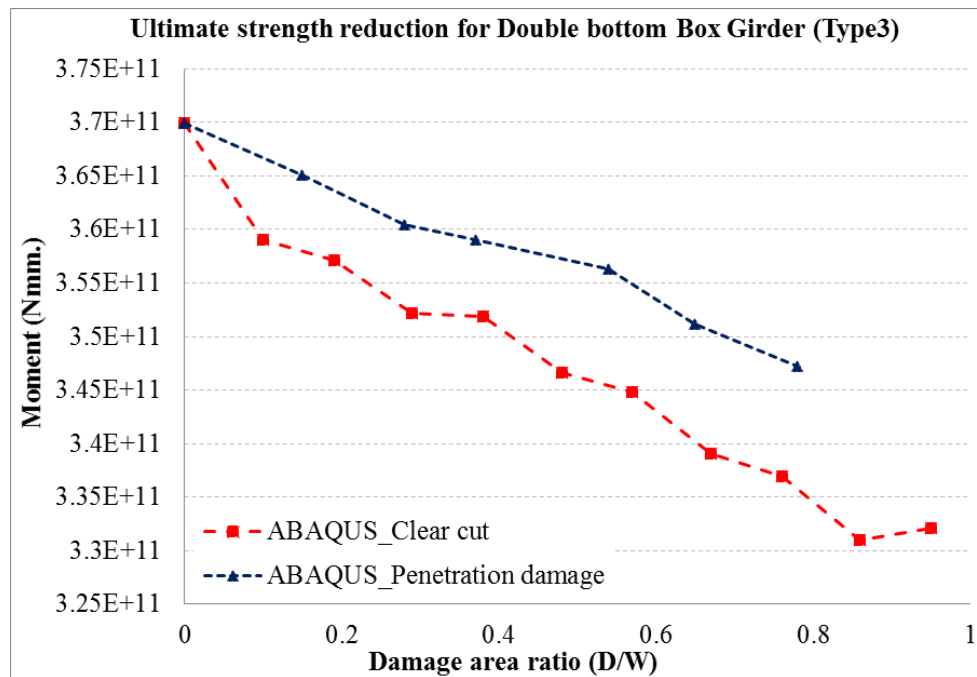


Figure 5.14 Comparison of ultimate strength for double bottom box girder between two different damage types in ABAQUS.

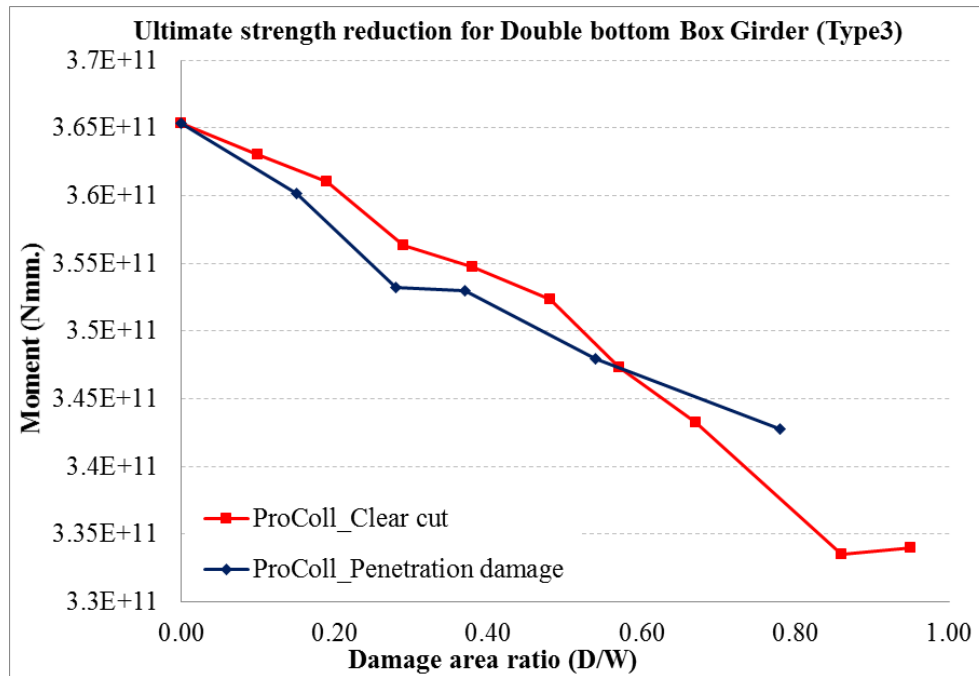


Figure 5.15 Comparison of ultimate strength for double bottom box girders between two different damage types in ProColl.

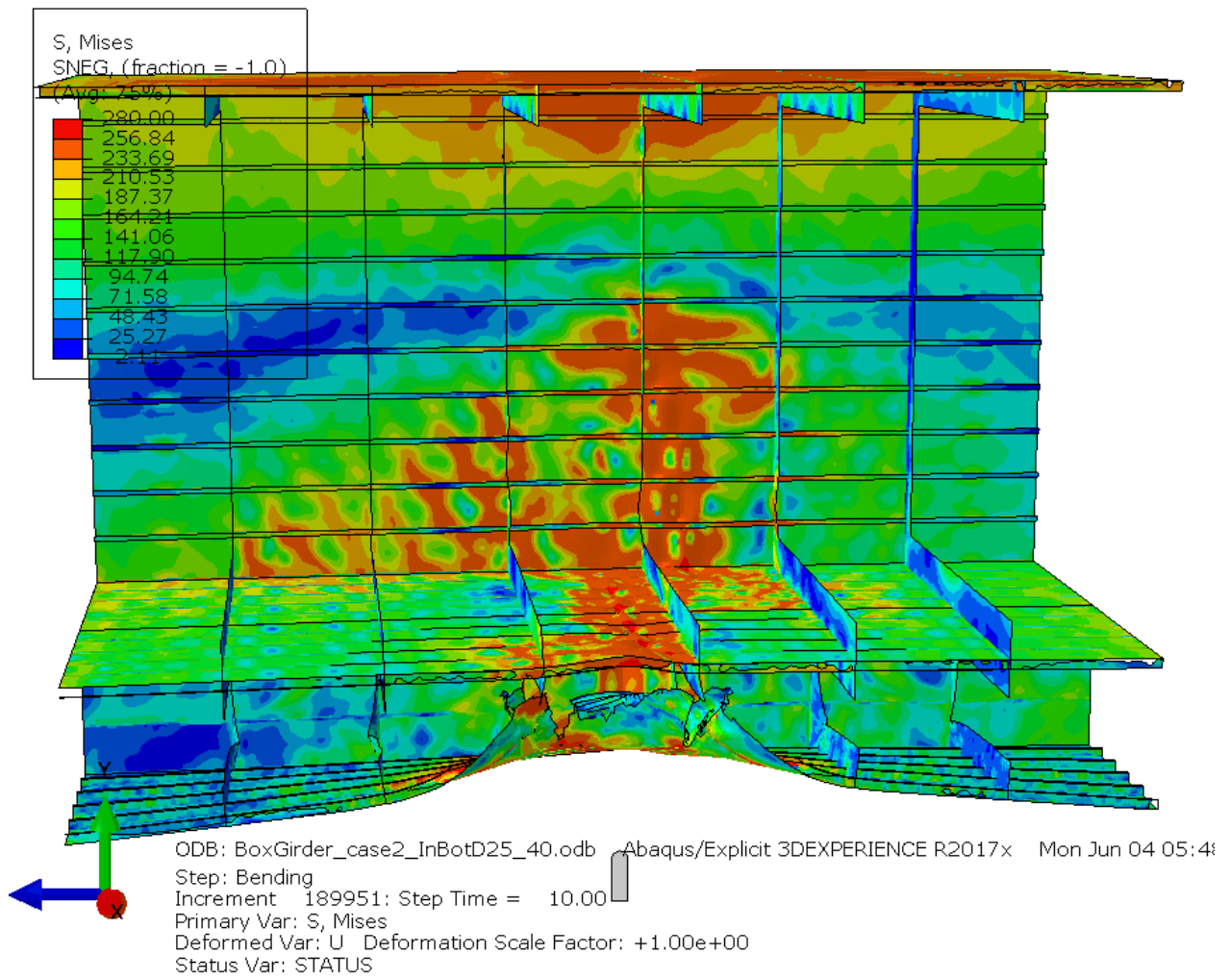


Figure 5.16 Penetration damage of double bottom box girder with damaged area ratio $\left(\frac{D}{W}\right) = 0.65$.

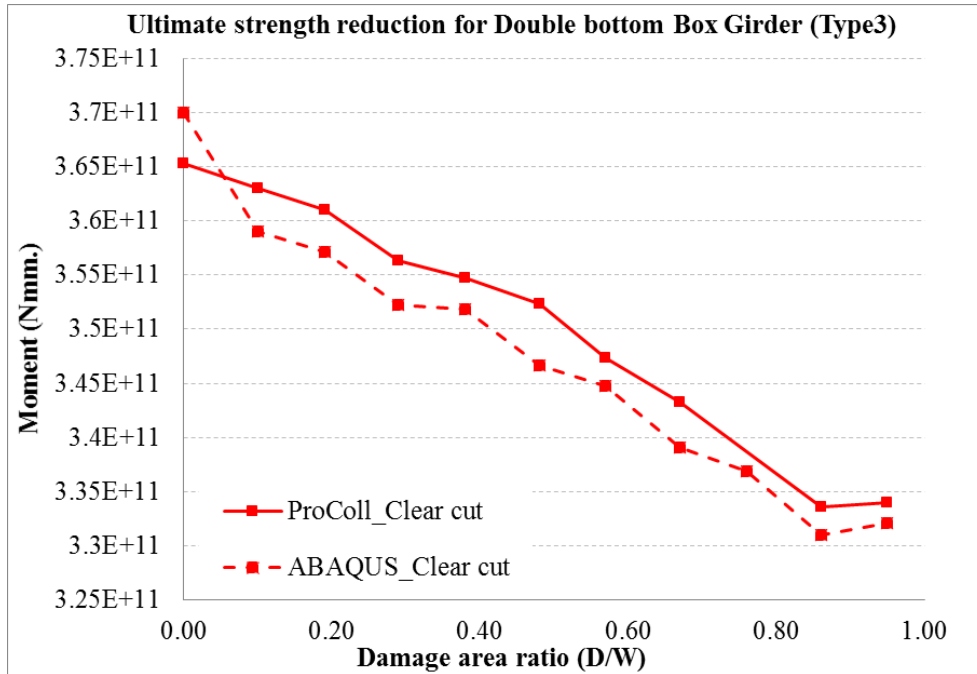


Figure 5.17 Comparison of ultimate strength for double bottom box girder with damage from a clear-cut hole between ABAQUS and ProColl.

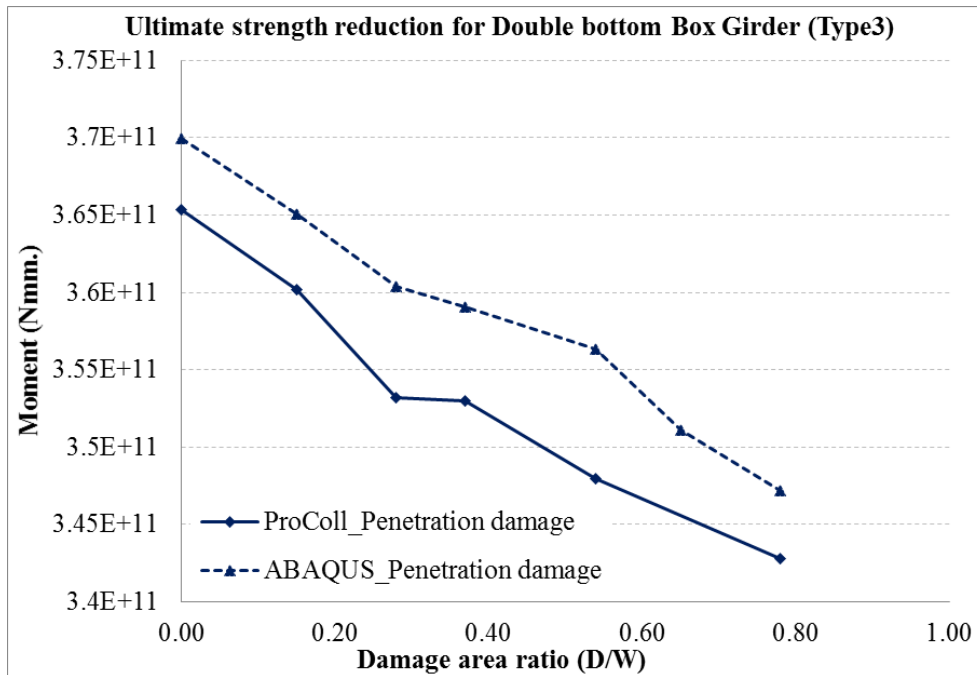


Figure 5.18 Comparison of ultimate strength for double bottom box girder with penetration damage with indenter between ABAQUS and ProColl.

5.6 ProColl results for other cases with box girder

5.6.1 Model description

Further analysis has been carried out with two cases using box girders which are described below. The purpose of these additional studies is to provide further validation of the damage progressive collapse method. The procedure followed for these analyses is the same as described in Section 5.5.

- Single bottom Box Girder (Case1)

A square steel box girder with a single bottom was used in this investigation. The box girder was 5931.55 millimetres long, 6409.964 millimetres high and wide. The T bar stiffener was type ALS3 with 582.724 millimetres spacing. The length of the box girder was divided into five bays by flat bars of transverse frame 450 millimetres high. Figure 5.19 shows a single bottom box girder (Case 1).

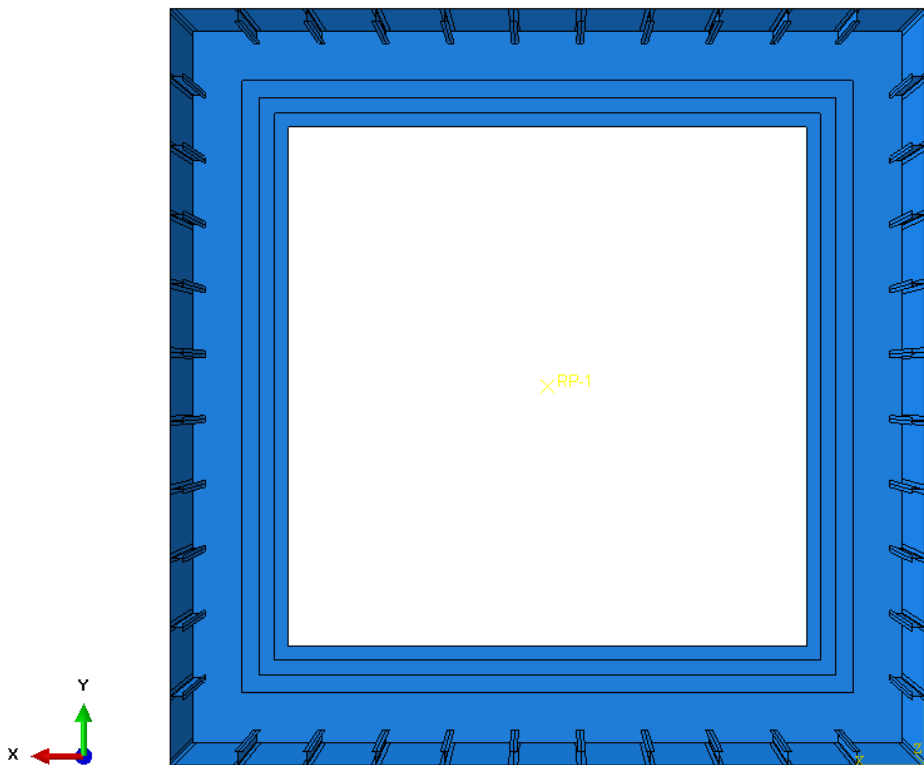


Figure 5.19 Front view of single bottom box girder (Case1).

- Single bottom Box Girder (Case2)

Figures 5.20 and 5.21 show a commercial single bottom box girder made from steel 12600 millimetres wide, 8400 millimetres high and 12600 millimetres long. A T-bar stiffener (ALS3) was used with 600 millimetre spacing. Using a flat bar transverse frame 180 millimetres high, the compartment was separated into seven bays.

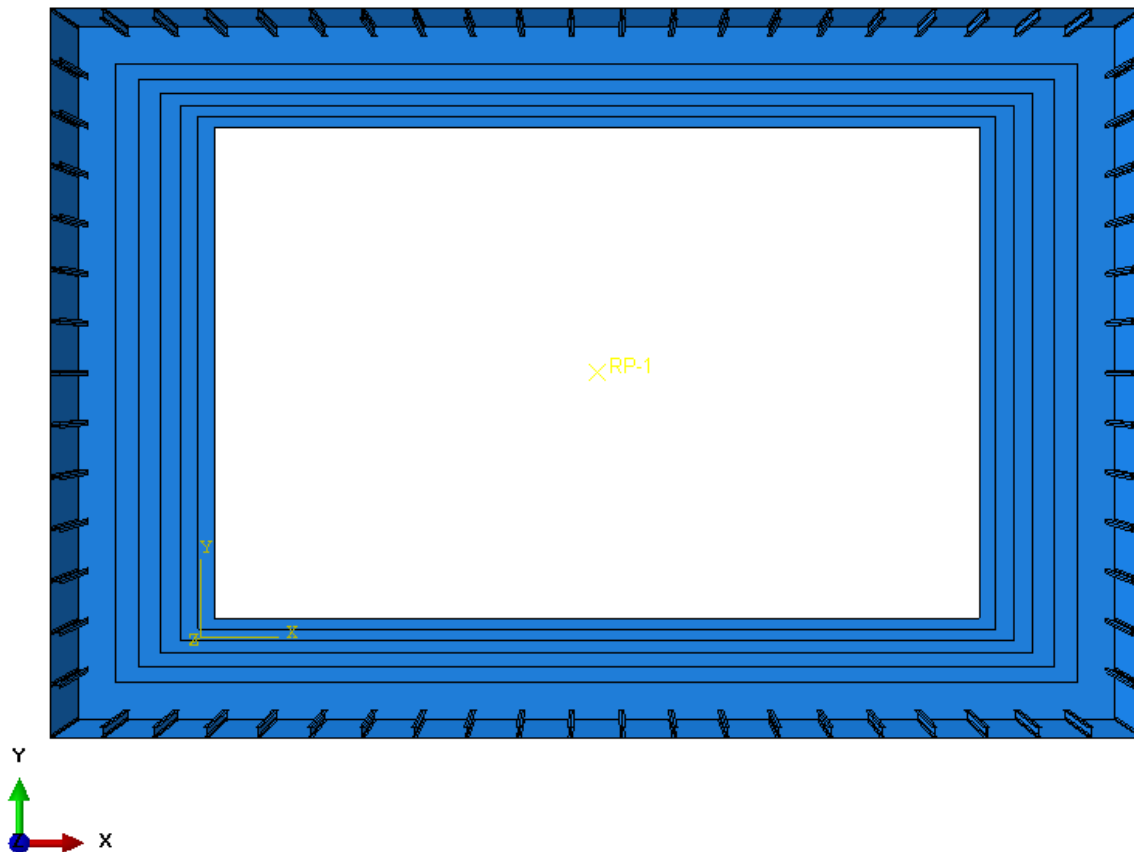


Figure 5.20 Front view of single bottom box girder (Case2).

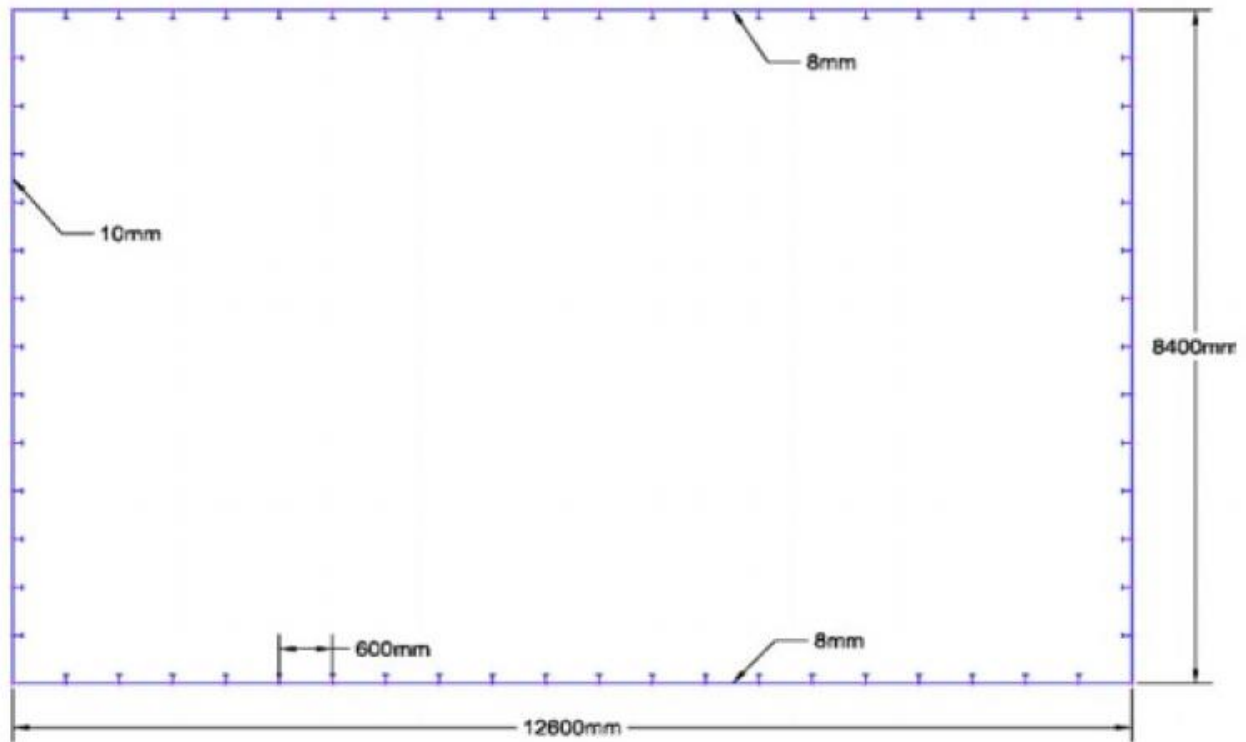


Figure 5.21 Layout of single bottom box girder (Case2).

5.6.2 Ultimate strength results from ProColl

The comparison between three case studies using the box girder for both damage scenarios is shown in Figure 5.22. The overall results present a close result between the damage represented by a circular clear-cut hole and damage represented by penetration with an indenter. The ultimate strength reduction occurs when the cross section area in the box girder decreases, which is similar to the stiffened panels' results in Chapter 4.

The strength of the box girder also depends on the type and shape of the box girder; for example, the strength of single bottom box girder (Case2) and the double bottom box girder. The double bottom box girder is stronger than the single bottom box girder in the same damage area ratio.

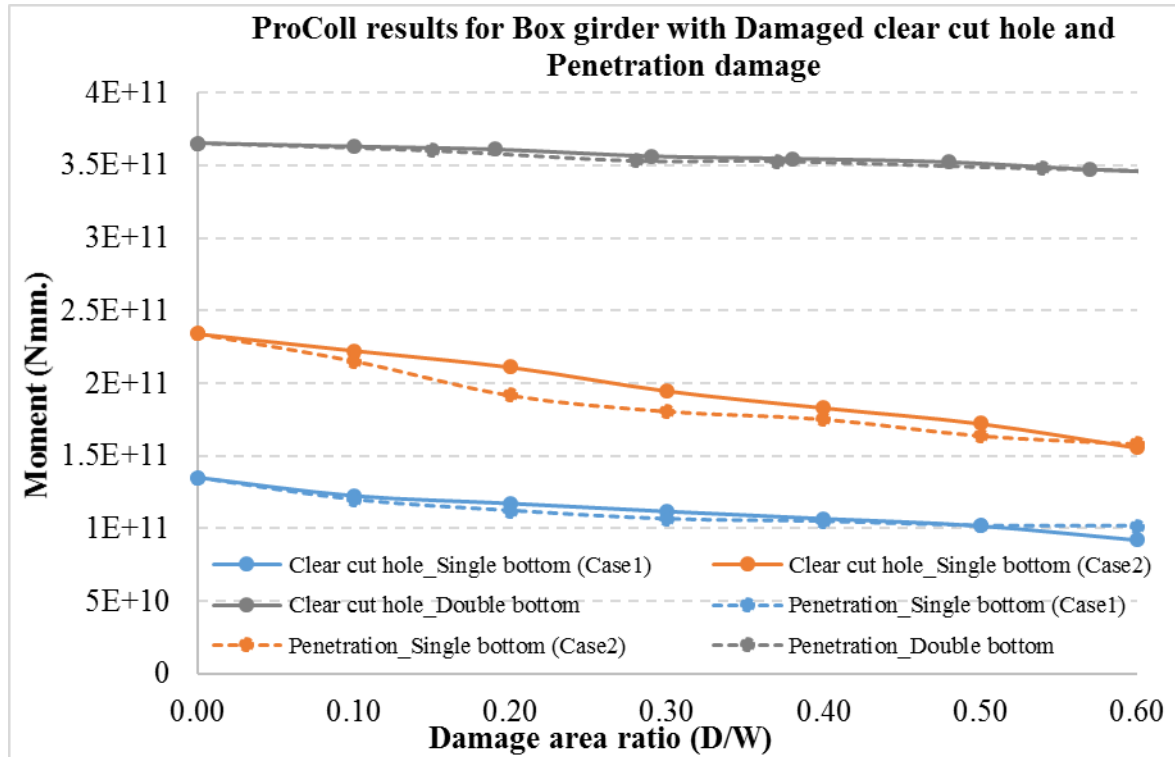


Figure 5.22 Ultimate strength of three cases of box girder with ProColl.

5.7 Summary

The modification of the simplified progressive collapse method (ProColl) is demonstrated in this chapter. The validation for the program has been carried on with a set of box girders, which is a rectangular cross section box girder. The box girder was analysed in ABAQUS as an intact and damaged structure. The results from both the finite element method and modified simplified progressive collapse method show a good correlation between them.

Chapter 6 Conclusions and Recommendations

6.1 Conclusions

The aim of this research was to investigate the effect of realistic damage mechanisms which occur on a ship's structure and to provide a better understanding of the residual ultimate strength behaviour of the damaged structure. This research was completed in three broad phases: firstly, by defining the strength of intact stiffened panels to provide a baseline dataset; secondly, by investigating the effect of different types of damage on the stiffened panels; and thirdly, by extending a progressive collapse method for calculating the ultimate strength of a ship's structure to include damage effects. Each of these phases produced novel contributions to the research field, which are described in the concluding remarks below.

6.1.1 *Intact stiffened panels*

A comprehensive and rigorous dataset of intact stiffened panel load shortening curves for large scale structures (multiple stiffeners and frames) was developed in this research with an in-plane compression. Previous datasets generally produced only ultimate strength values or were produced using small scale, single stiffener – frame models. The scale of the panel was selected to include 10 longitudinal stiffeners and 5 frame spaces to provide a large enough panel that gives representative results for any orthogonally stiffened panel with the same slenderness characteristics.

The intact stiffened panels have been analysed with the non-linear finite element method to generate a baseline dataset for the research; moreover, the results have been compared with the progressive collapse method (Smith et al., 1988) by using the standard design curve (Chalmers, 1993) at an average level of imperfection to represent the initial condition of the stiffened panels. In this particular group of analyses, a model of a stiffened panel was created and controlled with several parameters such as plate slenderness ratio (β), column slenderness ratio (λ) and stiffened area ratio $\left(\frac{A_s}{A}\right)$ with T-bar stiffener and flat bar for transverse frame, which are presented in Chapter 3.

The results are represented as a group. The size of stiffeners and column slenderness ratio (λ) do

not have much effect on the strength of the structure which is consistent with previous findings such as Chalmers collapse curves; in contrast, the plate slenderness ratio (β) is the main factor which affects the ultimate strength of the stiffened panels.

6.1.2 Damaged stiffened panels

A subset of the large-scale stiffened panels was analysed with controlled inclusion of damage. In this research the damage was applied to the centre of the stiffened panel. The range of damage size investigated in this research was large enough to represent some types of typical damage caused on a ship's structure in a collision, grounding incident or explosion. The dataset provides new understanding about the behaviour of large scale stiffened structures under controlled levels of damage. The range of damage scenarios focused on damage in the central region of the panel only. It is recognized that damage of different extents can occur in off-centre positions, and this could form the basis of further work to investigate the effect of damage position. It is envisaged that, because of the clear pattern of collapse behavior as discussed in Section 4, damage near the centre of the panel will produce a very similar response to the dataset in this study. Furthermore, the size of the stiffened panel was kept constant throughout the study to provide a rigorous comparable dataset. However, the dataset should still apply to panels with different numbers of stiffeners and in situations where damage is not centred on the central longitudinal.

The first scenario of damage investigated in this study was with the damaged area represented as a circular clear-cut hole. The dataset of analyses was narrowed down to focus on the models which had a stiffened area ratio equal to 0.2 and had 5' long stalk T stiffeners (ALS3). The set of damaged models was set up with different ranges of damage diameter areas. The static Riks analysis was adopted with an in-plane compression in order to generate the load shortening curve for damaged stiffened panels.

The results of the clear-cut hole analyses show that the plate stiffened area ratio still had a significant effect on the strength of stiffened panels. Furthermore, the cross-section area of the stiffened panel was reduced by the circular cut hole area. The damaged area created two different sets of ultimate strength results which are broadly termed the flat region area and a sharp drop of strength area in the structure. The flat region appeared for the group of damage that took place in unstiffened panel parts, while, the sharp drop of ultimate strength was located in the stiffened

panel area because the circular clear-cut hole damage took place in a middle of the panel and could remove two stiffeners at the same time when large enough. Overall, the behaviour with damage represented by a circular clear-cut hole panels still depended on the plate slenderness ratio (β) which separated results into a group with different plate slenderness ratio (β) values.

The second scenario of damage investigated in this study was penetration damage by an indenter. The damaged area was more complex and more realistic in this area of research. However, the study focused on producing a rigorous dataset with tightly controlled parameters for the indenter including its size and speed. This means that, although the results cannot directly capture all possible scenarios, the damage is representative for different types of damage occurrence. An indenter with a sphere head was used to create a damage effect in the stiffened panel. The penetration was controlled by the speed of the indenter under explicit analysis which was assumed to be a quasi-static analysis. The indenter was moved slowly to the stiffened panel in order to reduce the transfer of kinetic energy which can occur after collision. After penetration, the static Riks analysis was adopted in order to apply in-plane compression to stiffened panels.

The ultimate strength of the penetration damage shows that after generating the damaged area with an indenter, the panel absorbed the energy from the impact and built more initial residual stress into the structure. The ultimate strength in this case was collected by using the diameter of actual damage area. The circular area was placed on top of the actual damaged area. The centre of the damaged area and centre of the circular area were assumed to be in the same point at the centre of the stiffened panel. The results of the second damage scenario show similar behaviour on the effect of plate slenderness ratio (β) which separates results into a group.

The comparison between the two damage scenarios shows a slightly different behaviour for the stiffened panels, as presented in Figure 6.1. Furthermore, an analysis of the data scatter using a coefficient of variation measure showed much larger uncertainty in the indentation scenarios. This is expected because the nature of the damage event is much more complex and could vary significantly under different types of indentation. The behaviour of damage represented by a circular clear-cut hole can be demonstrated as a linear line by taking the mean value of an individual group of results. This example shows results of a group with a plate slenderness ratio of 2.0. On the other hand, a bi-linear line is adopted to represent the results of the penetration

damage.

In addition, both groups of damage scenarios show the difference of ultimate strength in the stiffened panels. The ultimate strength of penetration damage can be lower than circular clear-cut hole damage such as in the damage area ratio at 0.273 in Figure 6.1. However, the penetration damage can become stronger than damage with a clear-cut hole because of the conditions after penetration.

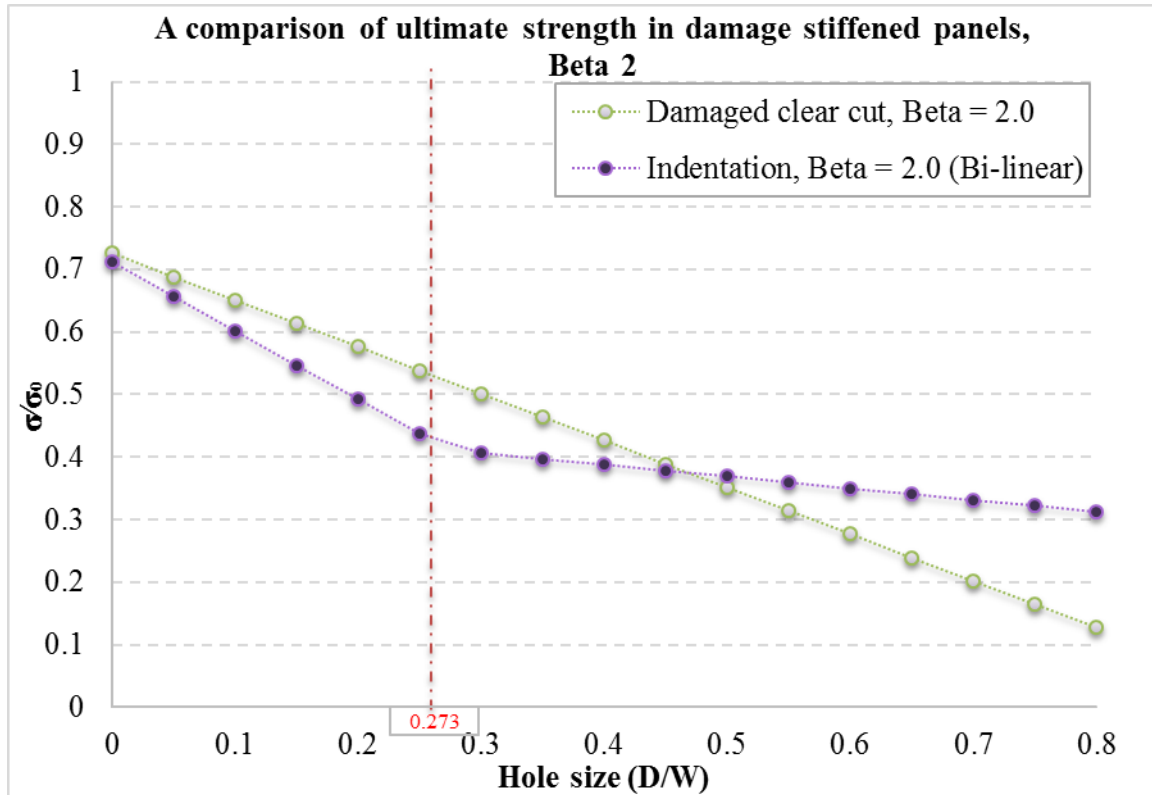


Figure 6.1 Comparison of ultimate strength in damaged stiffened panels with Beta 2.0.

6.1.3 Extended progressive collapse method

A principal outcome of this research is an extension of the simplified progressive collapse method, using ProColl (Benson et al., 2013c) as a basis and including the damage effect. The development began with a validation for the set of foundation models with intact stiffened panels. ABAQUS results were compared with results from the simplified method. The results showed good agreement between the results of both methods.

Knockdown factors were generated using results from both damage scenarios in the stiffened panels' analysis. The knockdown factors were used to re-generate load shortening curves for the damaged stiffened panel in the box girder. The new load shortening curves were sent back to the progressive collapse method to calculate the moment curvature relationship and determine the damage residual strength of the structure under consideration.

A set of box girders was used to validate the extended progressive collapse method. The damage scenarios were applied to the box girder, with a focus on damage to the bottom structure, and analysed with finite element analysis under moment curvature (hogging) before comparing the results with the modified simplified progressive method. The damage scenario used for this study is considered a worst case scenario where the bottom structure, which is under the largest bending stresses, is severely damaged. Further pilot analyses were undertaken with damage in the side shell and revealed that, although the damage was still reasonably represented by the extended progressive collapse method, the results show only a minor effect on the overall strength due to the damage location close to the neutral axis.

The comparison of moment curvature in double bottom box girder with damage effects showed a very good comparison between the two methods.

6.2 Recommendations for future work

Unpredictable accidents can occur anywhere in a ship's structure. This study has focused on the damage in the central region of a large regular stiffened panel. The range of damage scenarios that could be represented in the extended simplified progressive collapse method could be improved by investigating damage effects in different areas of stiffened panels. Furthermore, the speed and angle of the indenter could be changed in order to see different behaviours in the stiffened panel models.

On the other hand, external loads, such as wave load, temperature effect and lifespan of ship should be considered in the analysis in order to create a more realistic simulation of the ship's structure.

Finally, further studies could be carried out with different types of damage, for example, grounding, explosion or fire.

This study has application for industrially relevant improvements in the safety assessment of ship and offshore structures. Specifically, the study can be used as follows:

1. Improve the understanding about the behavior of the structure after accidents occur. This could be used within the design and analysis process of a new ship, and could also be an essential tool in damage assessment and decision making in the event of an accident. For example, it could be used as part of the Emergency Response Service offered by classification societies.
2. The research has developed a method which can reduce the computational time for the remaining strength of the damaged ship structure to be assessed. This can be used to validate high fidelity finite element analyses of damage scenarios.
3. This research can be used to reduce the consequences to the environment, economic and safety of life on board through a rapid assessment of the residual ship strength in the event of an accident. By shortening the time of the damaged strength estimation it decreases the likelihood of losses. For example, the use of this method could have altered the decision making process in the Prestige disaster, indicating that the ship did not have sufficient residual strength to remain in deepwater wave conditions.
4. The study can be used for the improvement of the ship maintenance process by identifying the loss in strength due to minor or major damage to the structure.

References

- ABUBAKAR, A. & DOW, R. S. 2013. Simulation of ship grounding damage using the finite element method. *International Journal of Solids and Structures*, 50, 623-636.
- ABUBAKAR, A., DOW, R. S., TIGKAS, I. G., SAMUELIDES, M. S. & SPYROU, K. J. 2010. Investigation of an actual collision incident between a tanker and a bulk carrier. 11th International Symposium on Practical Design of Ships and Other Floating Structures, 19-24 September 2010 2010 Rio de Janeiro, Brazil. Rio de Janeiro, Brazil: COPPE/UFRJ, 201-211.
- BENSON, S. 2011. *Progressive collapse assessment of lightweight ship structures*. Doctor of Philosophy, Newcastle University.
- BENSON, S., ABUBAKAR, A. & DOW, R. S. 2013a. A comparison of computational methods to predict the progressive collapse behaviour of a damaged box girder. *Engineering Structures*, 48, 266-280.
- BENSON, S., ABUBAKAR, A. & DOW, R. S. 2013. Progressive collapse analysis of a damaged box girder in longitudinal bending. 12th International Symposium on Practical Design of Ships and Other Floating Structures (The PRADS2013), 20-25 October 2013 2013b Gyeongnam Province, South Korea. Korea: PRADS, 2013.
- BENSON, S., DOWNES, J. & DOW, R. S. 2013c. Compartment level progressive collapse analysis of lightweight ship structures. *Marine Structures*, 31, 44-62.
- BENSON, S., DOWNES, J. & DOW, R. S. 2013d. Load shortening characteristics of marine grade aluminium alloy plates in longitudinal compression. In: NEWCASTLE UNIVERSITY, S. O. M. S. A. T. (ed.) *Thin-Walled Structures*. United Kingdom.
- BENSON, S., DOWNES, J. & DOW, R. S. 2015. Overall buckling of lightweight stiffened panels using an adapted orthotropic plate method. *Engineering Structures*, 85, 107-117.
- BENSON, S., LEELACHAI, A. & DOW, R. S. 2013. Ultimate strength of stiffened panels with circular cut-outs under in-plane compression. 12th International Conference on Fast Sea Transportation, 2-5 December 2013 2013e Amsterdam, Netherlands. Netherlands.
- BOLE, M. 2007. Introducing Damage Structural Assessment to Onboard Decision Support Tools. In: BERTRAM, V., ed. *Computer Applications and Information Technology in the Maritime Industries*, COMPIT, 23-25 April 2007 2007 Cortona, Italy. Cortona, Italy: INSEAN, 386-399.
- CALDWELL, J. B. 1965. Ultimate longitudinal strength. *Trans. RINA*, 107, 411-430.
- CARL T. F. ROSS, JOHN CASE & CRANFIELD, L. C. O. 1999. *Strength of Materials and Structures*, Oxford, United Kingdom, Butterworth-Heinemann.
- CHALMERS, D. W. 1993. *Design of ships' structures*, London, London : HMSO.
- CHEN, W. & HAN, D. 1988. *Plasticity for Structural Engineers*, Florida, United States, J. Ross Publishing, Inc.
- D. COOK, R., S. MALKUS, D., E. PLESHA, M. & J. WITT, R. 2002. *Concepts and*

Applications of Finite Element Analysis: 4th Edition.

- DOW, R. S. 1997. Structural redundancy and damage tolerance in relation to ultimate ship hull strength. *Advances in Marine Structures*, 3.
- DOW, R. S. & SMITH, C. S. 1984. Effects of localized imperfections on compressive strength of long rectangular plates. *Journal of Constructional Steel Research*, 4, 51-76.
- DOW, R. S. & SMITH, C. S. 1986. Fabstran: A Computer Program for Frame and Beam Static and Transient Response Analysis (Nonlinear). Admiralty Research Establishment, Dunfermline (England).; National Aeronautics and Space Administration, Washington, DC.: Admiralty Research Establishment, Dunfermline (England).; National Aeronautics and Space Administration, Washington, DC.
- GCAPTAIN 2016. ICS Raises Concerns Over Spanish Supreme Court's Ruling in Prestige Oil Spill Case. In: PRESTIGE, M. (ed.) *JPEG*. gCaptain.
- HUGHES, O. F. 1988. *Ship structural design : a rationally-based, computer-aided optimization approach*, Jersey City, N.J., Jersey City, N.J. : Society of Naval Architects and Marine Engineers.
- LEE, J.-S. 2012. On the Ultimate Compressive Strength of Stiffener Panels with Rectangular Opening. 5th PAAMES and AMEC2012, 10-12 Dec 2012 2012 Taiwan. Taiwan.
- LEE, S.-G., LEE, J.-S., LEE, H.-S., PARK, J.-H. & JUNG, T.-Y. 2017. Full-scale Ship Collision, Grounding and Sinking Simulation Using Highly Advanced M&S System of FSI Analysis Technique. *Procedia Engineering*, 173, 1507-1514.
- LEE, S. G., JAN, S. H. & KONG, G. Y. 2013. Modeling and simulation system for marine accident cause investigation. In: AMDAHL, J., EHLERS, S. & LEIRA, B. J., eds. 6th International conference on collision and grounding of ships and offshore structures, ICCGS, 17 - 19 June 2013 2013 Trondheim, Norway. Norway: Taylor & Francis Group, 39-47.
- LEELACHAI A, BENSON SD & RS, D. 2015. Progressive collapse of intact and damaged stiffened panels. 5th International Conference on Marine Structures, MARSTRUCT 2015, 2015 2015 Southampton, UK. CRC Press/Balkema, 505-512.
- REGISTER, L. S. 2014. General Information for the Rules and Regulations for the Classification of Ships. Lloyd's register: Lloyd's register.
- SGT. DON L. MAES, U. S. M. C. 2000. The USS Cole In: COLE, T. U. (ed.). 911 Memorial and Museum.
- SMITH, C. S. 1977. Influence of local compressive failure on ultimate longitudinal strength of a ship's hull. In: GAKKAI, N. Z., ed. Proceedings of the PRADS: International Symposium on Practical Design in Shipbuilding, 18 - 20 October 1977 1977 Tokyo. Tokyo: Society of Naval Architects of Japan, 1977, 73 - 79.
- SMITH, C. S. & ANDERSON, N. 1991. Strength of stiffened plating under combined compression and lateral pressure *Transactions of The Royal Institution of Naval Architects (RINA Trans)*, 134, 131-147.

- SMITH, C. S., DAVIDSON, P. C. & CHAPMAN, J. C. 1988. Strength and stiffness of ships' plating under in-plane compression and tension. *Annual report and transactions of the Royal Institution of Naval Architects.*, 130.
- SHIP STRUCTURES COMMITTEE. 2018. Case Study XII: PRESTIGE. N/A ed.: Ship Structure Committee (SSC) An Interagency Research and Development Committee for Safer Ship Structures.
- SYSTÈMES, D. 2013. ABAQUS 6.13. In: 6.13 (ed.) *ABAQUS 6.13*. 6.13 ed. United States: Dassault Systèmes Simulia Corp.
- UEDA, Y. & RASHED, S. 1974. *An Ultimate Transverse Strength Analysis of Ship Structure*.
- UNDERWOOD, J. M., SOBEY, A. J., BLAKE, J. I. R. & AJIT SHENOI, R. 2012. Ultimate collapse strength assessment of damaged steel-plated structures. *Engineering Structures*, 38, 1-10.
- WIKIPEDIA 2000 - 2017. USS Cole (DDG-67). *USS Cole (DDG-67)*. Wikipedia, The Free Encyclopedia.
- WIKIPEDIA 2002-2017. Prestige oil spill. *Prestige oil spill*. Wikipedia, The Free Encyclopedia.
- YAO, T. & NIKOLOV, P. I. 1991. Progressive Collapse Analysis of a Ship's Hull under Longitudinal Bending. *Journal of the Society of Naval Architects of Japan*, 1991, 449-461.
- YOSHIKAWA, T., BAYATFAR, A., J. KIM, B., P. CHEN, C., WANG, D., BOULARES, J., GORDO, J., JOSEFSON, L., SMITH, M., KAEDING, P., JENSEN, P., OJEDA, R., BENSON, S., VHANMANE, S., ZHANG, S. & JIANG, X. 2015. *Ultimate Strength, Committee III.1 - ISSC 2015*.
- YU, C.-L., FENG, J.-C. & CHEN, K. 2015. Ultimate uniaxial compressive strength of stiffened panel with opening under lateral pressure. *International Journal of Naval Architecture and Ocean Engineering*, 7, 399-408.
- YU, C. & LEE, J.-S. 2012. Ultimate Compressive Strength of Unstiffened Plate with Rectangular Opening. The 26th Asian-Pacific Technical Exchange and Advisory Meeting on Marine Structure, TEAM 2012, 3-6 September 2012 2012 Fukuoka, Japan. Japan.

Appendix A: Intact panels' details

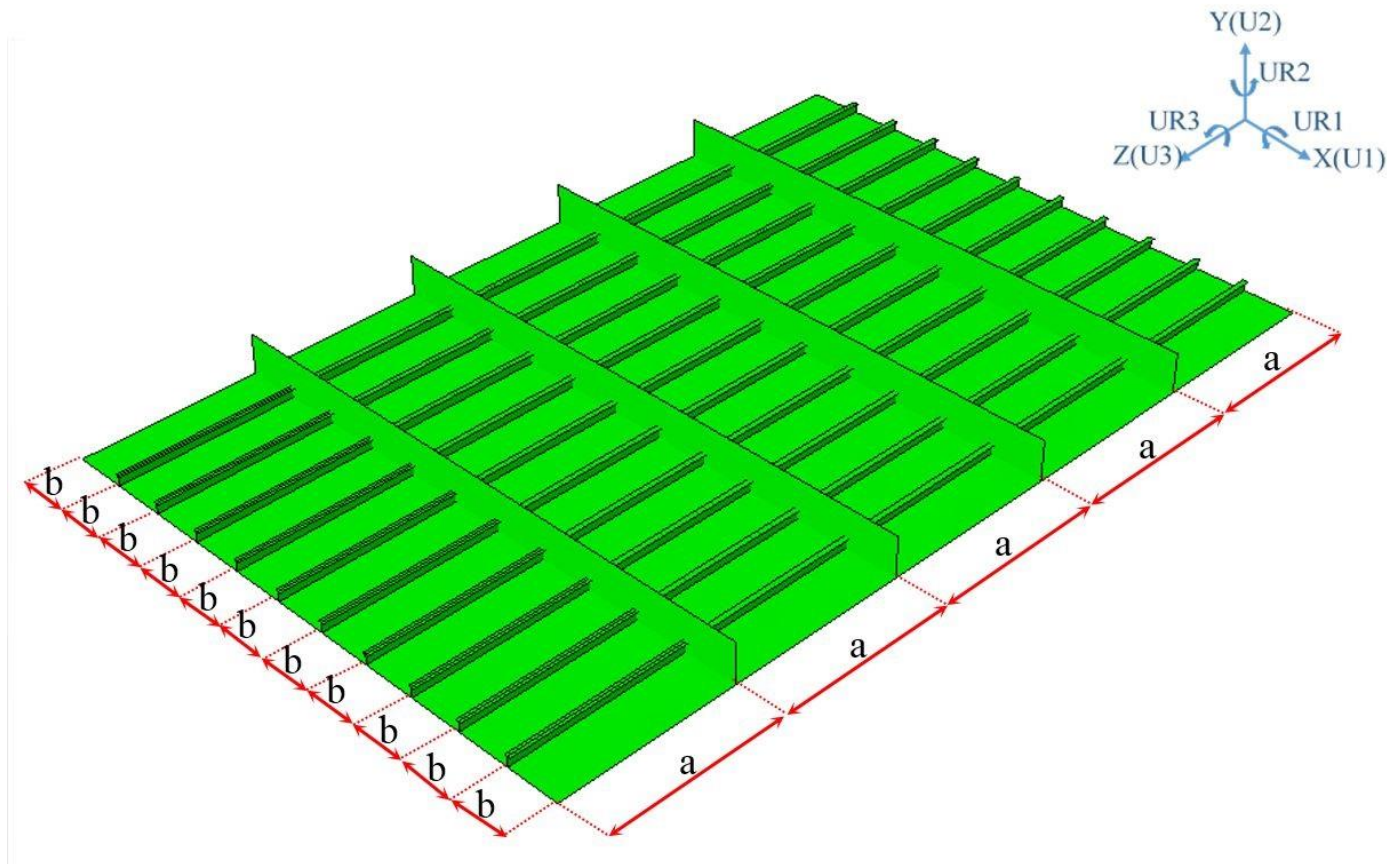


Figure A.0.1 Dimension of stiffened panel.

Plate slenderness ratio (β) = 1.0.

| β | b (mm.) | t_p (mm.) | Total area (mm ²) | a (mm.) | | | | | | | $\frac{A_s}{A}$ | Stiffener Type |
|---------|---------|----------------|-------------------------------------|-----------------|-----------------|-----------------|-----------------|-----------------|-----------------|-----------------|-----------------|-------------------|
| | | | | $\lambda = 0.2$ | $\lambda = 0.3$ | $\lambda = 0.4$ | $\lambda = 0.5$ | $\lambda = 0.6$ | $\lambda = 0.8$ | $\lambda = 1.0$ | | |
| 1 | 334.223 | 11.498 | 46969.8 | 344.548 | 516.822 | 689.096 | 861.370 | 1033.644 | 1378.193 | 1722.741 | 0.1 | ALS1 |
| 1 | 222.815 | 7.666 | 23484.8 | 442.943 | 664.414 | 885.885 | 1107.356 | 1328.828 | 1771.770 | 2214.713 | 0.2 | ALS1 |
| 1 | 170.178 | 5.855 | 15656.5 | 503.246 | 754.869 | 1006.492 | 1258.115 | 1509.738 | 2012.985 | 2516.231 | 0.3 | ALS1 |
| 1 | 136.446 | 4.694 | 11742.3 | 539.838 | 809.757 | 1079.676 | 1349.595 | 1619.514 | 2159.352 | 2699.189 | 0.4 | ALS1 |
| 1 | 477.120 | 16.414 | 95720.3 | 541.469 | 812.204 | 1082.938 | 1353.673 | 1624.407 | 2165.877 | 2707.346 | 0.1 | ALS2 |
| 1 | 318.080 | 10.943 | 47860.3 | 698.087 | 1047.130 | 1396.174 | 1745.217 | 2094.261 | 2792.348 | 3490.434 | 0.2 | ALS2 |
| 1 | 242.937 | 8.358 | 31907.0 | 792.815 | 1189.223 | 1585.631 | 1982.038 | 2378.446 | 3171.261 | 3964.076 | 0.3 | ALS2 |
| 1 | 194.783 | 6.701 | 23930.3 | 849.118 | 1273.677 | 1698.235 | 2122.794 | 2547.353 | 3396.471 | 4245.588 | 0.4 | ALS2 |
| 1 | 618.072 | 21.264 | 160630.4 | 630.098 | 945.148 | 1260.197 | 1575.246 | 1890.295 | 2520.394 | 3150.492 | 0.1 | ALS3 |
| 1 | 412.048 | 14.176 | 80315.4 | 806.400 | 1209.599 | 1612.799 | 2015.999 | 2419.199 | 3225.598 | 4031.998 | 0.2 | ALS3 |

Progressive collapse of damaged ship structure

| | | | | | | | | | | | | |
|---|---------|--------|----------|----------|----------|----------|----------|----------|----------|----------|-----|------|
| 1 | 314.707 | 10.827 | 53543.7 | 911.984 | 1367.976 | 1823.968 | 2279.960 | 2735.952 | 3647.936 | 4559.920 | 0.3 | ALS3 |
| 1 | 252.327 | 8.681 | 40157.9 | 973.026 | 1459.540 | 1946.053 | 2432.566 | 2919.079 | 3892.106 | 4865.132 | 0.4 | ALS3 |
| 1 | 701.669 | 24.140 | 207019.7 | 754.254 | 1131.380 | 1508.507 | 1885.634 | 2262.761 | 3017.014 | 3771.268 | 0.1 | ALS4 |
| 1 | 467.779 | 16.093 | 103509.7 | 968.102 | 1452.153 | 1936.204 | 2420.255 | 2904.306 | 3872.407 | 4840.509 | 0.2 | ALS4 |
| 1 | 357.272 | 12.291 | 69006.4 | 1096.137 | 1644.206 | 2192.274 | 2740.343 | 3288.411 | 4384.548 | 5480.685 | 0.3 | ALS4 |
| 1 | 286.455 | 9.855 | 51754.7 | 1170.390 | 1755.586 | 2340.781 | 2925.976 | 3511.171 | 4681.562 | 5851.952 | 0.4 | ALS4 |
| 1 | 785.618 | 27.028 | 259519.7 | 879.191 | 1318.787 | 1758.383 | 2197.979 | 2637.574 | 3516.766 | 4395.957 | 0.1 | ALS5 |
| 1 | 523.745 | 18.018 | 129759.7 | 1130.717 | 1696.075 | 2261.434 | 2826.792 | 3392.151 | 4522.868 | 5653.585 | 0.2 | ALS5 |
| 1 | 400.017 | 13.762 | 86506.4 | 1281.230 | 1921.845 | 2562.460 | 3203.075 | 3843.690 | 5124.920 | 6406.151 | 0.3 | ALS5 |
| 1 | 320.727 | 11.034 | 64879.7 | 1368.640 | 2052.960 | 2737.280 | 3421.600 | 4105.920 | 5474.560 | 6843.200 | 0.4 | ALS5 |
| 1 | 869.544 | 29.915 | 317930.2 | 1004.675 | 1507.013 | 2009.350 | 2511.688 | 3014.025 | 4018.700 | 5023.375 | 0.1 | ALS6 |
| 1 | 579.696 | 19.943 | 158965.2 | 1293.993 | 1940.989 | 2587.986 | 3234.982 | 3881.979 | 5175.972 | 6469.965 | 0.2 | ALS6 |

Progressive collapse of damaged ship structure

| | | | | | | | | | | | | |
|----------|----------|--------|----------|----------|----------|----------|----------|----------|----------|----------|-----|------|
| 1 | 442.750 | 15.232 | 105976.8 | 1467.019 | 2200.529 | 2934.039 | 3667.548 | 4401.058 | 5868.077 | 7335.097 | 0.3 | ALS6 |
| 1 | 354.990 | 12.213 | 79482.7 | 1567.561 | 2351.342 | 3135.122 | 3918.903 | 4702.683 | 6270.244 | 7837.805 | 0.4 | ALS6 |
| 1 | 1032.295 | 35.514 | 448079.6 | 1254.214 | 1881.322 | 2508.429 | 3135.536 | 3762.643 | 5016.858 | 6271.072 | 0.1 | ALS7 |
| 1 | 688.197 | 23.676 | 224039.6 | 1619.008 | 2428.512 | 3238.016 | 4047.520 | 4857.025 | 6476.033 | 8095.041 | 0.2 | ALS7 |
| 1 | 525.619 | 18.083 | 149359.6 | 1837.077 | 2755.615 | 3674.154 | 4592.692 | 5511.230 | 7348.307 | 9185.384 | 0.3 | ALS7 |
| 1 | 421.433 | 14.499 | 112019.6 | 1964.001 | 2946.001 | 3928.002 | 4910.002 | 5892.003 | 7856.004 | 9820.005 | 0.4 | ALS7 |

Plate slenderness ratio (β) = 2.0.

| β | b (mm.) | t_p (mm.) | Total area (mm ²) | a (mm.) | | | | | | | $\frac{A_s}{A}$ | Stiffener Type |
|---------|---------|----------------|-------------------------------------|-----------------|-----------------|-----------------|-----------------|-----------------|-----------------|-----------------|-----------------|-------------------|
| | | | | $\lambda = 0.2$ | $\lambda = 0.3$ | $\lambda = 0.4$ | $\lambda = 0.5$ | $\lambda = 0.6$ | $\lambda = 0.8$ | $\lambda = 1.0$ | | |
| 2 | 472.663 | 8.131 | 46969.8 | 333.615 | 500.422 | 667.230 | 834.037 | 1000.845 | 1334.460 | 1668.075 | 0.1 | ALS1 |
| 2 | 315.108 | 5.420 | 23484.8 | 434.800 | 652.201 | 869.601 | 1087.001 | 1304.401 | 1739.202 | 2174.002 | 0.2 | ALS1 |
| 2 | 240.668 | 4.140 | 15656.5 | 496.622 | 744.932 | 993.243 | 1241.554 | 1489.865 | 1986.487 | 2483.108 | 0.3 | ALS1 |
| 2 | 192.964 | 3.319 | 11742.3 | 534.454 | 801.681 | 1068.909 | 1336.136 | 1603.363 | 2137.817 | 2672.272 | 0.4 | ALS1 |
| 2 | 674.749 | 11.607 | 95720.3 | 526.002 | 789.004 | 1052.005 | 1315.006 | 1578.007 | 2104.010 | 2630.012 | 0.1 | ALS2 |
| 2 | 449.833 | 7.738 | 47860.3 | 686.392 | 1029.588 | 1372.784 | 1715.980 | 2059.176 | 2745.568 | 3431.960 | 0.2 | ALS2 |
| 2 | 343.565 | 5.910 | 31907.0 | 783.236 | 1174.854 | 1566.472 | 1958.090 | 2349.708 | 3132.944 | 3916.180 | 0.3 | ALS2 |
| 2 | 275.465 | 4.738 | 23930.3 | 841.295 | 1261.943 | 1682.590 | 2103.238 | 2523.885 | 3365.180 | 4206.475 | 0.4 | ALS2 |
| 2 | 874.086 | 15.036 | 160630.4 | 609.395 | 914.092 | 1218.790 | 1523.487 | 1828.184 | 2437.579 | 3046.974 | 0.1 | ALS3 |
| 2 | 582.724 | 10.024 | 80315.4 | 790.876 | 1186.314 | 1581.752 | 1977.190 | 2372.628 | 3163.504 | 3954.380 | 0.2 | ALS3 |

Progressive collapse of damaged ship structure

| | | | | | | | | | | | | |
|---|----------|--------|----------|----------|----------|----------|----------|----------|----------|----------|-----|------|
| 2 | 445.063 | 7.656 | 53543.7 | 899.286 | 1348.928 | 1798.571 | 2248.214 | 2697.857 | 3597.142 | 4496.428 | 0.3 | ALS3 |
| 2 | 356.844 | 6.138 | 40157.9 | 962.647 | 1443.970 | 1925.293 | 2406.617 | 2887.940 | 3850.587 | 4813.234 | 0.4 | ALS3 |
| 2 | 992.309 | 17.069 | 207019.7 | 731.022 | 1096.533 | 1462.044 | 1827.555 | 2193.066 | 2924.089 | 3655.111 | 0.1 | ALS4 |
| 2 | 661.540 | 11.380 | 103509.7 | 950.579 | 1425.869 | 1901.158 | 2376.448 | 2851.737 | 3802.316 | 4752.895 | 0.2 | ALS4 |
| 2 | 505.259 | 8.691 | 69006.4 | 1081.775 | 1622.663 | 2163.550 | 2704.438 | 3245.326 | 4327.101 | 5408.876 | 0.3 | ALS4 |
| 2 | 405.109 | 6.969 | 51754.7 | 1158.641 | 1737.961 | 2317.282 | 2896.602 | 3475.923 | 4634.564 | 5793.205 | 0.4 | ALS4 |
| 2 | 1111.032 | 19.111 | 259519.7 | 853.393 | 1280.090 | 1706.786 | 2133.483 | 2560.179 | 3413.572 | 4266.965 | 0.1 | ALS5 |
| 2 | 740.688 | 12.741 | 129759.7 | 1111.170 | 1666.754 | 2222.339 | 2777.924 | 3333.509 | 4444.678 | 5555.848 | 0.2 | ALS5 |
| 2 | 565.710 | 9.731 | 86506.4 | 1265.184 | 1897.777 | 2530.369 | 3162.961 | 3795.553 | 5060.738 | 6325.922 | 0.3 | ALS5 |
| 2 | 453.577 | 7.802 | 64879.7 | 1355.503 | 2033.255 | 2711.007 | 3388.759 | 4066.510 | 5422.014 | 6777.517 | 0.4 | ALS5 |
| 2 | 1229.721 | 21.153 | 317930.2 | 976.295 | 1464.442 | 1952.590 | 2440.737 | 2928.885 | 3905.180 | 4881.475 | 0.1 | ALS6 |
| 2 | 819.814 | 14.102 | 158965.2 | 1272.412 | 1908.618 | 2544.824 | 3181.030 | 3817.236 | 5089.649 | 6362.061 | 0.2 | ALS6 |

Progressive collapse of damaged ship structure

| | | | | | | | | | | | | |
|---|----------|--------|----------|----------|----------|----------|----------|----------|----------|----------|-----|------|
| 2 | 626.143 | 10.771 | 105976.8 | 1449.283 | 2173.924 | 2898.566 | 3623.207 | 4347.848 | 5797.131 | 7246.414 | 0.3 | ALS6 |
| 2 | 502.032 | 8.636 | 79482.7 | 1553.032 | 2329.547 | 3106.063 | 3882.579 | 4659.095 | 6212.126 | 7765.158 | 0.4 | ALS6 |
| 2 | 1459.885 | 25.112 | 448079.6 | 1220.847 | 1831.271 | 2441.695 | 3052.118 | 3662.542 | 4883.389 | 6104.236 | 0.1 | ALS7 |
| 2 | 973.257 | 16.742 | 224039.6 | 1593.498 | 2390.247 | 3186.996 | 3983.745 | 4780.493 | 6373.991 | 7967.489 | 0.2 | ALS7 |
| 2 | 743.337 | 12.787 | 149359.6 | 1816.074 | 2724.110 | 3632.147 | 4540.184 | 5448.221 | 7264.294 | 9080.368 | 0.3 | ALS7 |
| 2 | 595.996 | 10.252 | 112019.6 | 1946.781 | 2920.172 | 3893.562 | 4866.953 | 5840.343 | 7787.124 | 9733.906 | 0.4 | ALS7 |

Plate slenderness ratio (β) = 3.0.

| β | b (mm.) | t_p (mm.) | Total area (mm ²) | a (mm.) | | | | | | | $\frac{A_s}{A}$ | Stiffener Type |
|---------|----------|----------------|-------------------------------------|-----------------|-----------------|-----------------|-----------------|-----------------|-----------------|-----------------|-----------------|-------------------|
| | | | | $\lambda = 0.2$ | $\lambda = 0.3$ | $\lambda = 0.4$ | $\lambda = 0.5$ | $\lambda = 0.6$ | $\lambda = 0.8$ | $\lambda = 1.0$ | | |
| 3 | 578.891 | 6.639 | 46969.8 | 329.017 | 493.526 | 658.035 | 822.544 | 987.052 | 1316.070 | 1645.087 | 0.1 | ALS1 |
| 3 | 385.927 | 4.426 | 23484.8 | 431.278 | 646.917 | 862.557 | 1078.196 | 1293.835 | 1725.113 | 2156.391 | 0.2 | ALS1 |
| 3 | 294.757 | 3.380 | 15656.5 | 493.729 | 740.594 | 987.458 | 1234.323 | 1481.187 | 1974.916 | 2468.645 | 0.3 | ALS1 |
| 3 | 236.331 | 2.710 | 11742.3 | 532.093 | 798.140 | 1064.186 | 1330.233 | 1596.280 | 2128.373 | 2660.466 | 0.4 | ALS1 |
| 3 | 826.396 | 9.477 | 95720.3 | 519.471 | 779.206 | 1038.941 | 1298.677 | 1558.412 | 2077.883 | 2597.353 | 0.1 | ALS2 |
| 3 | 550.930 | 6.318 | 47860.3 | 681.320 | 1021.980 | 1362.640 | 1703.300 | 2043.960 | 2725.279 | 3406.599 | 0.2 | ALS2 |
| 3 | 420.780 | 4.825 | 31907.0 | 779.046 | 1168.568 | 1558.091 | 1947.614 | 2337.137 | 3116.182 | 3895.228 | 0.3 | ALS2 |
| 3 | 337.375 | 3.869 | 23930.3 | 837.860 | 1256.789 | 1675.719 | 2094.649 | 2513.579 | 3351.439 | 4189.298 | 0.4 | ALS2 |
| 3 | 1070.533 | 12.277 | 160630.4 | 600.673 | 901.010 | 1201.346 | 1501.683 | 1802.019 | 2402.692 | 3003.365 | 0.1 | ALS3 |
| 3 | 713.688 | 8.184 | 80315.4 | 784.153 | 1176.229 | 1568.306 | 1960.382 | 2352.459 | 3136.611 | 3920.764 | 0.2 | ALS3 |

Progressive collapse of damaged ship structure

| | | | | | | | | | | | | |
|---|----------|--------|----------|----------|----------|----------|----------|----------|----------|----------|-----|------|
| 3 | 545.089 | 6.251 | 53543.7 | 893.736 | 1340.603 | 1787.471 | 2234.339 | 2681.207 | 3574.942 | 4468.678 | 0.3 | ALS3 |
| 3 | 437.043 | 5.012 | 40157.9 | 958.091 | 1437.136 | 1916.182 | 2395.227 | 2874.273 | 3832.364 | 4790.455 | 0.4 | ALS3 |
| 3 | 1215.326 | 13.937 | 207019.7 | 721.219 | 1081.829 | 1442.438 | 1803.048 | 2163.658 | 2884.877 | 3606.096 | 0.1 | ALS4 |
| 3 | 810.217 | 9.291 | 103509.7 | 942.983 | 1414.474 | 1885.965 | 2357.456 | 2828.948 | 3771.930 | 4714.913 | 0.2 | ALS4 |
| 3 | 618.814 | 7.096 | 69006.4 | 1075.494 | 1613.241 | 2150.988 | 2688.735 | 3226.482 | 4301.976 | 5377.470 | 0.3 | ALS4 |
| 3 | 496.155 | 5.690 | 51754.7 | 1153.481 | 1730.222 | 2306.963 | 2883.704 | 3460.444 | 4613.926 | 5767.407 | 0.4 | ALS4 |
| 3 | 1360.730 | 15.604 | 259519.7 | 842.493 | 1263.739 | 1684.986 | 2106.232 | 2527.479 | 3369.972 | 4212.465 | 0.1 | ALS5 |
| 3 | 907.153 | 10.403 | 129759.7 | 1102.689 | 1654.033 | 2205.378 | 2756.722 | 3308.067 | 4410.756 | 5513.445 | 0.2 | ALS5 |
| 3 | 692.850 | 7.945 | 86506.4 | 1258.163 | 1887.245 | 2516.327 | 3145.409 | 3774.490 | 5032.654 | 6290.817 | 0.3 | ALS5 |
| 3 | 555.516 | 6.370 | 64879.7 | 1349.733 | 2024.599 | 2699.466 | 3374.332 | 4049.199 | 5398.932 | 6748.665 | 0.4 | ALS5 |
| 3 | 1506.095 | 17.271 | 317930.2 | 964.291 | 1446.437 | 1928.583 | 2410.729 | 2892.874 | 3857.166 | 4821.457 | 0.1 | ALS6 |
| 3 | 1004.063 | 11.514 | 158965.2 | 1263.044 | 1894.566 | 2526.087 | 3157.609 | 3789.131 | 5052.175 | 6315.219 | 0.2 | ALS6 |

Progressive collapse of damaged ship structure

| | | | | | | | | | | | | |
|---|----------|--------|----------|----------|----------|----------|----------|----------|----------|----------|-----|------|
| 3 | 766.866 | 8.794 | 105976.8 | 1441.519 | 2162.278 | 2883.038 | 3603.797 | 4324.557 | 5766.076 | 7207.595 | 0.3 | ALS6 |
| 3 | 614.861 | 7.051 | 79482.7 | 1546.647 | 2319.971 | 3093.295 | 3866.618 | 4639.942 | 6186.589 | 7733.237 | 0.4 | ALS6 |
| 3 | 1787.987 | 20.504 | 448079.6 | 1313.231 | 1969.846 | 2626.462 | 3283.077 | 3939.693 | 5252.923 | 6566.154 | 0.1 | ALS7 |
| 3 | 1191.991 | 13.669 | 224039.6 | 1730.093 | 2595.140 | 3460.186 | 4325.233 | 5190.280 | 6920.373 | 8650.466 | 0.2 | ALS7 |
| 3 | 910.398 | 10.440 | 149359.6 | 1982.942 | 2974.413 | 3965.884 | 4957.355 | 5948.826 | 7931.768 | 9914.710 | 0.3 | ALS7 |
| 3 | 729.943 | 8.371 | 112019.6 | 2106.899 | 3160.348 | 4213.798 | 5267.247 | 6320.696 | 8427.595 | 10534.49 | 0.4 | ALS7 |

Plate slenderness ratio (β) = 4.0.

| β | b (mm.) | t_p (mm.) | Total area (mm ²) | a (mm.) | | | | | | | $\frac{A_s}{A}$ | Stiffener Type |
|---------|----------|----------------|-------------------------------------|-----------------|-----------------|-----------------|-----------------|-----------------|-----------------|-----------------|-----------------|-------------------|
| | | | | $\lambda = 0.2$ | $\lambda = 0.3$ | $\lambda = 0.4$ | $\lambda = 0.5$ | $\lambda = 0.6$ | $\lambda = 0.8$ | $\lambda = 1.0$ | | |
| 4 | 668.446 | 5.749 | 46969.8 | 326.353 | 489.529 | 652.705 | 815.882 | 979.058 | 1305.410 | 1631.763 | 0.1 | ALS1 |
| 4 | 445.631 | 3.833 | 23484.8 | 429.204 | 643.807 | 858.409 | 1073.011 | 1287.613 | 1716.817 | 2146.022 | 0.2 | ALS1 |
| 4 | 340.356 | 2.927 | 15656.5 | 492.017 | 738.026 | 984.034 | 1230.043 | 1476.052 | 1968.069 | 2460.086 | 0.3 | ALS1 |
| 4 | 272.892 | 2.347 | 11742.3 | 530.693 | 796.039 | 1061.386 | 1326.732 | 1592.079 | 2122.771 | 2653.464 | 0.4 | ALS1 |
| 4 | 954.239 | 8.207 | 95720.3 | 515.675 | 773.513 | 1031.350 | 1289.188 | 1547.025 | 2062.701 | 2578.376 | 0.1 | ALS2 |
| 4 | 636.160 | 5.471 | 47860.3 | 678.329 | 1017.494 | 1356.658 | 1695.823 | 2034.987 | 2713.316 | 3391.645 | 0.2 | ALS2 |
| 4 | 485.875 | 4.179 | 31907.0 | 776.564 | 1164.845 | 1553.127 | 1941.409 | 2329.691 | 3106.254 | 3882.818 | 0.3 | ALS2 |
| 4 | 389.567 | 3.351 | 23930.3 | 835.821 | 1253.731 | 1671.641 | 2089.552 | 2507.462 | 3343.283 | 4179.103 | 0.4 | ALS2 |
| 4 | 1236.145 | 10.632 | 160630.4 | 595.613 | 893.419 | 1191.226 | 1489.032 | 1786.839 | 2382.452 | 2978.065 | 0.1 | ALS3 |
| 4 | 824.096 | 7.088 | 80315.4 | 780.192 | 1170.287 | 1560.383 | 1950.479 | 2340.575 | 3120.766 | 3900.958 | 0.2 | ALS3 |

Progressive collapse of damaged ship structure

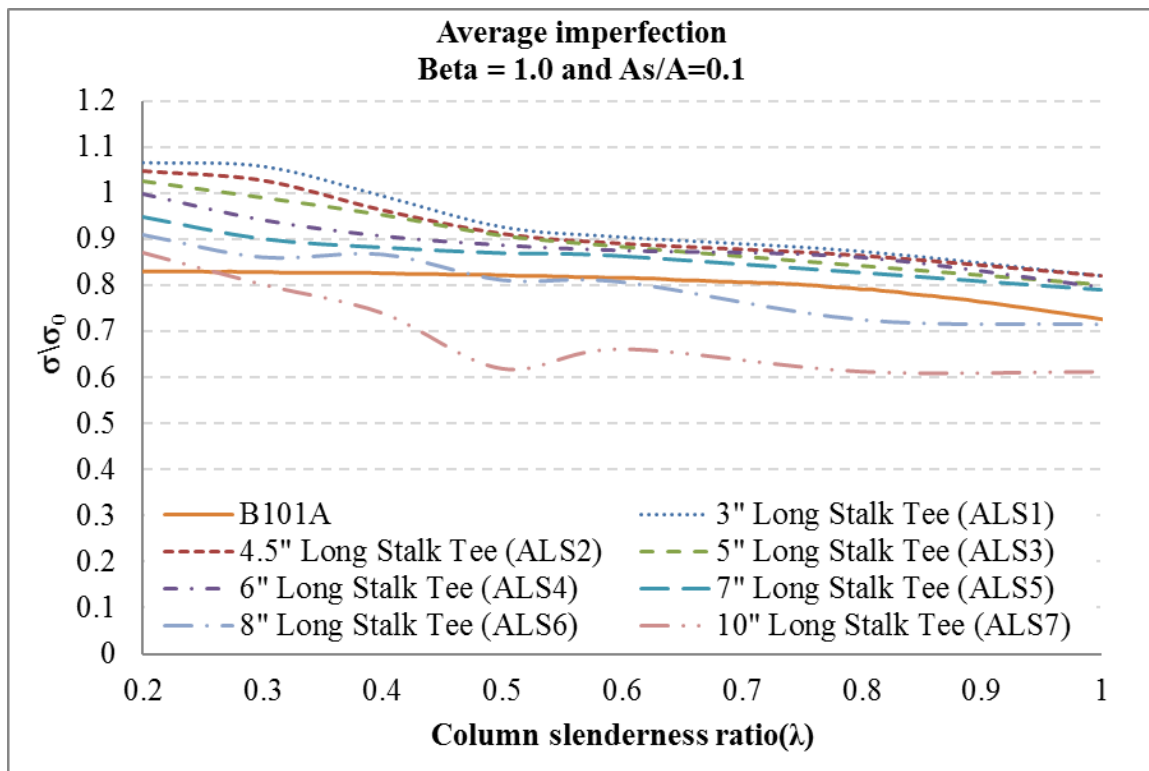
| | | | | | | | | | | | | |
|---|----------|--------|----------|----------|----------|----------|----------|----------|----------|----------|-----|------|
| 4 | 629.414 | 5.413 | 53543.7 | 890.450 | 1335.675 | 1780.899 | 2226.124 | 2671.349 | 3561.799 | 4452.249 | 0.3 | ALS3 |
| 4 | 504.654 | 4.340 | 40157.9 | 955.388 | 1433.082 | 1910.776 | 2388.469 | 2866.163 | 3821.551 | 4776.939 | 0.4 | ALS3 |
| 4 | 1403.337 | 12.070 | 207019.7 | 715.526 | 1073.289 | 1431.052 | 1788.815 | 2146.578 | 2862.104 | 3577.630 | 0.1 | ALS4 |
| 4 | 935.558 | 8.047 | 103509.7 | 938.504 | 1407.756 | 1877.008 | 2346.261 | 2815.513 | 3754.017 | 4692.521 | 0.2 | ALS4 |
| 4 | 714.544 | 6.146 | 69006.4 | 1071.774 | 1607.661 | 2143.548 | 2679.435 | 3215.322 | 4287.096 | 5358.870 | 0.3 | ALS4 |
| 4 | 572.910 | 4.927 | 51754.7 | 1150.419 | 1725.629 | 2300.839 | 2876.048 | 3451.258 | 4601.678 | 5752.097 | 0.4 | ALS4 |
| 4 | 1571.236 | 13.514 | 259519.7 | 836.158 | 1254.236 | 1672.315 | 2090.394 | 2508.473 | 3344.630 | 4180.788 | 0.1 | ALS5 |
| 4 | 1047.491 | 9.009 | 129759.7 | 1097.687 | 1646.531 | 2195.375 | 2744.218 | 3293.062 | 4390.749 | 5488.437 | 0.2 | ALS5 |
| 4 | 800.034 | 6.881 | 86506.4 | 1254.004 | 1881.006 | 2508.008 | 3135.011 | 3762.013 | 5016.017 | 6270.021 | 0.3 | ALS5 |
| 4 | 641.454 | 5.517 | 64879.7 | 1346.308 | 2019.461 | 2692.615 | 3365.769 | 4038.923 | 5385.230 | 6731.538 | 0.4 | ALS5 |
| 4 | 1739.089 | 14.958 | 317930.2 | 957.310 | 1435.966 | 1914.621 | 2393.276 | 2871.931 | 3829.242 | 4786.552 | 0.1 | ALS6 |
| 4 | 1159.392 | 9.972 | 158965.2 | 1257.517 | 1886.275 | 2515.034 | 3143.792 | 3772.550 | 5030.067 | 6287.584 | 0.2 | ALS6 |

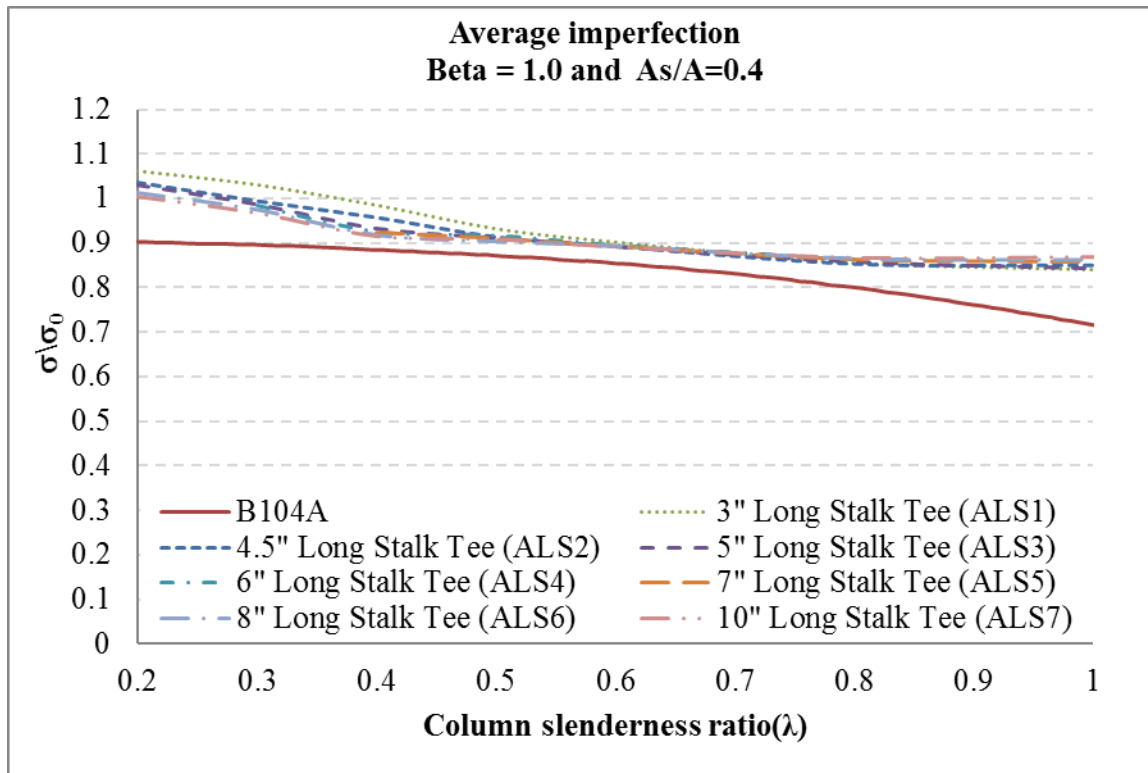
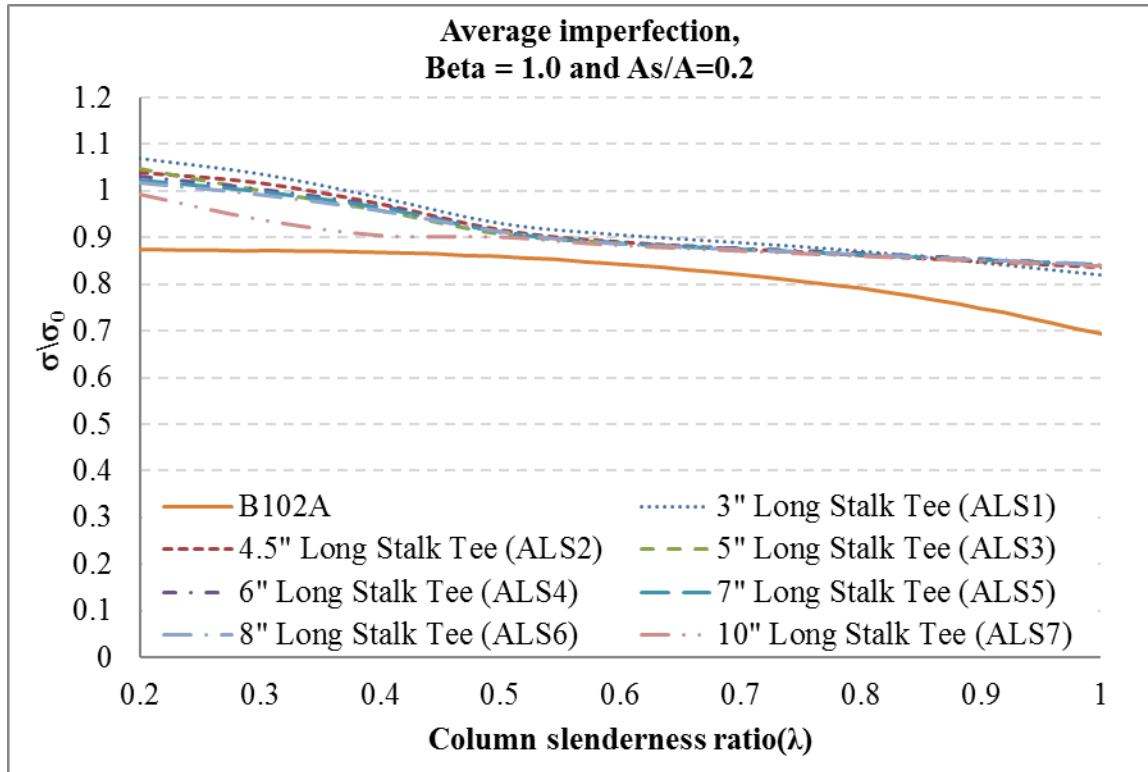
Progressive collapse of damaged ship structure

| | | | | | | | | | | | | |
|---|----------|--------|----------|----------|----------|----------|----------|----------|----------|----------|-----|------|
| 4 | 885.501 | 7.616 | 105976.8 | 1436.919 | 2155.378 | 2873.838 | 3592.297 | 4310.756 | 5747.675 | 7184.594 | 0.3 | ALS6 |
| 4 | 709.980 | 6.106 | 79482.7 | 1542.857 | 2314.286 | 3085.714 | 3857.143 | 4628.572 | 6171.429 | 7714.286 | 0.4 | ALS6 |
| 4 | 2064.590 | 17.757 | 448079.6 | 1198.484 | 1797.725 | 2396.967 | 2996.209 | 3595.451 | 4793.935 | 5992.418 | 0.1 | ALS7 |
| 4 | 1376.393 | 11.838 | 224039.6 | 1575.871 | 2363.807 | 3151.743 | 3939.679 | 4727.614 | 6303.486 | 7879.357 | 0.2 | ALS7 |
| 4 | 1051.238 | 9.041 | 149359.6 | 1801.422 | 2702.134 | 3602.845 | 4503.556 | 5404.267 | 7205.689 | 9007.112 | 0.3 | ALS7 |
| 4 | 842.865 | 7.249 | 112019.6 | 1934.717 | 2902.076 | 3869.434 | 4836.793 | 5804.151 | 7738.868 | 9673.585 | 0.4 | ALS7 |

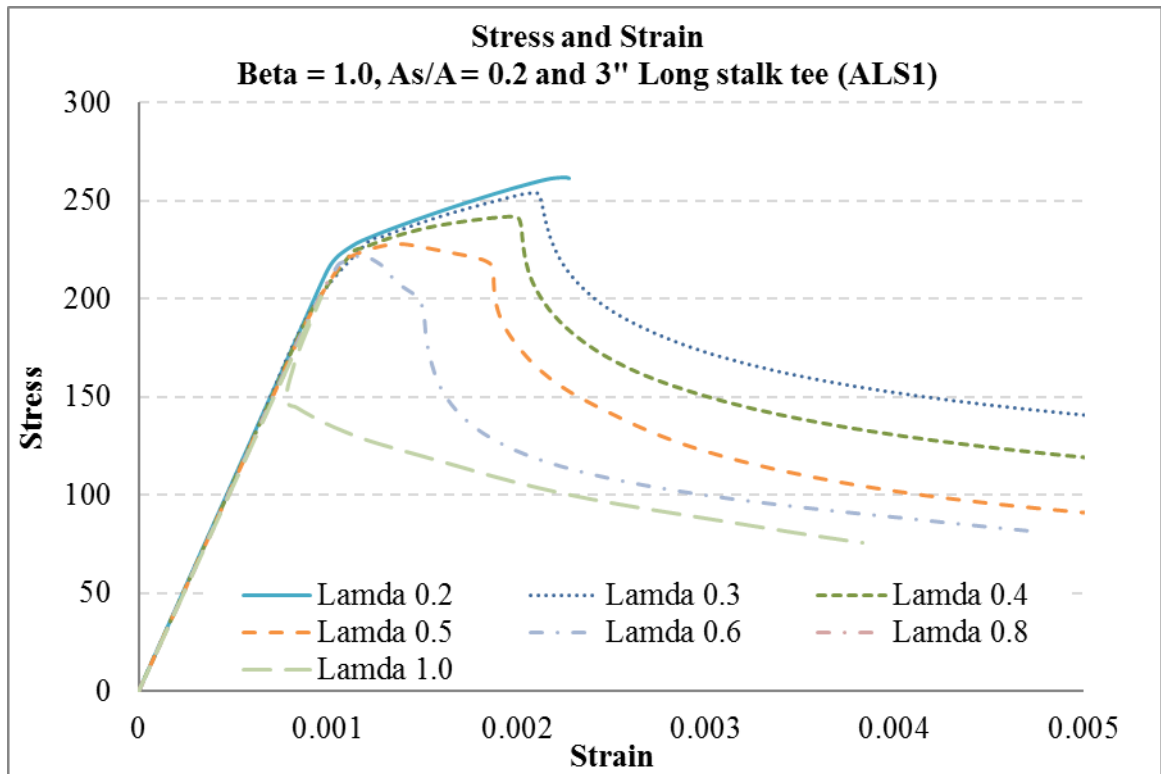
Appendix B: Strength of intact stiffened panels

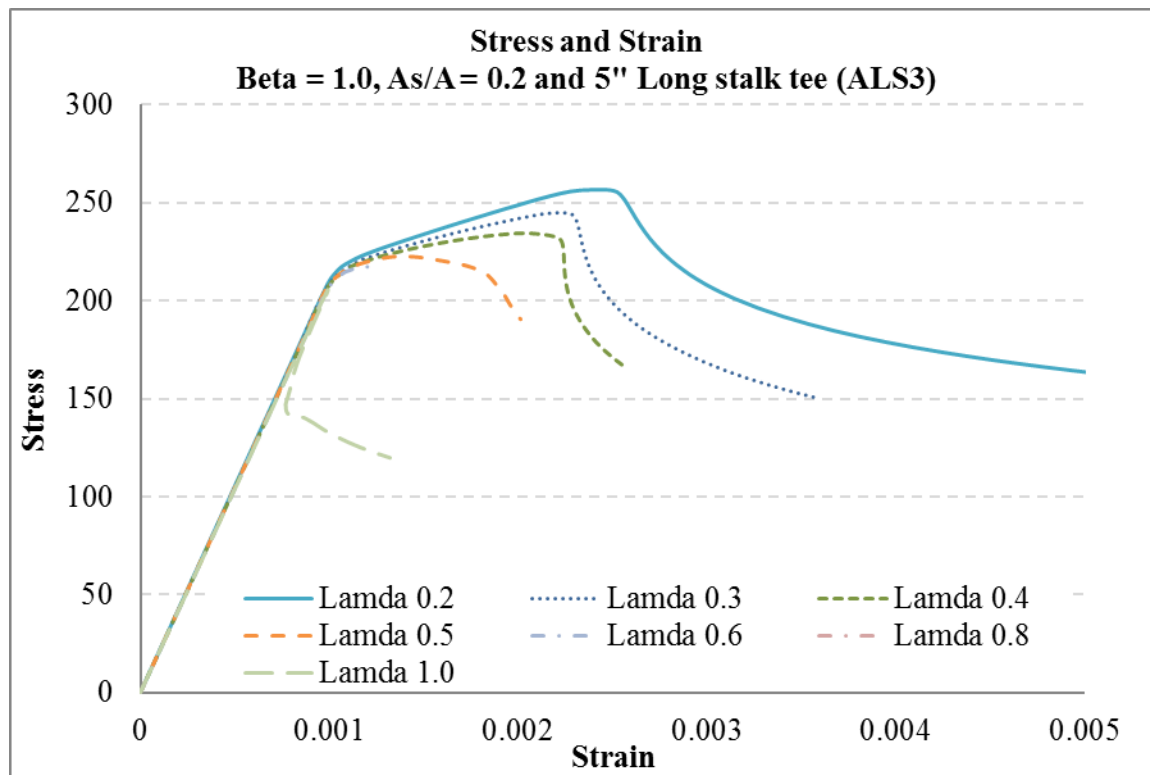
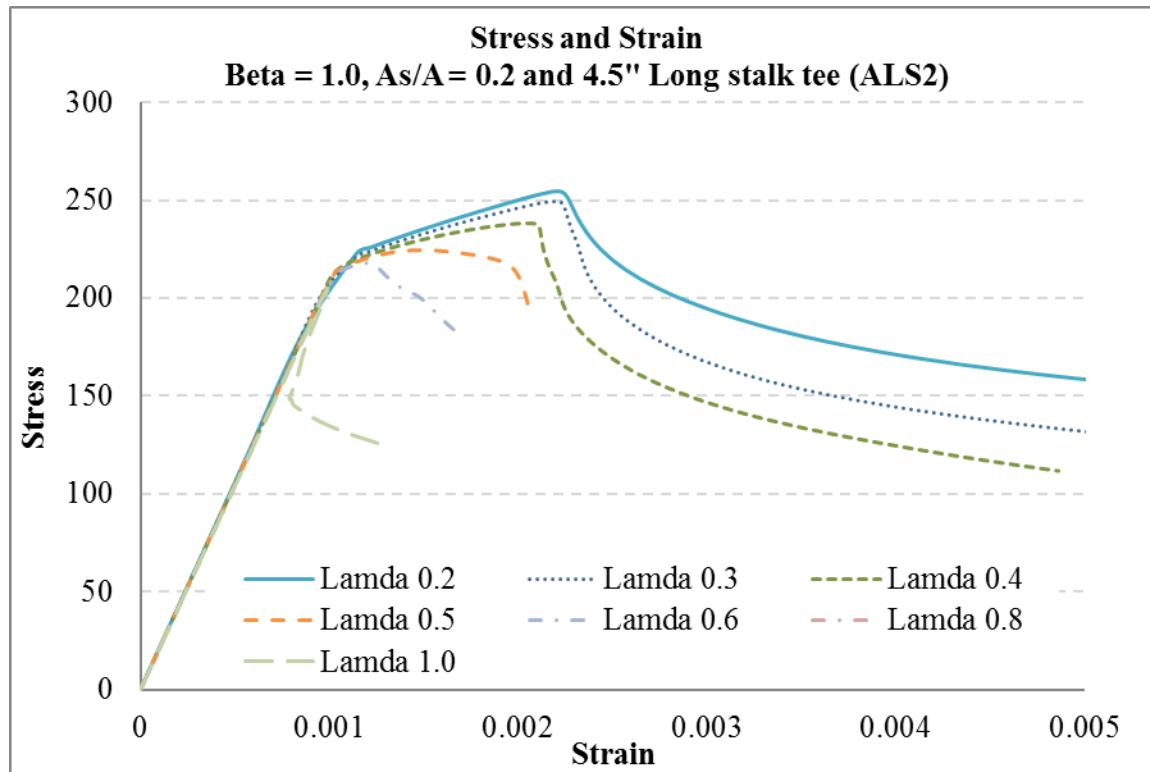
Beta 1.0: Average imperfection

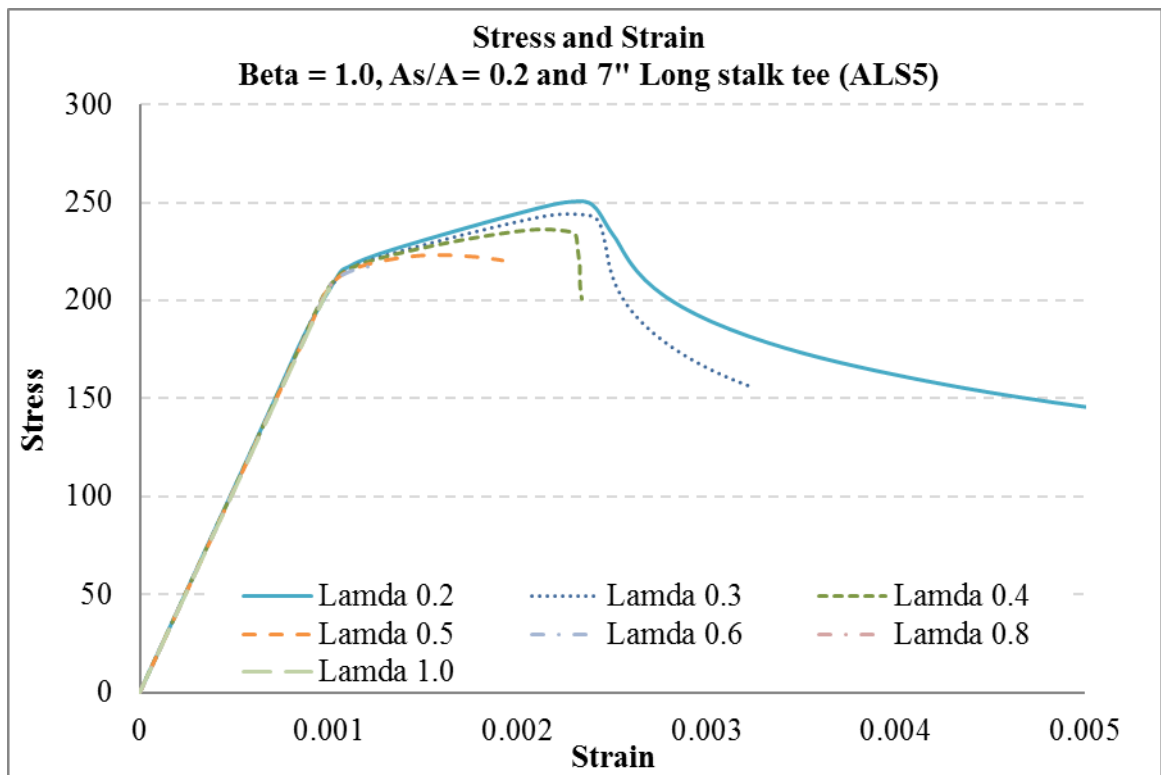
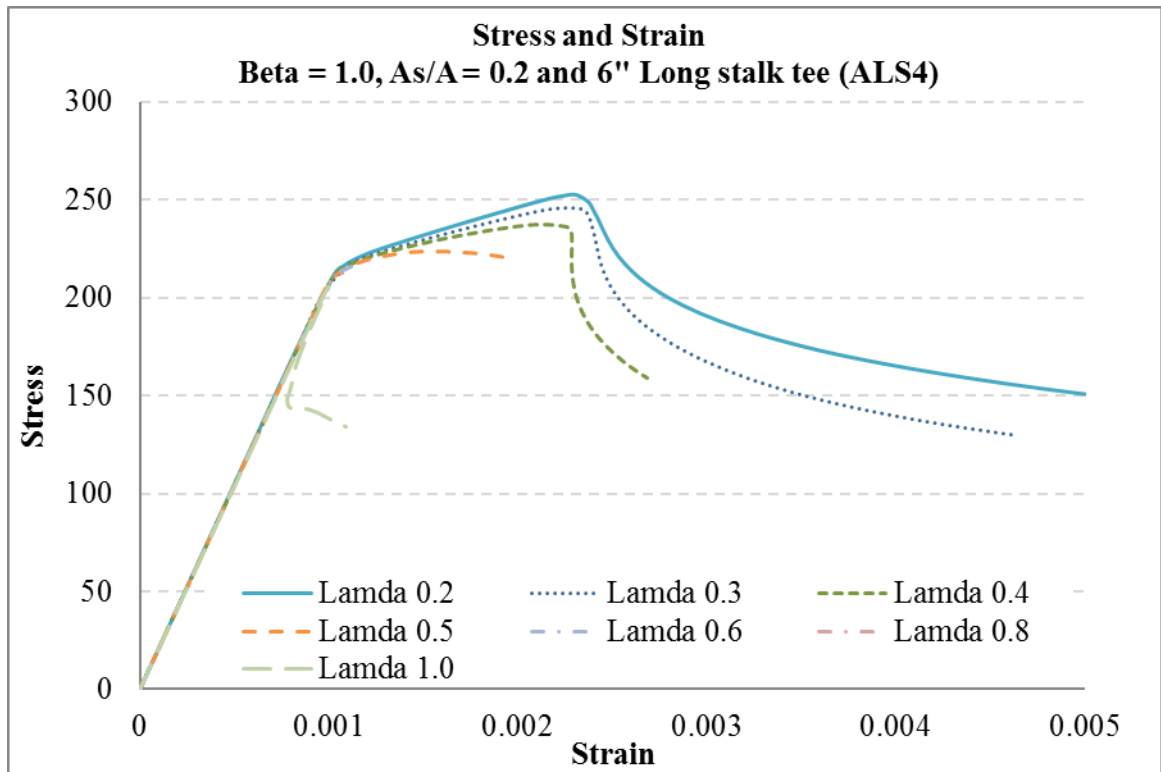


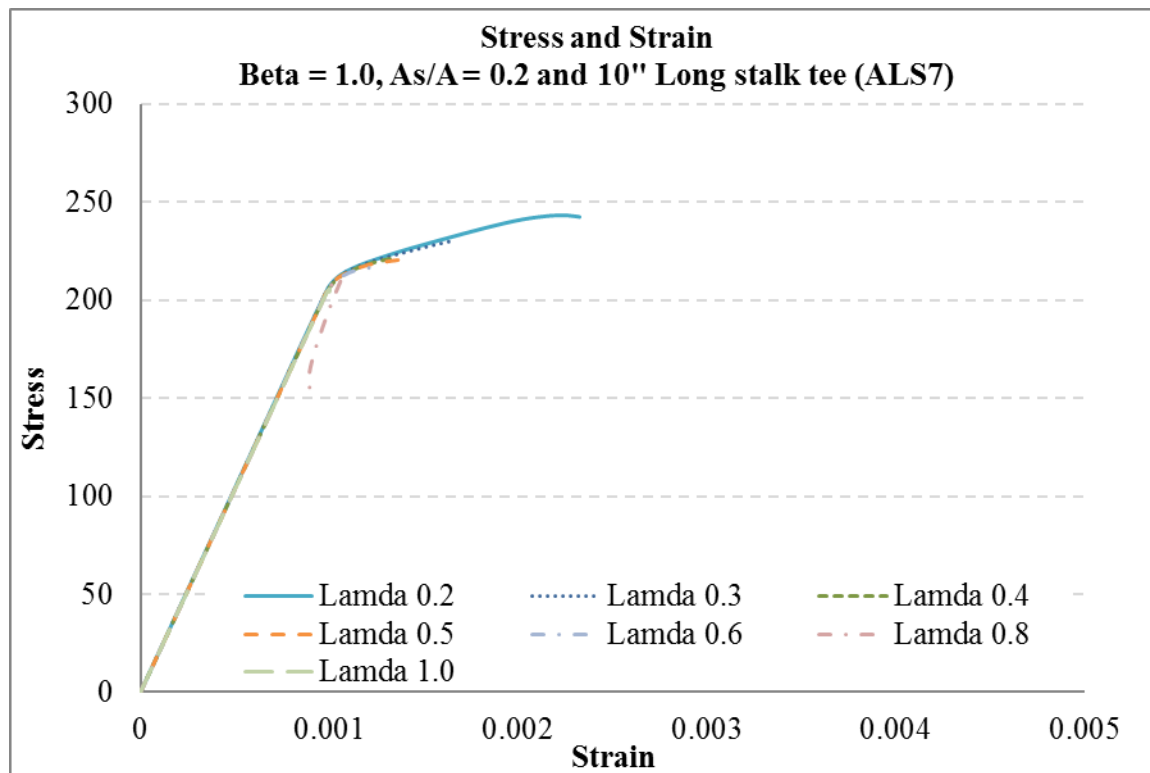
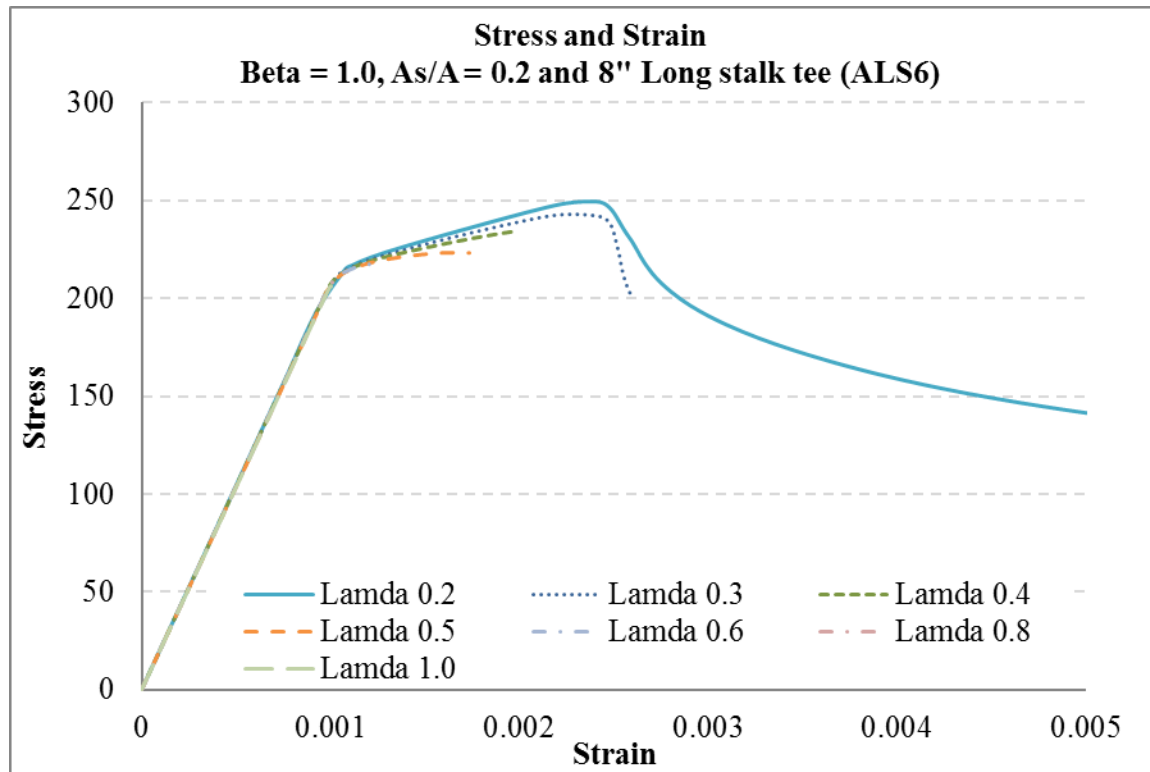


Beta 1.0: Stress and Strain curve

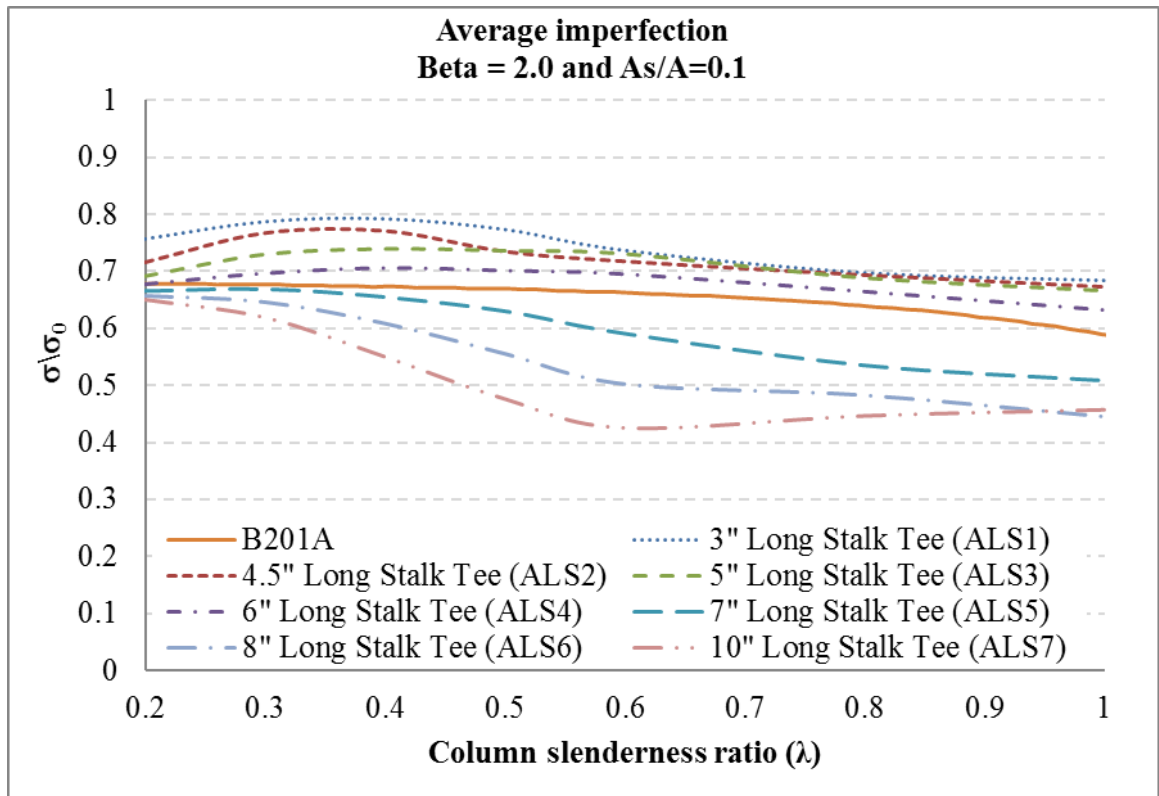


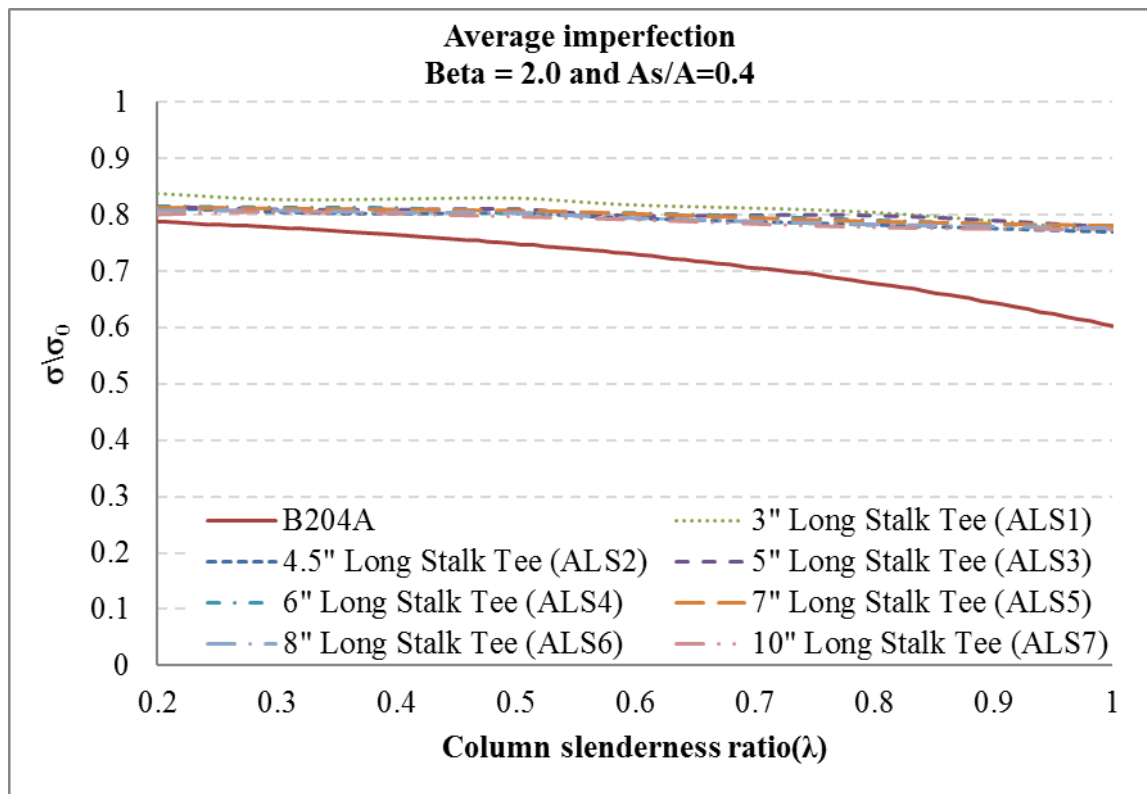
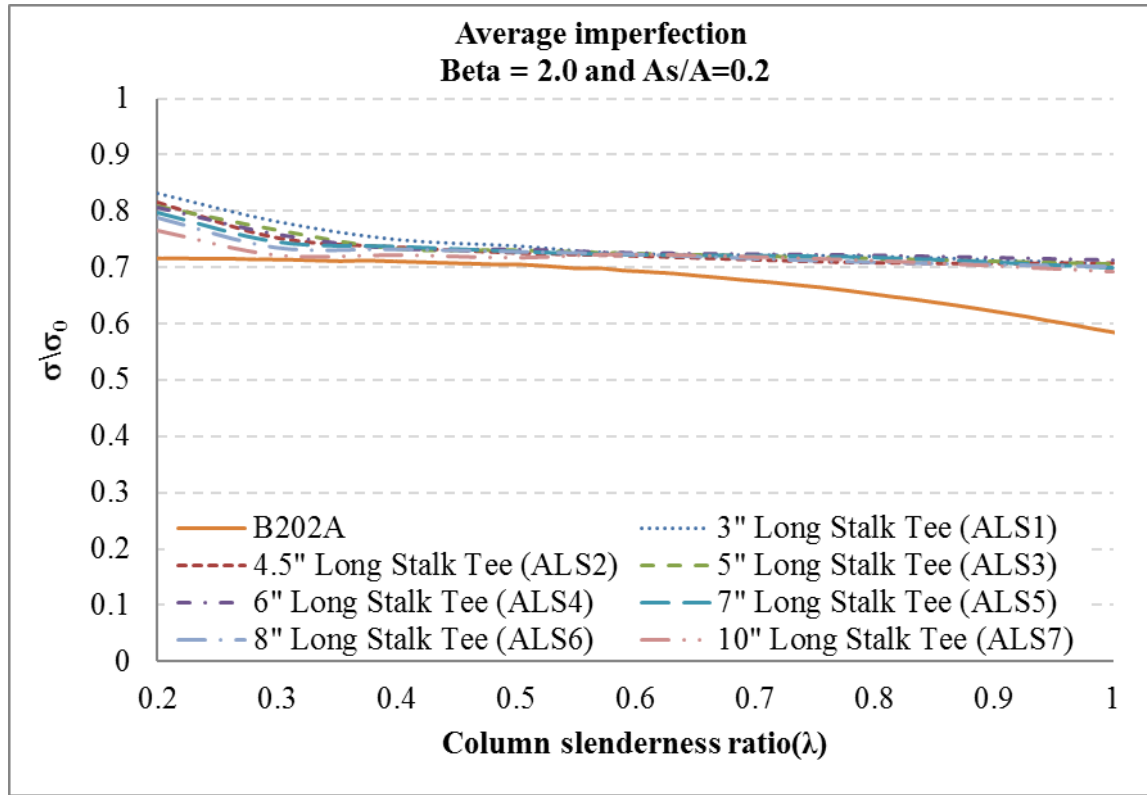




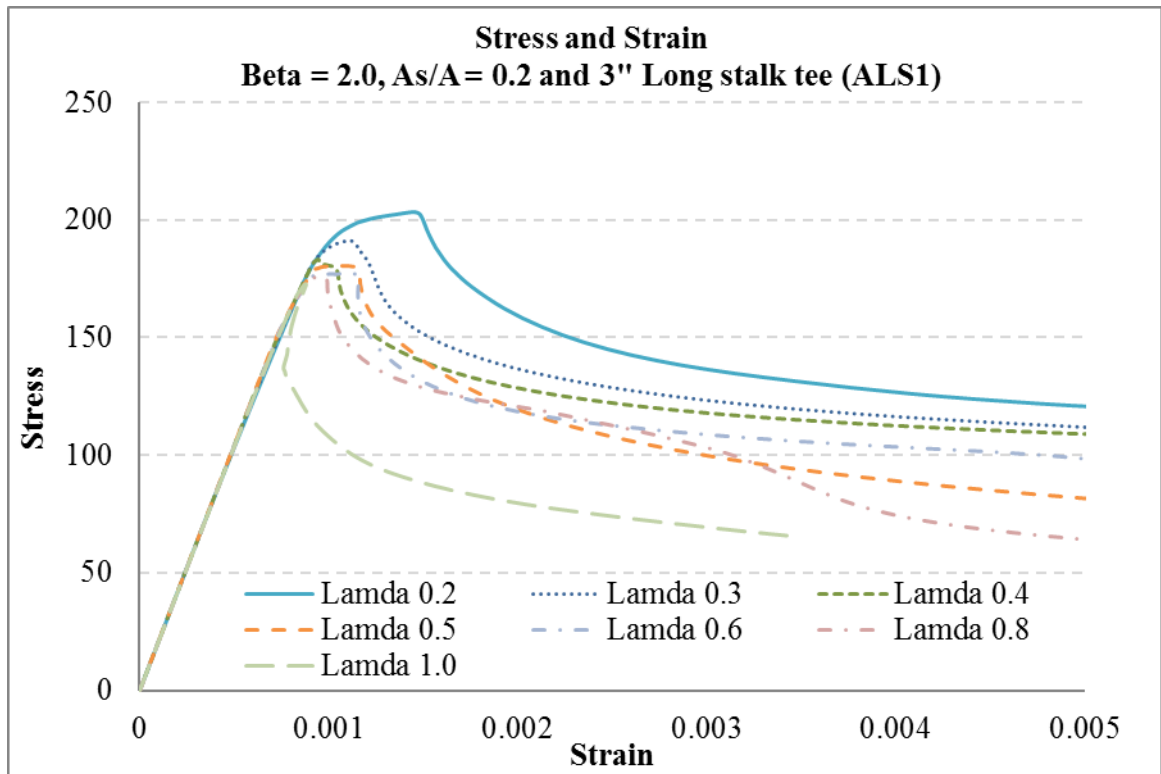


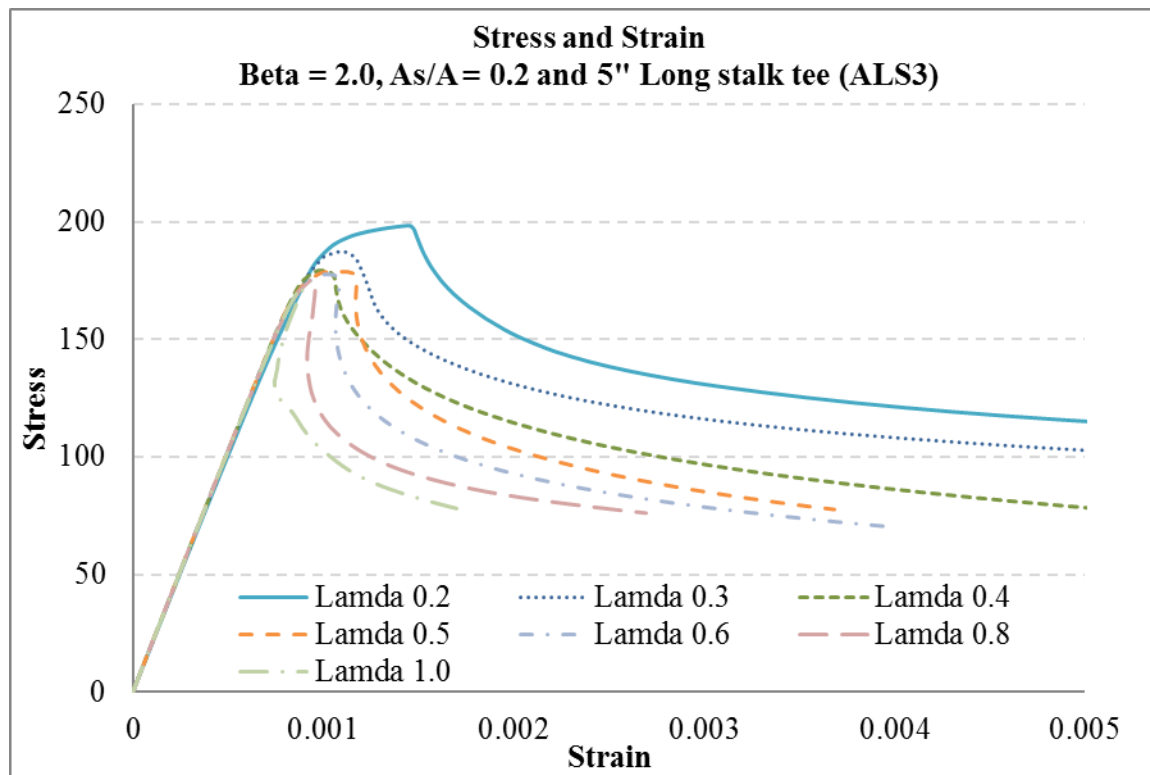
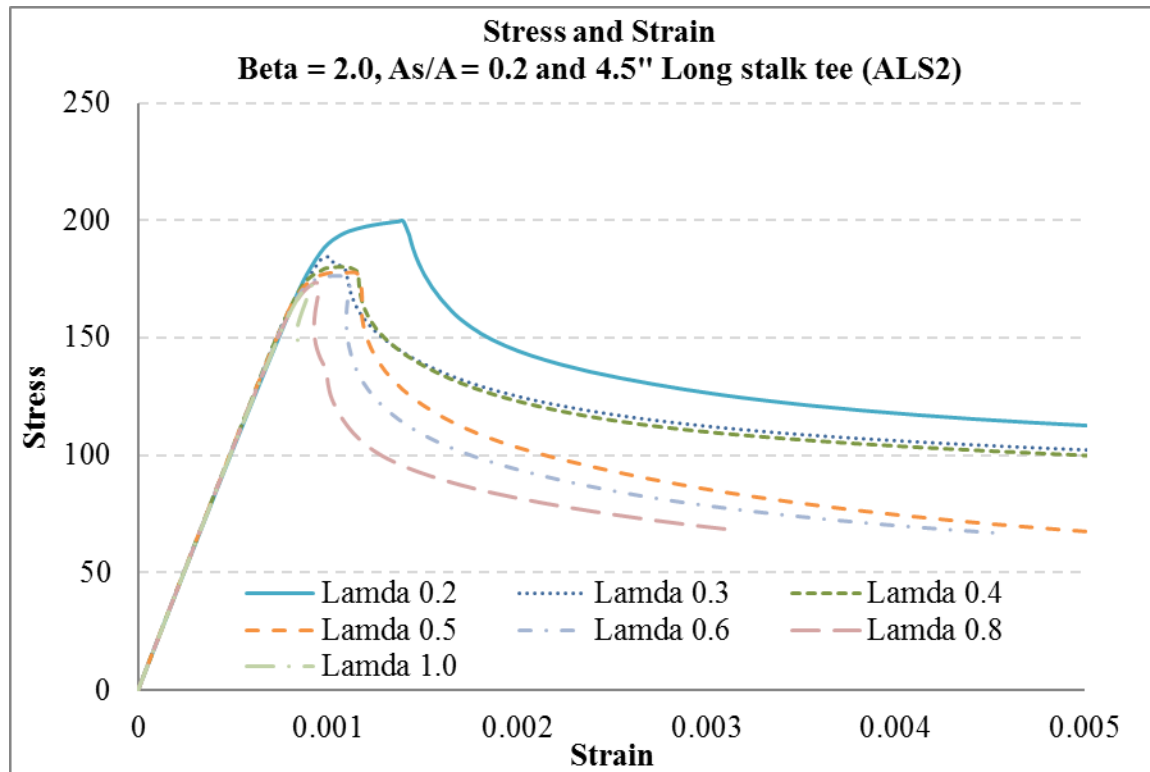
Beta 2.0: Average imperfection

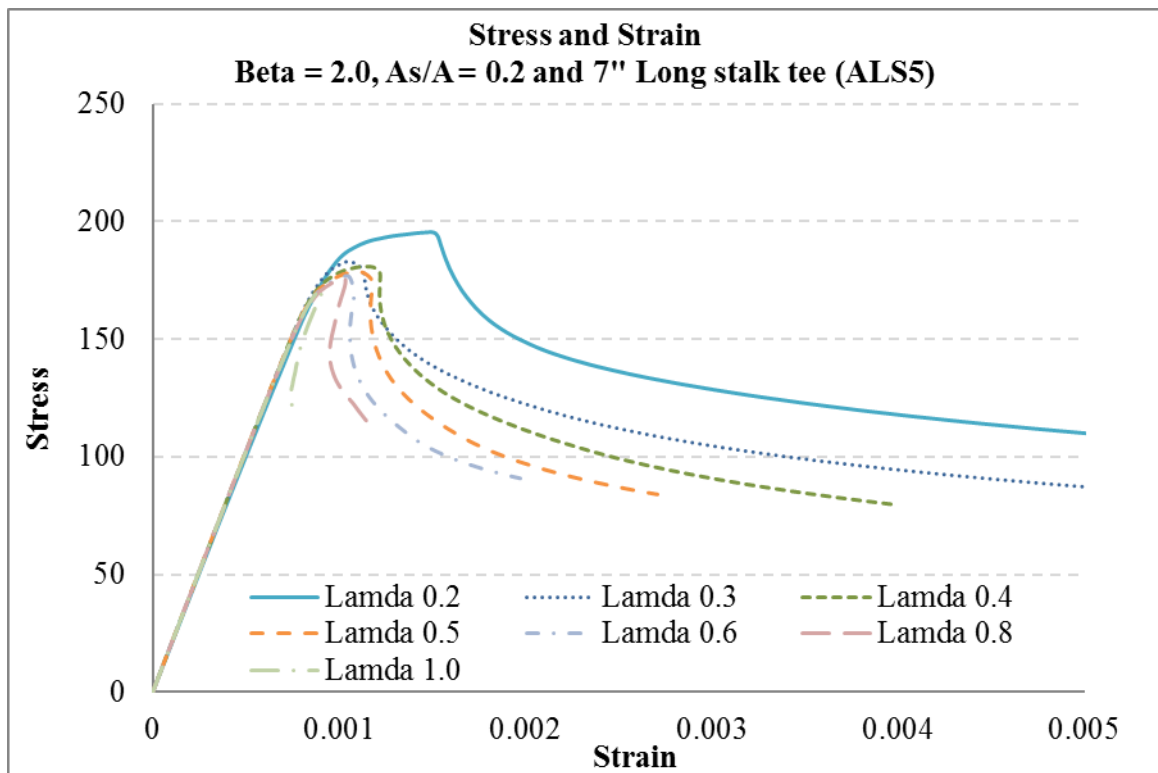
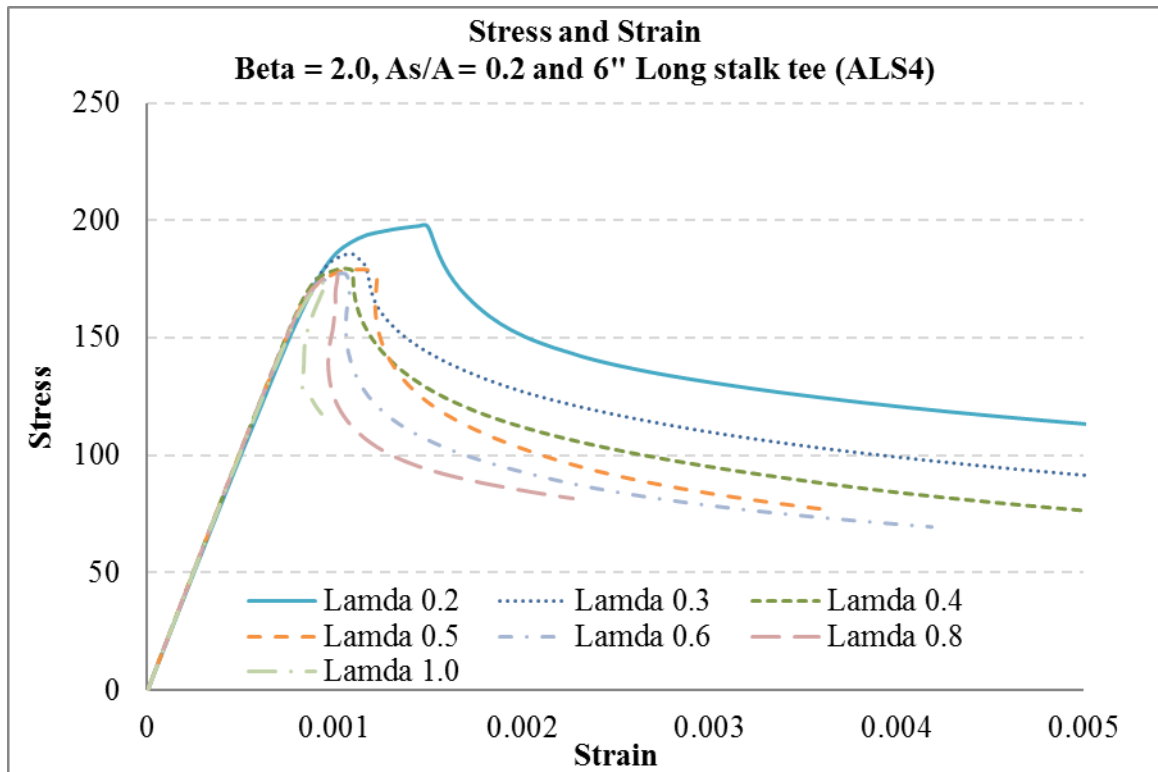


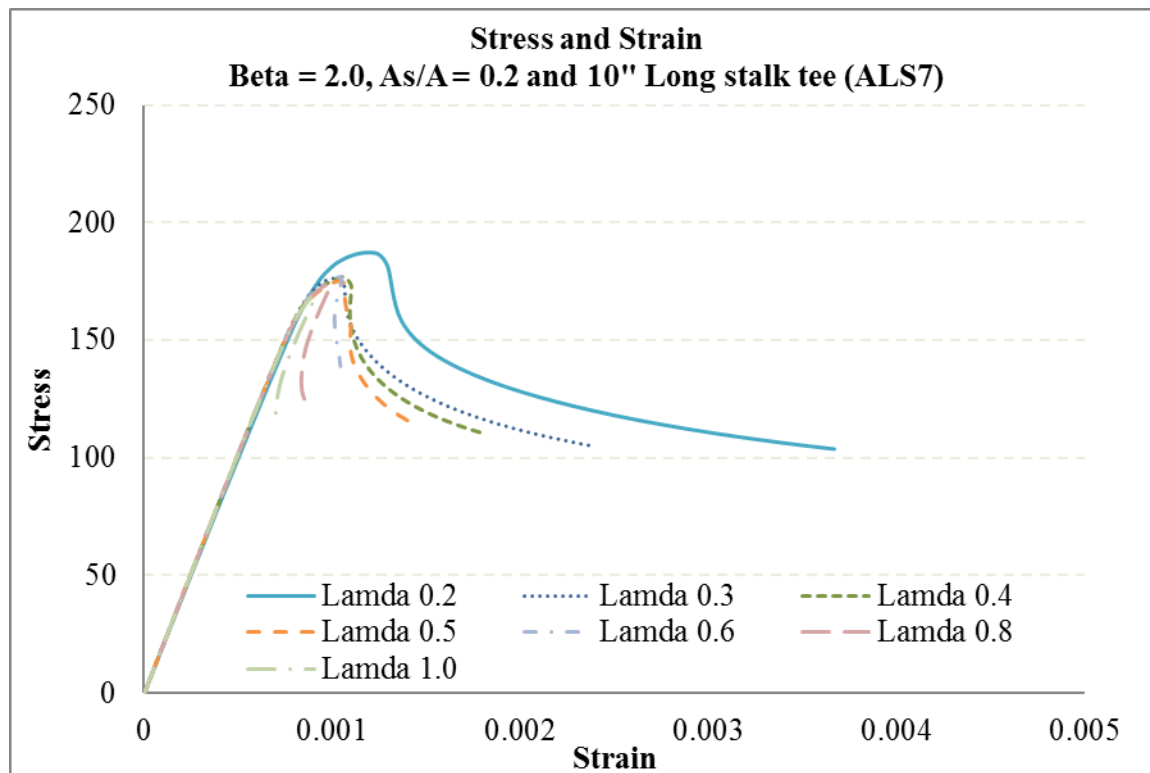
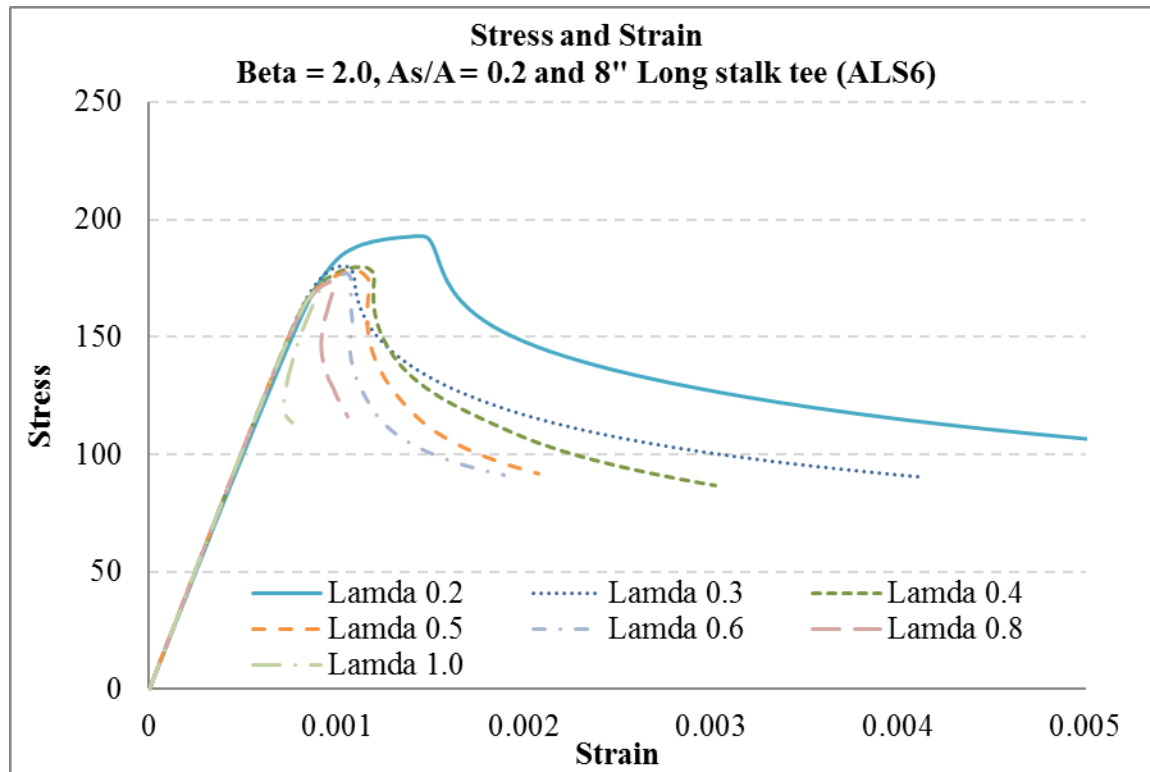


Beta 2.0: Stress and Strain curve

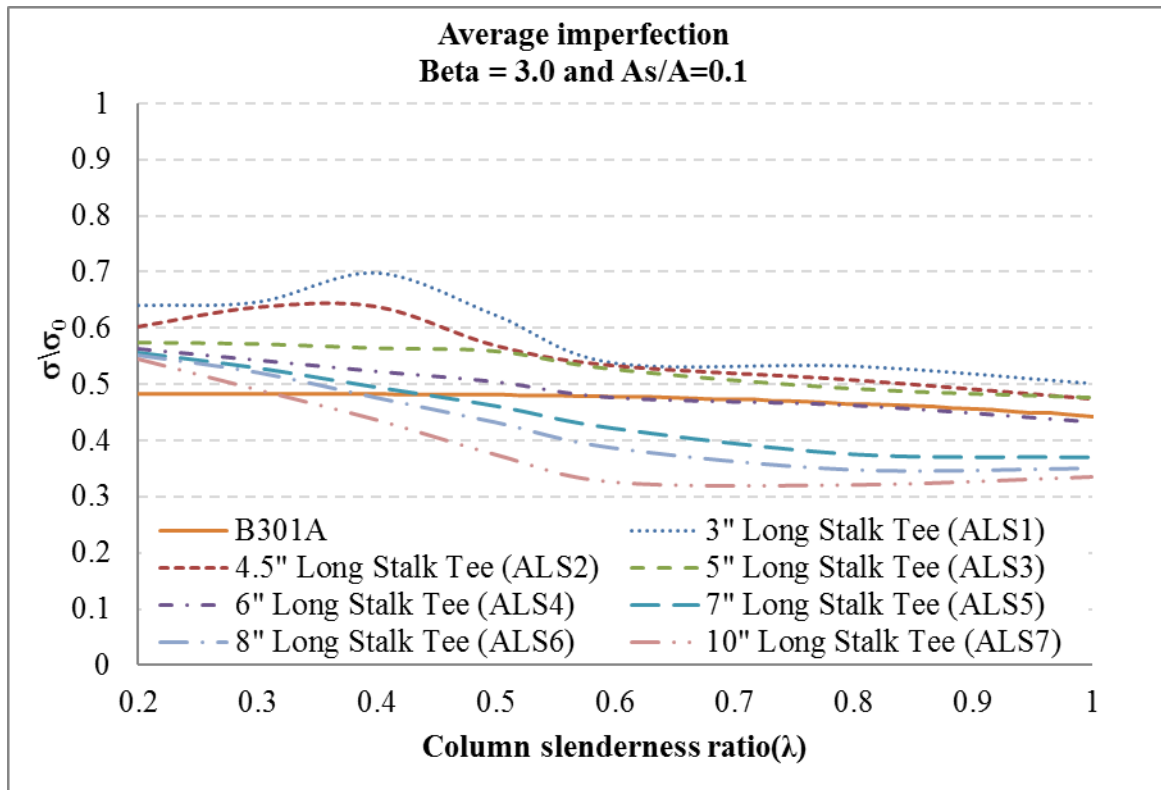


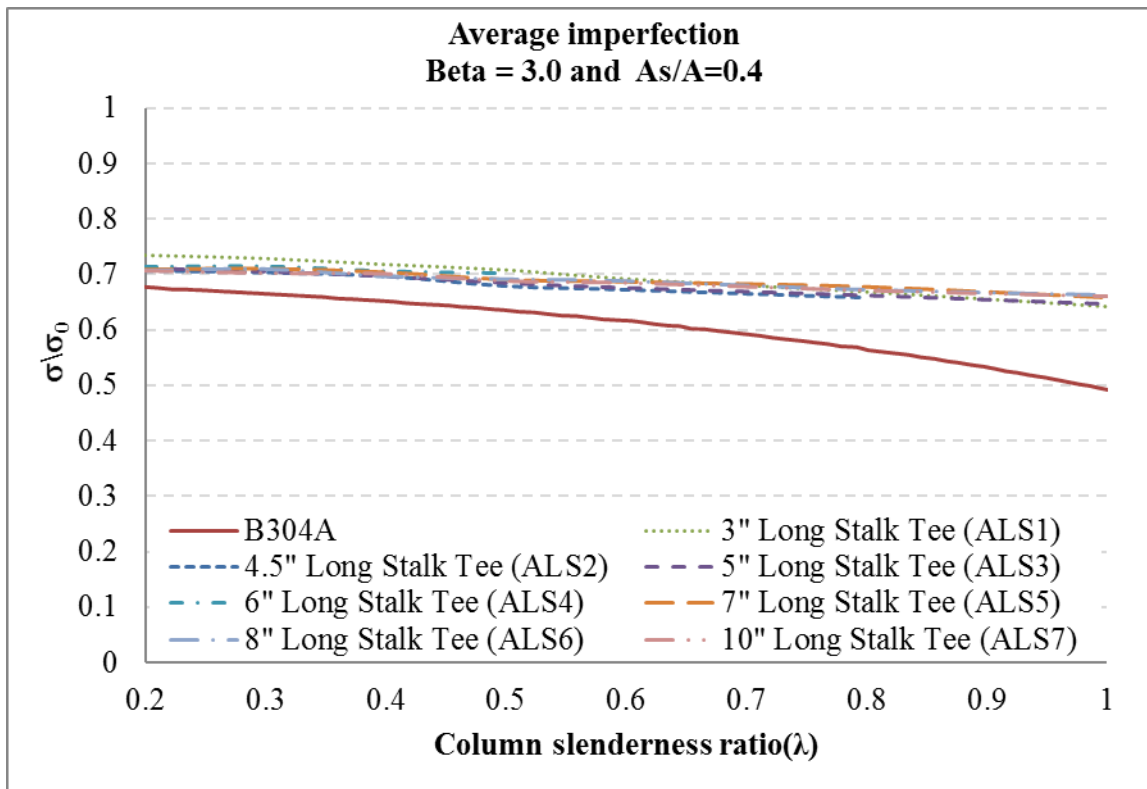
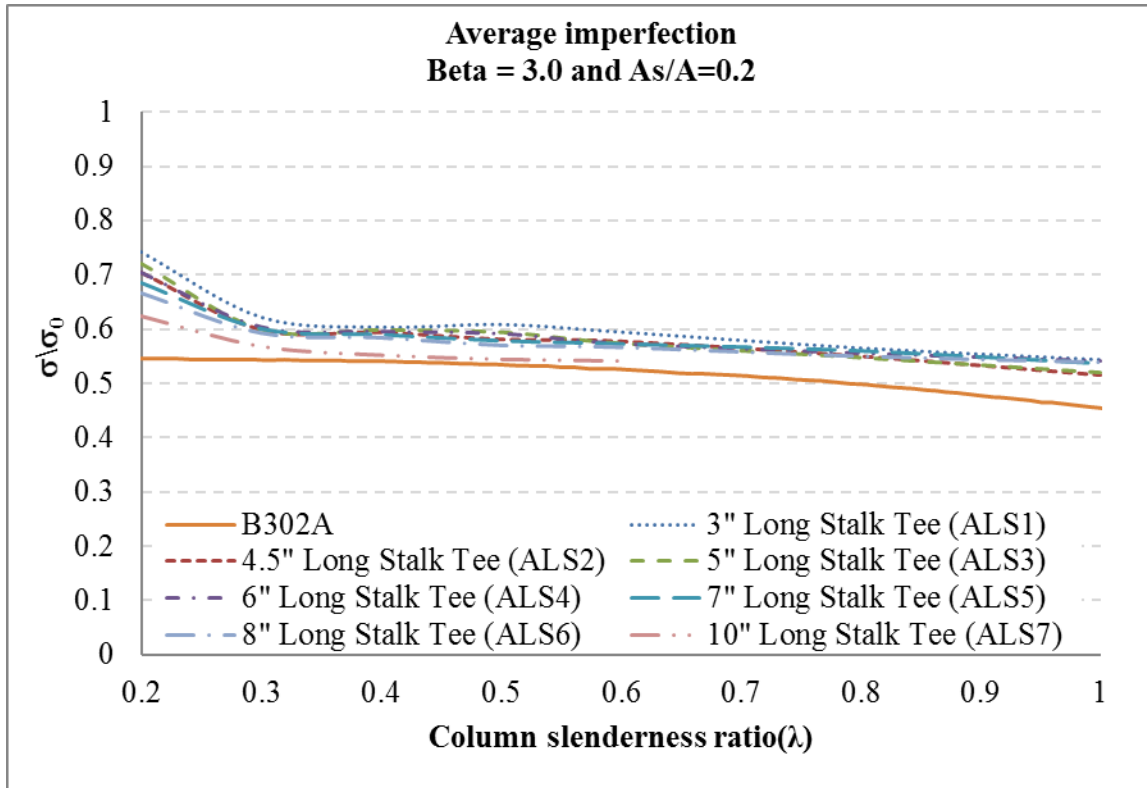




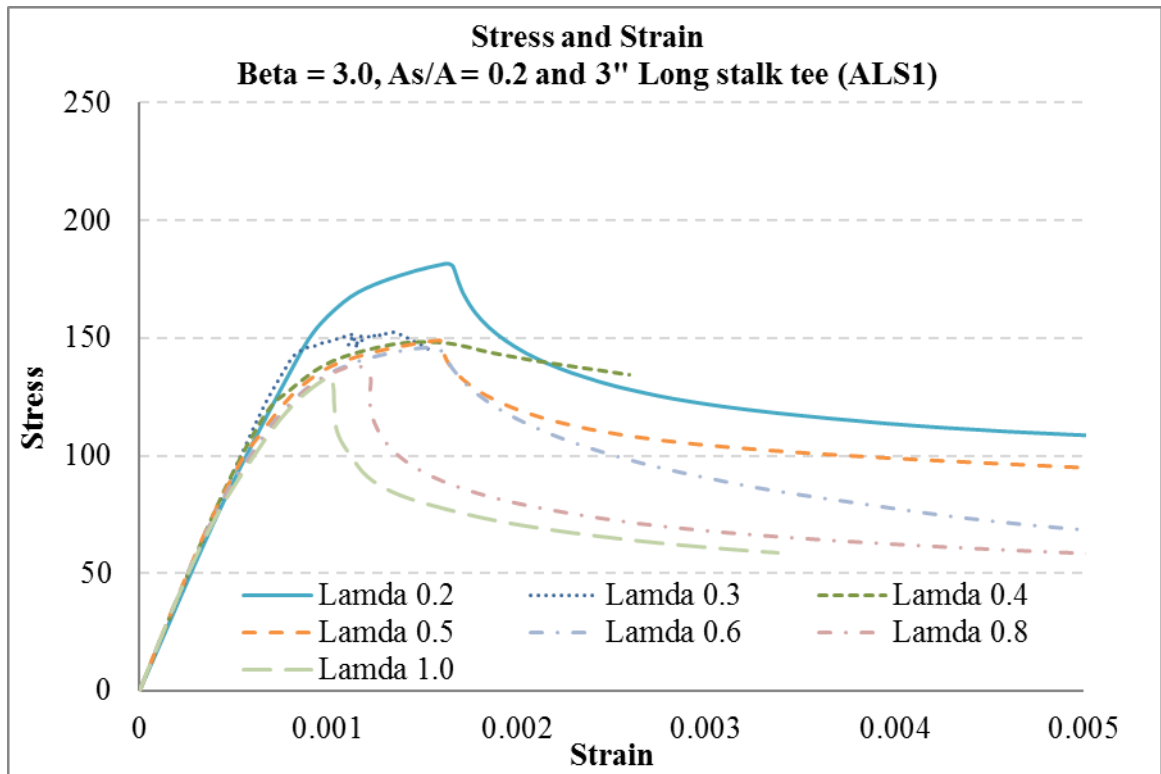


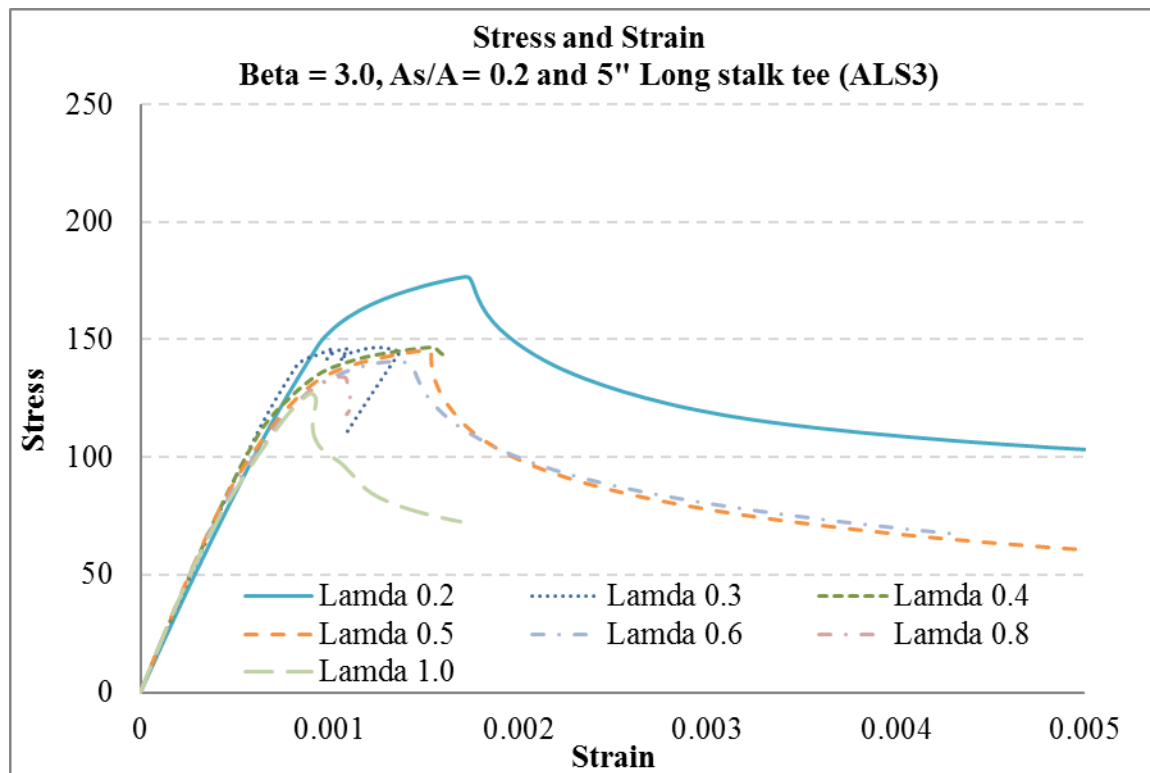
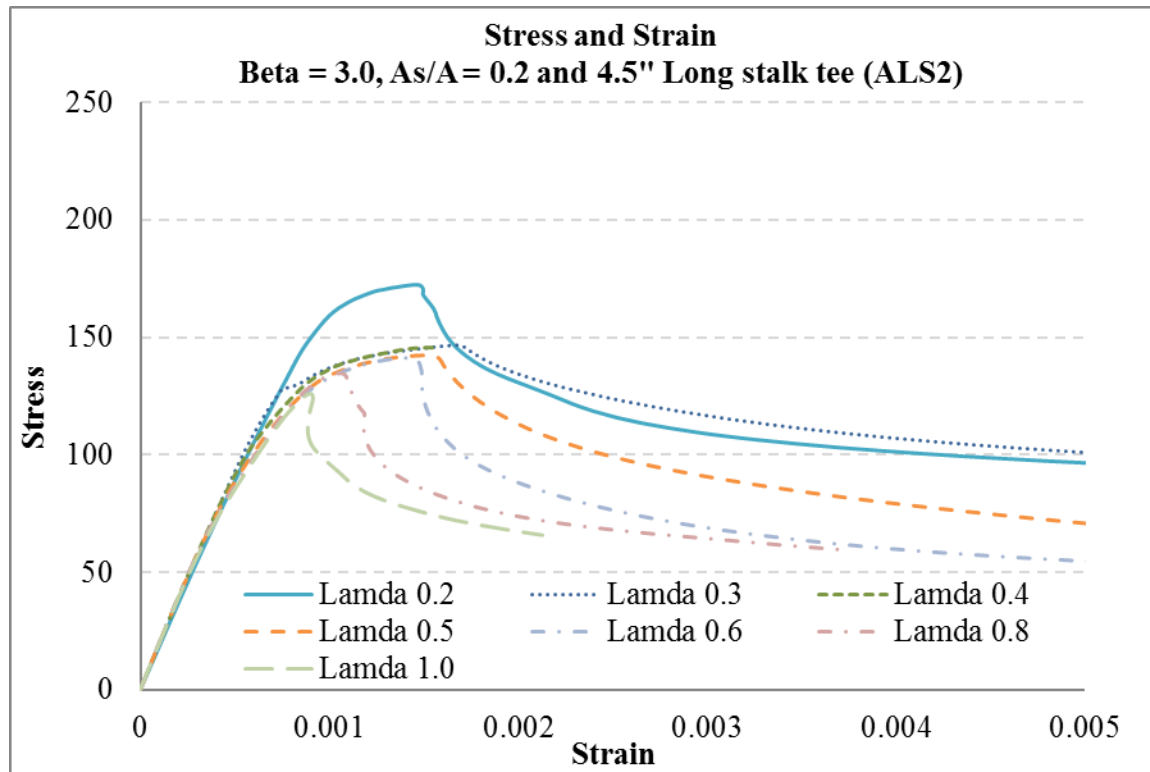
Beta 3.0: Average imperfection

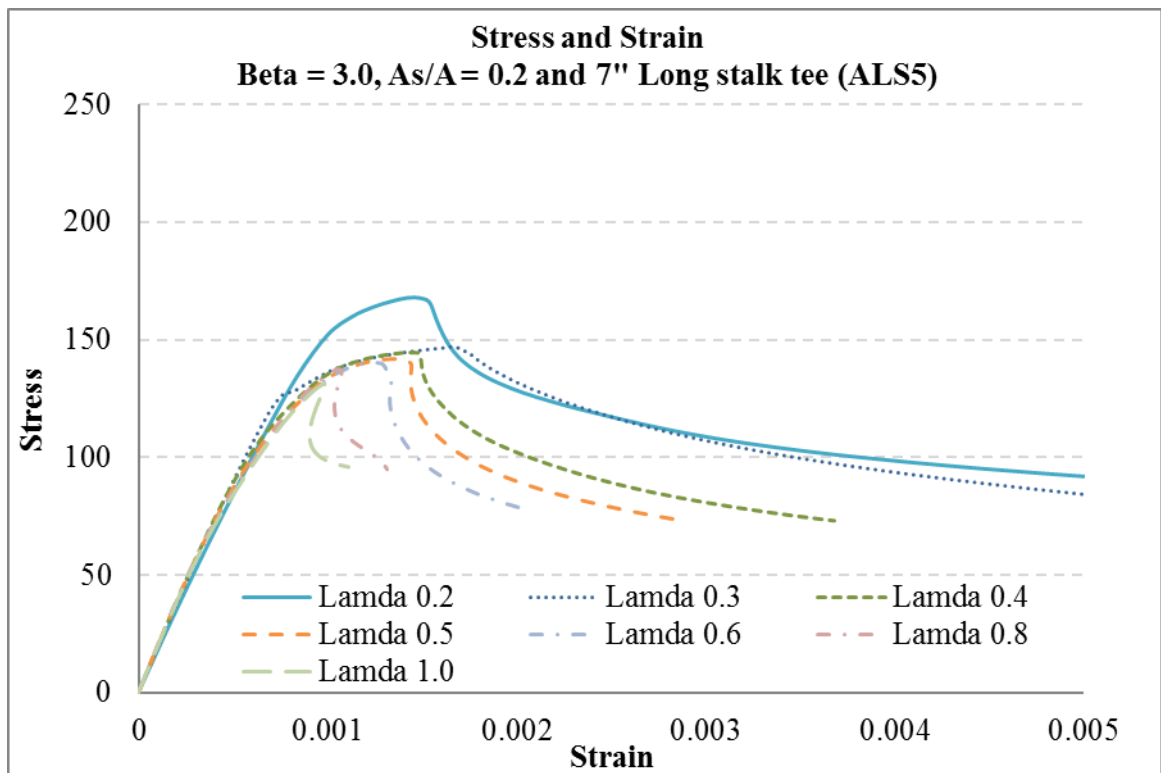
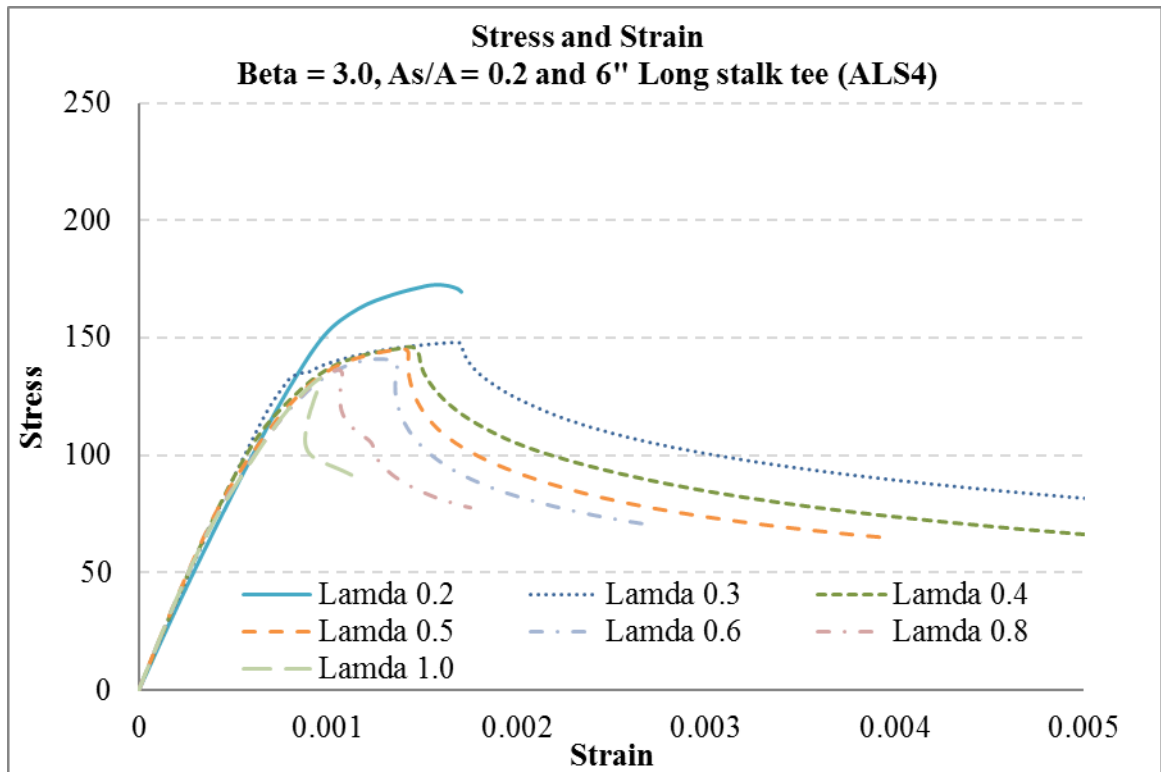


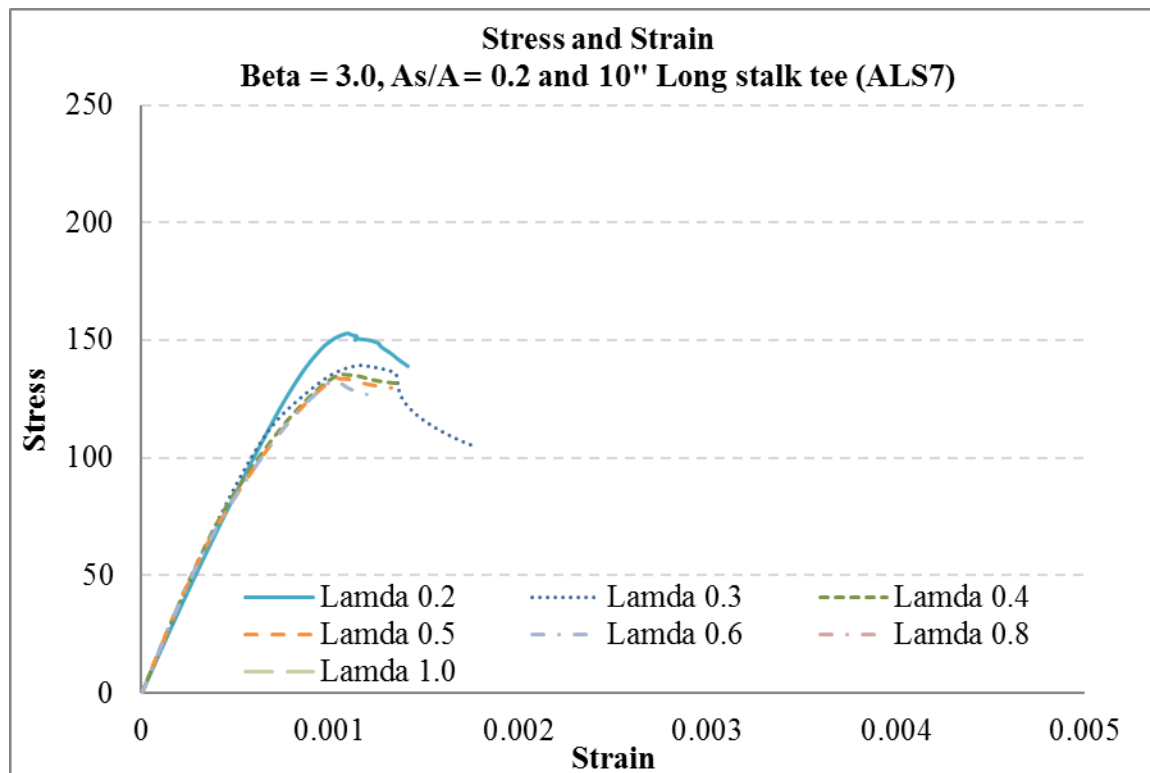
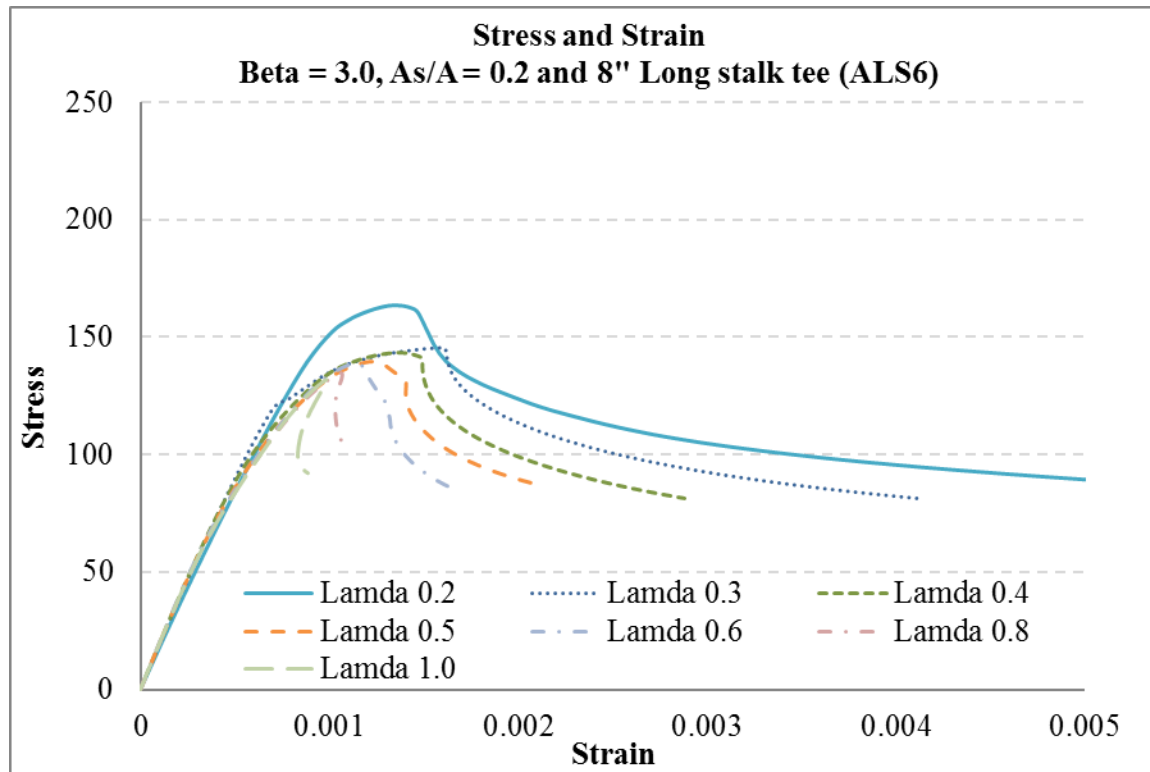


Beta 3.0: Stress and Strain curve

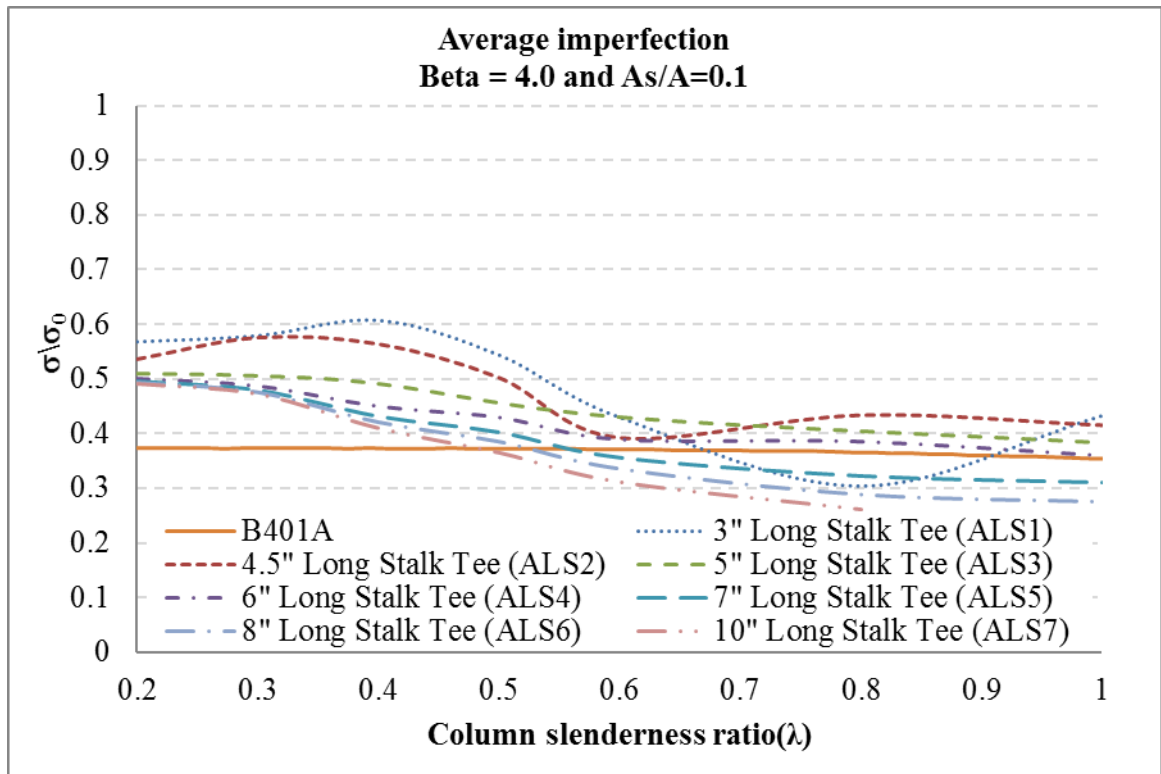


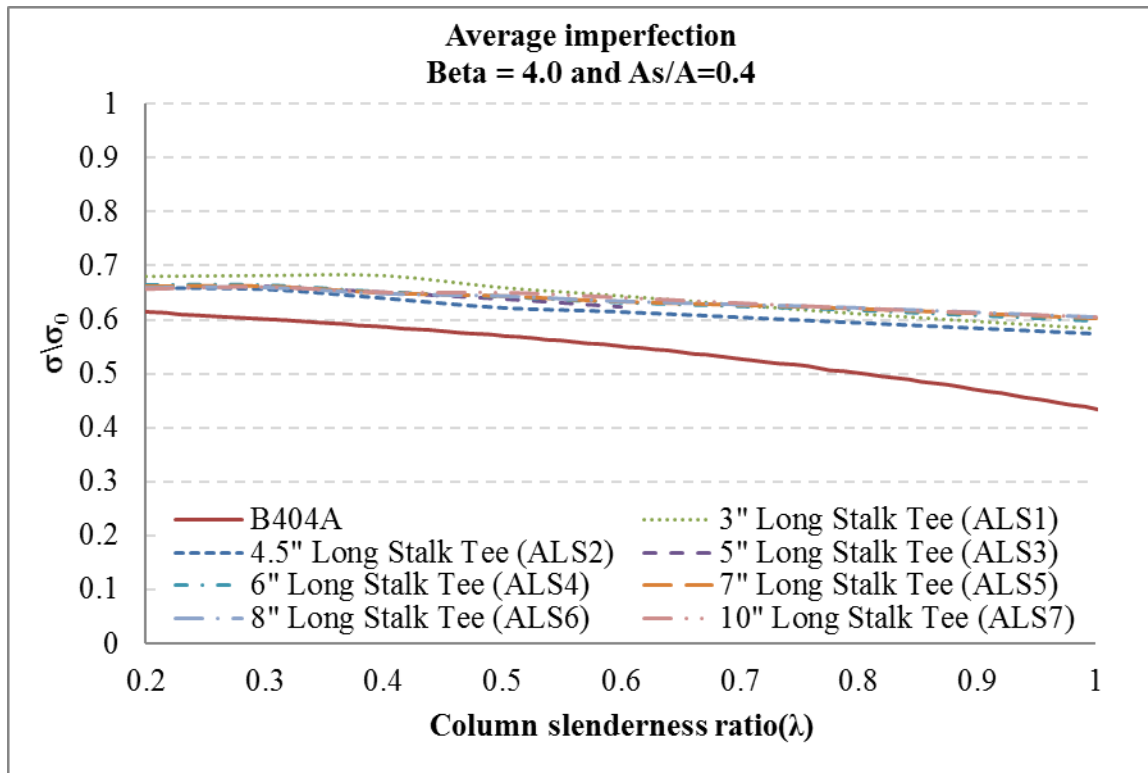
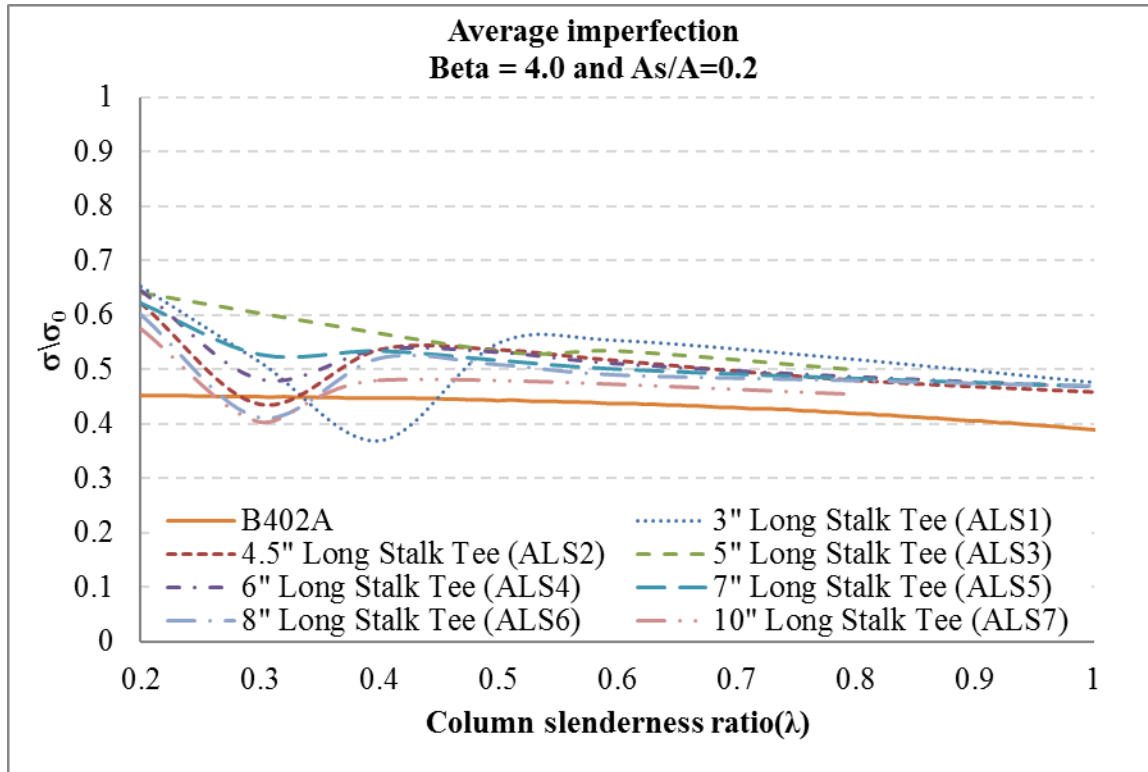




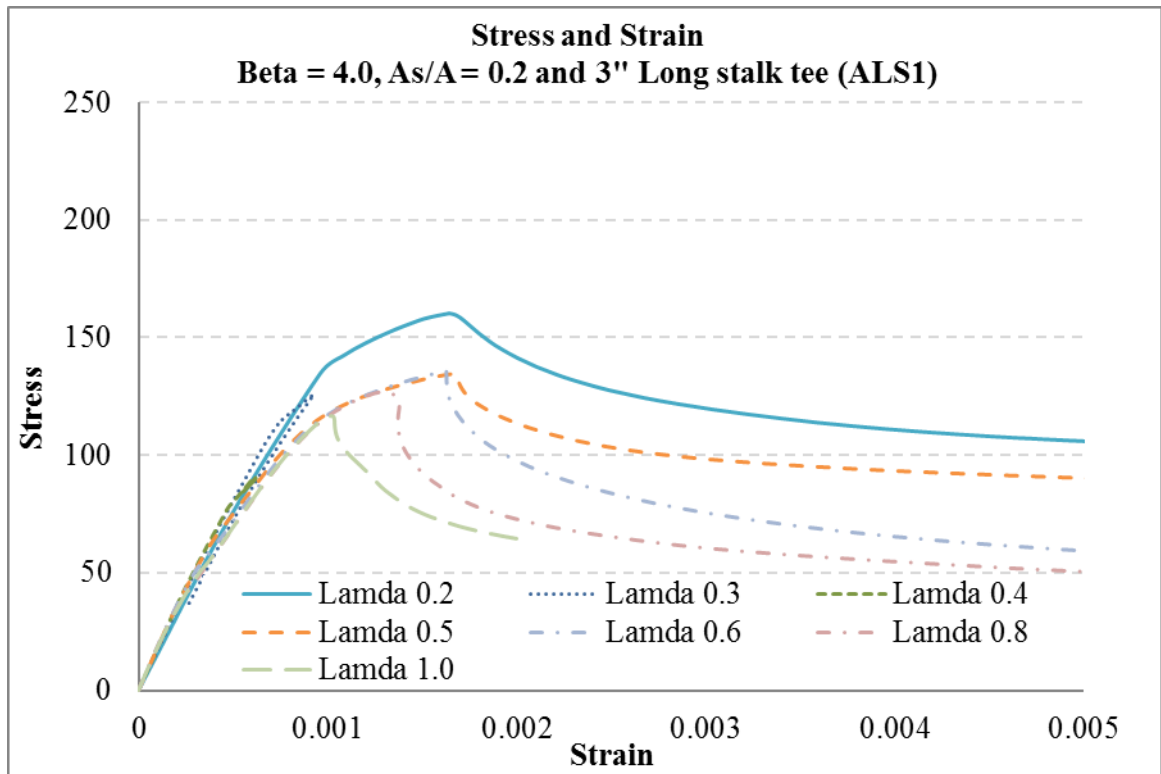


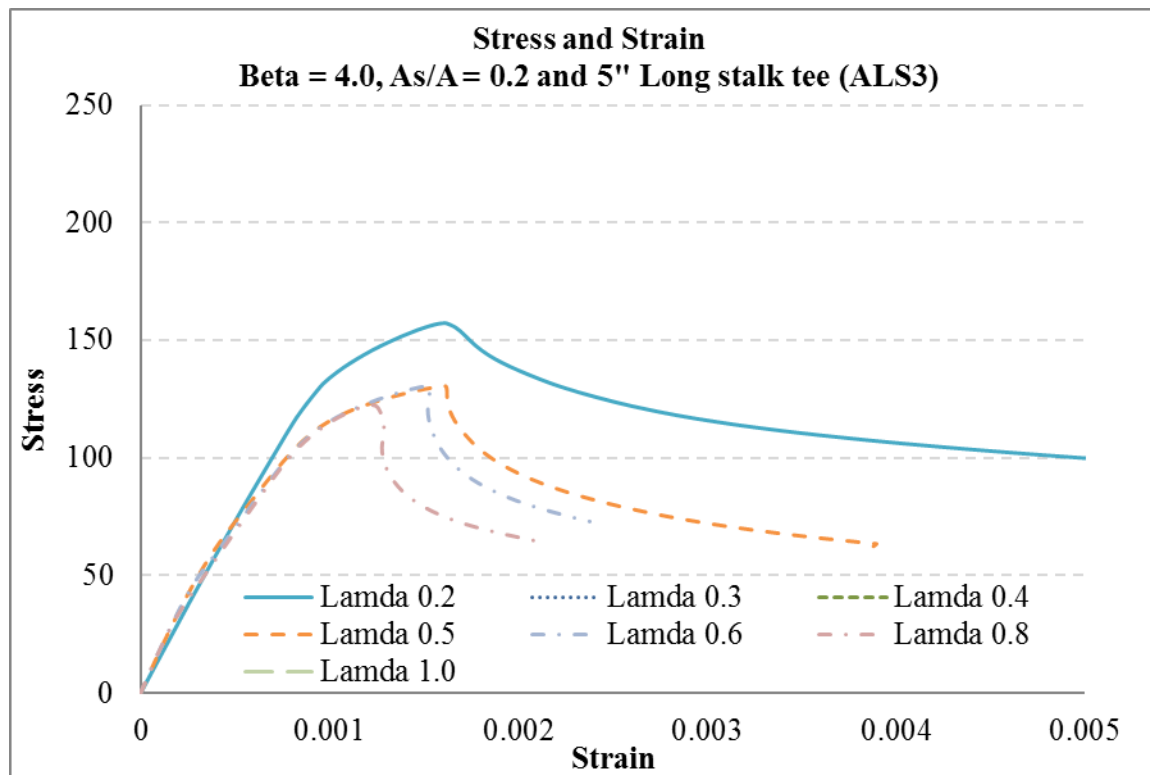
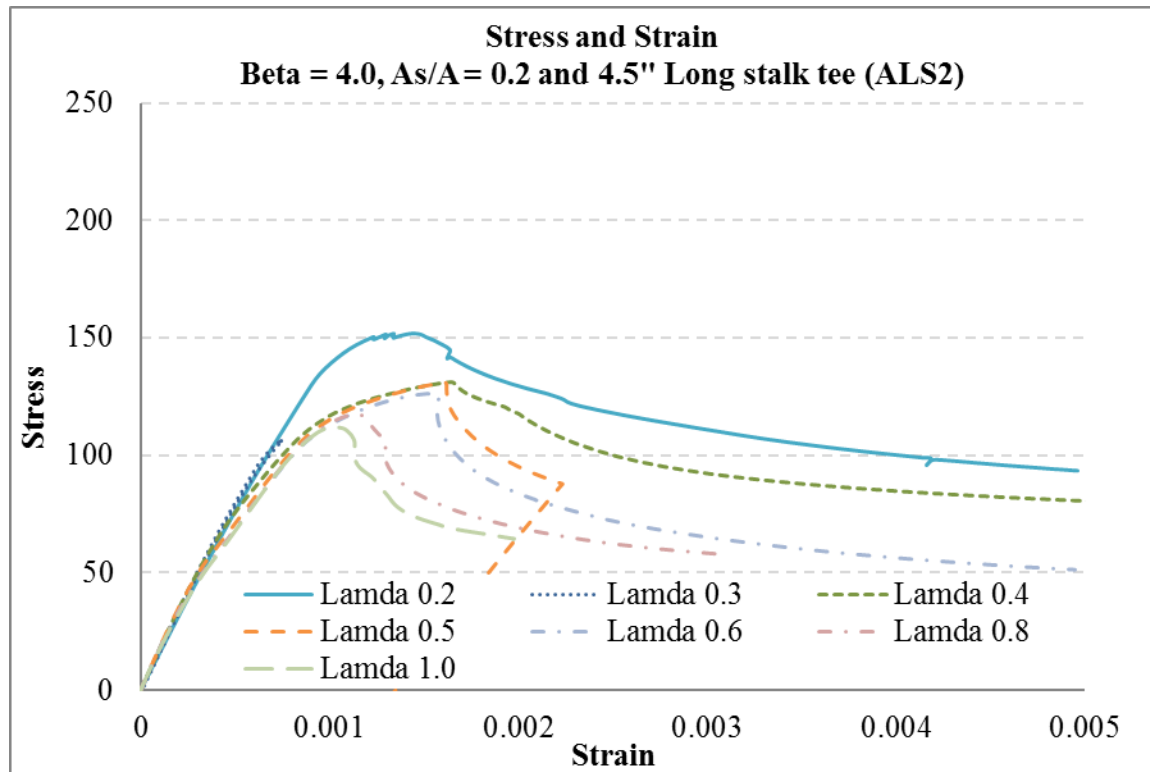
Beta 4.0: Average imperfection

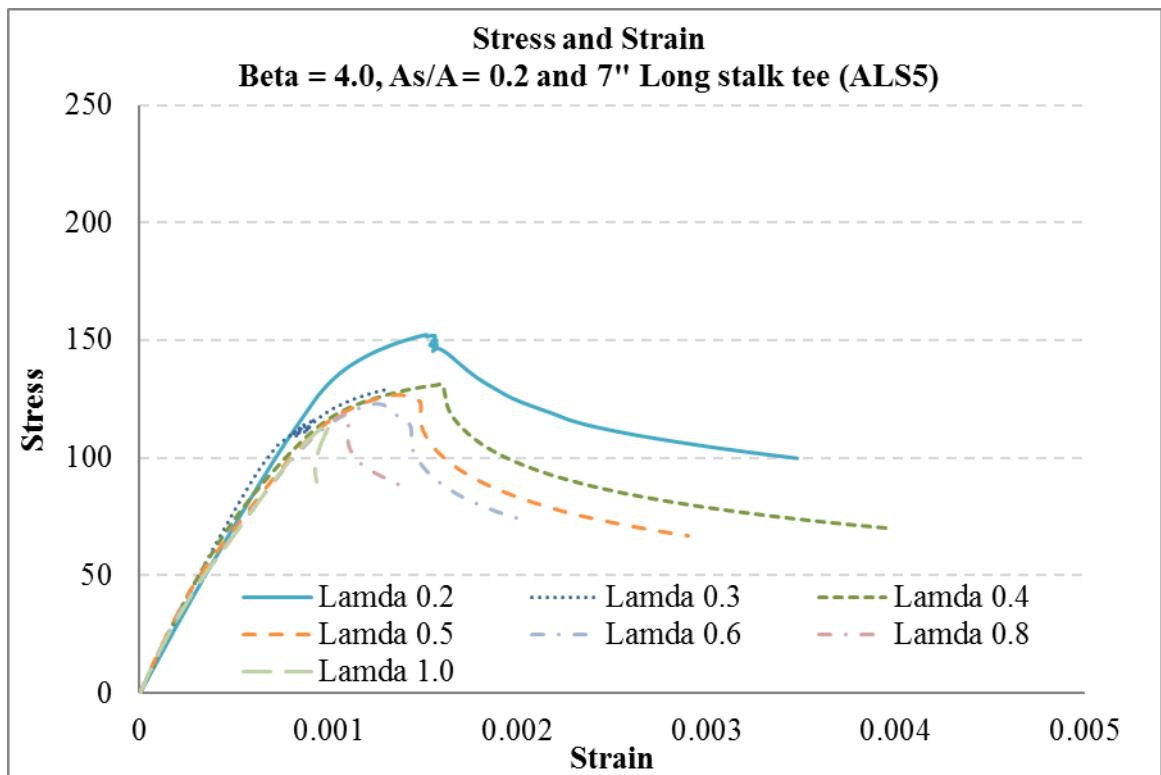
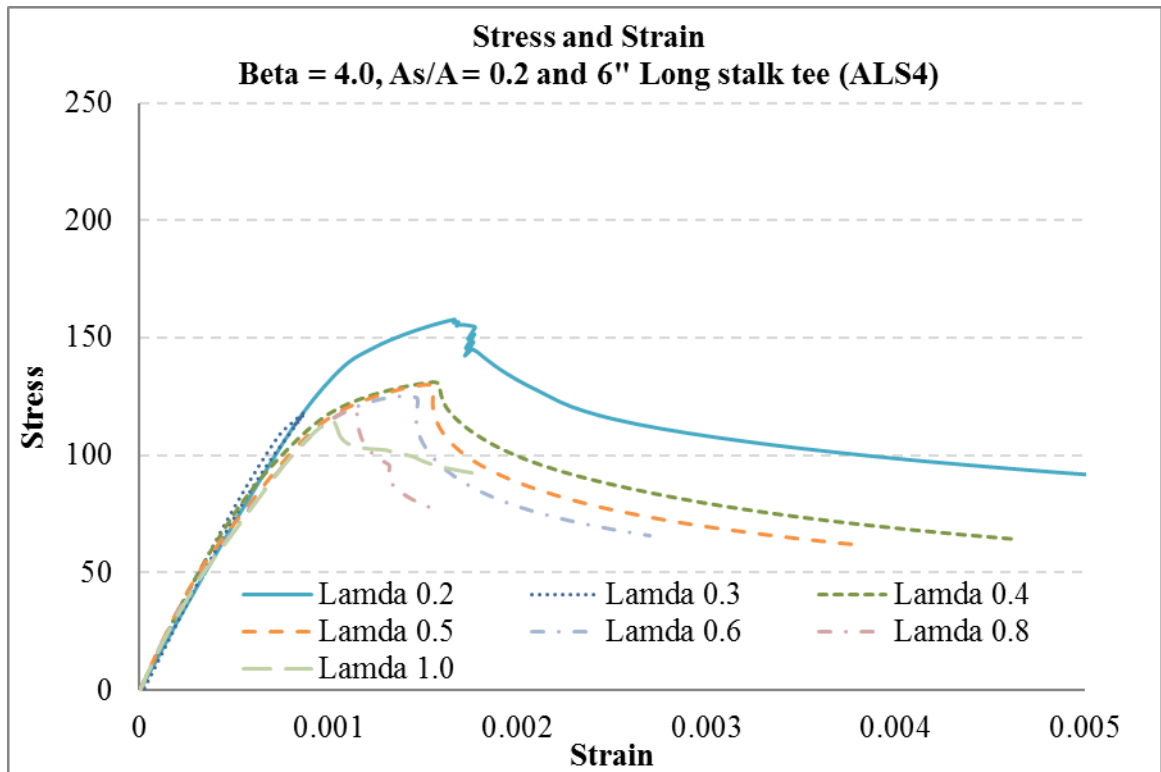


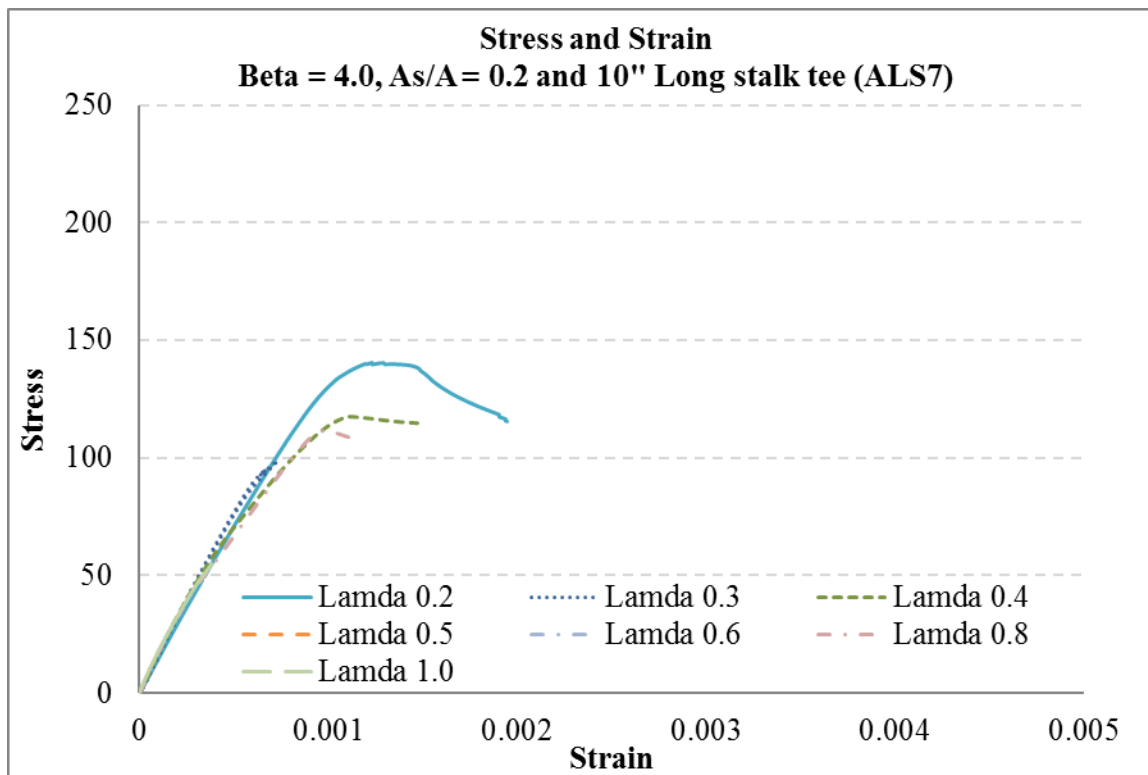
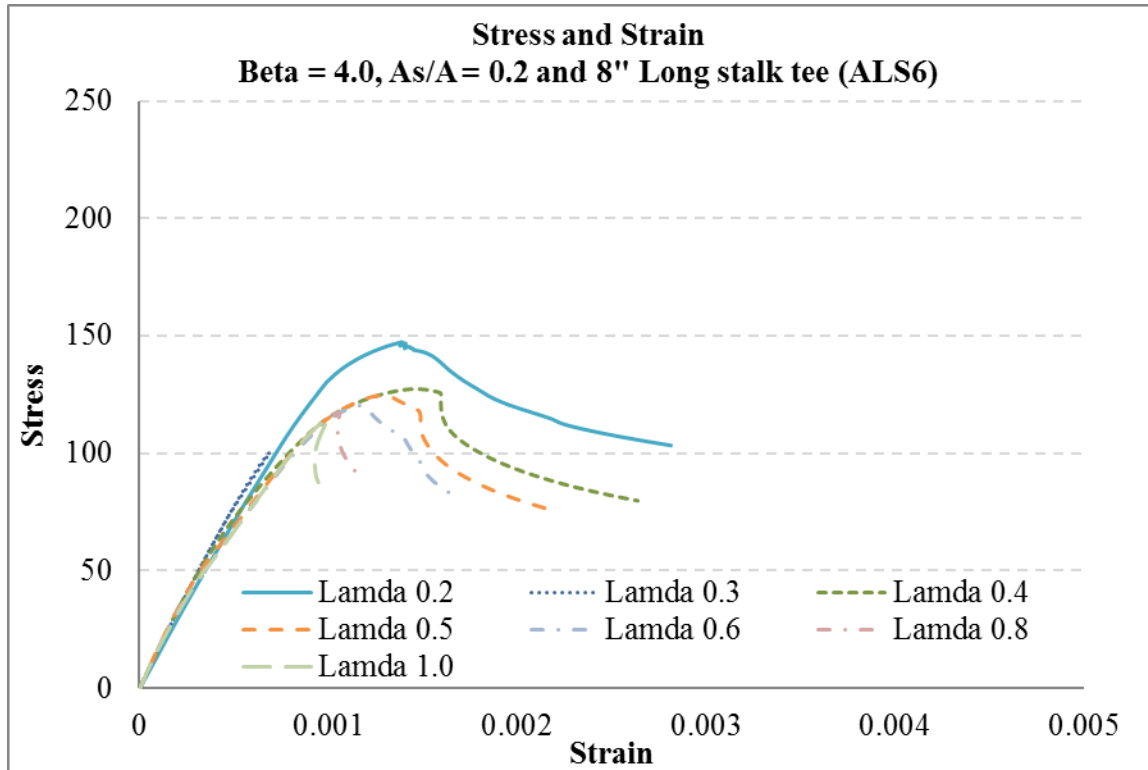


Beta 4.0: Stress and Strain curve



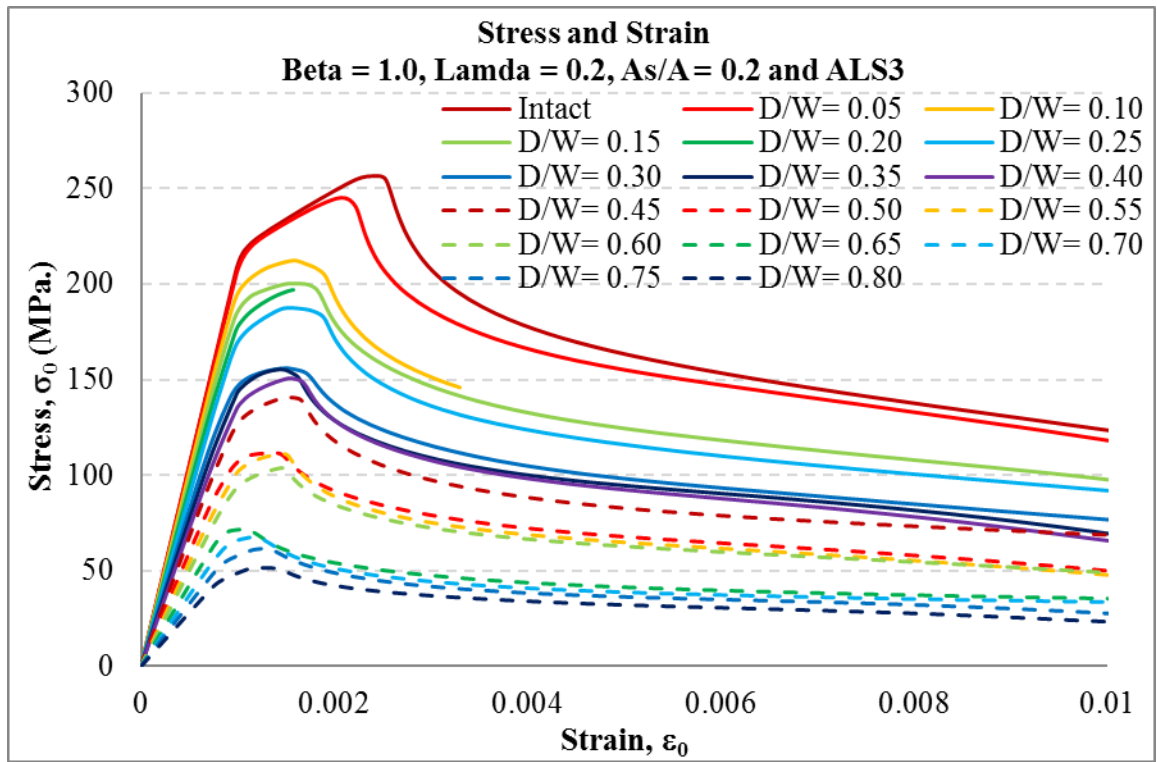


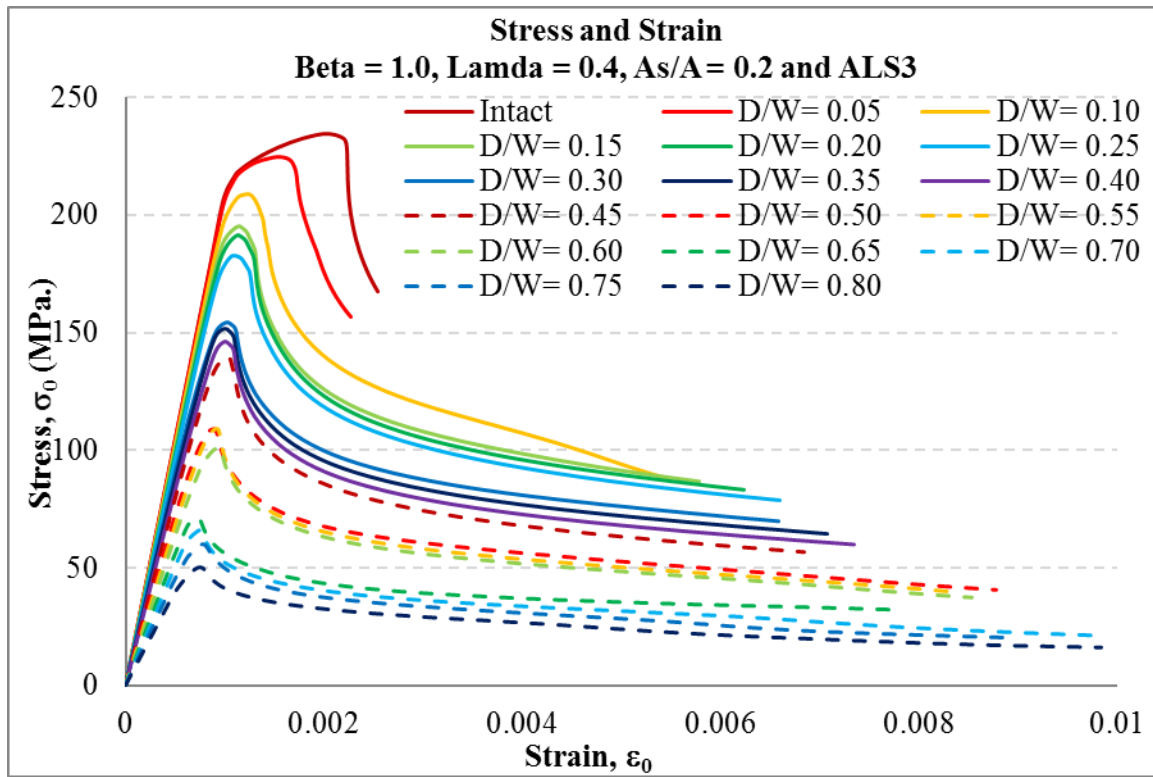
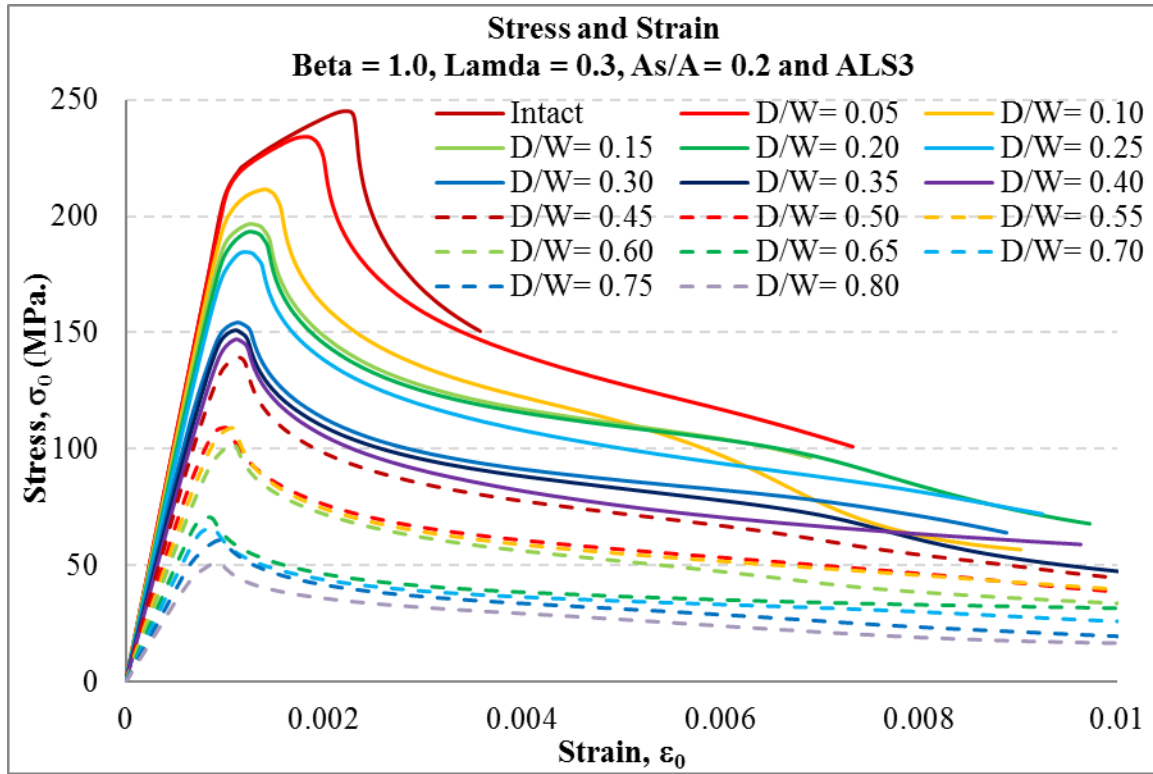


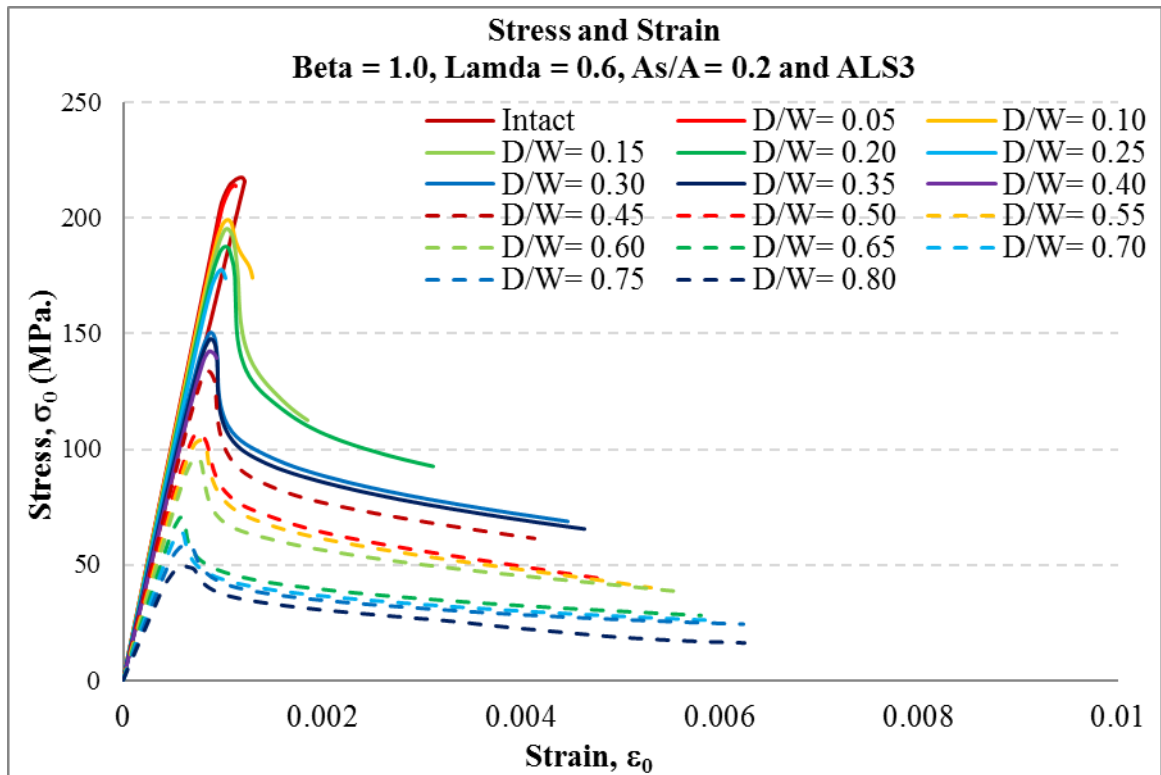
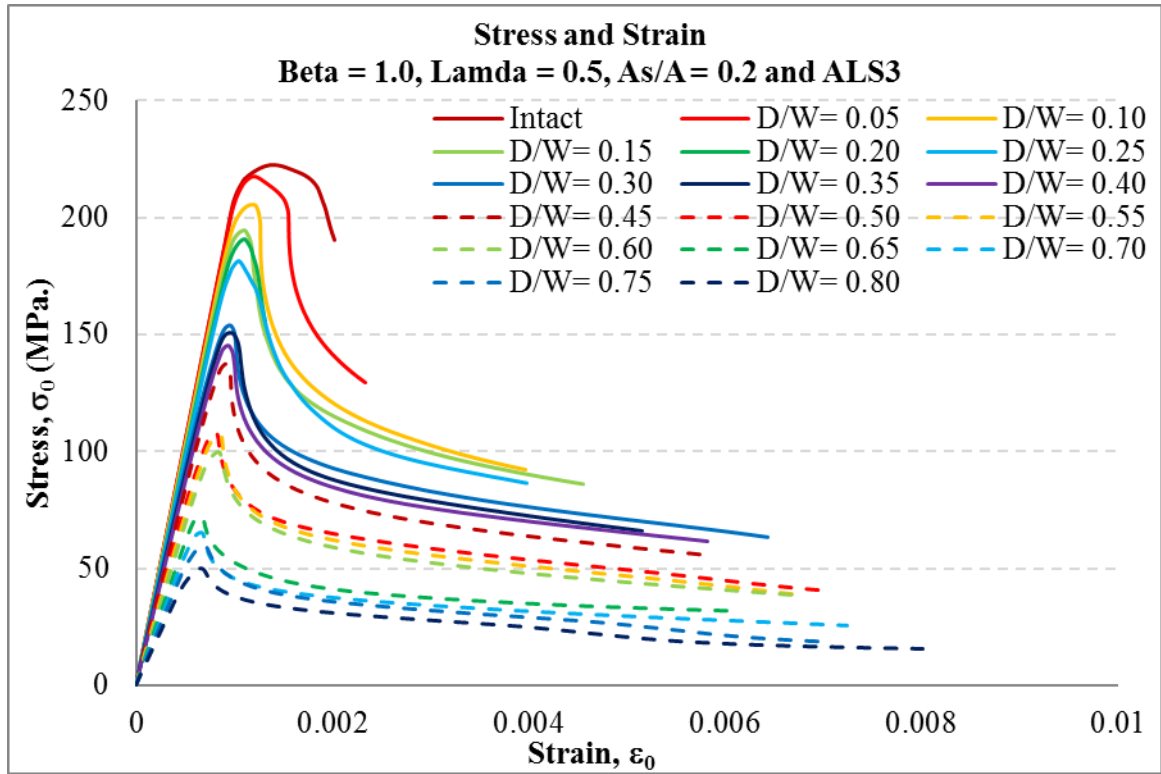


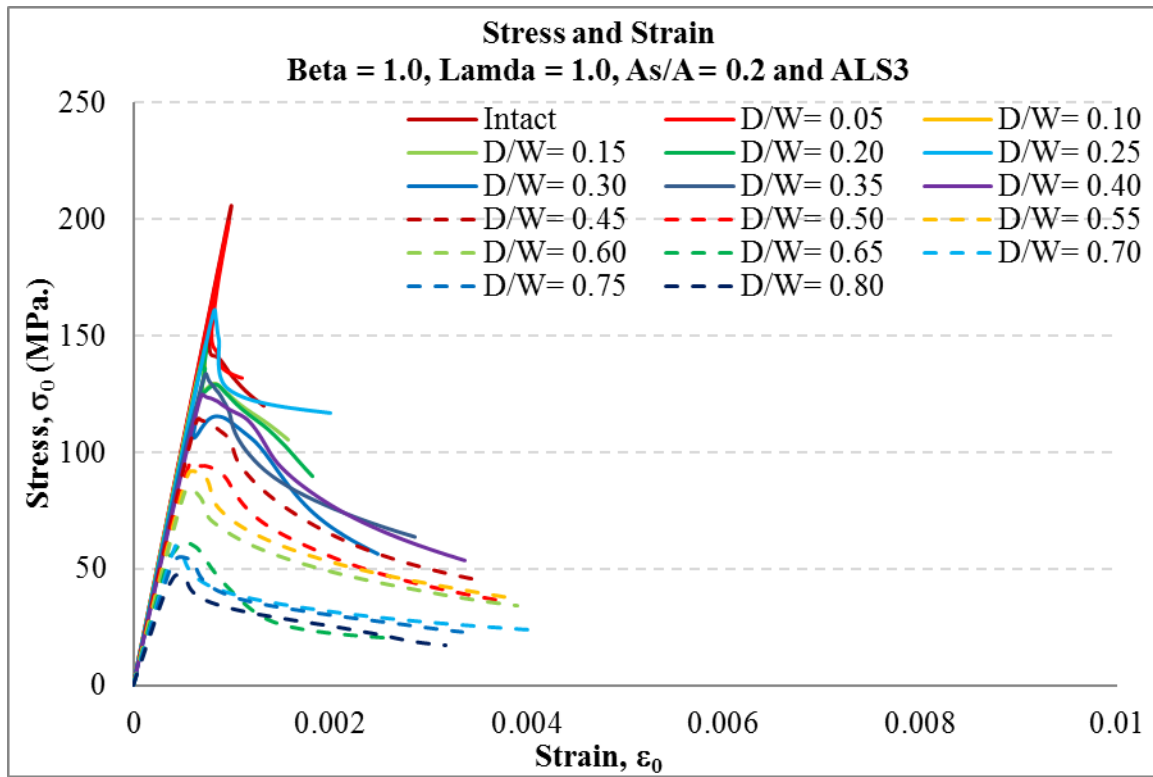
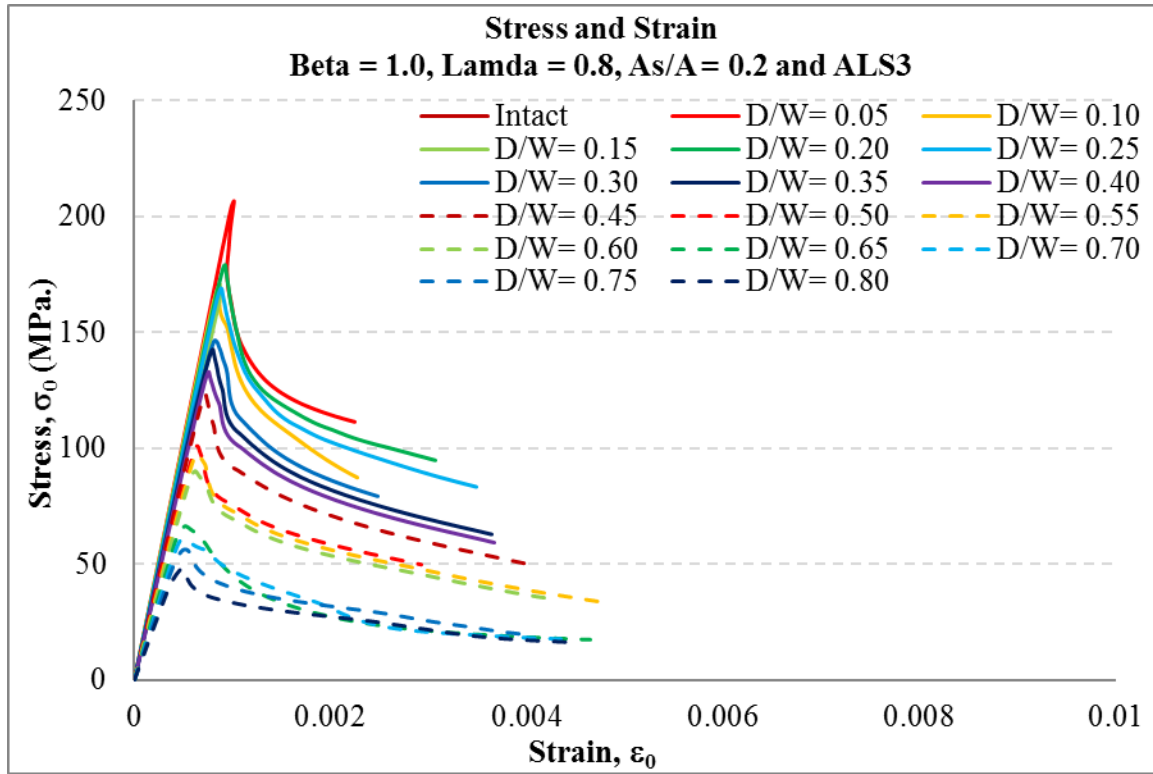
Appendix C: Strength of damaged clear-cut hole stiffened panels

Beta 1.0

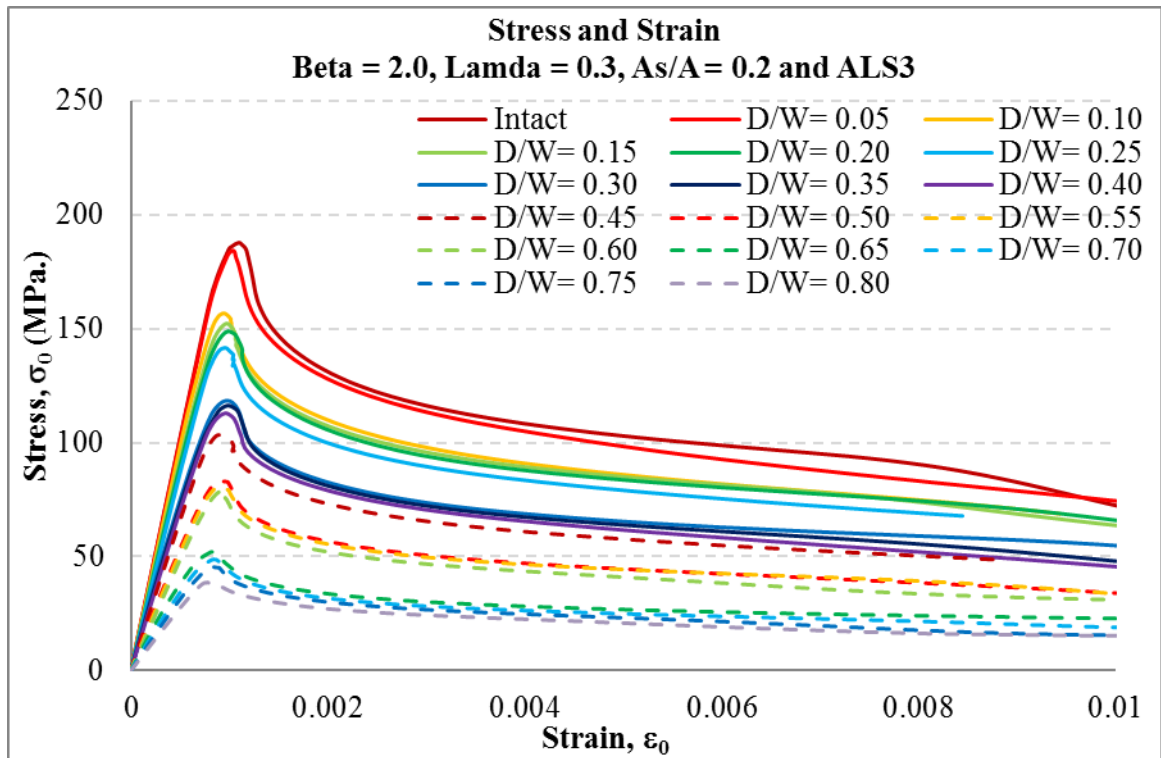
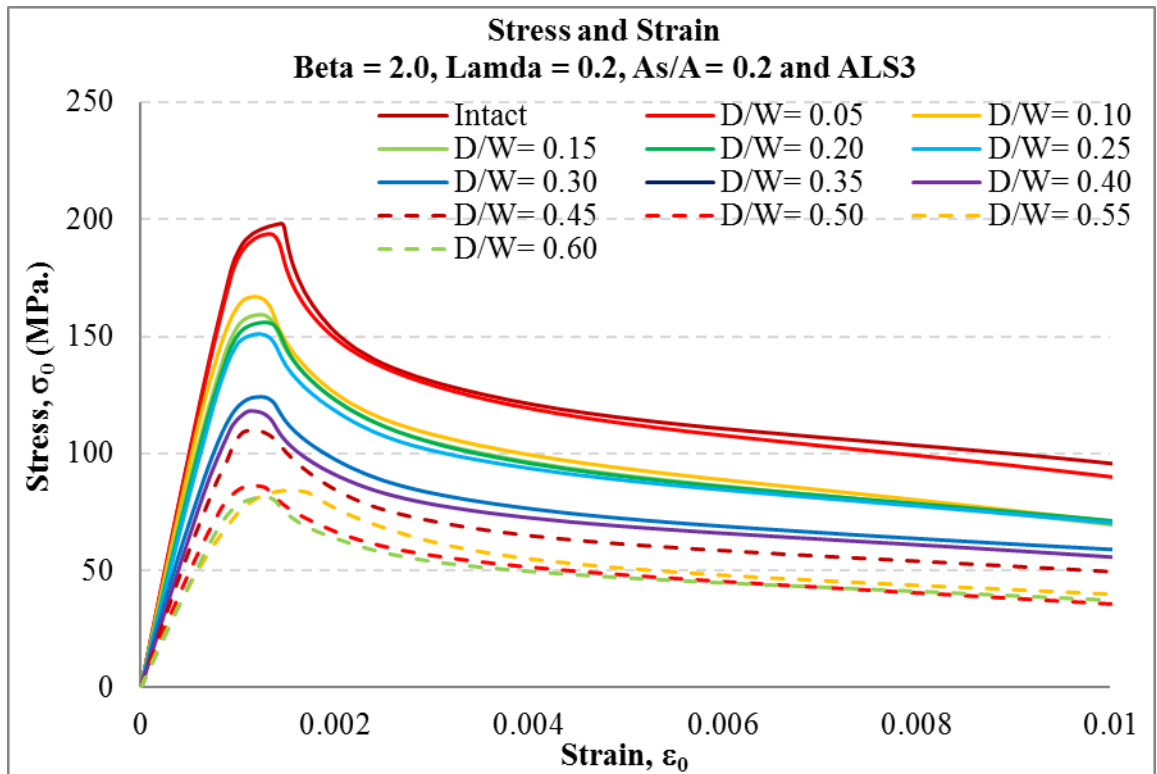


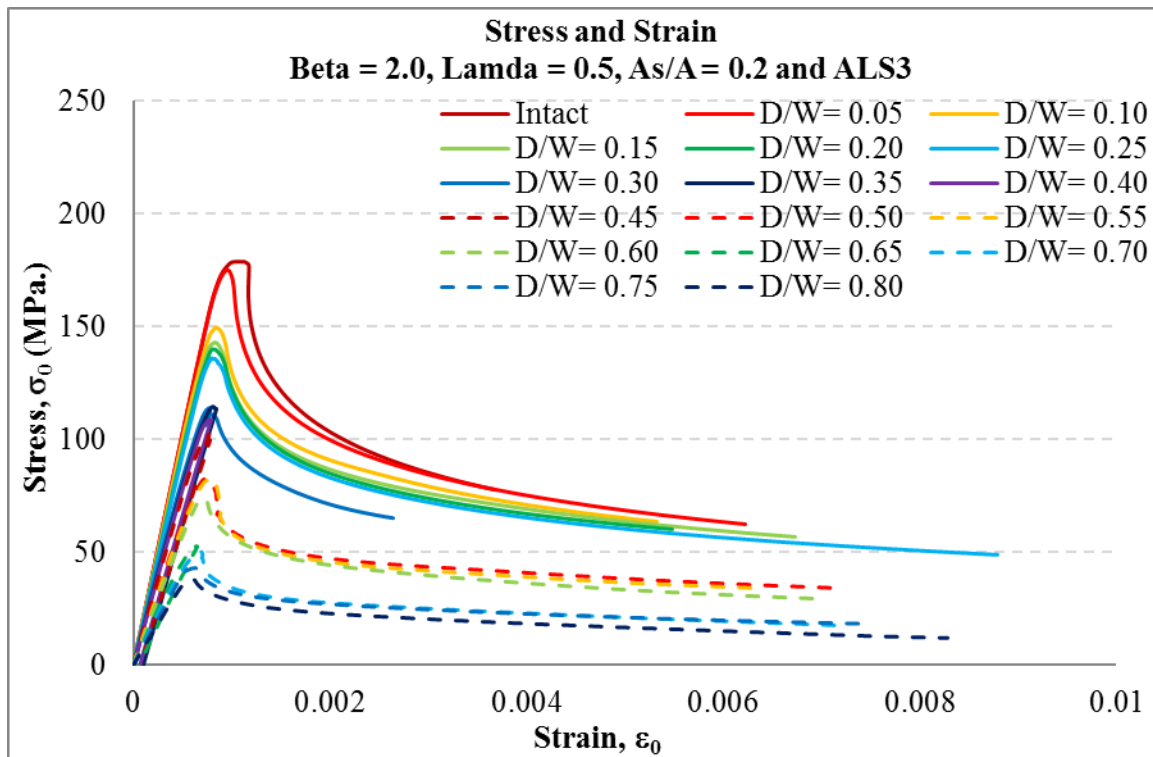
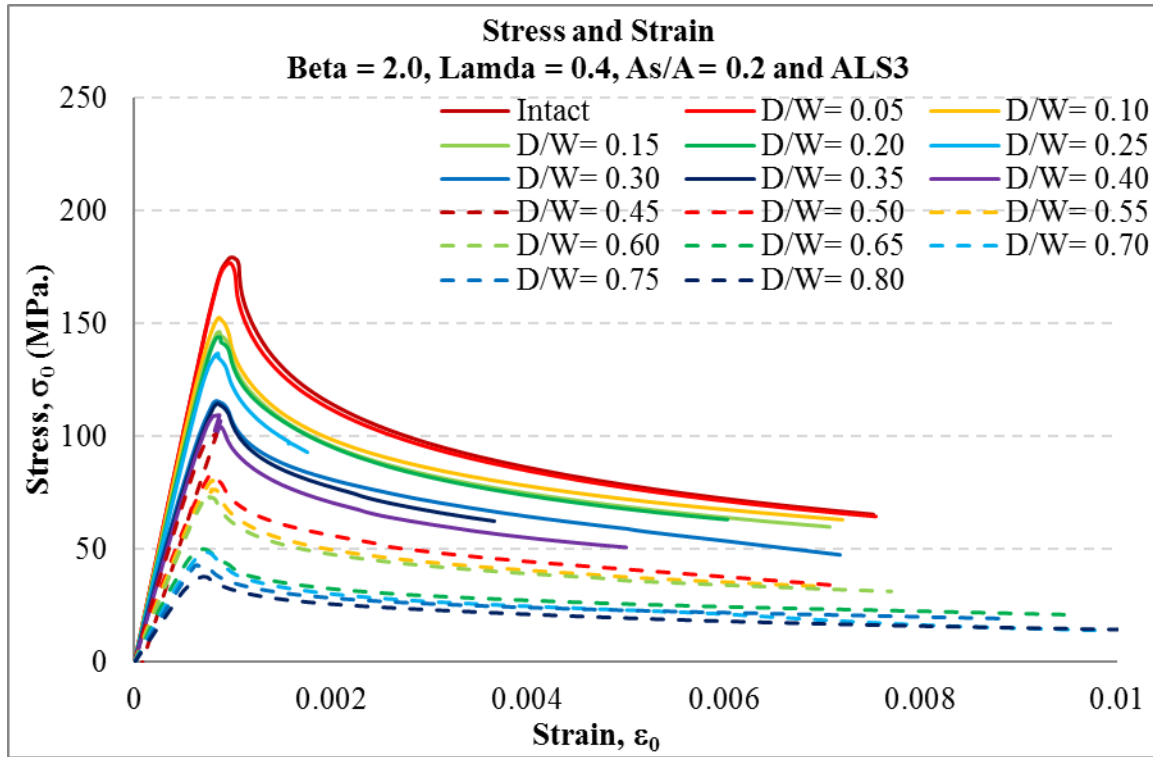


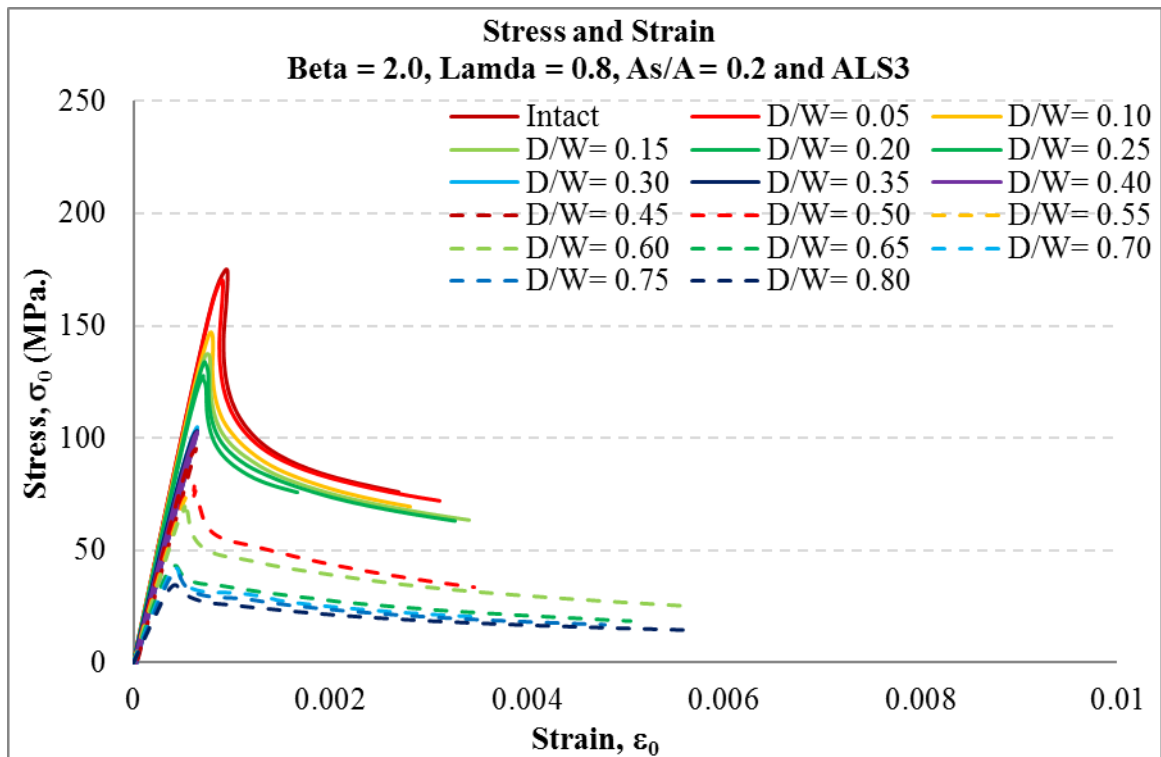
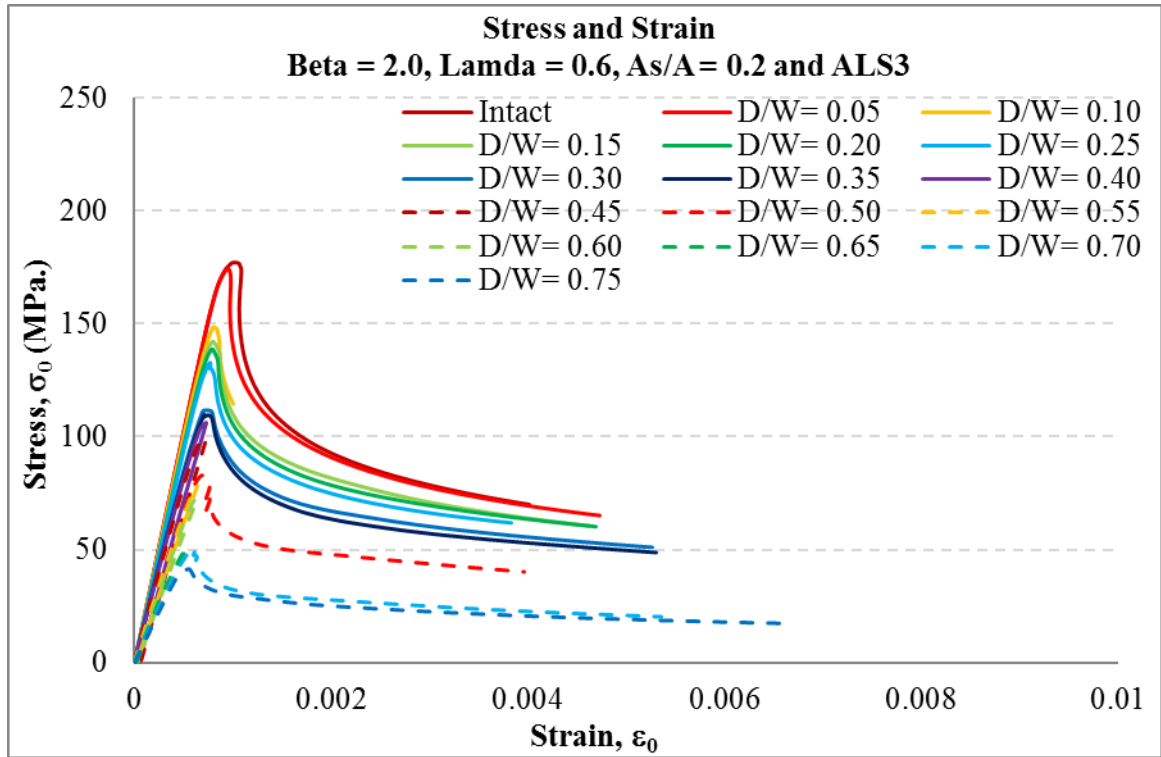


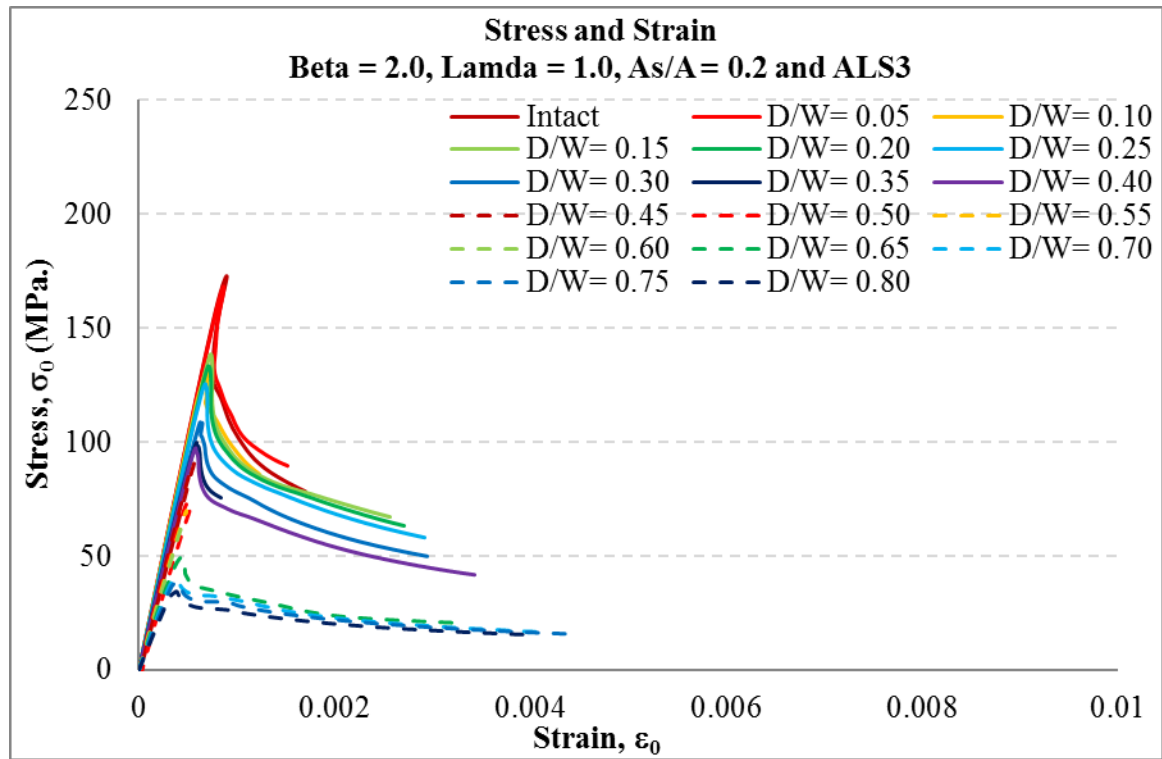


Beta 2.0

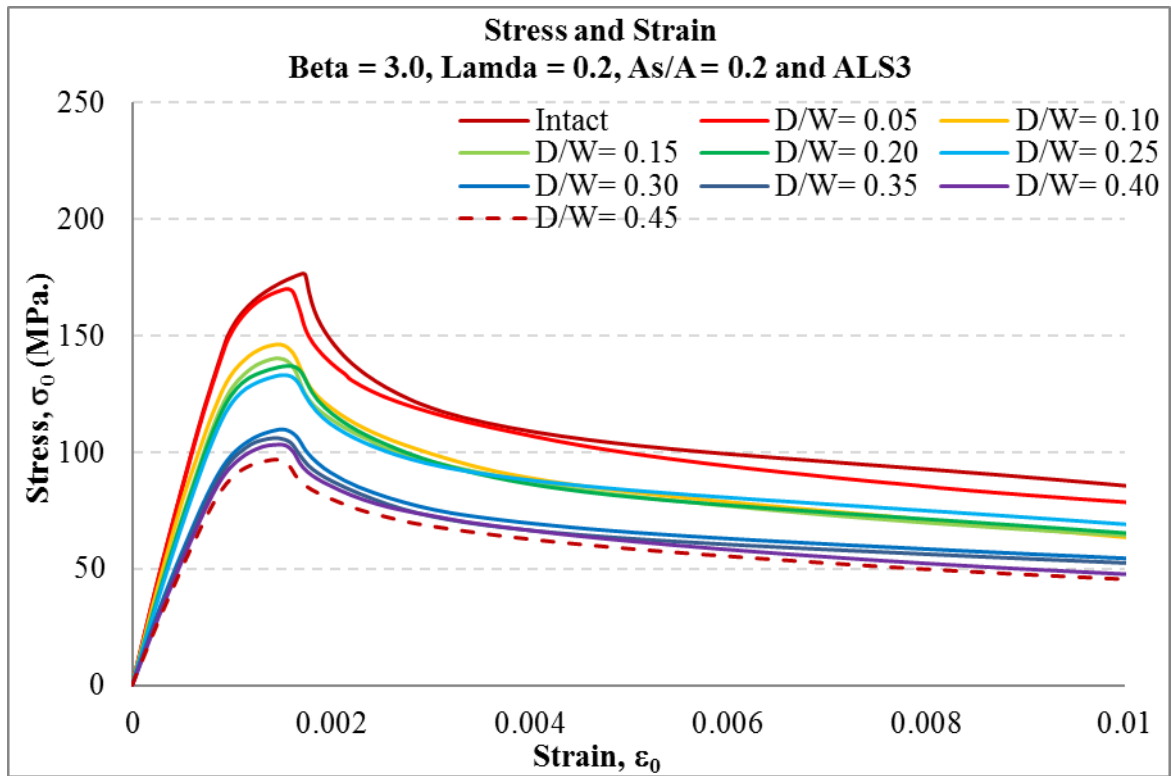


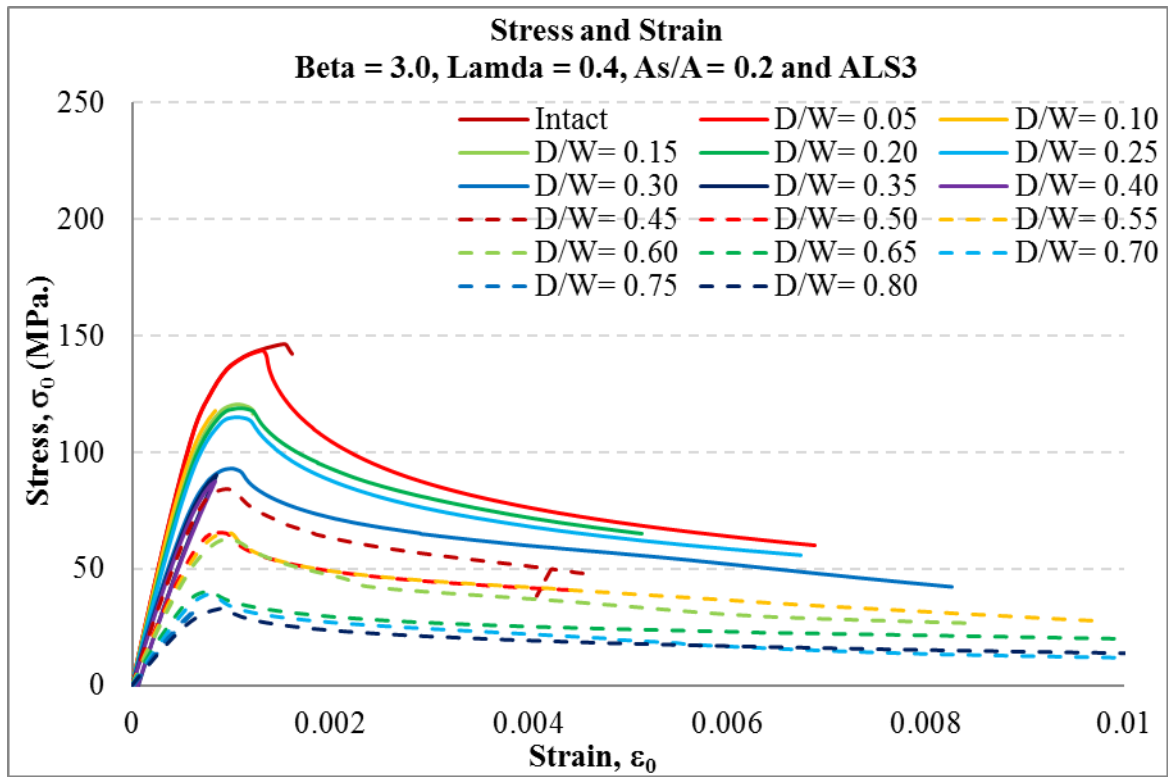
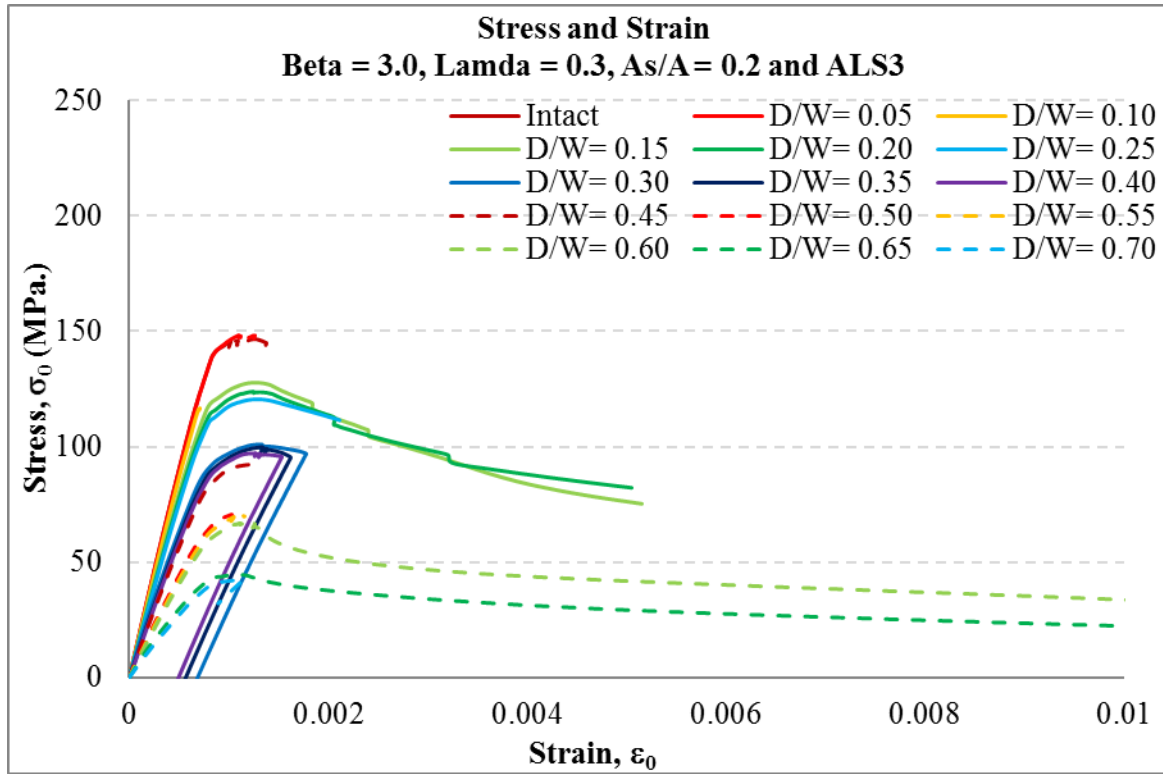


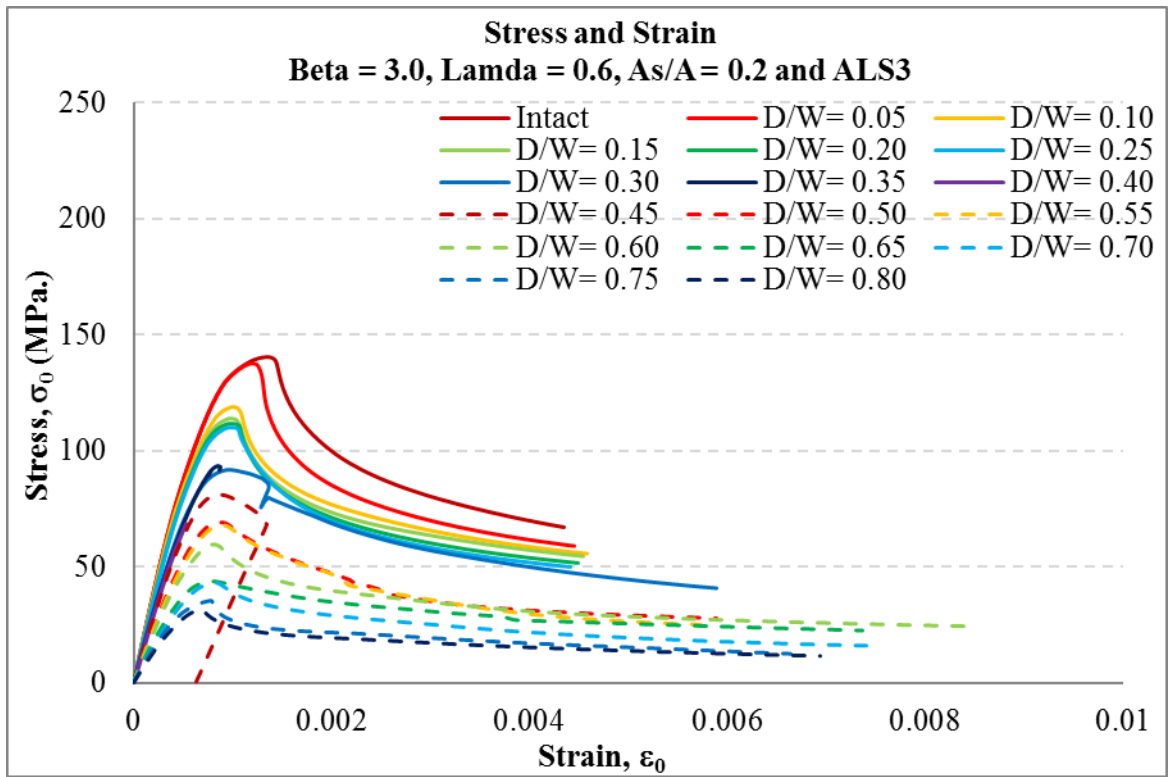
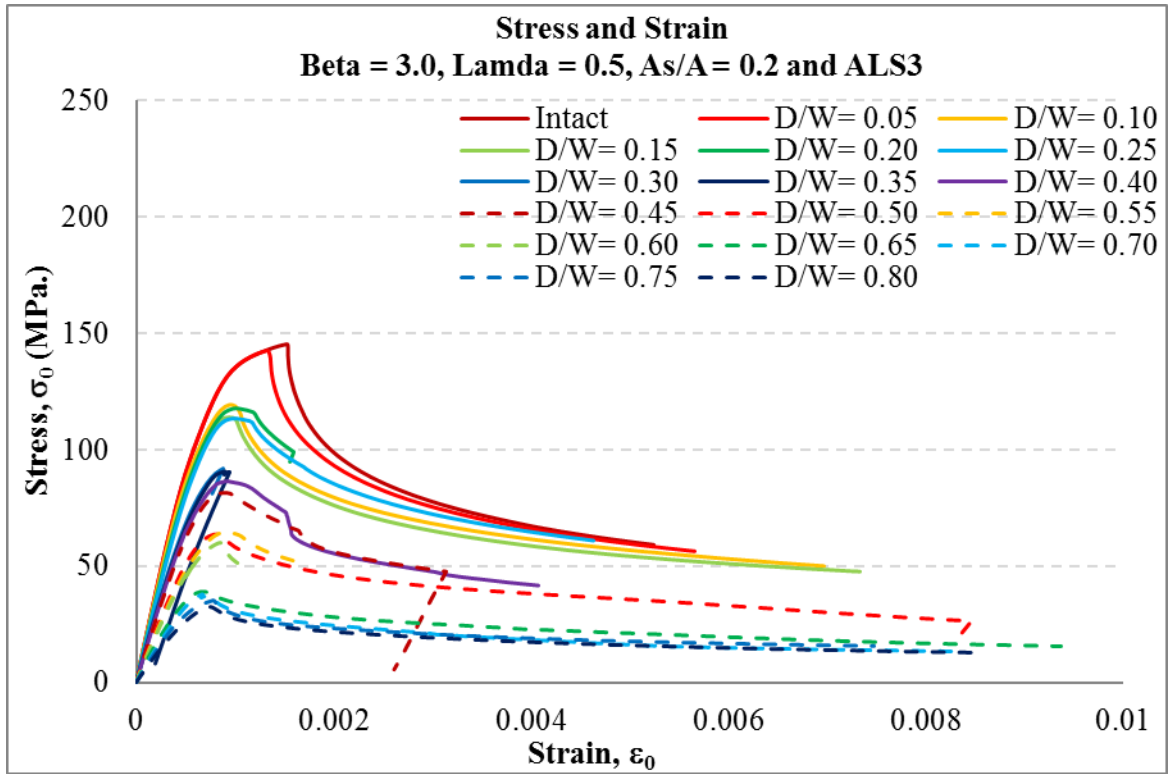


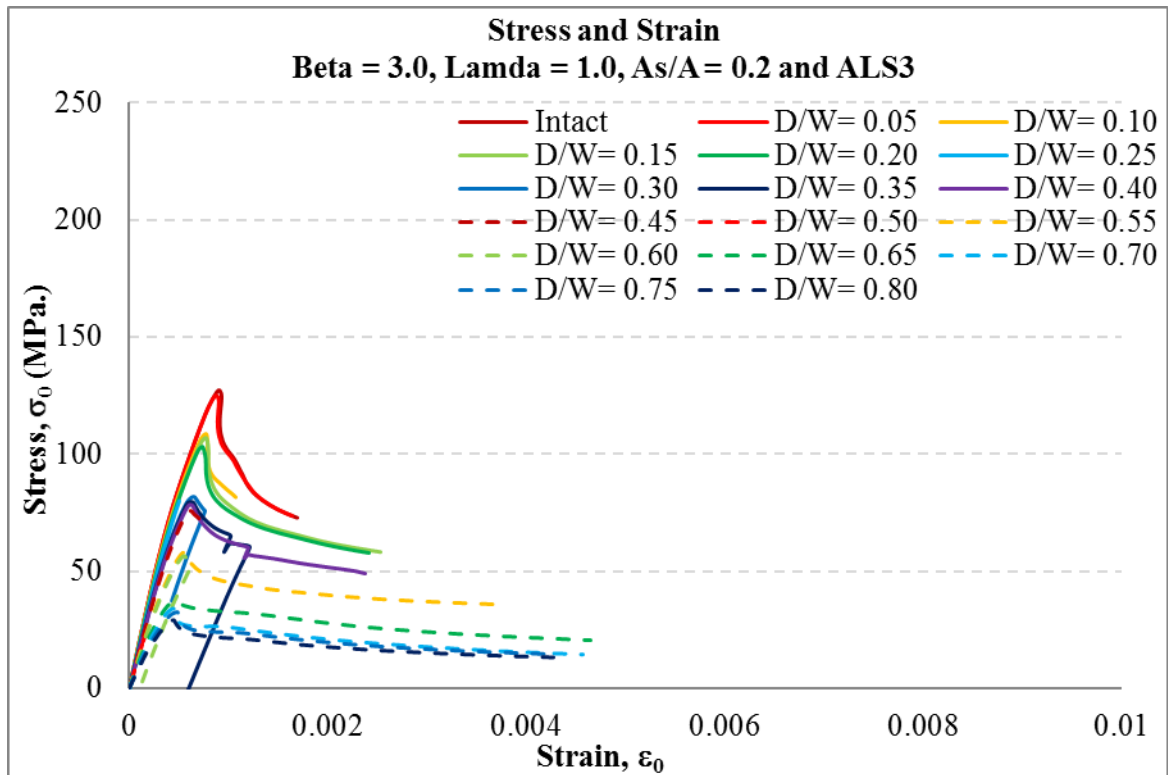
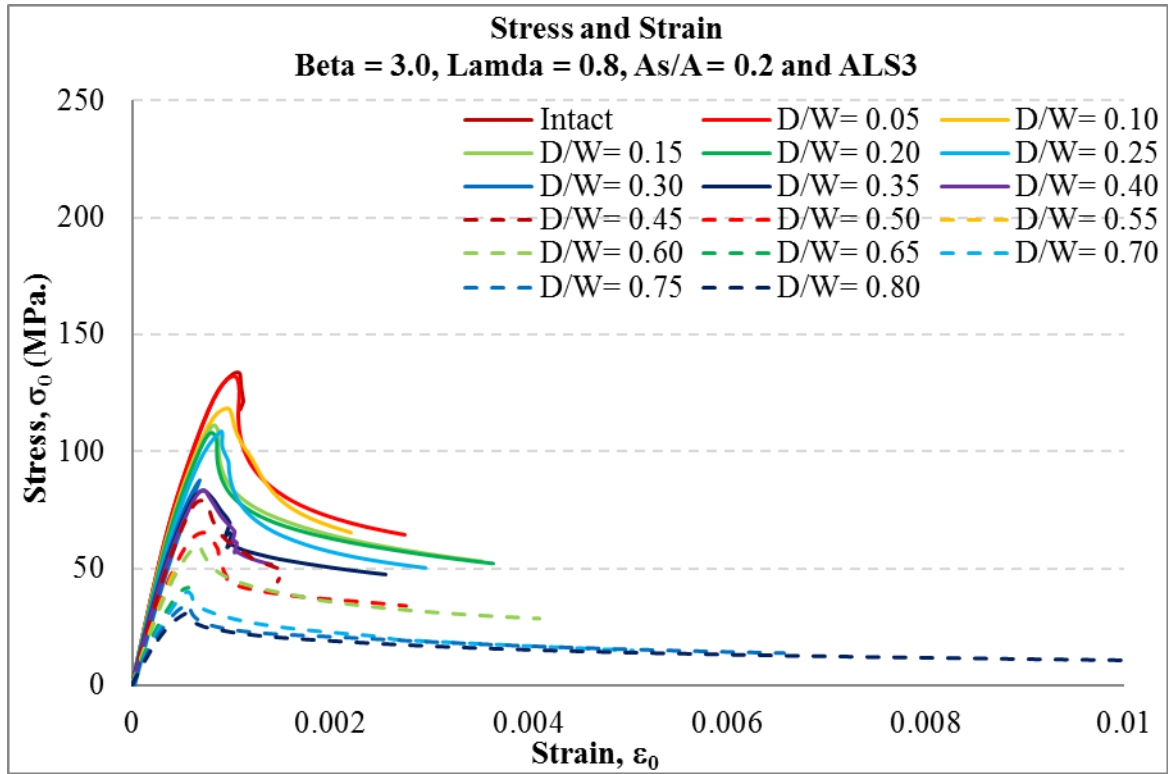


Beta 3.0

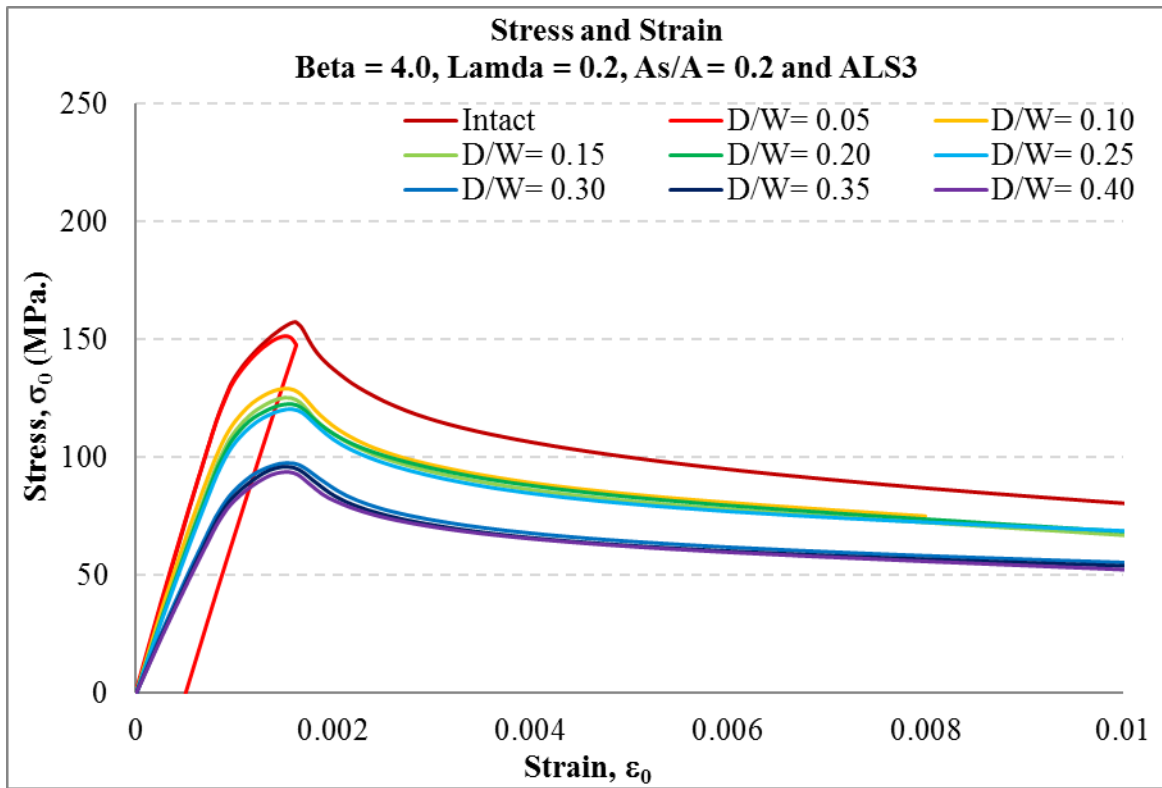


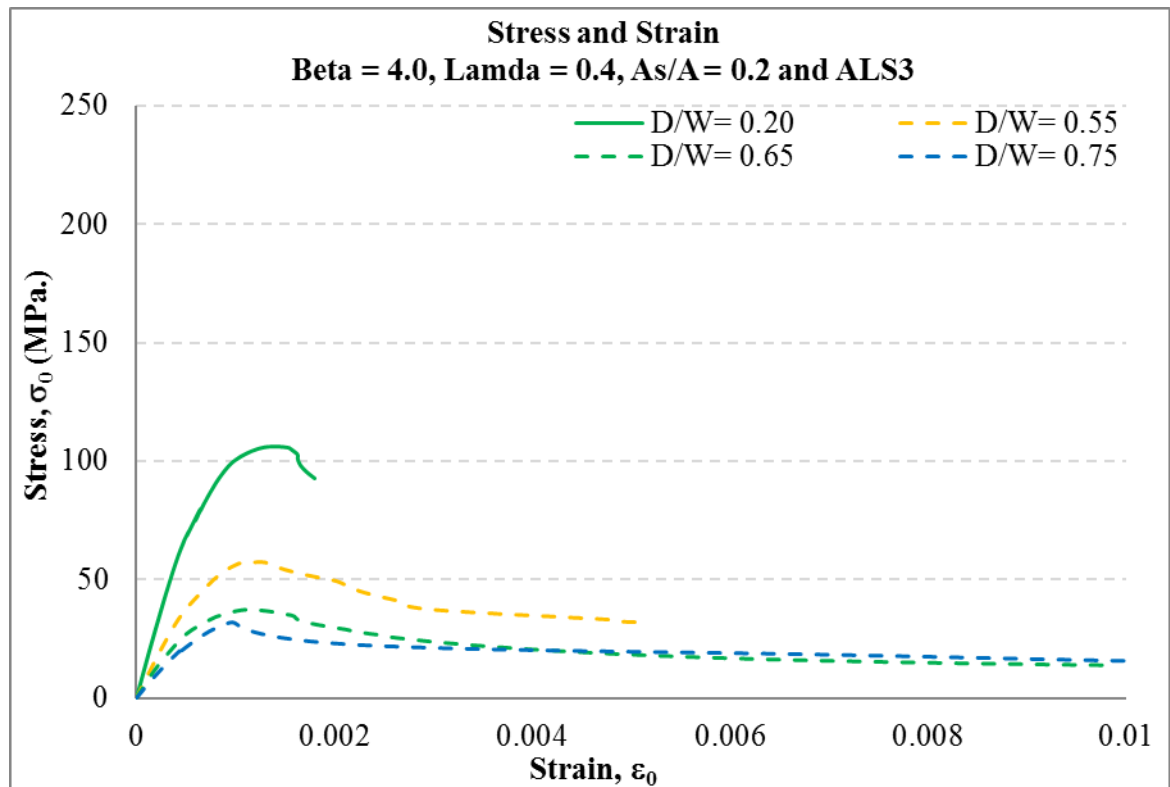
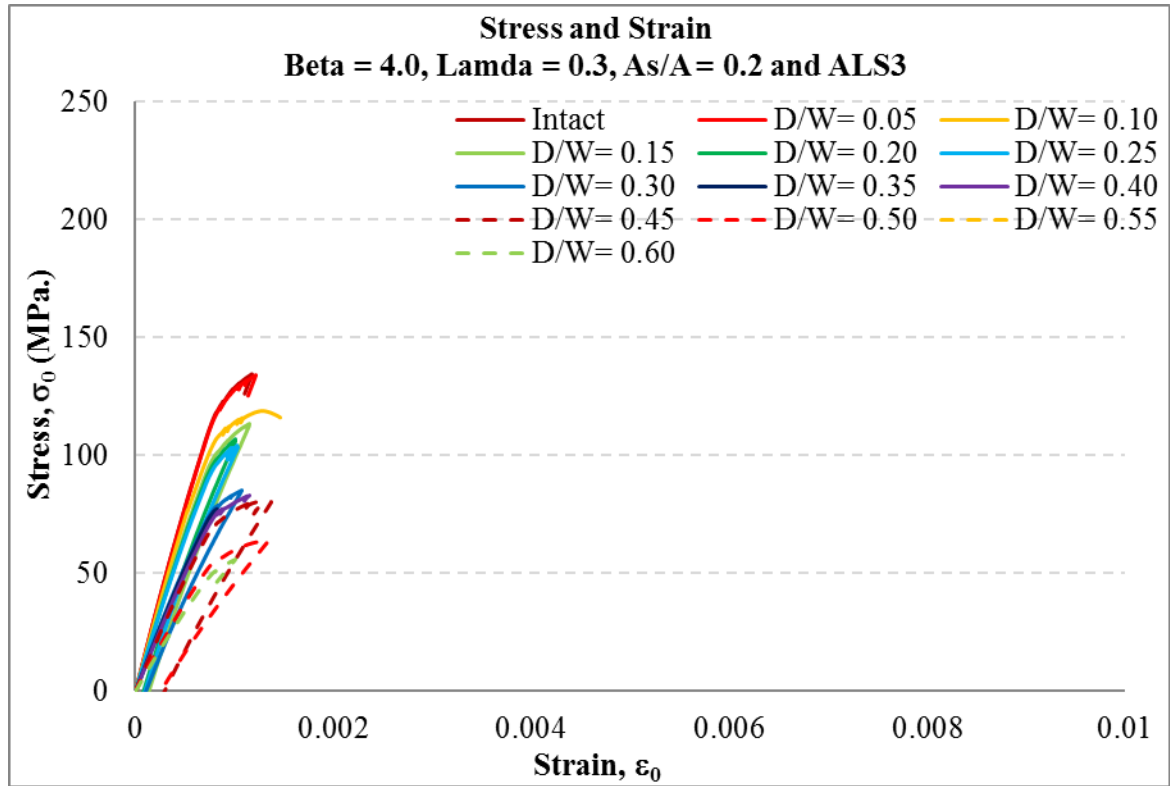


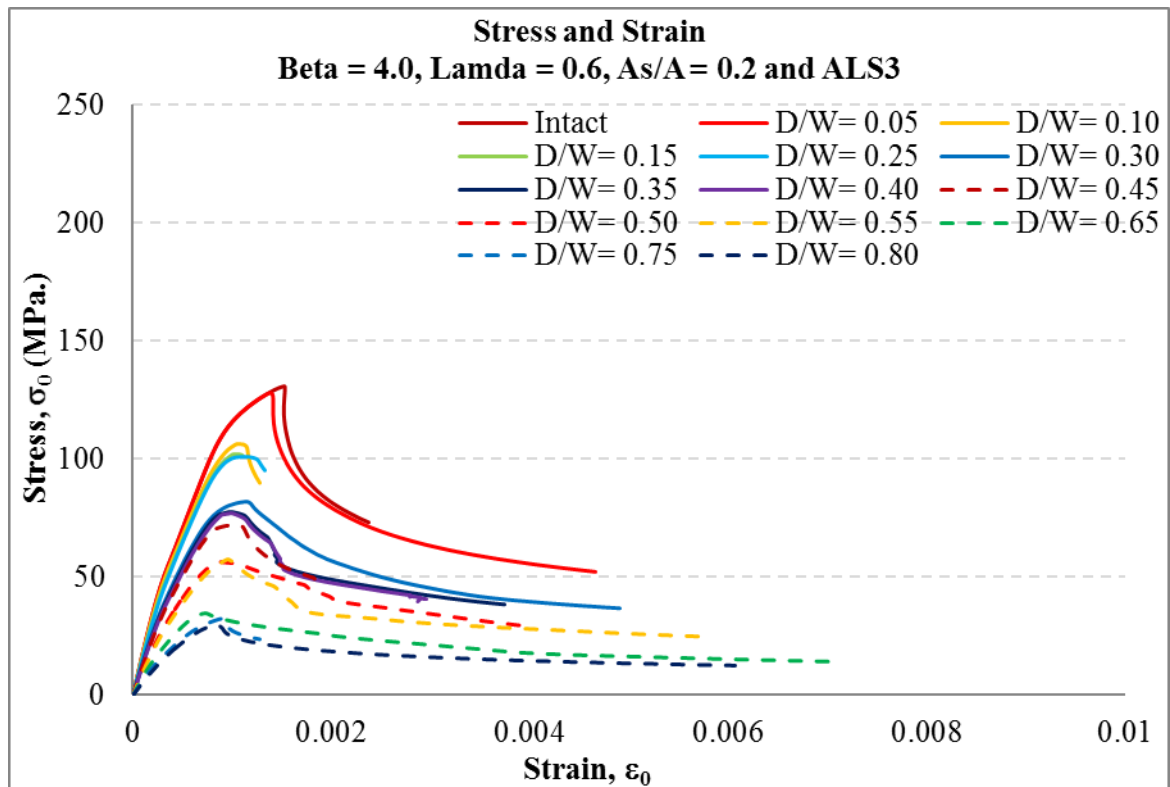
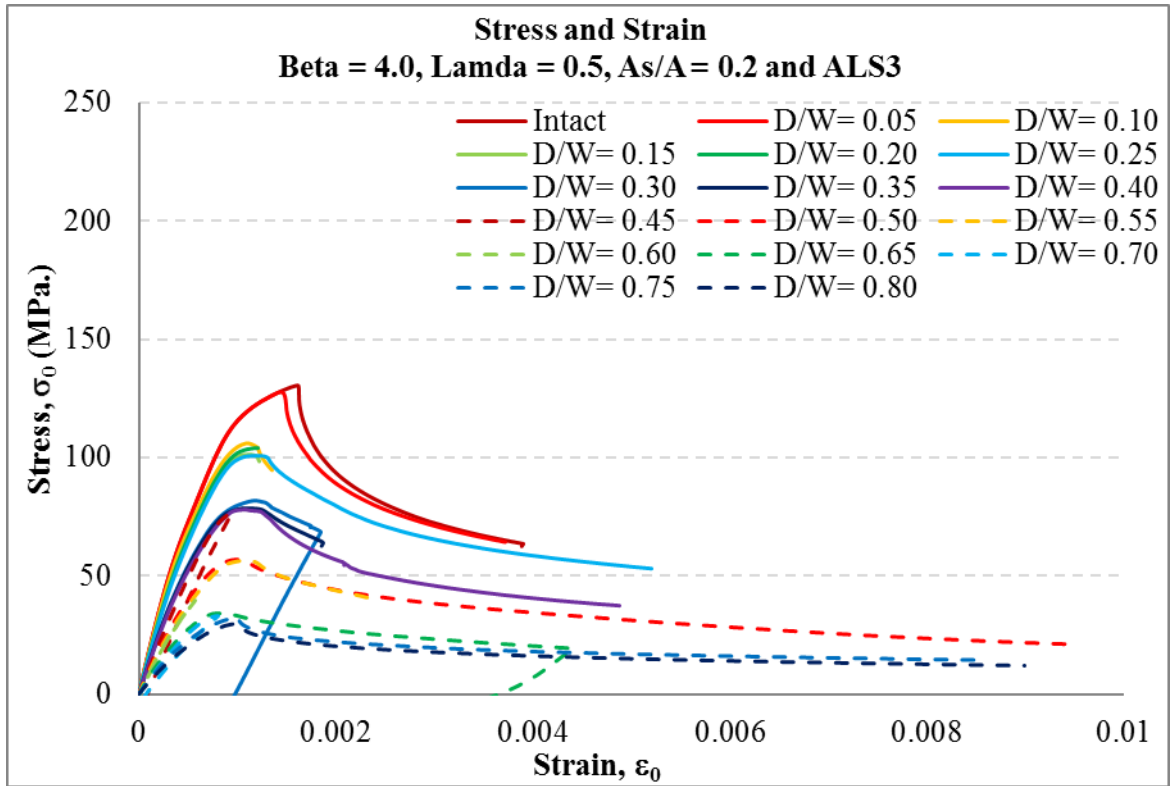


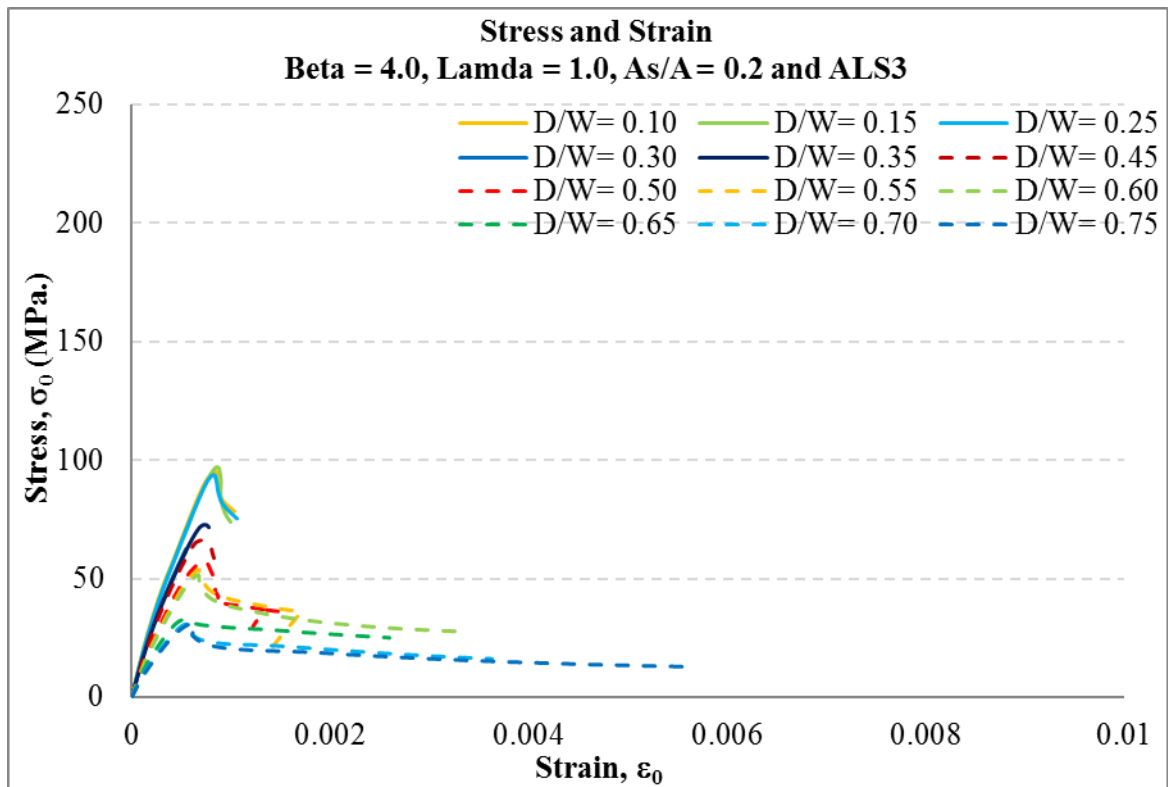
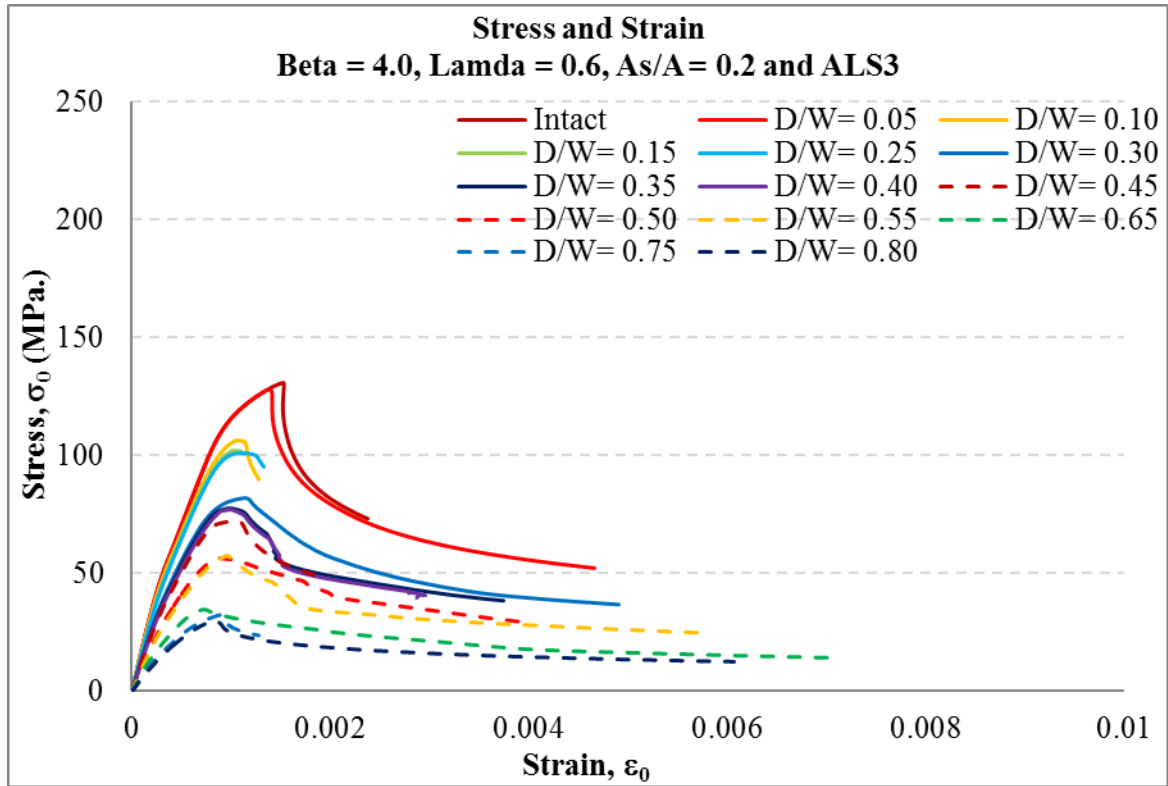


Beta 4.0



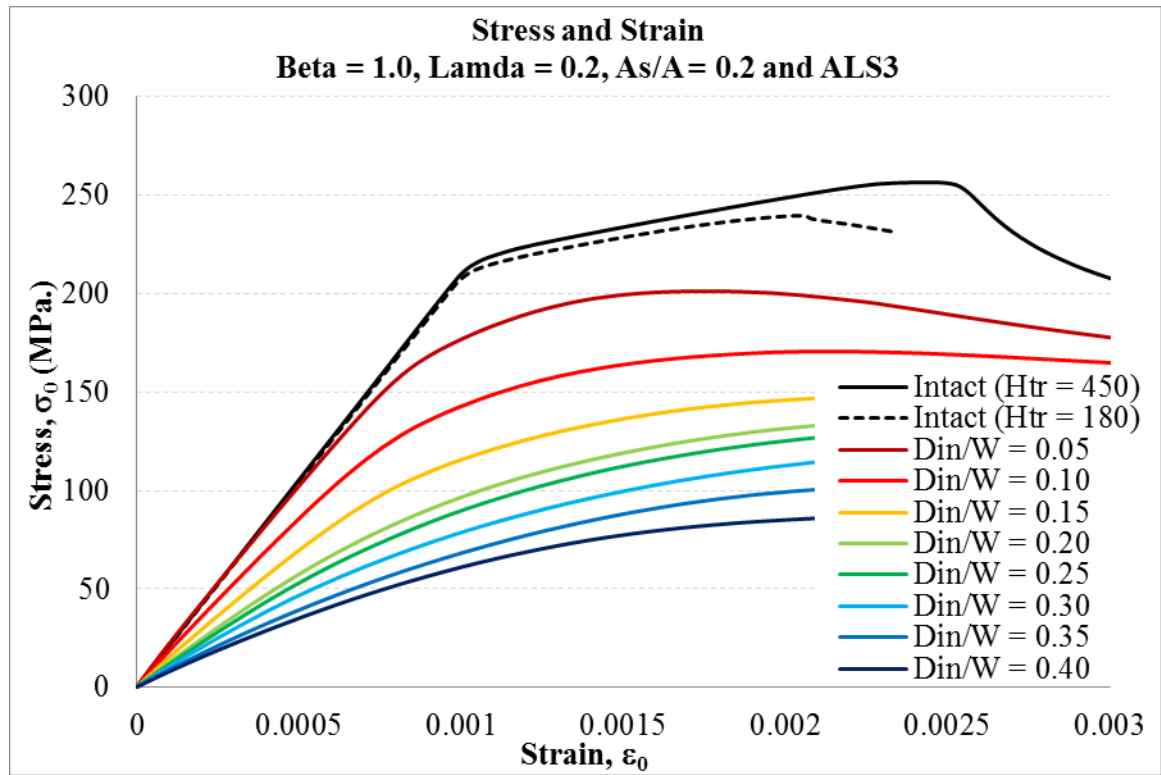


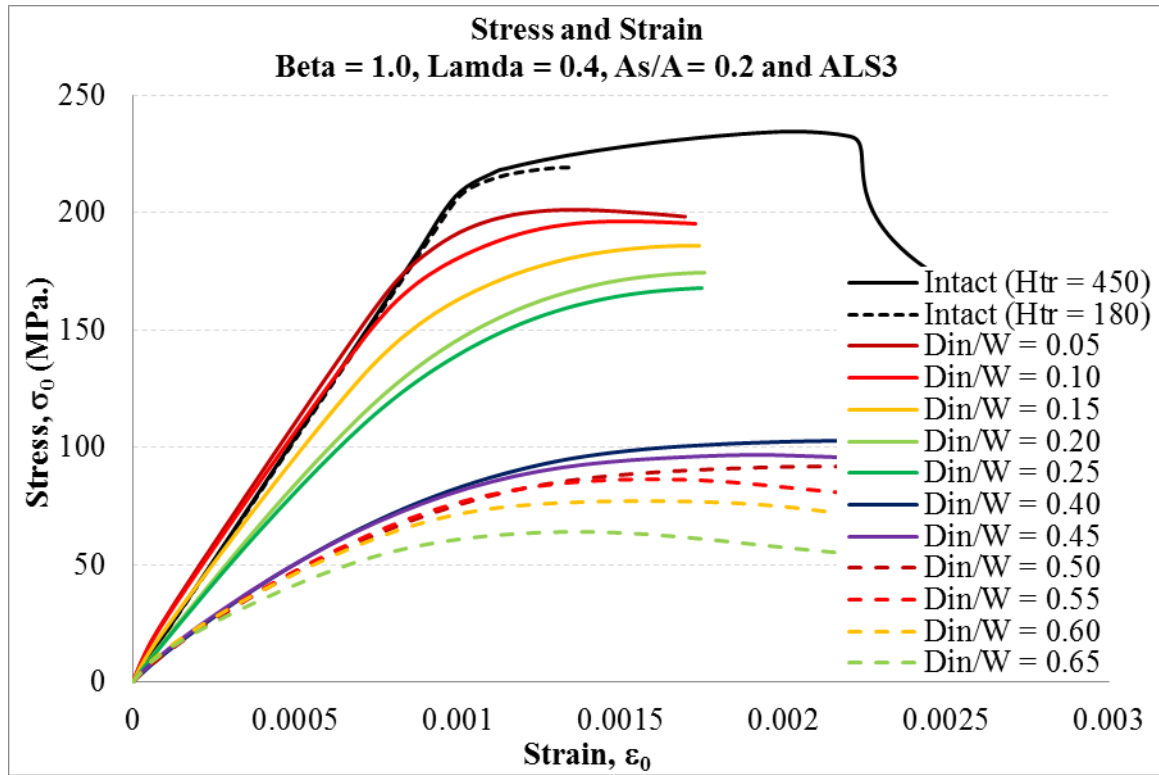
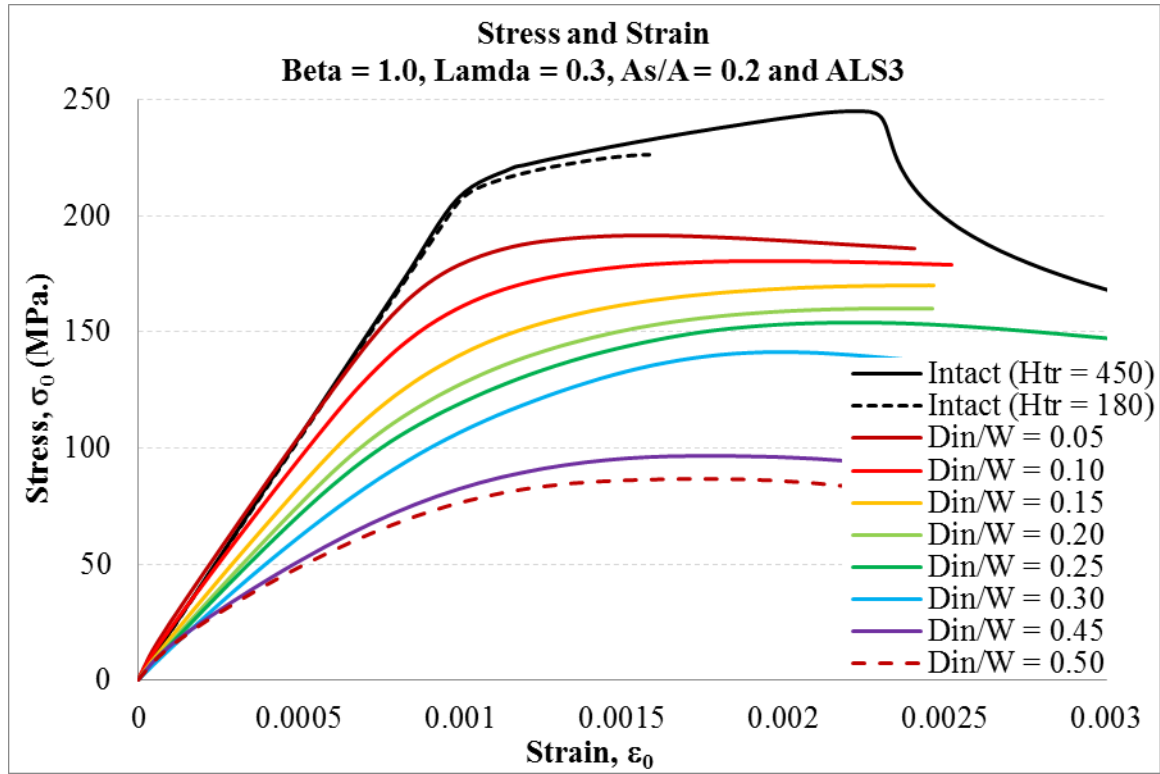


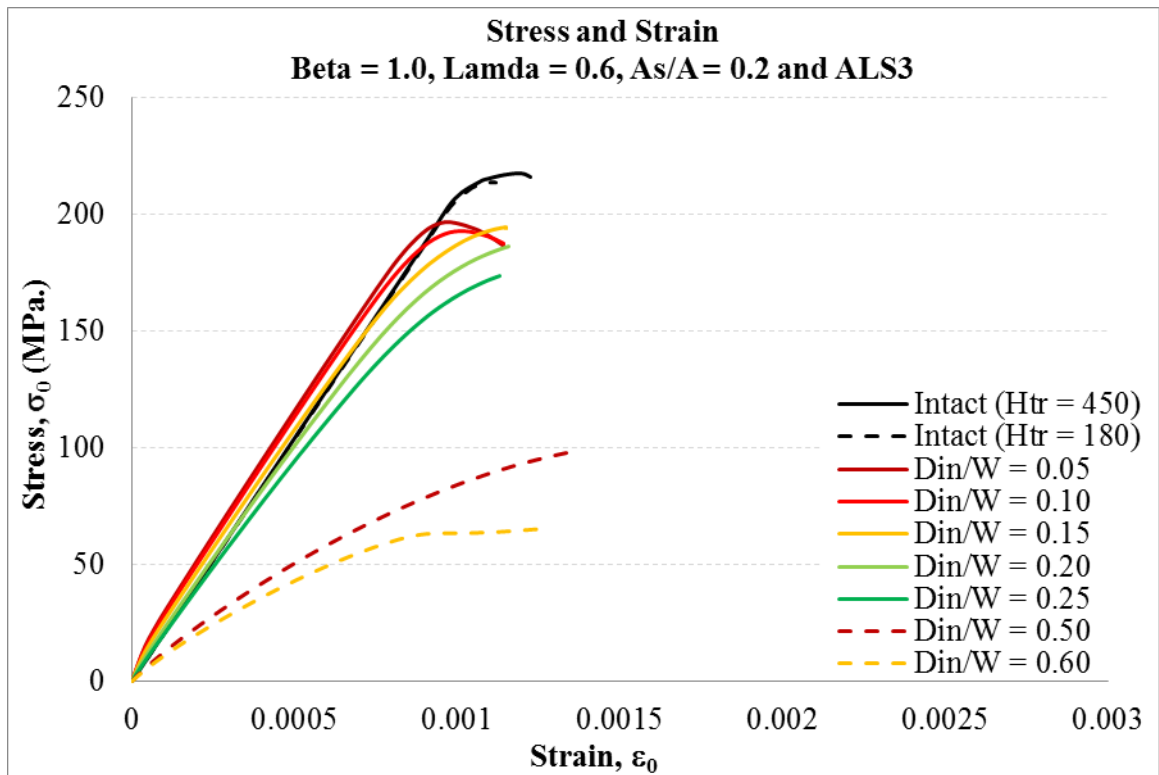
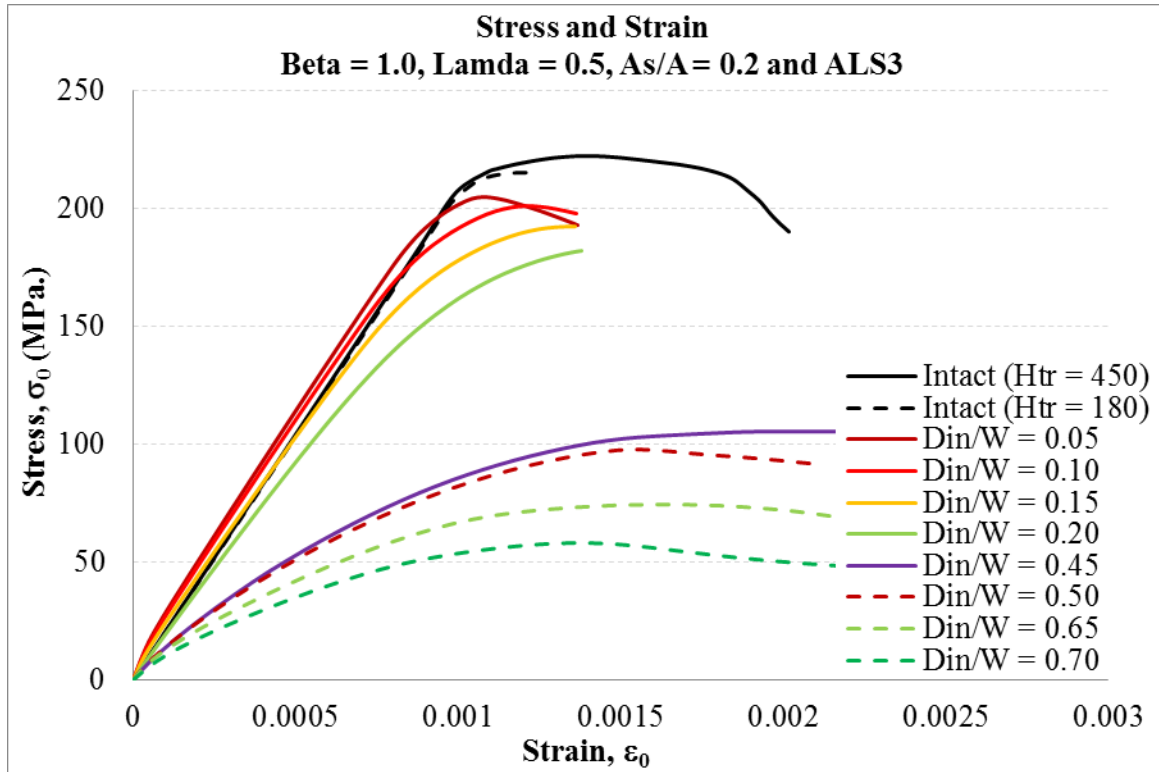


Appendix D: Strength of penetration damage with indenter.

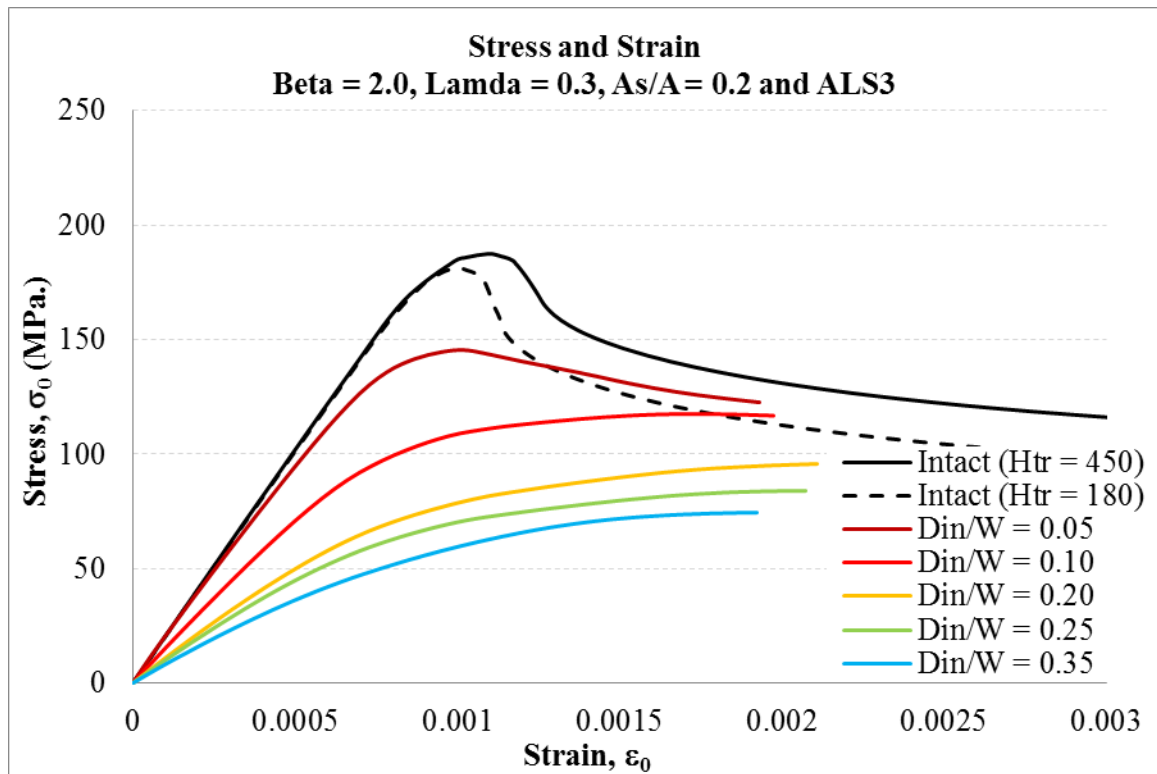
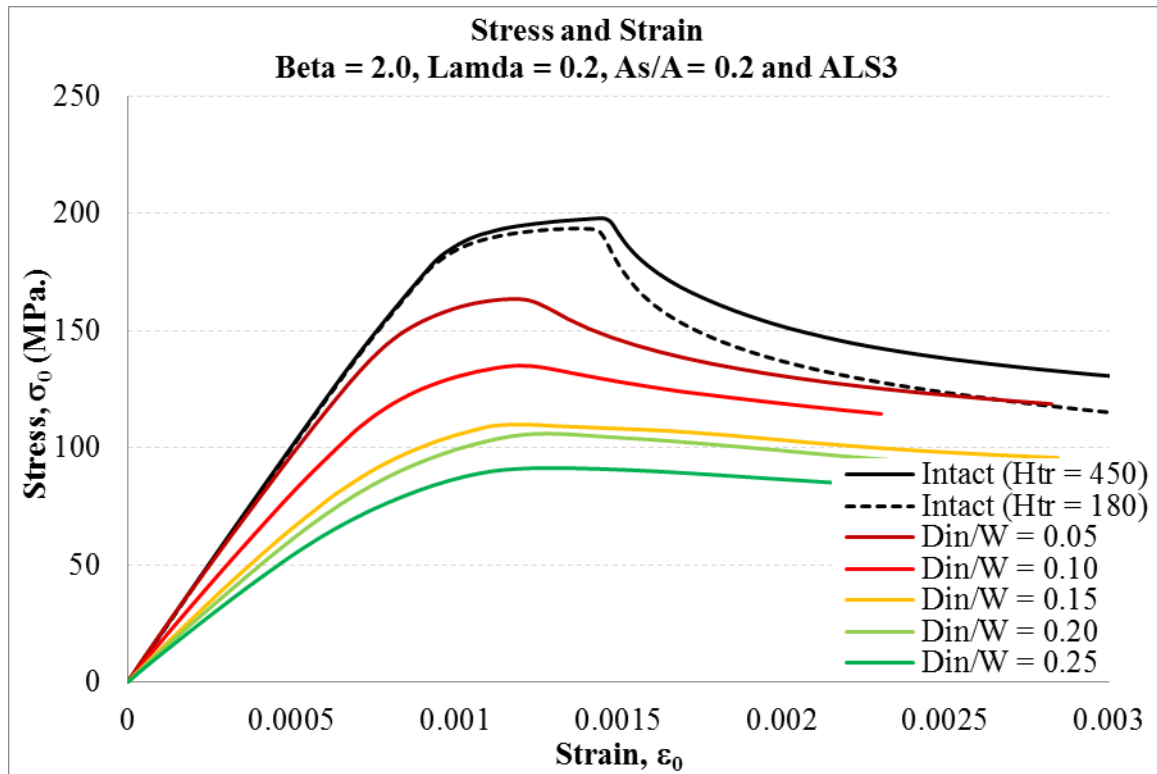
Beta 1.0

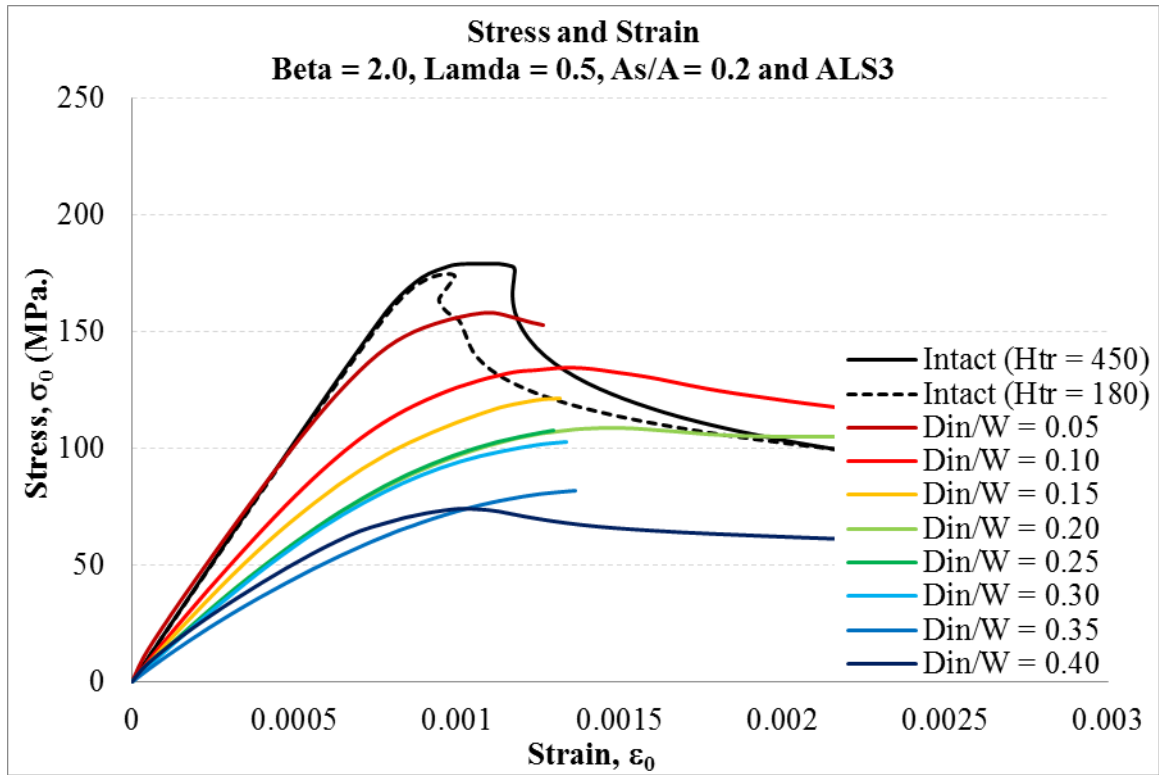
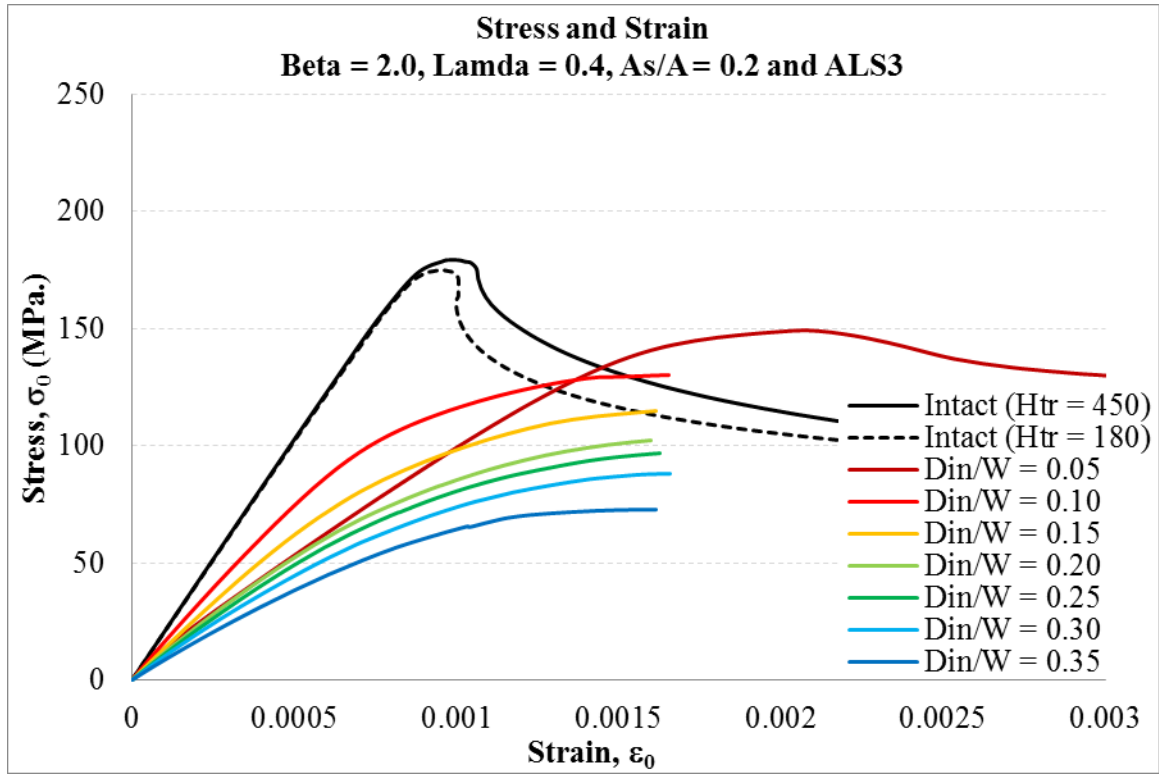


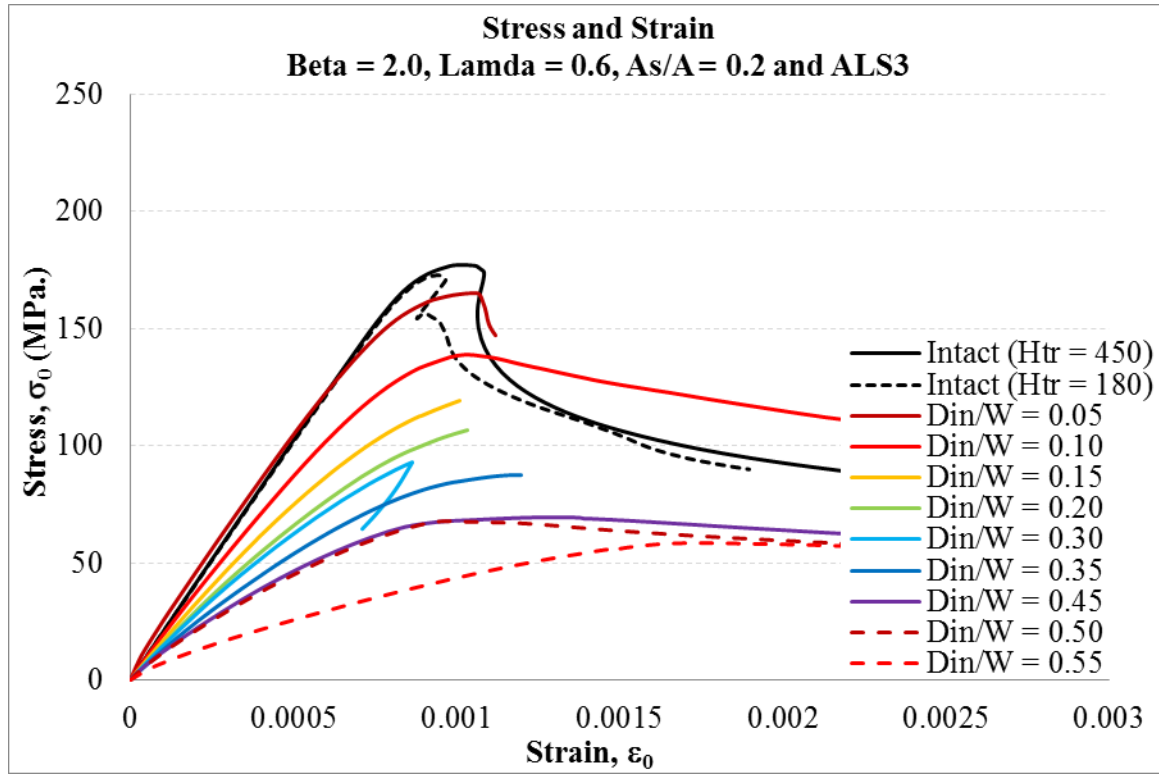




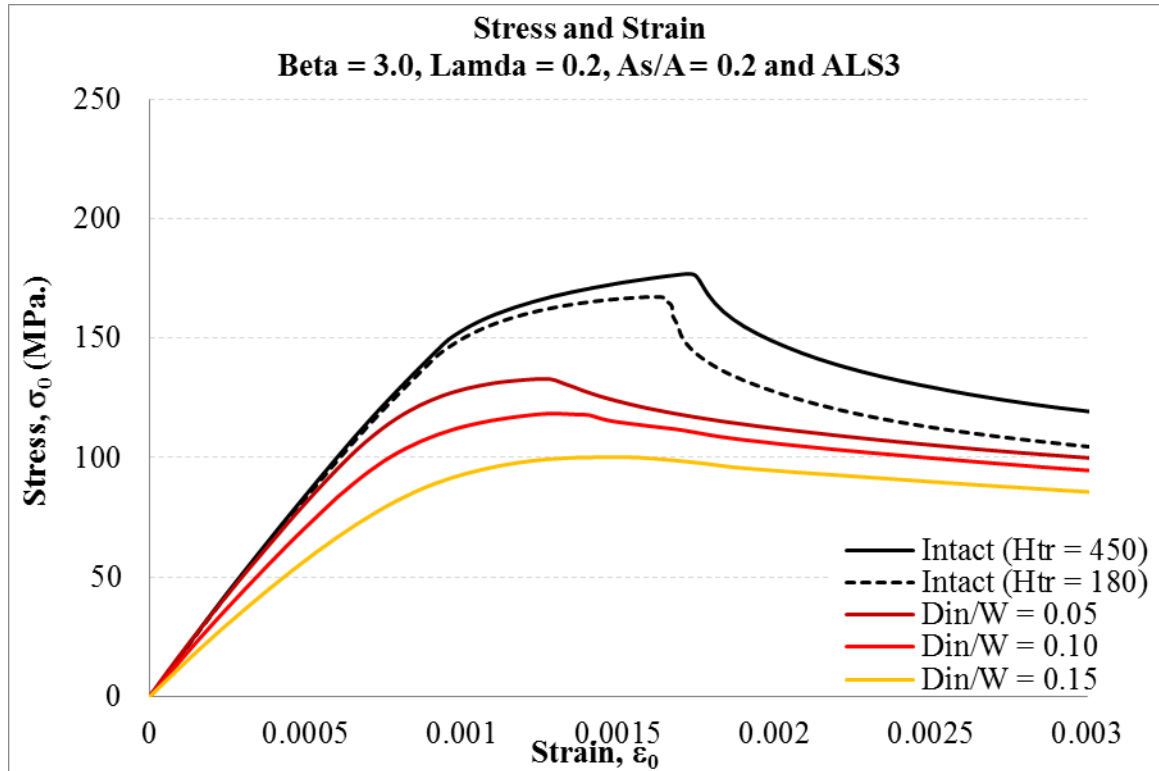
Beta 2.0

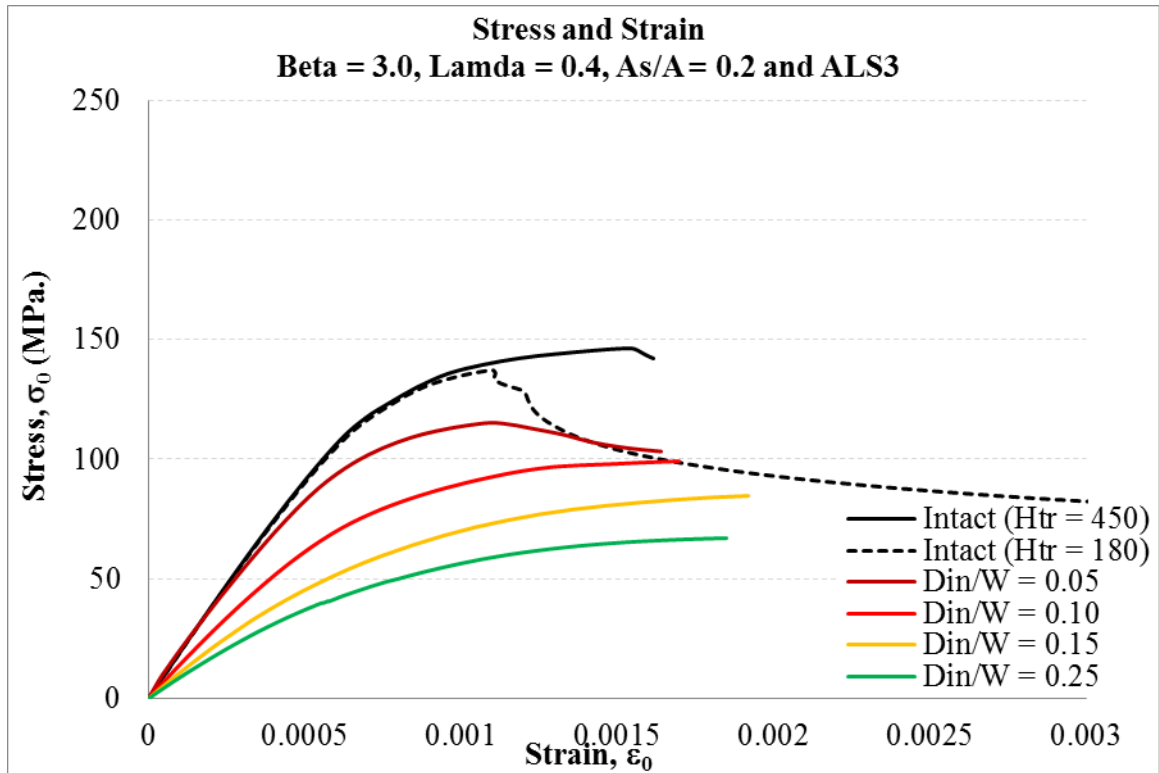
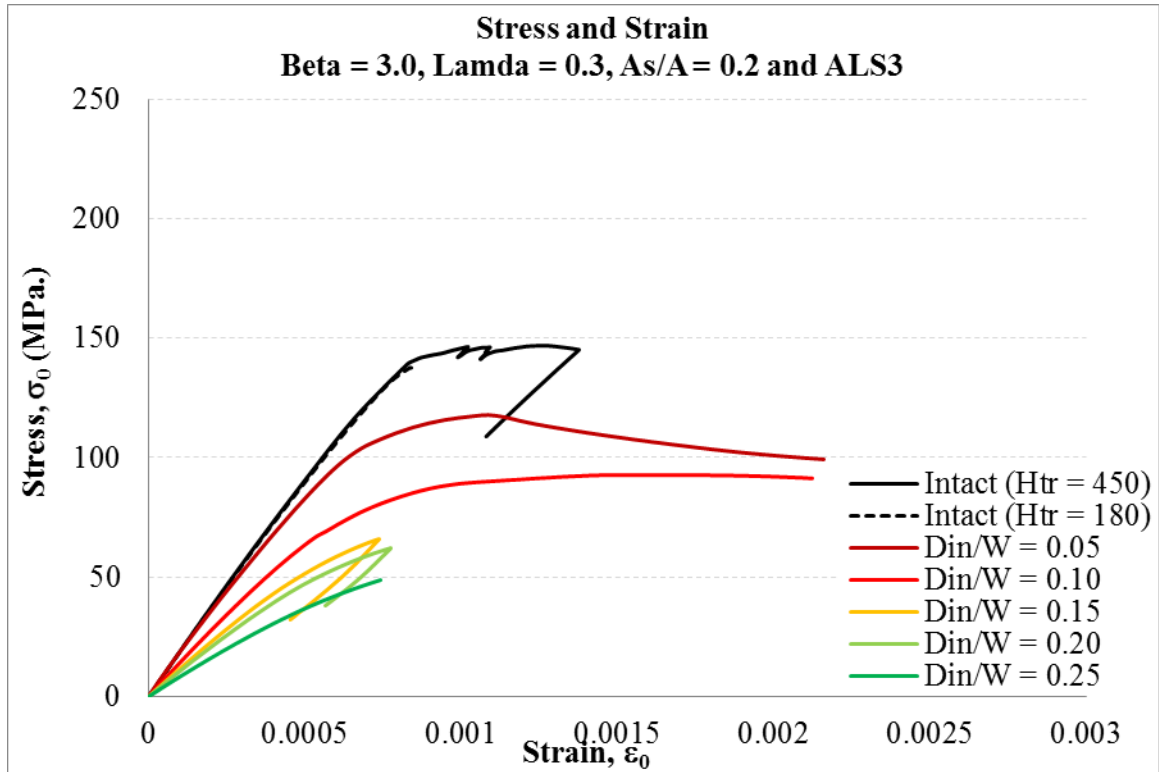


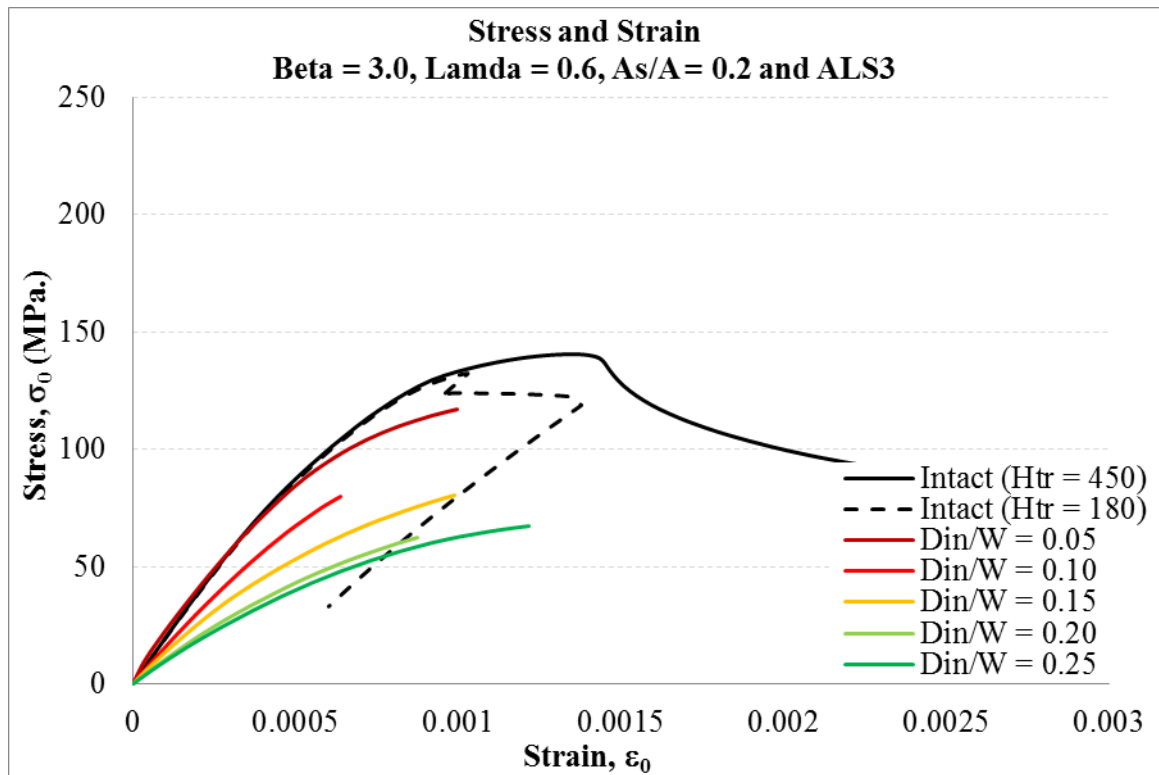
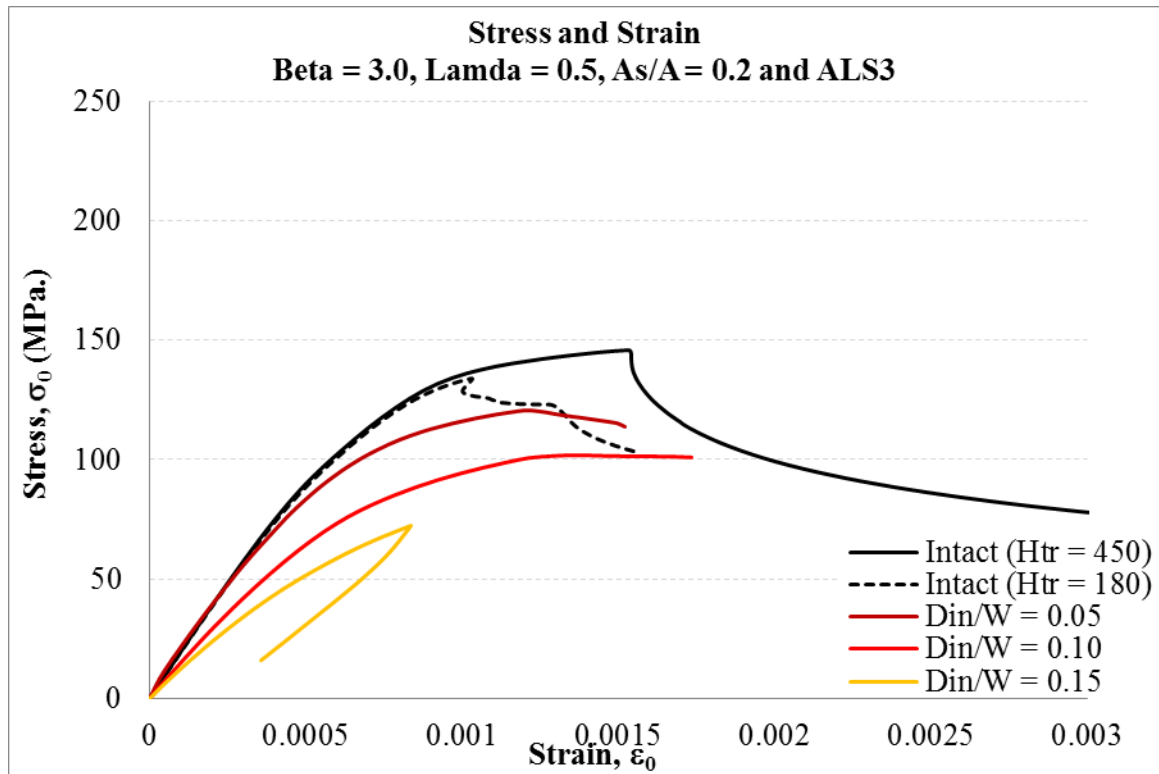




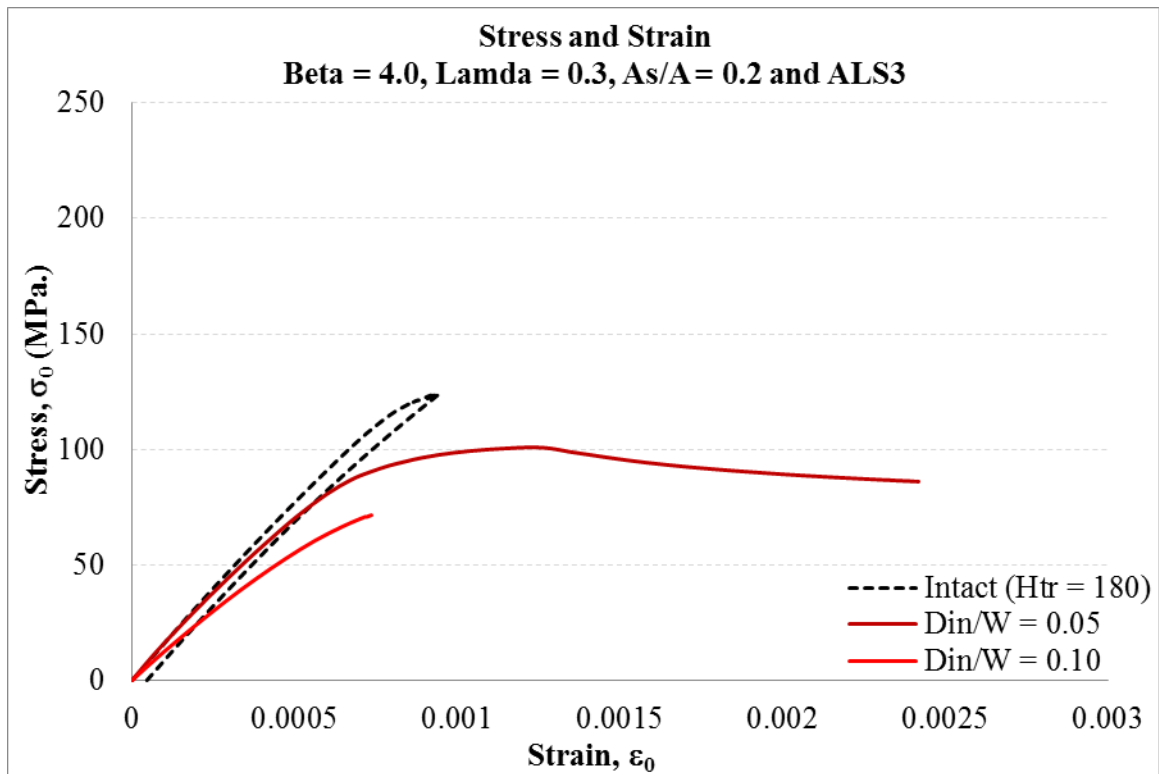
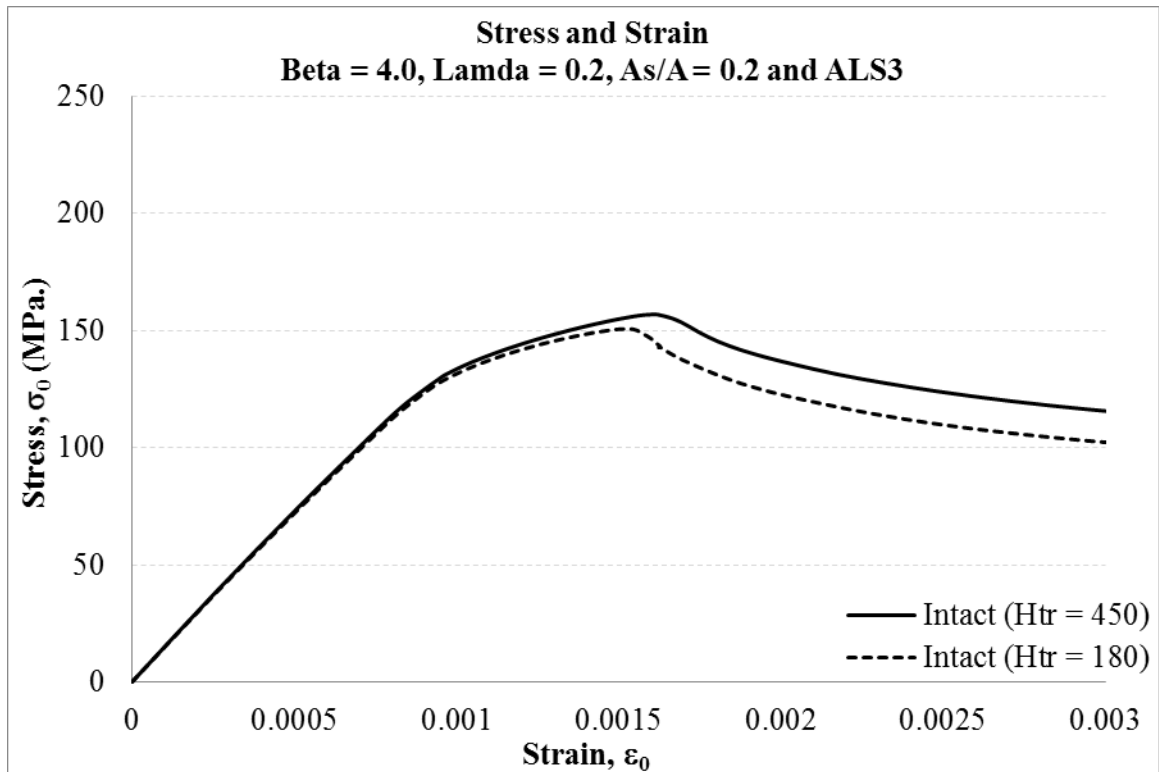
Beta 3.0

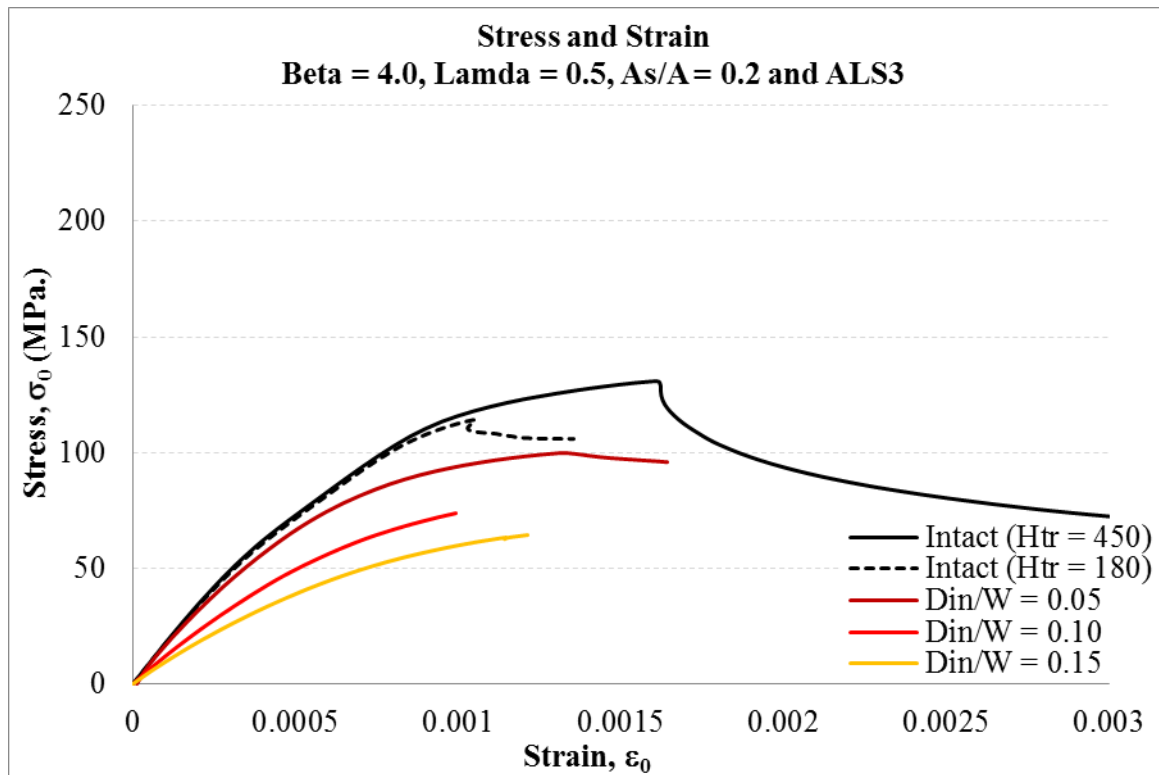
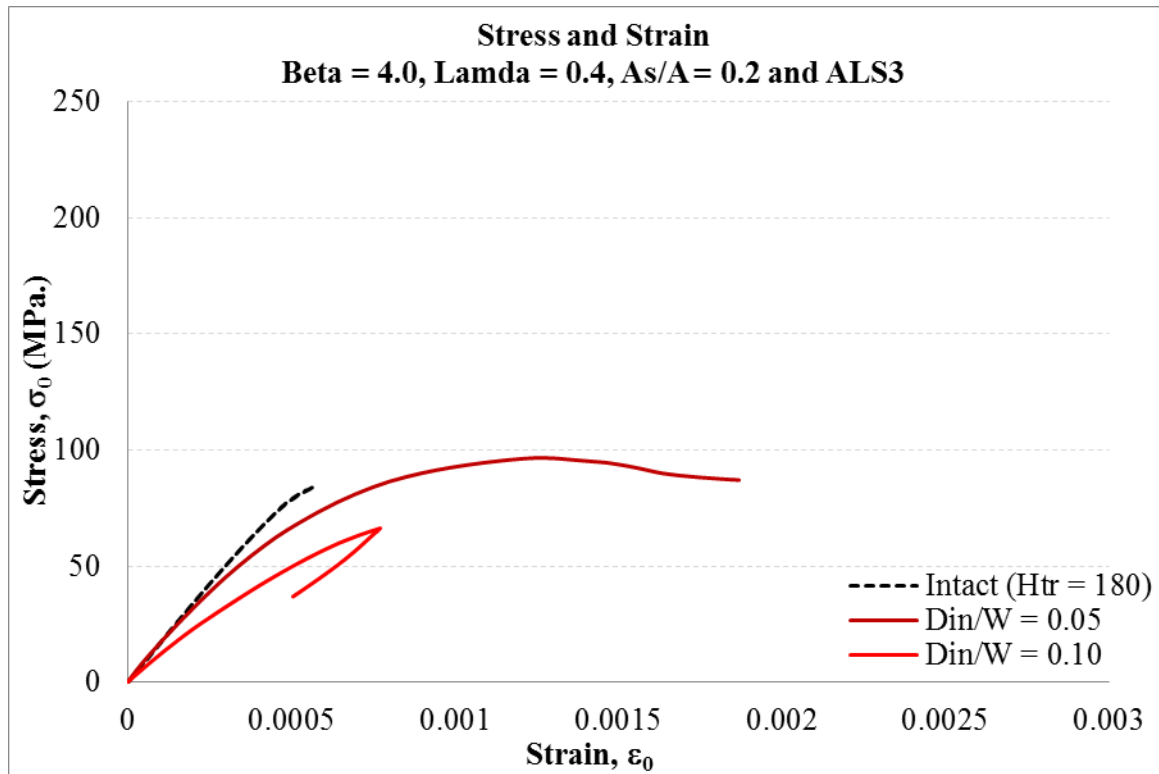


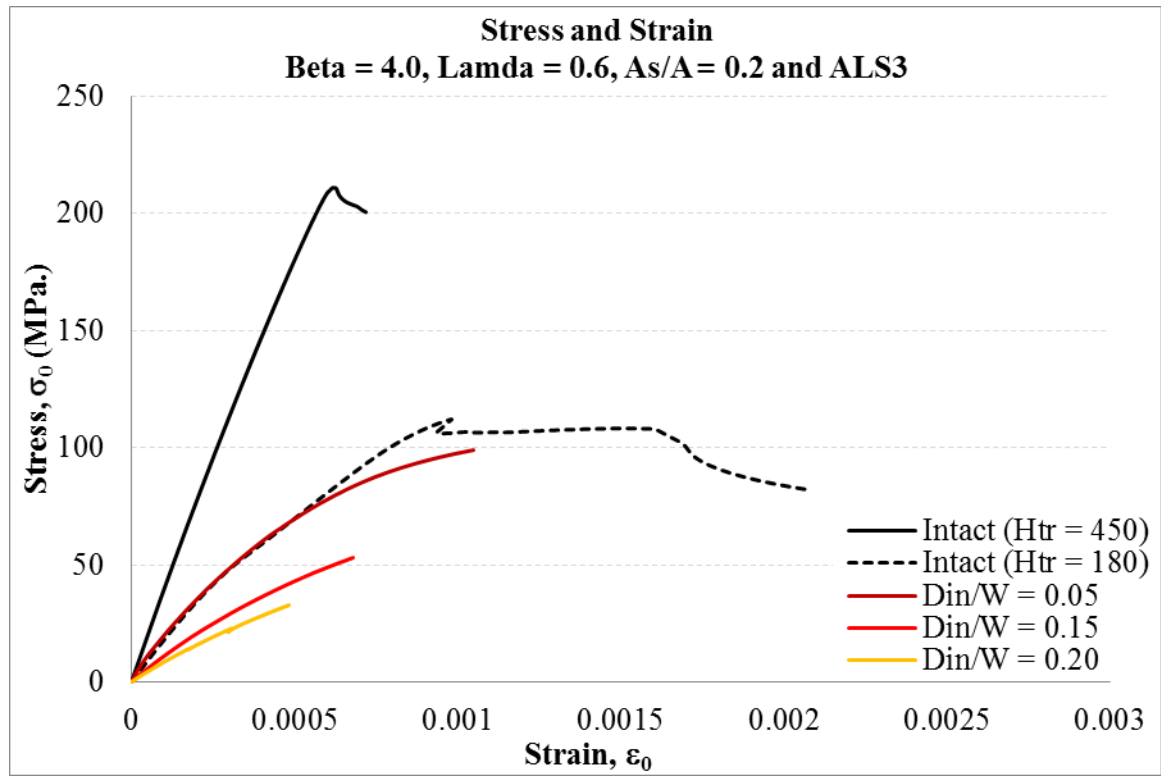




Beta 4.0

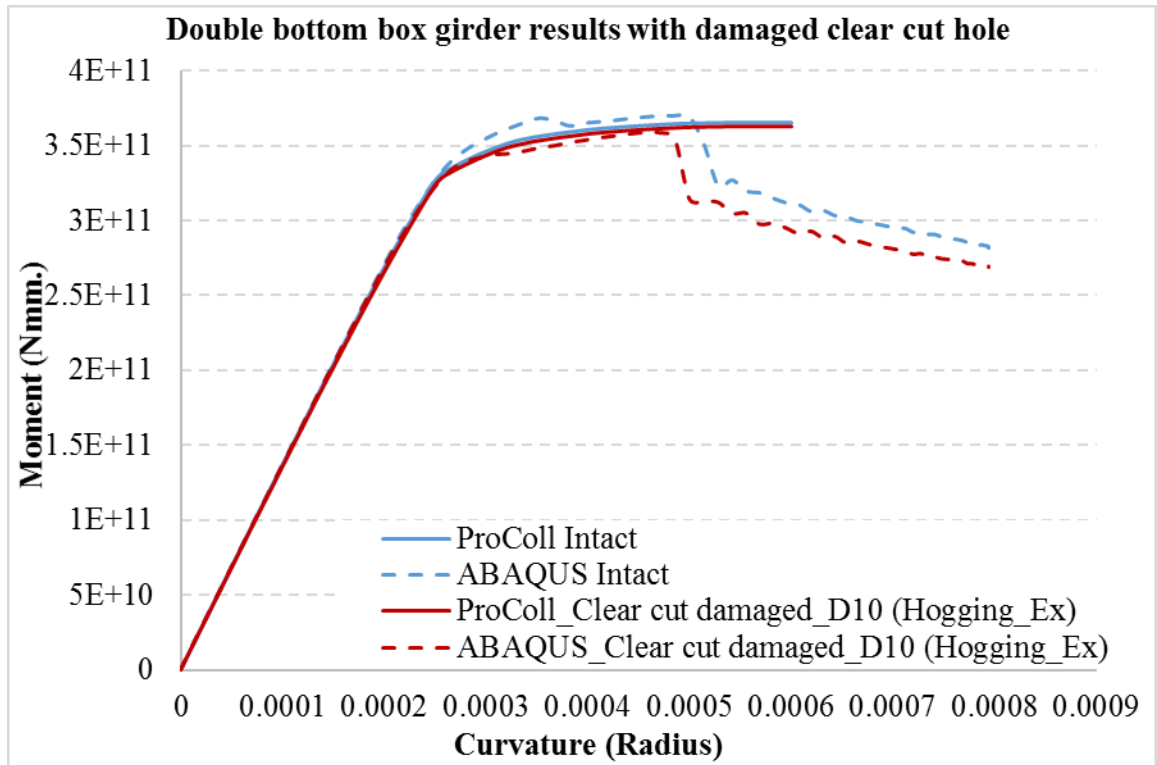


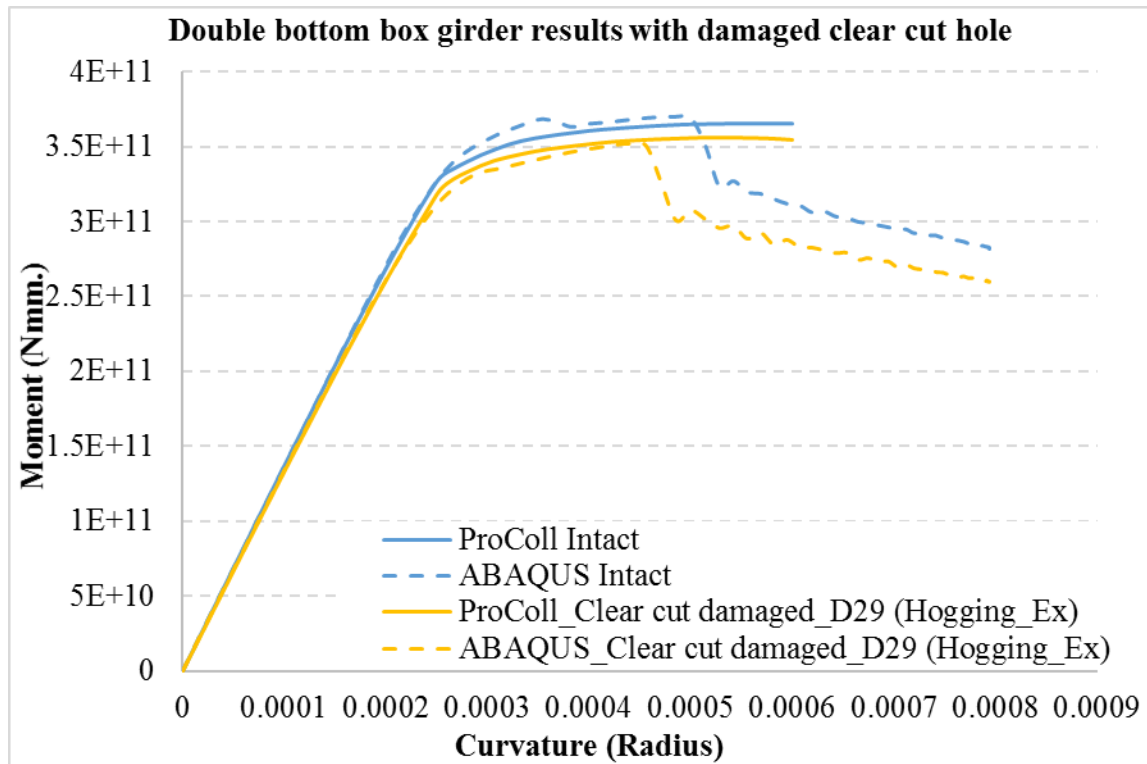
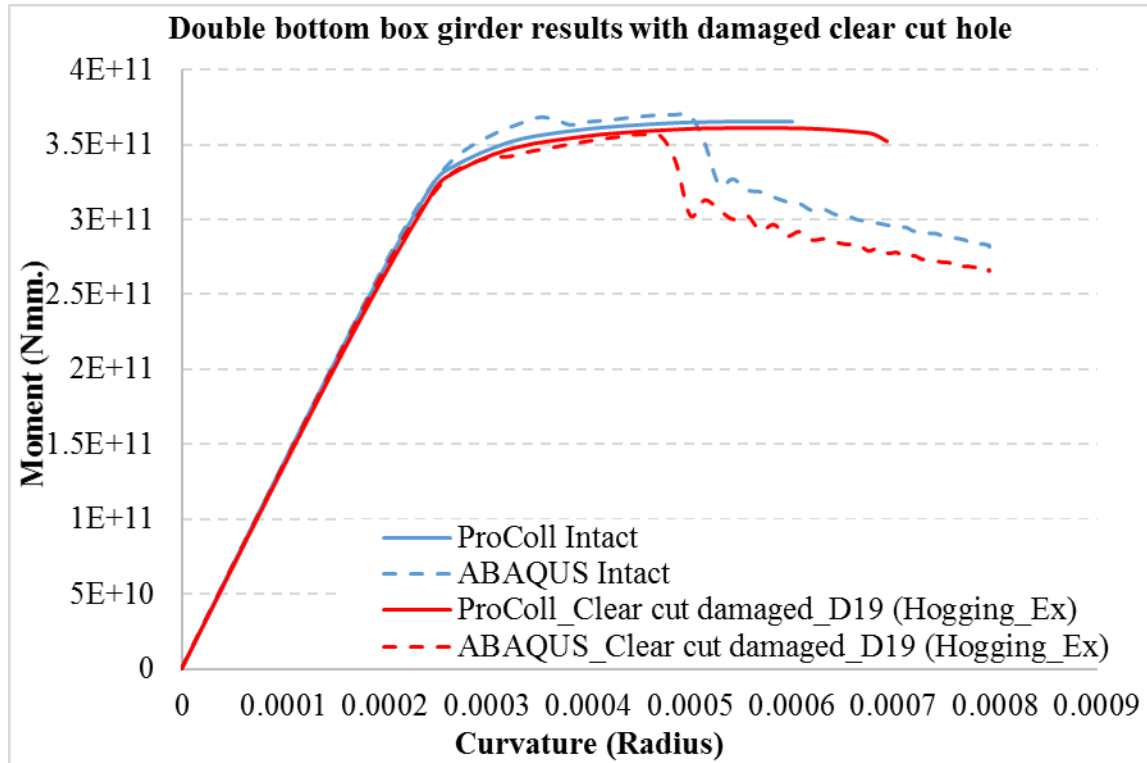


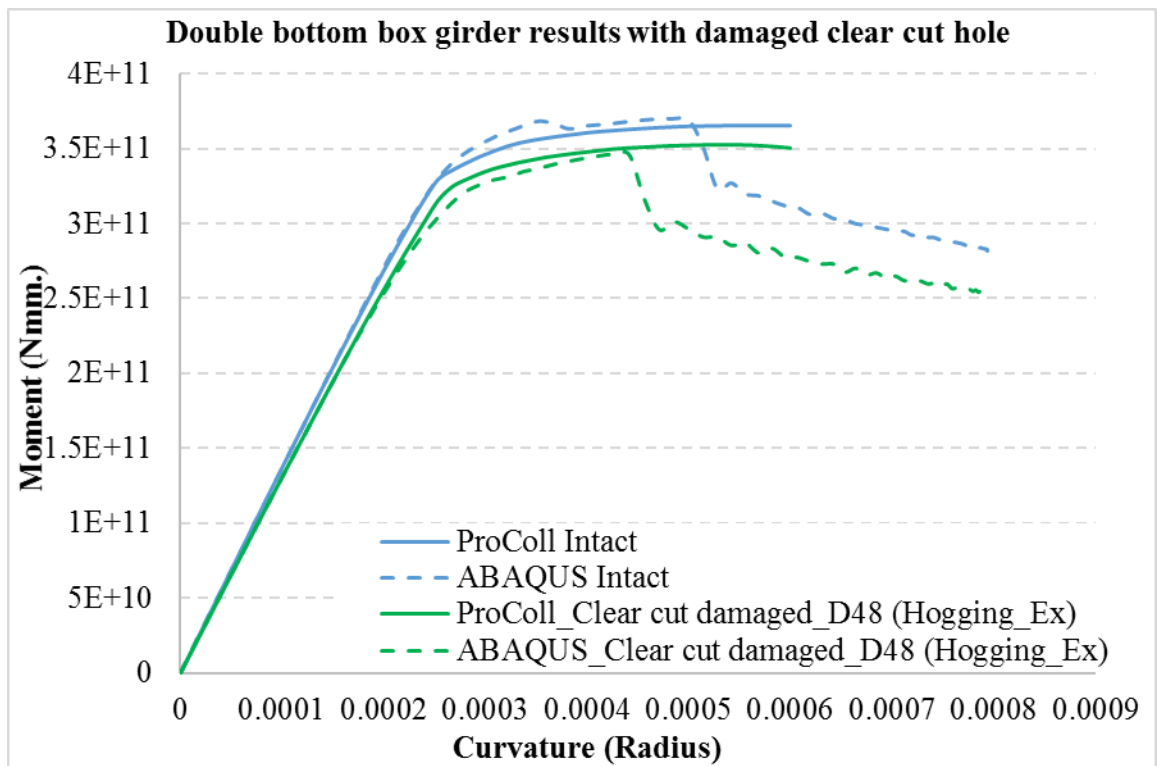
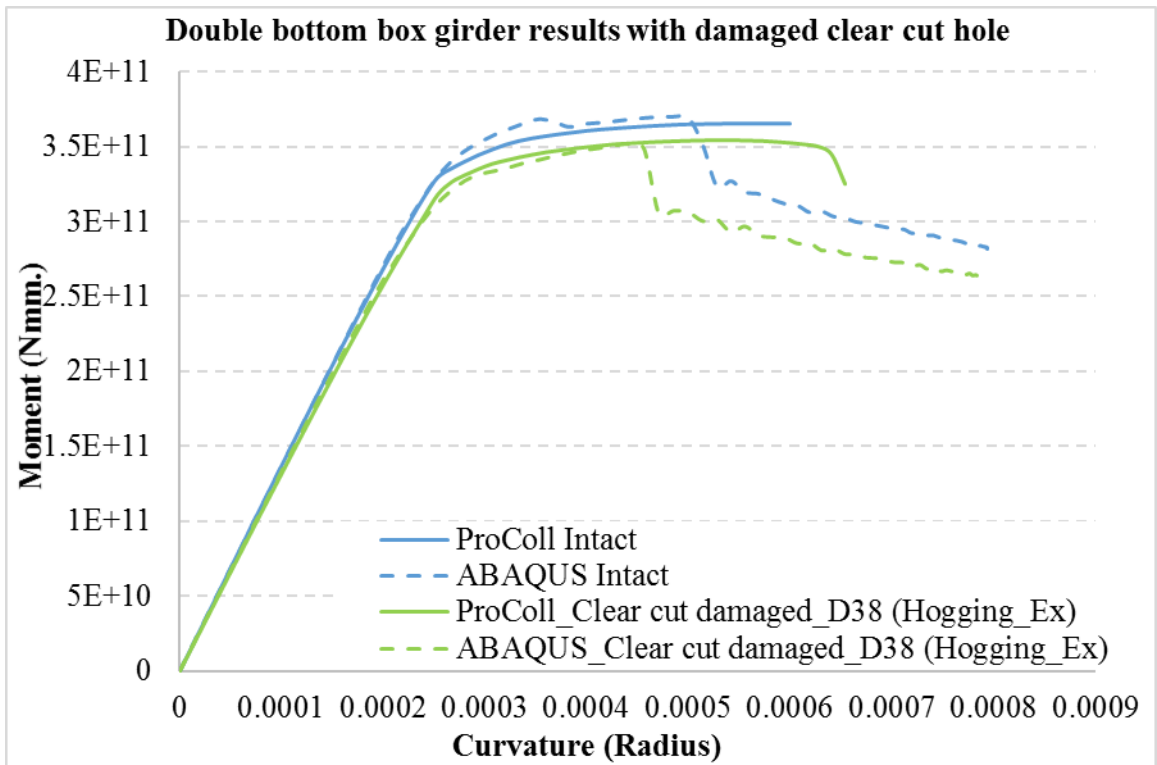


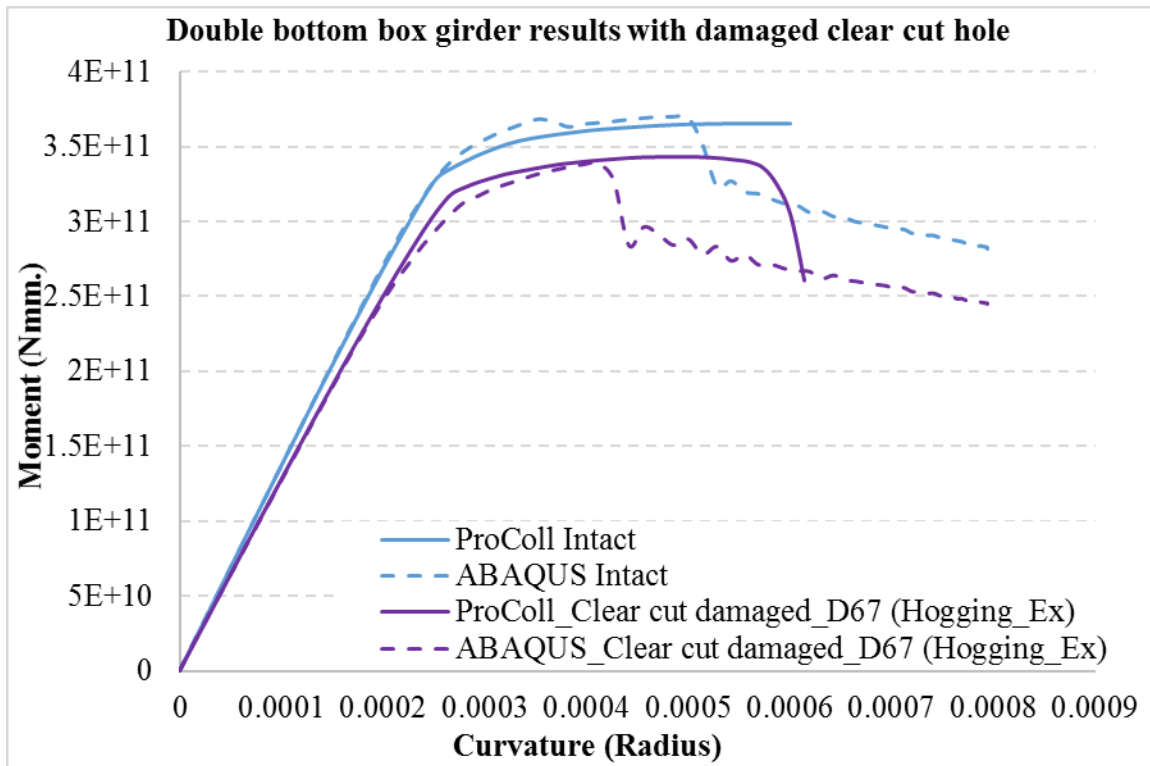
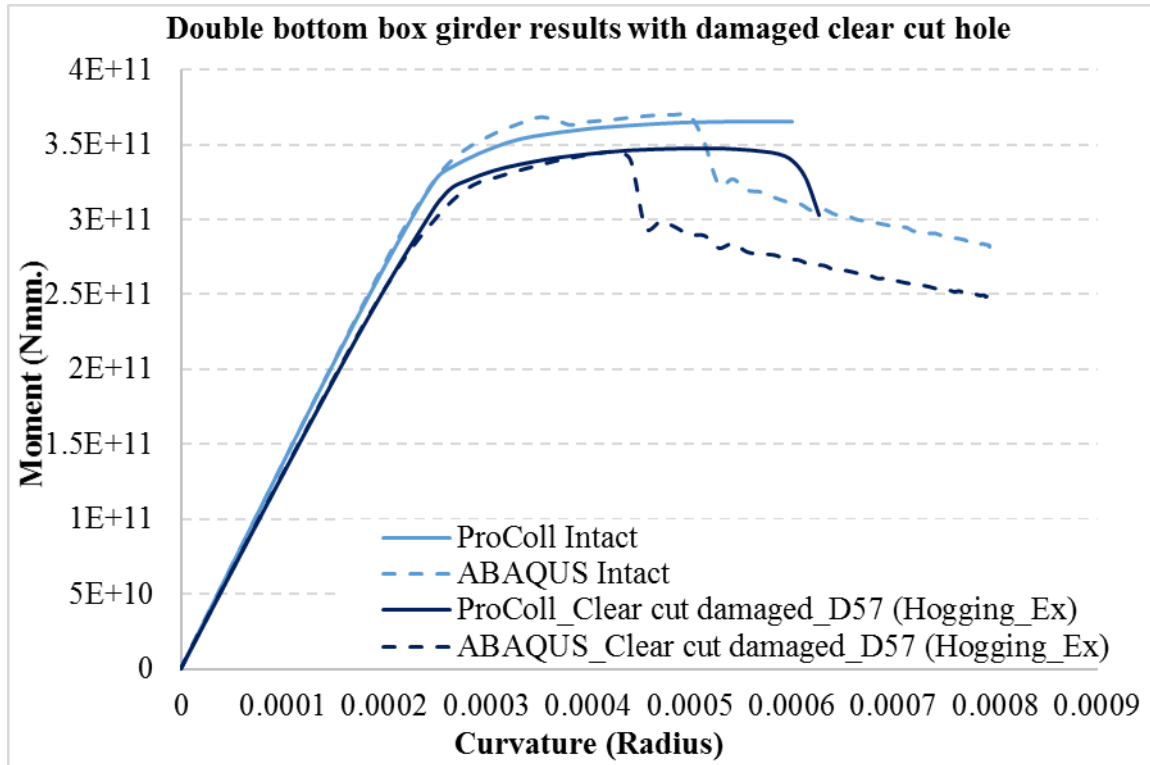
Appendix E: Strength of double bottom box girder.

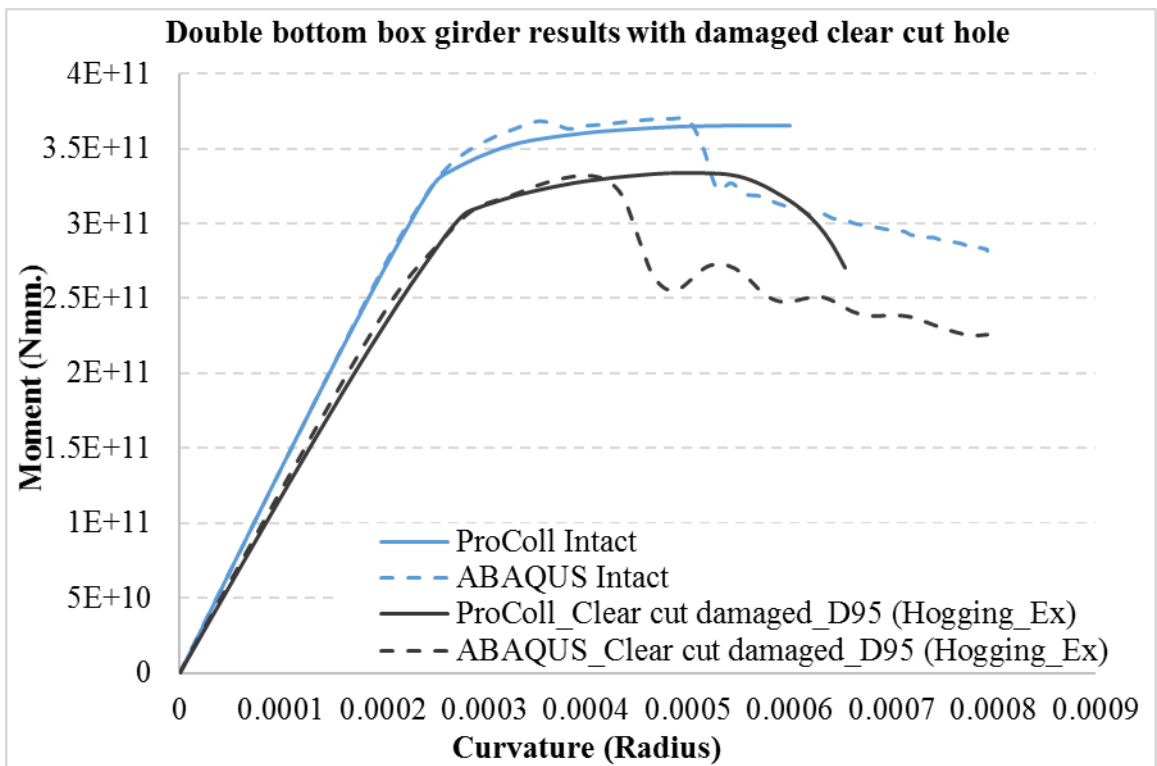
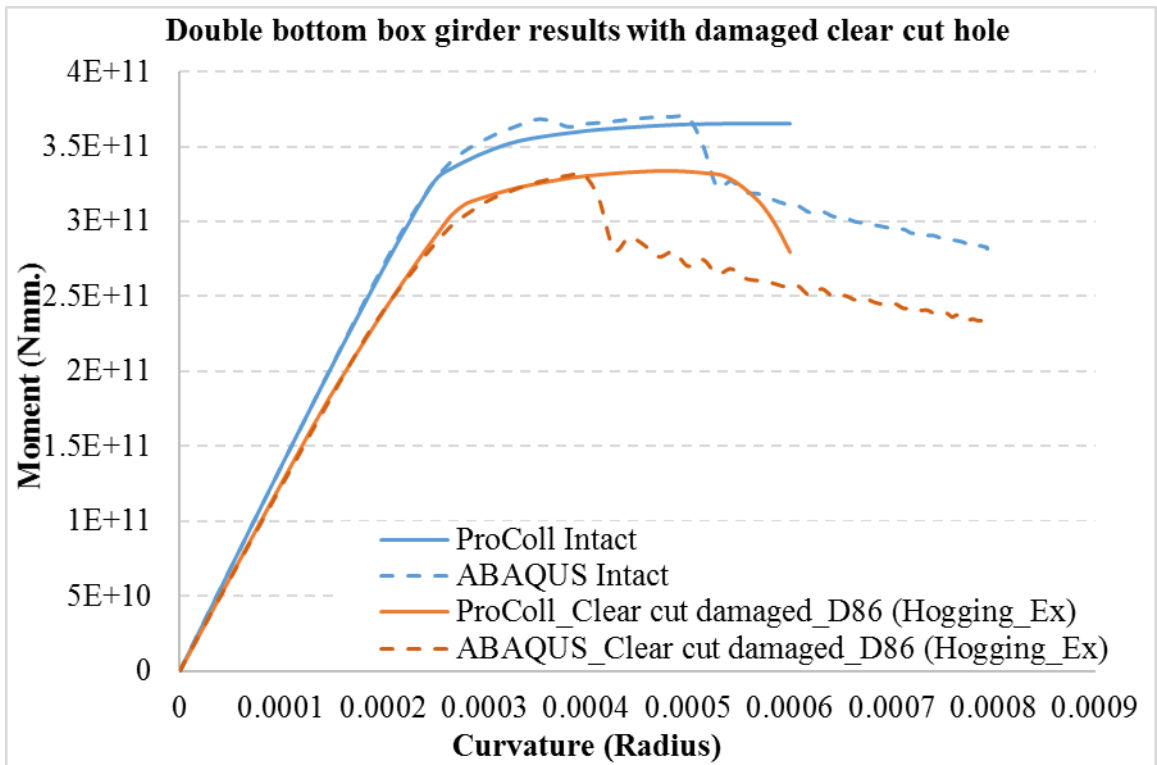
Comparison of double bottom box girder with damaged clear-cut hole between ABAQUS and ProColl.











Comparison of double bottom box girder with penetration damage with indenter between ABAQUS and ProColl.

